

Phylogeographic and morphometric studies on the Eurasian
pygmy shrew *Sorex minutus*: insights into its evolutionary history
and postglacial colonisation in Europe

Rodrigo Rafael Vega Bernal

PhD Thesis

University of York

Department of Biology

July 2010

Abstract

Here, I investigate the phylogeography and morphology of the Eurasian pygmy shrew *Sorex minutus*, searching for significantly differentiated lineages, colonisation routes and demographic parameters that would explain the effects of the Quaternary glaciations on the current distribution of the species. I also explore the genetic and morphological diversity and origin of pygmy shrew populations in the British Isles, particularly focusing on Ireland and the Orkney islands. Mitochondrial and nuclear DNA markers were used for the phylogeographic analyses, and a geometric morphometrics approach was implemented on mandible and skull samples. There was an evident phylogeographic structure across Eurasia consistent with occurrence of southern glacial refugia, and there were two distinct lineages in Northern-Central Europe and near the Pyrenees supporting the existence of northern glacial refugia through the characteristics of their distribution and population expansion. Haplotypes from Britain belonged to these two northern lineages, with the Pyrenean lineage forming a peripheral 'Celtic fringe'. I show that it is most likely that pygmy shrews on both Ireland and Orkney were introduced by humans from mainland British Celtic fringe rather than further afield, even though there is a haplotype found in Northern Spain identical to one in Ireland. Mandible size increased noticeably with decreasing latitude, but skulls showed no evident trend in size variation. Shape variation was significant but modest when analysing the sample divided into phylogeographical groups. However, the samples from different islands within the British Isles show that island evolution played an important role in morphological diversity, with mandible and skull shape divergence on small islands and low genetic diversity. These results notably expanded previous findings and indicate that *S. minutus* is an excellent model for understanding the effects of climate change on biological diversity, colonisation and differentiation in

refugia, and island evolution, useful for the conservation of genetic and morphological diversity.

List of contents

Abstract	i
List of contents	iii
List of tables	vii
List of figures	ix
List of appendices	xv
Dedication	xvii
Acknowledgements	xviii
Author declaration	xx
Chapter 1 General introduction	1
1.1 Structure of the thesis	1
1.2 The European peninsula as a geographical setting	2
1.3 Shrews including <i>Sorex minutus</i>	3
1.4 The Quaternary glaciations	6
1.5 Phylogeography defined	8
1.6 Geometric morphometrics defined	10
1.7 Aims	11
Chapter 2 Phylogeography of <i>Sorex minutus</i> in Europe	13
2.1 Introduction	13
2.2 Materials and methods	17
2.2.1 Samples and GenBank sequences for molecular analysis	17
2.2.2 DNA extraction, gel electrophoresis and visualization	18
2.2.3 PCR amplification, purification and sequencing	19
2.2.4 Analysis of sequence polymorphism	20
2.2.5 Phylogenetic analyses	21
2.2.6 Analysis of sequence diversity	26

2.2.7 Divergence and genetic structure of populations.....	27
2.2.8 Estimation of historical demographic parameters	29
2.3 Results	33
2.3.1 Sequence polymorphism.....	33
2.3.2 Phylogenetic analyses	34
2.3.3 Sequence diversity.....	45
2.3.4 Divergence and genetic structure of populations.....	46
2.3.5 Historical demography	53
2.4 Discussion and conclusions	58
2.4.1 Phylogenetic findings and genetic population structure	58
2.4.2 Insights on the colonisation routes into Europe	60
2.4.3 Colonisation and historical demography of southern peninsulas	61
2.4.4 Northern refugia of the North-Central European phylogroup	64
2.4.5 Colonisation history of Northern Europe and Britain.....	66
2.4.6 Northern refugium of the Pyrenean phylogroup?.....	67
2.4.7 Origins of the Irish pygmy shrew	67
2.4.8 Other considerations.....	69
Chapter 3 Morphological diversity of <i>Sorex minutus</i> across Europe	71
3.1 Introduction.....	71
3.2 Materials and methods.....	73
3.2.1 Collection and preparation of samples	73
3.2.2 Digitization of mandibles and skulls	75
3.2.3 Statistical analysis of landmark coordinates data	77
3.3 Results	82
3.3.1 Landmark placing error	82
3.3.2 Asymmetry and sex differences	82
3.3.3 Morphometric analysis of mandibles	83

3.3.4 Morphometric analysis of skulls	94
3.4 Discussion and conclusions.....	104
3.4.1 Mandible and skull size variation in <i>Sorex minutus</i>	104
3.4.2 Mandible and skull shape variation in <i>Sorex minutus</i>	105
3.4.3 Taxonomic implications.....	107
Chapter 4 Island phylogeography and morphometrics of <i>Sorex minutus</i>	109
4.1 Introduction.....	109
4.2 Materials and methods.....	111
4.2.1 Samples for genetic and morphological analysis.....	111
4.2.2 Sequence diversity, divergence and differentiation	113
4.2.3 Estimation of migration routes.....	114
4.2.4 Geometric morphometric analysis.....	115
4.3 Results	116
4.3.1 Genetic diversity and structure.....	116
4.3.2 Migration routes	120
4.3.3 Geometric morphometrics findings.....	122
4.4 Discussion and conclusions.....	129
Chapter 5 General discussion and conclusions	134
5.1 Phylogeographic structure of <i>Sorex minutus</i> in Europe.....	134
5.2 Historical demography and colonisation routes.....	137
5.3 An emerging pattern of northern glacial refugia	141
5.4 Natural and human-mediated colonisation	143
5.5 Morphological diversity of <i>Sorex minutus</i> in Europe.....	145
5.6 Insights into island evolution of <i>Sorex minutus</i>	147
5.7 Conservation implications	150
5.8 Future directions	150
5.9 Conclusions	153

References	156
Appendix 1. Genetic and morphological variation in a Mediterranean glacial refugium: evidence from Italian pygmy shrews, <i>Sorex minutus</i> (Mammalia: Soricomorpha)	180
Appendix 2. Northern glacial refugia for the pygmy shrew <i>Sorex minutus</i> in Europe revealed by phylogeographic analyses and species distribution modelling	194
Appendix 3. List of samples of <i>Sorex minutus</i> for genetic analysis	206
Appendix 4. List of mandible and skull samples for geometric morphometric analysis	218
Appendix 5. Analysis of Variance (ANOVA) post-hoc tests on Centroid Size (CS) for <i>Sorex minutus</i> mandibles	229
Appendix 6. Multivariate Analysis of Variance (MANOVA) post-hoc tests on shape variables for <i>Sorex minutus</i> mandibles	231
Appendix 7. Analysis of Variance (ANOVA) post-hoc tests on Centroid Size (CS) for <i>Sorex minutus</i> skulls.....	233
Appendix 8. Multivariate Analysis of Variance (MANOVA) post-hoc tests on shape variables for <i>Sorex minutus</i> skulls.....	235
Appendix 9. Analysis of Variance (ANOVA) of <i>Sorex minutus</i> mandibles.	237
Appendix 10. Analysis of Variance (ANOVA) of <i>Sorex minutus</i> skulls	238
Appendix 11. Multivariate Analysis of Variance (MANOVA) of <i>Sorex minutus</i> mandibles	240
Appendix 12. Multivariate Analysis of Variance (MANOVA) of <i>Sorex minutus</i> skulls	242

List of tables

Table 2.1. Primer sequences used in this study.

Table 2.2. Cytochrome *b* sequence diversity of phylogroups, island and continental samples of *Sorex minutus*.

Table 2.3. Pairwise sequence divergence values D_a (SD), below diagonal, and pairwise geographic distances (in Km), above diagonal, among cytochrome *b* phylogroups of *Sorex minutus*.

Table 2.4. Pairwise F_{ST} values (below diagonal) among cytochrome *b* phylogroups and phylogroup specific F_{ST} values (diagonal) of *Sorex minutus*.

Table 2.5. Analysis of Molecular Variance (AMOVA) among cytochrome *b* phylogroups of *Sorex minutus* and phylogroup F_{ST} .

Table 2.6. Time of divergence (\pm SD) among cytochrome *b* phylogroups of *Sorex minutus* (in MYA).

Table 2.7. Population expansion analyses for the whole cytochrome *b* dataset (Eurasian) and phylogroups of *Sorex minutus* (p values are given between parentheses).

Table 2.8. Time of expansion parameters for the whole cytochrome *b* dataset (Eurasian) and phylogroups of *Sorex minutus*.

Table 3.1. Centroid size statistics for *Sorex minutus* mandibles.

Table 3.2. Centroid size statistics for *Sorex minutus* skulls.

Table 4.1. Cytochrome *b* sequence diversity of *Sorex minutus* groups of the Pyrenean lineage.

Table 4.2. Demographic parameters obtained for *Sorex minutus* Pyrenean groups based on cytochrome *b* data.

Table 4.3. Centroid Size statistics for *Sorex minutus* mandibles of the Pyrenean lineage.

Table 4.4. Centroid Size statistics for *Sorex minutus* skulls of the Pyrenean lineage.

List of figures

Figure 1.1. A) Map of Eurasia showing the geographical distribution of the Eurasian pygmy shrew *Sorex minutus* (modified from Corbet and Harris 1991). B) Map of Europe showing the three Mediterranean peninsulas (namely Iberian, Italian and Balkan) and the glaciated areas at the Last Glacial Maximum (gray shaded polygons delimited by thick black lines; modified from Ehlers and Gibbard 2004).

Figure 2.1. Sample localities of *Sorex minutus* from Europe divided into cytochrome *b* phylogroups: ● North-Central European (three Russian samples from Siberia are not shown in map), ○ Pyrenean, ☆ South Italian, □ North-Central Italian, ▽ Balkan and ▲ Iberian; ■ *S. volnuchini* (outgroup). Relief illustrated in grey tones.

Figure 2.2. Bayesian inference tree of cytochrome *b* data showing the phylogenetic relationships among *Sorex minutus* haplotypes. Phylogroups (North-Central European, Pyrenean, South Italian, North-Central Italian, Balkan and Iberian) and four other groups (Britain, Ireland, Orkney and Celtic fringe) are represented with different colours. Letters 'A – F' correspond to ancestral (central) haplotypes in the MJ network (Fig. 2.3). Values on branches correspond to posterior probability support. The scale bar represents 0.3 nucleotide substitutions per site.

Figure 2.3. Median-Joining network of cytochrome *b* data showing the relationships among *Sorex minutus* haplotypes. A) Full network showing the main phylogroups (dashed lines). B) The North-Central European phylogroup (with British group). C) The Pyrenean (with Ireland, Orkney and Celtic fringe groups), North-Central Italian and South Italian phylogroups. D) The Balkan and Iberian phylogroups. Ancestral (central) haplotypes from where all other haplotypes derive from are marked with

letters 'A – F' (see text for explanation). Numbers in parentheses represent mutation steps. Dotted line in centre of A) shows where the network was cut.

Figure 2.4. Bayesian inference tree of A) Y-chromosome introns and B) BRCA1 gene showing the phylogenetic relationships among *Sorex minutus* sequences. Values on branches represent posterior probability branch support.

Figure 2.5. Neighbor-Joining tree showing the pairwise distances among cytochrome *b* phylogroups of *Sorex minutus* and estimated divergence times (in MYA) assuming a molecular clock.

Figure 2.6. Bayesian inference tree of cytochrome *b* data showing the genetic relationships among phylogroups of *Sorex minutus*. Values on nodes correspond to Times to the Most Recent Common Ancestor with 95% Highest Probability Density confidence intervals (in MYA). The ingroup (*) was calibrated with the oldest known fossil record of *S. minutus* (5 MYA, SD = 0.2).

Figure 2.7. Mismatch distribution (frequency of pairwise nucleotide differences) of cytochrome *b* phylogroups of *Sorex minutus*.

Figure 2.8. Bayesian Skyline Plots of cytochrome *b* phylogroups of *Sorex minutus* showing the historical demographic trends. The solid lines are median estimates and the shaded areas represent 95% Highest Probability Densities (confidence intervals).

Figure 3.1. Samples of *Sorex minutus* for morphological analysis. A) Mandible dataset. B) Skull dataset. The symbols correspond to the different lineages detected

previously with mtDNA. ● North-Central European, □ North-Central Italian, ▽ Balkan, ☆ South Italian, ▲ Iberian, ⊕ Pyrenean, △ Orkney Mainland, ○ Westray, ★ South Ronaldsay, X Ireland, ◊ *S. volnuchini* (outgroup).

Figure 3.2. Landmarks placed on A) mandibles and B) skulls of *Sorex minutus*. For simplicity, only the left sides are shown. The diagrams show the observed dispersion of landmarks for all the aligned specimens.

Figure 3.3. Box plots of mandible Centroid Size (CS; transformed with natural logarithms) of *Sorex minutus*. There is a decrease of CS from Southern (left) to Northern (right) latitudes. The horizontal dashed line corresponds to the sample mean. The outgroup (*S. volnuchini*) is shown for purposes of comparison.

Figure 3.4. Linear regressions of Centroid Size (CS; natural log-transformed) on A) latitude and B) longitude for *Sorex minutus* mandible samples.

Figure 3.5. Multiple regressions of shape on A) Centroid Size (CS), B) latitude and C) longitude for *Sorex minutus* mandibles. Transformation grids were exaggerated 3 times for purposes of visualisation. Arrows help to evaluate the relative movements of landmarks.

Figure 3.6. Relative Warp Analysis of shape variables of *Sorex minutus* mandibles. The maximum and minimum transformation grids on the first two Relative Warps (RW1 and RW2), and the average configuration are shown for purposes of visualisation.

Figure 3.7. Canonical Variate Analysis of shape variables of *Sorex minutus* mandibles showing group differences. The first two canonical variates (CV) were used to describe variation among groups.

Figure 3.8. A) Unrooted and B) rooted Neighbor-Joining (NJ) trees constructed using mandible Procrustes distances among *Sorex minutus* groups. Branch support is shown as bootstrap values (10,000 replications). The grids on the right correspond to shape deformation per group from the average configuration. Inset: NJ trees based on genetic distances obtained in Chapter 2, shown for purposes of comparison.

Figure 3.9. Box plots of skull Centroid Size (CS; natural log-transformed) of *Sorex minutus*. There is no apparent tendency from Southern (left) to Northern (right) latitudes. The horizontal dashed line corresponds to the sample mean. The outgroup (*S. volnuchini*) is shown for purposes of comparison.

Figure 3.10. Linear regressions of Centroid Size (CS; transformed with natural logarithms) on A) latitude and B) longitude for *Sorex minutus* skull samples.

Figure 3.11. Multiple regressions of shape on A) Centroid Size (CS), B) latitude and C) longitude for *Sorex minutus* skulls. Transformation grids were exaggerated 3 times for purposes of visualisation. Arrows help to evaluate the relative movements of landmarks.

Figure 3.12. Relative Warp Analysis of shape variables of *Sorex minutus* skulls. The maximum and minimum transformation grids on the first two Relative Warps

(RW1 and RW2), and the average configuration are shown for purposes of visualisation.

Figure 3.13. Canonical Variate Analysis of shape variables of *Sorex minutus* skulls showing group differences. The first two canonical variates (CV) were used to describe variation among groups.

Figure 3.14. A) Unrooted and B) rooted Neighbor-Joining (NJ) trees constructed using skull Procrustes distances among *Sorex minutus* groups. Branch support is shown as bootstrap values (10,000 replications). The grids on the right correspond to shape deformation per group from the average configuration. Inset: NJ trees based on genetic distances obtained in Chapter 2, shown for purposes of comparison.

Figure 4.1. Samples of *Sorex minutus* for genetic analysis. ☞ Continental, ■ British Celtic fringe, ○ Ireland and △ Orkney islands.

Figure 4.2. Median-Joining network of cytochrome *b* data showing the relationships among *Sorex minutus* haplotypes belonging to the Pyrenean lineage. The Pyrenean lineage is divided into a 'Continental' group (light green), a 'Celtic fringe' group distributed on Britain and some islands off the coast of Britain (light blue), excluding the Orkney islands, 'Ireland' (dark green) and 'Orkney islands' groups (purple). Pointed lines indicate the central (ancestral) haplotypes from where all other haplotypes derive from (see text for explanation). Some loops in the network are not on scale and mutations are shown with numbers. For the 'Continental' group, the country of origin for the haplotypes is shown (FR = France, ES = Spain).

Figure 4.3. Migration rates and routes of *Sorex minutus* among the Continental, Celtic fringe, Ireland and Orkney islands groups estimated from cytochrome *b* data. Values next to arrows are the estimated migration rates from one group to the other. Larger arrow heads and bold numbers represent the migration rate trends, mainly from continent to island and from larger island to smaller island.

Figure 4.4. Box plots of A) mandible and B) skull Centroid Size (CS; natural log-transformed) of *Sorex minutus* samples ordered latitudinally (with south to the left).

Figure 4.5. Canonical Variate Analysis of shape variables of A) mandibles and B) skulls of *Sorex minutus* from the Pyrenean lineage showing group differences. The first two canonical variates (CV) were used to describe variation among groups. O = Orkney, SR = South Ronaldsay, W = Westray.

Figure 4.6. Canonical Variate Analysis of shape variables of A) mandibles and B) skulls of *Sorex minutus* from the Pyrenean lineage showing island size differences. The first two canonical variates (CV) were used to describe variation among groups. Continent = Continental European samples, Large size island = Ireland, Medium size island = Orkney Mainland, Small size island = South Ronaldsay, Westray and Belle Île.

Figure 5.1. Three paradigms of postglacial colonisation routes from Southern Europe: A) the bear, B) the grasshopper and C) the hedgehog (Hewitt 2000). The addition of D) the pygmy shrew gives a more complete picture and exemplifies an emerging pattern of northern refugia. Arrows represent general colonisation routes. Coloured areas are an approximation of the geographical distribution of the cytochrome *b* lineages obtained in this study (see Fig. 2.2 for lineages).

List of appendices.

Appendix 1. Genetic and morphological variation in a Mediterranean glacial refugium: evidence from Italian pygmy shrews, *Sorex minutus* (Mammalia: Soricomorpha).

Appendix 2. Northern glacial refugia for the pygmy shrew *Sorex minutus* in Europe revealed by phylogeographic analyses and species distribution modelling.

Appendix 3. List of samples of *Sorex minutus* for genetic analysis.

Appendix 4. List of mandible and skull samples for geometric morphometric analysis.

Appendix 5. Analysis of Variance (ANOVA) post-hoc tests on Centroid Size (CS) for *Sorex minutus* mandibles.

Appendix 6. Multivariate Analysis of Variance (MANOVA) post-hoc tests on shape variables for *Sorex minutus* mandibles.

Appendix 7. Analysis of Variance (ANOVA) post-hoc tests on Centroid Size (CS) for *Sorex minutus* skulls.

Appendix 8. Multivariate Analysis of Variance (MANOVA) post-hoc tests on shape variables for *Sorex minutus* skulls.

Appendix 9. Analysis of Variance (ANOVA) of *Sorex minutus* mandibles.

Appendix 10. Analysis of Variance (ANOVA) of *Sorex minutus* skulls.

Appendix 11. Multivariate Analysis of Variance (MANOVA) of *Sorex minutus* mandibles.

Appendix 12. Multivariate Analysis of Variance (MANOVA) of *Sorex minutus* skulls.

Dedication

To my nieces and nephews, Ximena, Alejandro, Evelyn, Oriana and Federico, and to my grand-niece Amalia.

Acknowledgements

Firstly, I would like to thank my supervisor Jeremy B. Searle for his support, advice and friendship over the years, and for sending me to wonderful places for fieldwork! I would also like to thank Angela E. Douglas for her support and giving me the chance to do the final years of my PhD in her lab at Cornell University. I am grateful to my training committee, Jane K. Hill and Paul O'Higgins for their advice throughout the development of this thesis and for making sure that everything was going smoothly during the course (or curse?) of my PhD. The CONACyT (México) provided essential financial support (Reg. No. 181844).

This thesis would have not been possible without the specimens provided by several museums and private collections (acknowledged here and elsewhere). Particularly, I thank Giovanni Amori, Gaetano Aloise, Jacques Hausser, Jan Wójcik, Jan Zima, Heidi Hauffe, Richard Sabin, Patrick Brunet-Lecomte, Glenn Yannic, Enrique Castiens, Carlos Nores Quesada, Paulo Célio Alves, Alberto Goza, Giuliano Doria, Sandro Bertolino and Boris Kryštufek, who provided advice and samples asking for nothing in return.

I had a great time in Britain with Mabel Giménez, Ellie Jones, Fríða Jóhannesdóttir, Natalia Martinková, Tom White, Joana Pauperio, Sofia Gabriel and Allan McDevitt, past, present and future members of the Searle Lab. I hope we will meet again. At Cornell, the Douglas Lab members made sure I would not get bored being in an insect physiology lab, and I would like to thank Emma Ridley, Calum Russell, Adam Wong, Tomás Lazo, Stephanie Westmiller, Erick van Fleet, George Lin and the undergrads.

Back in York, my flatmates from Ainsty Court, Soar, Kiran, Jan, Nicole, Lulu, Venkat and Nuria, my housemates from Saint Paul's Terrace, Michelle, Mary, Erica and George the rabbit, and the Mexican gang, Tizbe, Arturo and Horacio, made all

these years unforgettable. The time while in the US would have been less fun without my friends Guillermo, Mathieu, Marie-Line, Aldo, Patricia, Sergio and the rest of the Spanish gang.

Back in México and Argentina, Juan Pablo, Rodrigo, Alfredo, Julieta, Andrés, Giuseppe, Yoshi, Mariana and Ariel always reminded me of the joys of life. I missed you.

My parents have given me endless support, love and courage to keep going this far. I hope they enjoy their well deserved retirement. My brother and sister, uncles and cousins have also been there for me when I needed them the most.

And finally, I would like to thank my wife Sophie for giving me more than I ever thought I could get from a relationship.

Author declaration

I declare that this is my own work, unless stated otherwise.

Chapter 1

General introduction

1.1 Structure of the thesis

In this thesis I explore the genetic and morphological diversity of the Eurasian pygmy shrew *Sorex minutus* (Linnaeus 1766) by means of a phylogeographic and geometric morphometrics approach.

This chapter (Chapter 1) gives a general introduction to the subject species in a biogeographical, taxonomic and evolutionary setting, and I provide the aims of this study. In Chapter 2, I perform a phylogeographic analysis using mitochondrial and nuclear DNA markers, and discuss the findings in the context of the Quaternary glaciations and the processes of Eurasian colonisation and evolutionary divergence. Chapter 3 is devoted to the analysis of morphological variation using a geometric morphometric technique on mandible and skull datasets of *S. minutus* obtained across Europe. In Chapter 4, I present a combined analysis of phylogeography and geometric morphometrics on the genetic and morphological variation of *S. minutus* belonging to a Pyrenean lineage, distributed in Western continental Europe, the Orkney islands, Ireland and Britain, to understand the colonisation patterns and divergence in an island setting. In the final chapter (Chapter 5), I discuss the main findings and future directions, and present the general conclusions of my phylogeographic and morphometric studies on *S. minutus*. The appendices 1 and 2 correspond to two published works in scientific journals that originated from this thesis, one in the Biological Journal of the Linnean Society (Vega et al. 2010a) and the other in Ecography (Vega et al. 2010b), made in collaboration with other researchers; the former explores the genetic and morphological distinction of *S.*

minutus in the Italian peninsula, while the later examines the northern glacial refugia hypothesis with a phylogeographic and ecological niche modelling approach.

1.2 The European peninsula as a geographical setting

Europe is a macropeninsula with an east-west orientation on the western-most region of the Eurasian landmass forming part of the Palaearctic biogeographic region. Europe is delimited in the east by the Ural Mountains, in the southeast by the Caspian Sea, Caucasus Mountains and the Black Sea, in the south by the Mediterranean Sea, in the west by the Atlantic Ocean and in the north by the Arctic Ocean (Fig. 1.1A, B; Temple and Terry 2007). The total area (including European Russia) is more than 10 million square kilometres, and the most important mountain ranges are the Pyrenees, the Alps, the Apennines, the Carpathians, the Caucasus and the Balkan mountain range (Temple and Terry 2007).

There are 219 species of terrestrial mammals in Europe, of which 59 (26.9%) are endemic (Temple and Terry 2007, Mitchell-Jones et al. 1999). Biogeographic studies indicate that there are low levels of mammalian diversity but high levels of endemism compared to Asia and North America (Maridet et al. 2007). Europe has 23 species of shrews (Temple and Terry 2007), 12 of which belong to the genus *Sorex* which has 74 extant species worldwide (Rzebik-Kowalska 2005).

The biogeographical patterns that explain mammal diversity and distribution in the European peninsula include: 1) a 'peninsular effect', with highest diversity in east-central regions and a lower diversity westwards and northwards, possibly as a result of historical and environmental factors affecting mammal distributions during the Quaternary; 2) isolation and allopatric speciation during the glaciations in the Pleistocene; 3) species evolution and presence of relict species from the Tertiary; and 4) ancient and current human pressures, introduction and extinction of species (Baquero and Tellería 2001).

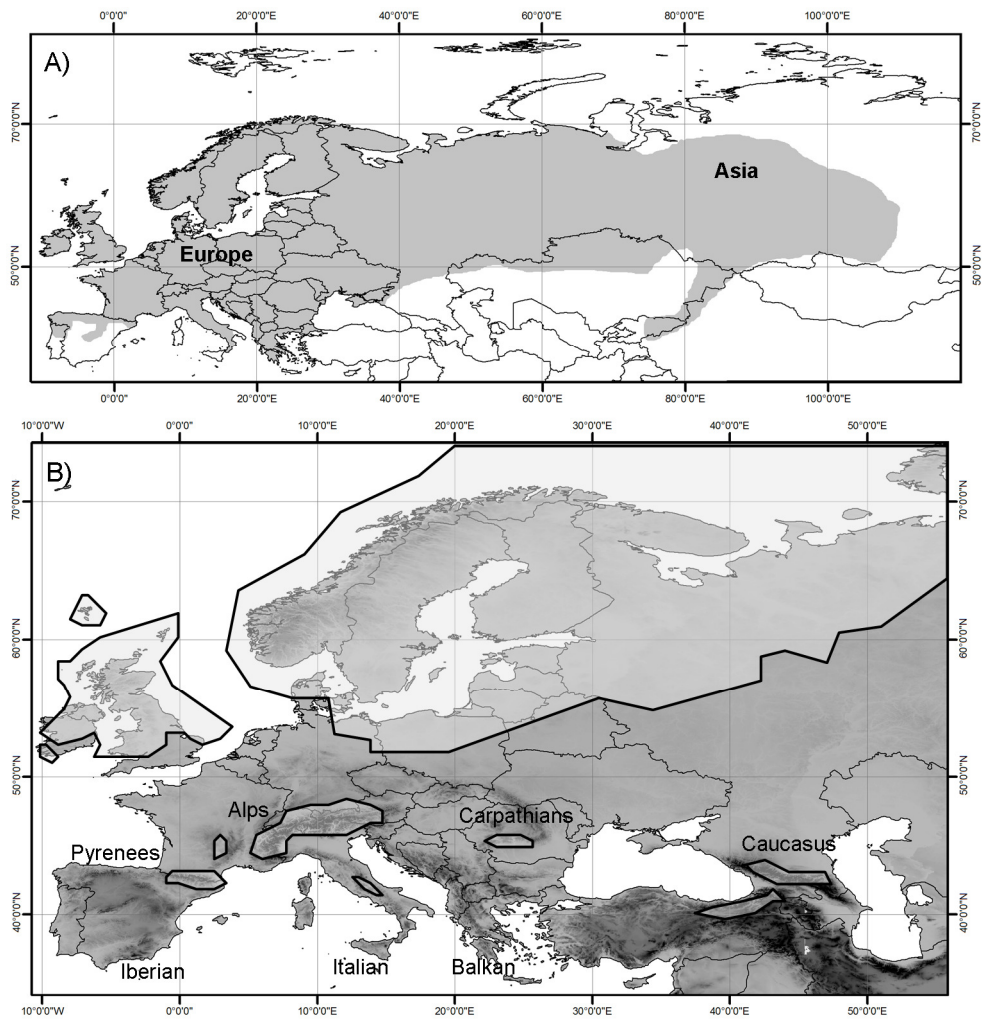


Figure 1.1. A) Map of Eurasia showing the geographical distribution of the Eurasian pygmy shrew *Sorex minutus* (modified from Corbet and Harris 1991). B) Map of Europe showing the three Mediterranean peninsulas (namely Iberian, Italian and Balkan) and the glaciated areas at the Last Glacial Maximum (grey shaded polygons delimited by thick black lines; modified from Ehlers and Gibbard 2004).

1.3 Shrews including *Sorex minutus*

Shrews are among the smallest of all extant mammals, frequently confused with mice because of their small size, short legs, small rounded ears, short dense fur, usually dark colour, and long snouts. However, shrews are classified as insectivores, but do not specialize on insects and may be considered predatory generalists (Crowcroft 1957, Churchfield 1990).

One of the most speciose groups of mammals, shrews occupy moist and terrestrial environments at different altitudes (from sea level to 3000 m.a.s.l), where there is adequate vegetation cover and diversity of invertebrate prey, are found in woodlands, forests, grasslands, hedgerows and scrublands in temperate and tropical regions, and some are aquatic (Churchfield 1990, Corbet and Harris 1991).

Among the primitive characters shown by shrews are the generalized and unspecialized body plan, plantigrade mode of locomotion, each foot with five digits terminating in a simple claw, the skull is long and narrow with a small brain with small cerebral hemispheres but relatively large and well developed olfactory lobes, there are no zygomatic arches, the mandible has a double articulating surface, the genital and urinary systems have a common cloaca, and the testes are retained in an abdominal cavity and do not descent to a scrotum (Churchfield 1990). The teeth are specialized and characteristic with large prominent incisors, which, unlike rodents, do not keep growing all their life span. The first upper incisors are enlarged and have two cusps that project downward, plus a large cusp at the base, and the first lower incisors are also large and slightly procumbent, pointing forward and upwards (Churchfield 1990).

Sorex minutus, commonly known as the Eurasian pygmy shrew, has a wide Eurasian range (Fig. 1.1A) and it is the most widespread species of the Holarctic genus *Sorex*, extending from Northern Portugal across most of Central and Northern Europe to Lake Baikal in Siberia. This species is present in the three Mediterranean peninsulas of Iberia, Italy and the Balkans, but is limited to higher altitudes where its distribution becomes patchy (Hutterer 2005). However, humans are also believed to be involved in the distribution of this species, particularly for the populations in Ireland and the islands off the coast of Britain (Mascheretti et al. 2003). The widespread distribution of *S. minutus* makes it an excellent model for studies of genetic and morphological evolution in a continental and island setting.

To classify taxonomically the study species, I follow the recent splitting up of the paraphyletic Order 'Insectivora' into the Orders Soricomorpha (moles, shrews and *Solenodon*), Erinaceomorpha (hedgehogs) and Afrosoricida (tenrecs and golden moles) (Stanhope 1998, Hutterer 2005). Then, I follow the two-family classification of shrews by Reumer (1998), which distinguishes the extinct Heterosoricidae and the extant Soricidae. Therefore, the Eurasian pygmy shrew *Sorex minutus* (Linnaeus 1766) belongs to: Class Mammalia, Order Soricomorpha, Family Soricidae, Subfamily Soricinae, Tribe Soricini (with a Holarctic distribution), Genus *Sorex*, Species *minutus*. The morphological features of *S. minutus* described here follow Crowcroft (1957): the adults have a nose to anus length of 55-66 mm, tail length of 30-45 mm, hind foot of 10-11.5 mm and weight around 3-6 g; the juveniles have a length of 45-55 mm and weight between 2.5 and 4.5 g. The tail is hairy and usually exceeds 2/3 of the body length. The colour is sandy brown and the ears are never white, as found in some species (Crowcroft 1957, Corbet and Harris 1991). *Sorex minutus* has 339% of the expected basal metabolic rate for mammals of that body weight (Sparti and Genoud 1989), and it requires 125% of its body weight daily in food or 9.7-13.0 KJ per gram body weight per day (Churchfield 1990). The diet of *S. minutus* includes flies, spiders, woodlice and earthworms, and less frequently millipedes and centipedes (Churchfield 1990).

Five valid subspecies, which should be regarded with caution, were recognized by Hutterer (1990): *S. m. minutus* in Northern and Central Europe to Siberia, *S. m. gymnurus* (Chaworth-Musters 1932) in Greece, *S. m. becki* (von Lehman 1963) in the Alps, *S. m. carpetanus* (Rey 1971) in Spain, and *S. m. lucanius* (Miller 1909) in the Basilicata and Calabria ridges of Southern Italy; however, he did not resolve the taxonomic status of pygmy shrew populations in Central Italy. The populations appear to follow a clinal gradient within regions (Hutterer 1990). The karyotype has a diploid number (2n) of 42 chromosomes, and

a fundamental number of 56, but $2n = 40$ and 36 are found in the Baltic islands of Öland and Gotland (Hutterer 2005).

The fossil record of the Soricidae in Europe starts in the Early Oligocene, while the oldest record of the Soricini in Europe dates probably to the Late Miocene, including the genus *Sorex* (Rzebik-Kowalska 1998). The oldest record of *S. minutus* was found in Podlesice and Mała Cave, Poland in the Early Pliocene (Mammal Neogene 14), between 5.3 and 3.6 MYA (Rzebik-Kowalska 1998).

1.4 The Quaternary glaciations

For this study, a geological timeframe is needed to fully understand the main findings. Most of the events discussed here occurred within the Quaternary period (2.58 – 0.0117 MYA; Gibbard et al. 2010), commonly recognized as the ice ages. The Quaternary was marked by significant changes in climate that led to periods of ice-sheet expansion or 'glaciations', and intervening temperate (warm) stages or 'interglacials' (Ehlers 1996), with profound effects on the current distribution of European biota and their intraspecific genetic variation (Hewitt 2000, 2004). The Quaternary is further subdivided in two epochs: the Pleistocene (2.58 – 0.0117 MYA) with the subepochs Early, Middle and Late, and the Holocene (11.7 KYA to present) (Gibbard et al. 2010).

About 30 warm and 30 cold stages are distinguished in the Pleistocene, with cold stages every ca. 41 KY cycles from the beginning of the Pleistocene until ca. 0.9 MYA and every 100 KY from then to the present (Hewitt 2000), caused by periodic changes of the Earth's orbit around the Sun that affect the influx of solar radiation. The factors affecting the radiation influx are: 1) the Earth's eccentricity or deviation from a circular orbit, which enhances the contrast in temperature between summer and winters, and varies between 0.5 to 6% within 100,000 years; 2) the tilt of the Earth's axis, which changes over 40,000 years between 22.1° and 24.5°; and

3) the Earth's precession, or rotation of the Earth's axis around the pole, which together with the orbital ellipse determine the perihelium with a periodic change every 20,000 years and enhances the annual temperature gradient on one hemisphere and smoothes it on the other (Ehlers 1996). However, the mechanisms that cause the climatic fluctuations may be more complex involving a combination of astronomical, geological and biological factors.

During the Quaternary ice ages substantial areas of Northern Europe were covered by ice sheets (Fig. 1.1B) while permafrost existed in large areas of Central Europe, which restricted the distribution of many temperate and warm-adapted species to the three Southern European peninsulas of Iberia, Italy and the Balkans at the Last Glacial Maximum (LGM; Hewitt 2000). These species are interpreted to have recolonised Central and Northern Europe from the traditionally recognized southern glacial refugia in response to the late-glacial and postglacial warming, and this process became established as a biogeographical paradigm (Taberlet et al. 1998, Hewitt 2000, 2004). In addition, there is evidence supporting glacial refugia for some temperate and boreal species further north than traditionally recognized, from where the postglacial colonisation of Central and Northern Europe occurred, implying a more complex pattern of glacial survival and postglacial recolonisation (Bilton et al. 1998, Stewart and Lister 2001, Kotlík et al. 2006, Stewart et al. 2010).

The isolation and recolonisation during the climatic fluctuations of the Quaternary must have had profound effects on population demographic parameters and must have left genetic signatures that can be explored using a phylogeographic approach. Moreover, the latitudinal and altitudinal range shifts and isolation of populations because of the presence of geographical barriers to dispersal such as glaciers could have provided an opportunity for adaptation to occur, which could have affected the intraspecific levels of morphological variation.

1.5 Phylogeography defined

The term phylogeography implies the integration of phylogenetic analyses of organismal data with a geographical context. This term was coined by Avise et al. (1987) and stemmed from the idea that species are genetically structured due to environmental, geographical, geological or behavioural factors. Phylogeography is generally defined as "...a field of study concerned with the principles and processes governing the geographic distributions of genealogical lineages, especially those within and among closely related species." (Avise 2000).

Phylogeography is considered as a subdiscipline of biogeography, bridging the gap between microevolutionary and macroevolutionary disciplines, and it is used to infer historical (evolutionary) patterns, gene flow, colonisation and genetic bottlenecks among populations within and between species, and to delimit species boundaries and define conservation units (Domínguez-Domínguez and Vázquez-Domínguez 2009). It is an integrative field of evolutionary biology because it exploits very different scientific disciplines such as molecular biology, population genetics, geographical information systems, geology, taxonomy and systematics, conservation biology, ecology, etc.

Traditionally, the topology of the phylogenetic trees, the geographic distribution of lineages and the estimated dates of branching events of the trees were used to provide a direct qualitative interpretation of the demographic history of the taxa under study (Hickerson et al. 2010). The favoured statistics were based on the hierarchically partitioned Wright's F statistics (Wright 1969) and Nei's summary statistics (Nei and Li 1979, Nei 1987). Since then, the field of phylogeography has gone through a methodological and philosophical transformation in how the genetic data are used to infer the demography. The breakthrough was the shift to the use of genealogy samplers such as the coalescent to derive parameter estimates.

The coalescent, or simply coalescence, is the retrospective process in which genes from the present merge into their common ancestor going back in time, and it is represented as a gene genealogy of a sample of individuals taken from a population (Knowles 2009). The gene genealogy can be modelled using a priori information, or knowledge of the biological system under study, or it can be modelled using a variety of possible demographies. When using different models to infer population demographic history, no competing model is true, but it is instead a probabilistic approximation to a particular demographic history that explains better the observed patterns of the gene genealogies (Hickerson et al. 2010). The use of statistical approaches based on coalescent models that take into account the stochasticity of genetic processes for parameter estimation and hypothesis testing is termed statistical phylogeography (Knowles and Maddison 2002).

The marker of choice for microevolutionary phylogenetic inference since the development of phylogeography has been the mitochondrial (mt) DNA because of its rapid sequence evolution (Avice 2000). However, there has also been a shift towards the use of multilocus data in statistical phylogeography to provide a more robust basis for statistical inference (Knowles 2009), usually incorporating nuclear genes or strictly paternally non-recombining inherited molecular markers, such as Y-chromosome introns (Hellborg and Ellegren 2003). The mitochondrion is an intracellular organelle that has its own genome, and it can move, divide and fuse within a cell. The genome consists of 15,000 – 17,000 bp of a double stranded and circular DNA molecule that encodes 37 genes. Twenty-four genes encode the translational molecules for the mtDNA (22 transfer RNAs and two ribosomal RNAs) and 13 genes encode subunits of the electron transfer chain involved in cellular respiration and ATP production (Ballard and Whitlock 2004). The mtDNA is characterized by the lack of recombination, asexual inheritance and almost strictly maternal mode of inheritance (no heteroplasmy, although there are a few

exceptions), exists in high number of copies per cell and has extensive intraspecific polymorphism, all of which are useful for estimating population demographic parameters (Avise 2000). Within the mtDNA, the cytochrome (cyt) *b* gene has been the marker of choice for phylogeographic studies of recently separated mammalian taxa because of its moderate substitution rate, compared to the hypervariable mtDNA control region, for example, and because its levels of genetic divergence are in the phylogenetically informative range without saturation effects (Johns and Avise 1998). The cyt *b* is the central catalytic subunit of the ubiquinol cytochrome *c* reductase complex and encodes a transmembrane enzymatic protein subunit involved in the electron transfer of the cellular respiratory chain of all eukaryotic organisms (Esposti et al. 1993).

1.6 Geometric morphometrics defined

Morphometrics, considered as a subfield of statistics or a branch of mathematical shape analysis, is an old discipline etymologically defined as the measurement of shape (Mitteroecker and Gunz 2009). The objective of morphometrics is to characterize, analyze and compare biological forms quantitatively. Traditionally, the measurements that needed to be taken from an object to describe its shape were the length, depth and width, but more recently the field of morphometrics experienced a 'revolution' by the invention of coordinate-based methods, the development of the statistical theory of shape and the use of transformation grids to visualize shape variation (Rohlf and Marcus 1993, Adams et al. 2004, Mitteroecker and Gunz 2009). This new morphometrics approach was termed 'geometric morphometrics' because it preserves the geometry of the landmark coordinates throughout the analysis. Geometric morphometric methods give a precise and accurate description of shape variation, and a better

visualization, interpretation and communication of the results in comparison to traditional morphometrics (Zelditch et al. 2004).

Under the statistical theory of shape, any object has a form that is composed of shape and size. Shape is mathematically defined as all the information that is independent of the object's size, position and orientation, while size is the scale of the object, and it can be measured by any interlandmark distance or by a series of single size measures (Mitteroecker and Gunz 2009). Size measurements and the analysis of shape variation depend on the selection of landmarks, which are defined as discrete anatomical points present in all the specimens in the study, i.e., biological homologous anatomical loci that must be represented on each object and must exist between and within populations (Dryden and Mardia 1998). Landmarks contain the information about their relative position in their Cartesian coordinates and simple algebraic manipulations can separate that information into independent statistically uncorrelated components of size and shape; that information can then be used as variables for statistical analysis (Zelditch et al. 2004).

1.7 Aims

In this study, two different techniques and areas of scientific research are to be implemented for the understanding of the genetic and morphological diversity of *S. minutus*. First, a phylogeographical approach will help understand several aspects of the past and current distribution of the genetic lineages. Second, a geometric morphometrics approach will examine the morphological variation within and among the genetic lineages. The use of both approaches can give very powerful insights regarding the evolutionary history of this small mammal. The knowledge acquired through this project will be a significant piece of the puzzle for the understanding of the recent evolutionary history of European small mammals.

The general aims of this study are:

- To estimate the phylogeographic structure (i.e., the geographical distribution of genealogical lineages) of the Eurasian pygmy shrew *Sorex minutus* using different molecular markers. Where different lineages are found, to estimate the genetic diversity and structure, time of divergence and historical demographic processes of those lineages.
- To determine the glacial refugia and colonisation routes for *S. minutus* in Europe using a more detailed study than previously, and compare the results with the phylogeographic paradigms of glacial refugia in the Southern Mediterranean peninsulas.
- To estimate the morphological variability of *S. minutus* in Europe using a geometric morphometrics approach and compare it with the phylogeographic structure. Where significant differences are found, to identify any geographical or genetic pattern to which it could be related.
- To explore the origin, colonisation routes, genetic diversity and structure, and morphological variation of *S. minutus* in the British Isles.

Chapter 2

Phylogeography of *Sorex minutus* in Europe

2.1 Introduction

It is widely recognized that the three Southern European peninsulas, namely the Iberian, Italian and Balkan (Fig. 1.1B), acted as Mediterranean glacial refugia for many temperate and warm-adapted species during the Quaternary ice ages (Hewitt 2000). Under this scenario, populations and species in the southern peninsulas remained isolated during cold stages by ice sheets covering most of the Alps and the Pyrenees and by unsuitable climatic conditions further north, which acted as geographical barriers to dispersal. Different genealogical lineages evolved in these refugial areas; thus, the Southern European peninsulas became current hotspots of intra-specific diversity (Bilton et al. 1998, Hewitt 2000, Myers et al. 2000, Petit et al. 2003). As glaciers retreated and suitable habitat became available, it is also posited that populations at the northern limits of the southern refugia expanded and colonised territories further north, but with subsequent loss of alleles and heterozygosity because of founder events at the leading edge, whereas populations in the south maintained higher genetic diversity (Hewitt 1996).

The concept of glacial refugia has been mostly applied to the isolation and differentiation of species and/or populations in Mediterranean peninsulas during cold phases of the Quaternary, with glaciations as the major force shaping population divergence in allopatry (Stewart et al. 2010). However, it has been shown that this biogeographic pattern is further complicated by the existence of cryptic northern glacial refugia, further north than the traditionally recognized southern refugia. There is palaeontological, palynological, phylogeographic and species distribution modelling (SDM) evidence for some temperate and boreal species that support this hypothesis of 'northern refugia' (Bilton et al. 1998, Willis

and van Andel 2004, Kotlík et al. 2006, Magri et al. 2006, Sommer and Nadachowski 2006, Svenning et al. 2008, Fløjgaard et al. 2009, Vega et al. 2010b). Moreover, recent findings of intra-specific genetic and morphological differentiation within multiple micro-refugia in Iberia (Gómez and Lunt, 2007), Italy (Canestrelli et al. 2007, Canestrelli et al. 2008) and the Balkans (Kryštufek et al. 2007) add to the current understanding of the genetic diversification and biological diversity in southern refugia. Additionally, interglacial refugia, the reverse phenomenon of glacial refugia, have been hypothesised to explain the persistence of cold adapted species through interglacials (Hilbert et al. 2007). Hence, the term Quaternary refugia can be broadly defined as the geographical region that a species inhabits during periods of adverse climate (either glacial or interglacial) that represent the species' maximum contraction in geographical range (Stewart et al. 2010), highlighting the idea that different species can respond to climate change independently.

Previous phylogeographic studies on *Sorex minutus* using mitochondrial (mt) DNA and Y-chromosome introns revealed a genetic structure over Eurasia, with isolation and differentiation in different southern and northern refugia (Bilton et al. 1998, Mascheretti et al. 2003, McDevitt et al. 2010). Bilton et al. (1998) analysed a partial sequence of the cytochrome (cyt) *b* gene (581 bp) based on 14 individuals and found 13 haplotypes distributed in four clades: three geographically restricted lineages corresponding to 'Balkan', 'Central Italian' and 'Iberian' clades, and a 'major lineage' linking together individuals from Northern-Central Europe to Lake Baikal in Siberia, which gave support to the hypothesis of northern refugia. However, these authors used a restricted number of samples and did not cover the full extent of the geographical range of the species. In a more detailed study, Mascheretti et al. (2003) explored the colonisation of Ireland based on 74 specimens of *S. minutus* with 1110 bp of the cyt *b* gene. They recovered a similar

tree topology as previously, with a northern and three peninsular lineages, but also an 'Andorran-Irish' lineage, interpreted as evidence for human-mediated colonisation of Ireland from South-Western Europe. The sequence similarity between Ireland and the Pyrenees resembled a Lusitanian element, linking together several species from South-Western Ireland with Portugal and North-Western Spain (Corbet 1961, Yalden 1982). McDevitt et al. (2009, 2010) analysed a larger dataset of *S. minutus* using microsatellite, mitochondrial and Y-chromosomal molecular markers and found that the Irish populations were introduced most likely in the Neolithic period, had smaller genetic diversity than the British population and presented a signature of rapid population expansion in Ireland. They also found a similar tree topology with the mitochondrial Control Region as found previously with *cyt b*, showing Northern, Balkan, Iberian, Italian and Western (composed of Andorran-Irish-French) lineages, plus a single individual with distinct mitochondrial and Y-chromosome DNA from Southern Italy. Additionally, Vega et al. (2010a) showed that the South Italian pygmy shrew is genetically and morphologically different from populations in Central and Northern Italy and Europe, and Vega et al. (2010b) showed that the northern lineage has a strong signature of population expansion and it is genetically different from southern lineages, favouring the northern refugia hypothesis. However, more sampling in southern peninsulas and Northern-Central Europe is needed to rule out completely the hypothesis of southern peninsulas as source areas for the northern lineage, to estimate the amount of differentiation, colonisation routes and contact zones among them after the Last Glacial Maximum (LGM), to pinpoint the origin of Irish and British populations and to evaluate the demographic parameters within peninsulas and other lineages.

Here, I undertake a statistical phylogeographic approach to further this aim. In particular, I address the following specific study questions: 1) Does a more

detailed phylogeographic analysis, using more samples and molecular markers, detect the same genetic lineages that have been previously found? 2) Do different molecular markers recover the same phylogenetic tree topology or distinguish the same genetic lineages? 3) What is the geographic distribution of the genetic lineages of *S. minutus* within Europe, and are there areas of contact between the different lineages? 4) What is the genetic diversity within the lineages and are they significantly structured over Eurasia? 5) Is the South Italian pygmy shrew genetically distinctive from other Italian populations, as suggested by previous analyses? 6) What were the colonisation routes, times of divergence and historical demographies of the genetic lineages? 7) Do the genetic lineages show a signature of population expansion or have the populations remained constant through time? 8) Are the new data on the northern lineage still compatible with the northern refugia hypothesis? 9) Can the origin of the Irish and British populations be determined with more detailed sampling in continental Europe? To answer these questions I employ a substantial battery of software for the analysis of genetic variation and three molecular markers, the *cyt b* gene, two Y-chromosome introns and the nuclear BRCA1 gene, on a larger number of samples than previously.

The detailed study of phylogeography of *S. minutus* has broader significance. The nature of southern and northern glacial refugia has important implications for the understanding of their biogeographical roles as sources of genetic diversity, areas of speciation, identification of conservation units and preservation of species, and the results presented here should be put in the wider context of European biodiversity. Such information is relevant for understanding how species responded to past climate changes and may be useful to forecast how climate change may affect the current distribution of species, and contributes towards an emerging new synthesis of the full-glacial distributions of the European biota.

2.2 Materials and methods

2.2.1 Samples and GenBank sequences for molecular analysis

A total of 544 samples and sequences were obtained for the *cyt b* analysis (Appendix 3). Of that total, 236 *S. minutus* samples, plus two *S. volnuchini* samples used as an outgroup, were obtained from fieldwork, museum collections or were kindly provided by colleagues (this includes 78 *S. minutus* samples distributed among 68 haplotypes deposited in GenBank: GQ494305 – GQ494350, GQ272492 – GQ272518, Vega et al. 2010a, b). Three hundred and five *S. minutus cyt b* sequences were obtained from studies reported by other researchers, using haplotypes deposited in GenBank (AJ535393 – AJ535457, Mascheretti et al. 2003; AB175132 and AB175133, Ohdachi et al. 2006; FJ623774 – FJ623893, Searle et al. 2009), plus one *cyt b* sequence of *S. volnuchini* (AJ535458, Mascheretti et al. 2003).

A total of 127 sequences of DBY-7 and UTY-11 introns were obtained for the Y-chromosome analysis (Appendix 3). From the total, 71 DBY-7 and UTY-11 sequences were obtained from *S. minutus* samples from fieldwork, museum collections and provided by colleagues. This includes 11 sequences reported in Vega et al. (2010a) distributed among the following eight sequence variants deposited in GenBank (GQ272519 – GQ272521 for DBY-7 and GQ272522 – GQ272526 for UTY-11). Data on 55 sequences, plus one sequence of *S. volnuchini*, were obtained from McDevitt et al. (2010), using the following sequence variants recorded in GenBank: EU564415 – EU564422 for DBY-7 and EU564423 – EU564434 for UTY-11.

For the BRCA1 gene, 36 new sequences were obtained (Appendix 3), plus one sequence of *S. volnuchini* from GenBank which was used as outgroup (DQ630236, Dubey et al. 2007).

Fieldwork was done in several regions of Southern, Central and North-Western Italy, Northern Spain and Ireland to improve the sample size of previous studies and to cover sampling gaps in Europe. Tissue samples from the specimens collected were placed in 90% or 100% Ethanol until use, and whole body specimens were deposited at the National Museums of Scotland for long term storage. Tissue samples from museum specimens were obtained by toe clipping or by cutting a small piece of skin, to avoid damage to the specimen, or by removing residual desiccated brain tissue from skulls using a surgical curette.

2.2.2 DNA extraction, gel electrophoresis and visualization

Sorex minutus DNA was obtained from fresh and collection samples using the Blood and Tissue DNA Extraction Kit (Qiagen) following the protocols provided and stored at -20°C . Prior to extraction, fresh ethanol-preserved samples were dried at room temperature and digested at 56°C for ca. 5 h in the cell lysis solution with 20 mg/ml Proteinase K provided with the kit, while museum samples that might have been stored in Formalin were dried first and then digested overnight. To visualise the quality of the extracted DNA, 5 μl of sample mixed with 2 μl of Loading Buffer were run in a 1% Agarose 1X TAE (Tris base-Acetic acid-Ethylenediaminetetraacetic acid pH 8.0) buffer gel at 100 V for 35 min, next to a standard ladder containing known molecular weights for comparison. The gel was placed under UV light and photographed.

Good quality DNA, usually from fresh samples or well preserved specimens, appears in the Agarose gels as a single bright band of high molecular weight, evidence of no degradation and good extraction yields. Degraded DNA, on the other hand, appears as a smear of varying molecular weights. Old museum samples usually appear as a light smear of low molecular weight between 600 and 200 bp.

2.2.3 PCR amplification, purification and sequencing

Partial *cyt b* sequences from good quality DNA (obtained from fresh samples or well-preserved museum specimens) were obtained by the Polymerase Chain Reaction (PCR) using two primer (oligonucleotide) pairs that amplified ca. 700 bp of overlapping fragments. Partial *cyt b* sequences from samples with highly degraded DNA were obtained by PCR using a combination of five primer pairs that amplified an overlapping set of fragments of ca. 250 bp (Table 2.1).

Table 2.1. Primer sequences used in this study.

Sequence	Forward primer 5'-3'	Reverse primer 5'-3'	Approx. fragment length (bp)
<i>Cyt b</i>	GACAGGAAAAATCATCGTTG	GTAGTAGGGGTGGAAAGGAATT	700
<i>Cyt b</i>	GAGGACAAATGTCATTCTGAGGC	TTCATTACTGGTTTACAAGAC	700
<i>Cyt b</i>	GACAGGAAAAATCATCGTTG	CGACGTGAAGGAATAGACAGA	250
<i>Cyt b</i>	CCGAGACGTAAACTACGGATG	AGAAGCCCCCTCAGATTCAT	250
<i>Cyt b</i>	TTCTGAGGCGCAACAGTTATT	AATGAGGAGGAGCACTCCTAGA	250
<i>Cyt b</i>	CCTGTCTCAGACGCAGATA	GTTTGGAGGTGTGGAGGAAA	250
<i>Cyt b</i>	TCCCGAATAAACTAGGAGGTGT	TTCATTACTGGTTTACAAGAC	250
DBY-7 ¹	GGTCCAGGAGARGCTTTGAA	CAGCCAATTCTCTTGTTGGG	500
UTY-11 ¹	CATCAATTTTGTAYMAATCCAAAA	TGGTAGAGAAAAGTCCAAGA	1000
BRCA1 ²	TGAGAACAGCACTTTATTACTCAC	ATTCTAGTTCCATATTGCTTATACTG	750

¹Hellborg and Ellegren (2003).

²Dubey et al. (2006).

PCR amplification of *cyt b* was performed in a 50 µl final volume containing: 1X Buffer, 1 µM each primer, 1 µM dNTP's, 3 mM MgCl₂ and 0.5 U Platinum *Taq* Polymerase (Invitrogen), with cycling conditions: 94 °C for 4 min, 40 cycles at 94 °C for 30 s, 55 °C for 30 s and 72 °C for 45 s, and a final elongation step at 72 °C for 7 min, using a C1000 thermal cycler (BIO-RAD). Negative controls were included during the PCR amplification to check for contamination.

PCR amplification of the Y-chromosome introns was done using one primer pair for each intron, DBY-7f with DBY-7r and UTY-11f with UTY11r (Table 2.1,

Hellborg and Ellegren 2003), in a 25 µl final volume containing: 1X Buffer, 5 µM each primer, 2 µM dNTP's, 2.5 mM MgCl₂ and 0.25 U Platinum *Taq* Polymerase (Invitrogen), with cycling conditions: 95 °C for 10 min, 20 cycles of 95 °C for 30 s, touchdown temperatures from 65 – 55 °C (for UTY-11) or 55 – 45 °C (for DBY-7) for 60 s decreasing by 0.5 °C/cycle and 72 °C for 90 s, followed by 20 cycles of 95 °C for 30 s, 55 °C (for UTY-11) or 45 °C (for DBY-7) for 60 s and 72 °C for 90 s, and a final elongation step at 72 °C for 10 min (Hellborg and Ellegren 2003). Known female and male samples were used as controls, and negative controls were included in all PCRs for the Y-chromosome introns to check for contamination. The sequences of DBY-7 and UTY-11 introns were concatenated and analysed jointly.

Amplification of the BRCA1 nuclear gene was performed using the primer pair BRCA1f and BRCA1r (Table 2.1, Dubey et al. 2006) in a 50 µl final volume containing: 1X Buffer, 0.6 µM each primer, 1 µM dNTP's, 3 mM MgCl₂ and 0.5 U Platinum *Taq* Polymerase (Invitrogen), with cycling conditions: 94 °C for 4 min, 40 cycles at 94 °C for 60 s, 50 °C for 60 s and 72 °C for 120 s, and a final elongation step at 72 °C for 7 min (Dubey et al. 2006). Negative controls were included in all PCRs to check for contamination.

The purification of PCR products was done with a commercial kit (Qiagen). DNA was quantified by spectrophotometry in a NanoDrop 1000 (Thermo Scientific) at 260 nm and sequenced in an ABI 3730XL DNA Sequencer using Big Dye Terminator chemistry (Macrogen, Inc. and Cornell University Core Laboratories Center).

2.2.4 Analysis of sequence polymorphism

DNA sequences of *cyt b*, Y-chromosome introns and BRCA1 were edited in BioEdit version 7.0.9.0 (Hall 1999) and aligned using ClustalX version 2.0 (Larkin et al. 2007). The software DnaSP version 5.10 (Librado and Rozas 2009) was used to

calculate for all molecular markers: the number of monomorphic and polymorphic sites, sites with alignment gaps, the number of parsimony informative sites and singleton mutations, and the number of haplotypes or sequence variants within the sample; and for the *cyt b* data only: the haplotype frequency and the number of synonymous and non-synonymous substitutions in the codons using a conservative approach. The parsimony informative sites were counted as the number of sites where at least two types of nucleotides were found and were represented at least twice in the sample. The singleton mutations were counted as the number of sites where only one mutation was found in all the samples.

The neutral hypothesis for the *cyt b* gene was tested between *S. minutus* and the outgroup using the McDonald-Kreitman (MK) test (McDonald and Kreitman 1991), where the ratio of non-synonymous to synonymous fixed substitutions among populations should be the same as the ratio of non-synonymous to synonymous polymorphisms within populations if evolution of the protein coding gene occurs by neutral processes.

2.2.5 Phylogenetic analyses

The haplotypes and sequence variants found in *cyt b*, Y-chromosome introns and the BRCA1 gene datasets were used for the phylogenetic reconstructions. A phylogeny is a graphic representation of the evolutionary relationships among species or, in this case, among individuals of the same species.

The use of models of evolution, or models of nucleotide substitution, allows for different probabilities of change among nucleotides, and the failure to allow unequal substitution rates can lead to underestimates of the genetic distances between sequences and problems with long branch attraction (Waddell and Steel 1997). To identify the most appropriate substitution model for the molecular data

available, I used the software jModelTest version 0.1.1 (Posada 2008) that statistically selects the best-fit model with a hierarchical likelihood ratio test. I set a fixed tree with the BIONJ algorithm (a variation of the Neighbor-Joining method described below; Gascuel 1997) to estimate the branch lengths as model parameters, and used the Bayesian Information Criterion (BIC) value to select the best of 56 candidate models. The BIC selects the model with the maximum posterior probability when all models have the same prior.

The model of evolution that best fit the *cyt b* data was the General Time Reversible (GTR) with a gamma shape parameter (Γ) of 0.2720 and no specified proportion of invariable sites (I), base frequencies for A = 0.2819, C = 0.3062, T = 0.1318 and G = 0.2800, and six substitution types (A–C = 0.2384, A–G = 14.4125, A–T = 0.7193, C–G = 1.3882, C–T = 9.2882, G–T = 1.000). Similarly, the Akaike Information Criteria, with a weaker penalization for increased model complexity, suggested the GTR + Γ + I. The GTR model is a distance calculation method that gives the expected average number of substitutions per site by comparing all pairs of sequences (Lanave et al. 1984, Waddell and Steel 1997). It allows unequal substitution rates across sites because of invariable sites, incapable of changing due to biological constraints (Waddell and Steel 1997), and accommodates rate heterogeneity among codon positions by fitting a gamma distribution (i.e., a probability model) with an alpha shape parameter which is inversely correlated with increasing rate heterogeneity (Xia 1998).

For the concatenated Y-chromosome introns, the best fit model was the Hasegawa-Kishino-Yano (HKY, Hasegawa et al. 1985) with no specified proportion of invariable sites, no gamma correction, equal rates for all sites, a transition/transversion ratio = 1.6681 and nucleotide frequencies of A = 0.2832, C = 0.1904, G = 0.1969 and T = 0.3295. For the BRCA1 gene, the model selected was again the HKY, with no gamma correction and equal rates for all sites, a

transition/transversion ratio = 12.1998 and nucleotide frequencies of A = 0.3825, C = 0.1749, G = 0.2130 and T = 0.2296. The HKY model allows for a different transition/transversion ratio and unequal base frequencies, and is a generalization of simpler models of evolution (Felsenstein 2004).

The phylogenetic relationships among *cyt b* haplotypes and among nuclear markers sequence variants were inferred with a variety of traditional phylogenetic methods, including Neighbor-Joining (NJ), Maximum Parsimony (MP) and Maximum Likelihood (ML). I used PAUP* version 4.0b10 (Swofford 2000) complemented with PAUPUp version 1.0.3.1 (by F Calendini and J-F Martin, available at <http://www.agro-montpellier.fr/sppe/Recherche/JFM/PaupUp/main.htm>) to infer NJ trees with the BIONJ method (described below; Gascuel 1997) and the appropriate evolutionary model, and MP trees with a heuristic search with simple stepwise addition of taxa, branch swapping (tree bisection reconnection, one million rearrangements) and 100 random replicates. ML trees were inferred with RAxML version 7.0.4 software (available at <http://www.phylo.org/news/RAxML>; Stamatakis 2006) using the appropriate evolutionary model.

In brief, NJ is a fast distance clustering method that does not assume a molecular clock and it is based on the principle of minimum evolution, where the sum of the branch lengths is minimized (Felsenstein 2004). NJ uses an agglomerative algorithm that chooses two sequences iteratively, creates a new node that represents the cluster of the two sequences and reduces the distance matrix by replacing the two sequences by this node, and repeats the operation until all sequences are chosen. The BIONJ method is a variant of the NJ method where the variances and co-variances of the evolutionary distances of the distance matrices are reduced (Gascuel 1997). MP reconstructs a phylogeny with the fewest evolutionary events possible, and searches among all possible phylogenies for the one that minimizes the number of evolutionary events making use of the parsimony

informative sites (Felsenstein 2004). This method does not take into account the substitution rate among nucleotides and it uses parsimony as its evolutionary model. ML is a method for the statistical estimation of phylogenies that evaluates different hypotheses of evolutionary history (i.e., phylogenies or trees) in terms of probability of the observed data given a certain evolution model, taking into account the substitution rates among nucleotides, where the phylogeny with the highest probability (or maximum likelihood) of reaching the observed data is preferred over the others (Felsenstein 2004).

Statistical support for the phylogenetic relationships was assessed by 10,000 bootstrap replicates for NJ and 1000 bootstrap replicates for MP and ML. The bootstrap involves resampling from the nucleotide site data with replacement to assess the uncertainty of the estimated phylogeny. With this method, sites are drawn independently from the aligned full dataset, replaced and resampled until a new dummy dataset with the same number of sites is created from which a new tree can be built, and the process is repeated several times. Then, the topology (i.e., the branching pattern) of the generated trees is compared and a proportion value is given to all the branches (Felsenstein 2004); if a branching pattern is found several times in the bootstrap replicates, that branch will have a high proportional value and higher certainty.

Additionally, a Bayesian analysis (BA) for phylogenies was performed in MrBayes version 3.1 (Huelsenbeck and Ronquist 2001) using the appropriate evolutionary model. BA is similar to likelihood methods, but makes use of prior information of the quantities being inferred and implements a Markov Chain Monte Carlo (MCMC) method using the Metropolis-Hastings algorithm (Metropolis et al. 1953, Hastings 1970). The MCMC is run for several thousand generations (or cycles) to approximate the highest probability of the data, where the first tree is stochastically perturbed and the new tree is either accepted or rejected based on

the ratio of probabilities of the new and previous trees (Huelsenbeck et al. 2001). The acceptance ratio between trees is calculated using the prior probabilities of the new and previous trees, multiplied by the likelihood ratio (Felsenstein 2004). Then, after several generations, the acceptance ratio reaches an equilibrium distribution where the probability of accepting a new tree is smaller than the probability of accepting the previous tree (Felsenstein 2004). All the proposed trees before this equilibrium can be discarded as a “burn-in” and trees can be recorded every several steps during the equilibrium phase. The MCMC in BA draws a random sample from the posterior distribution of trees after burn-in and, with enough samples, it is possible to give a probability value to the branches within a tree (Felsenstein 2004), named as posterior probability.

For the BA of *cyt b* data, two runs were performed with 10 million generations, a sampling frequency every 1000 generations (to give a total of 10,000 samples for each run), a temperature of 0.01 for four heated chains, six rate parameters (equivalent to the GTR model) and checked for convergence with the program Tracer version 1.4.1 (Drummond and Rambaut 2007, available at <http://beast.bio.ed.ac.uk/Tracer>). Trees were summarised after a burn-in value of 2500 to obtain the posterior probabilities of each phylogenetic split with a 50% majority rule consensus. For nuclear genes and Y-chromosome introns I used similar settings, but changed the temperature to 0.1 and the number of rate parameters to two (equivalent to the HKY model).

To complement the tree-generating programs, a phylogenetic network was constructed only for the *cyt b* data using the software Network version 4.5.1.0 (Fluxus-Engineering) with a Median-Joining (MJ) algorithm and a ‘greedy’ method (Foulds et al. 1979, Bandelt et al. 1999). The phylogenetic MJ network first creates a minimum spanning network, which is a network with the least number of steps, without reticulations (loops or cycles) among sequences and without inferring

additional sequences, so that the total distance is kept minimal or parsimonious. Then, it adds triplets of closely related sequences connecting them to the minimum spanning network by median vectors (hypothetical nodes) in a 'greedy' manner, where the least number of median vectors is added only if they result in branching nodes (Bandelt et al. 1999).

Phylogenetic networks provide an explicit graphic representation of the evolutionary history between sequences in which taxa are represented as nodes and their evolutionary relationships are represented by edges. The most internal nodes represent ancestral states from which more recent and peripheral nodes derive (Avice 2000). Also, networks have the advantages of representing non-hierarchical evolutionary relationships as multifurcations and loops, being able to work with very few mutations, extant ancestral nodes among haplotypes and large sample sizes, typical characteristics of intraspecific data (Posada and Crandall 2001).

2.2.6 Analysis of sequence diversity

Nucleotide diversity for all sequence sets (*cyt b*, Y-chromosome introns and BRCA1 gene) and haplotype diversity for the *cyt b* dataset only were calculated using DnaSP. Nucleotide diversity (π) was calculated as the average number of nucleotide substitutions per site between two sequences (Lynch and Crease 1990), but using the Jukes-Cantor correction (Jukes and Cantor 1969) performed in each pairwise comparison. Haplotype (gene) diversity (H_d) was calculated as the frequency of the haplotype in the population, but using the total number of samples, not twice as much (Nei 1987, equation 8.5) because *cyt b* is a haploid (mitochondrial) gene.

2.2.7 Divergence and genetic structure of populations

The amount of divergence and genetic structure was estimated for the phylogenetically coherent groups detected by the *cyt b* phylogenetic analysis and for the geographically delimited group of samples. These groups included the full monophyletic dataset (excluding the outgroup), the phylogroups detected by the phylogenetic methods (including the outgroup as another phylogroup), and continental and island samples. I decided to analyse the samples by phylogroups because I cannot delimit “true” populations based solely on the geographical locations from where the samples were obtained, at least in continental Europe where the distribution of *S. minutus* is continuous. In contrast, island and full continental samples of the phylogroups can be easily distinguished and were analysed separately.

The average number of nucleotide substitutions (D_{xy}) between two populations (x and y) was calculated using the average number of nucleotide substitutions among all pairs of haplotypes from each population (Nei 1987, equations 10.19 and 10.20). D_{xy} was used to calculate D_a , the net number of nucleotide substitutions between two populations (Nei 1987, equation 10.21). The matrix of D_a values, which represent the proportional sequence divergence among populations, was used to construct a NJ tree to depict the evolutionary distances between phylogroups. D_a was corrected subtracting the average nucleotide diversity of each population from D_{xy} , being the corrected $D_a = D_{xy} - (D_x + D_y) / 2$ (Nei 1987, equation 10.23), where D_x and D_y are the average nucleotide diversity within each population (π).

The time of divergence between the phylogroups (or groups of samples) was calculated as $T = D_a / 2\mu$ (Nei 1987, equation 10.22), where μ is the nucleotide substitution rate per site per year (using the standard mammal substitution rate of 2% per million years averaged over the whole mtDNA molecule, Wilson et al. 1985)

and D_a is the corrected net number of nucleotide substitutions between two populations. The corrected D_a values were used because the average time since divergence between haplotypes from two populations is longer than the time of population split, and for recently diverged populations there is a risk of overestimating the divergence time (Edwards 1997). The variance of D_a was obtained with DnaSP and used to calculate the standard deviation (SD) for the estimated values of time of divergence between populations.

The geographic midpoints (mid-geographic location between two or more coordinates) for the phylogroups using the samples' coordinates were calculated with the Geographic Midpoint Calculator (available at <http://www.geomidpoint.com/>). The geographic midpoints were used to obtain the pairwise geographic distances among phylogroups with the Geographic Distance Matrix Calculator version 1.2.3 (by PJ Ersts, available at http://biodiversityinformatics.amnh.org/open_source/gdmq). A Mantel test was performed in Arlequin version 3.1 (Excoffier et al. 2005) to test the significance of the correlation between the pairwise D_a or Wright's F_{ST} genetic structure values (Wright 1969) with the pairwise geographic distances among phylogroups. The significance was obtained through a permutation procedure used to create an empirical null distribution (100,000 permutations).

The genetic structure of populations, including the global and phylogroup specific genetic differentiation (F_{ST}) values, pairwise F_{ST} among phylogroups and Analysis of Molecular Variance (AMOVA), was estimated using the software Arlequin. Phylogroup specific F_{ST} indices were calculated as a weighted value of the global population differentiation, which represent the degree of evolution from the ancestral population and are provided as a measure of the contribution of each phylogroup to the global F_{ST} . Pairwise F_{ST} among phylogroups, given as a matrix, were calculated as a measure of the degree of genetic differentiation or distance

(Slatkin 1995). The significance values of genetic differentiation were calculated using a non-parametric approach (Excoffier et al. 1992) obtaining a null distribution while permuting haplotypes between populations (10,000 permutations), with p values showing the proportion of permutations giving F_{ST} values larger or equal than the observed ones. The AMOVA follows a similar implementation of the analysis of variance in traditional statistics, but transformed into a hierarchical analysis of molecular data (Weir and Cockerham 1984). The total variance was partitioned into covariance components within the global sample and among phylogroups, and used to compute fixation indices in terms of coalescent times (Slatkin 1995). The significance of the AMOVA was calculated using a non-parametric approach (Excoffier et al. 1992) obtaining a null distribution while permuting haplotypes among phylogroups (10,000 permutations).

The nuclear marker data (Y-chromosome introns and the BRCA1 gene) were not used to estimate genetic divergence and structure among populations because of the low number of informative sites and lack of variation in comparison to the mitochondrial data.

2.2.8 Estimation of historical demographic parameters

Mismatch distributions were obtained with DnaSP for the full *cyt b* dataset and for the main phylogroups computing the distribution of the number of observed pairwise differences among haplotypes and plotting it against their frequency. The mismatch distribution travels as a wave through the horizontal axis, with its crest at an estimated value of $\tau = 2uT$, where the value T corresponds to the time of population expansion in $\frac{1}{2}u$ generations and u is the mutation rate per sequence (Rogers and Harpending 1992, Rogers 1995). Moreover, the mismatch distribution is unimodal for populations that have been under a sudden expansion, but multimodal for populations with constant population size or demographic equilibrium

(Rogers and Harpending 1992, Slatkin and Hudson 1991). I calculated with DnaSP the theoretical mismatch distribution for a population expansion that would best fit the observed data by implementing a nonlinear least squared approach assuming no recombination, an infinite-sites model (only useful for short periods of time) and that the population size after the expansion is infinite (only reasonable if the population expansion is large) (Rogers and Harpending 1992).

I performed four different tests to verify the hypothesis of sudden population expansion for the full dataset, phylogroups, and continental and island samples. The first method, Tajima's D statistic, tests the null hypothesis that the average number of pairwise nucleotide differences and number of segregating sites in the sample are equal (Tajima 1989). This method explicitly tests for selective neutrality and it is based on an infinite-sites model assuming no recombination; however, significant values can also be related to factors other than selection such as bottlenecks, population expansions or heterogeneity of mutation rates (Tajima 1989). The second method, Fu's F_s statistic, is also a selective neutrality test based on the infinite-sites model, assumes no recombination and tests the probability of having no fewer haplotypes than the observed number in the sample (Fu 1997). This statistic tends to be negative if there is an excess of recent mutations and small pairwise differences among haplotypes (Fu 1997). The third test, Ramos-Onsins and Rozas's R_2 statistic (Ramos-Onsins and Rozas 2002), is based on the difference between the number of singleton mutations and the average number of nucleotide differences, where lower R_2 values are expected under a population expansion scenario. Coalescent computer simulations were performed in DnaSP to provide confidence intervals and significant values for Tajima's D, Fu's F_s and R_2 statistics based on parametric bootstrapping (10,000 replicates). In the fourth method, the occurrence of population expansion was tested using the sum of square deviations between the observed and expected mismatch distributions under

a sudden population expansion model using parametric bootstrapping (10,000 replicates), as implemented in Arlequin. However, Fu's F_s and R_2 have been shown to be the most powerful statistics for detecting population growth (Ramos-Onsins and Rozas 2002).

Using the mismatch distributions, the parameters of a sudden population expansion and values of τ were calculated for the full dataset and all phylogroups with a unimodal distribution. The time of expansion T for the full dataset and phylogroups with a unimodal mismatch distribution was calculated by estimating T from the equation above, being $T = \tau / 2u$, where $u = 2\mu k$, μ is the mutation rate per nucleotide (assuming a mutation rate per nucleotide of 2% per million years, Wilson et al. 1985) per generation (considering one generation per year for *S. minutus*) and k is the number of nucleotide sites (1110 bp for cyt *b* data) (Rogers 1995). It has been shown that this method underestimates τ and the age of the population expansion because it does not consider mutation rate heterogeneity and uses an unrealistic infinite-sites model (Schneider and Excoffier 1999). Moreover, the assumption of a molecular clock is often invalid, and the use of a phylogenetic rate (an estimate of evolutionary rate calculated by comparing interspecific molecular sequence data) instead of a pedigree rate for intraspecific studies and the time dependency of molecular rates (exponential decay of substitution rate with time) may result in an overestimation of divergence times and population expansion events (Ho et al. 2005, Ho and Larson 2006, but see also Bandelt 2008). Therefore, I also estimated the values of τ and parameters of population expansion using a generalized non-linear least-squares approach with Arlequin, which takes into account possible heterogeneity of mutation rates and obtains confidence intervals using a parametric bootstrap approach (10,000 replicates) (Schneider and Excoffier 1999).

The use of Bayesian analysis with a relaxed clock model that does not assume a molecular clock and allows for rate heterogeneity can estimate divergence events more accurately. I calculated the Time of divergence from the Most Recent Common Ancestor (TMRCA) for the full *cyt b* dataset using BEAST version 1.5.2 (Drummond and Rambaut 2007) which does a BA using an MCMC algorithm (the input file was created in BEAUti version 1.5.2 included with BEAST). Several short runs were conducted to check the behaviour of the program with the *S. minutus* dataset. Parameters for the final MCMC run reported here were as follows: one run of 50 million generations sampling every 1000 generations (50,000 samples), a prior assumption that the population has remained constant, a random starting tree, a monophyletic group including all *S. minutus* data (without the outgroup), a fossil calibration of 5 MYA (SD = 0.2) with a normal prior distribution, an uncorrelated relaxed clock model (Drummond et al. 2006) to calculate the evolutionary rate, and an GTR substitution model. The trace files were analysed in Tracer version 1.5 and the tree information was summarized using TreeAnnotator version 1.5.2 with a burn-in of 30,000 (20,000 trees summarized) (all software included with BEAST). However, intraspecific data evolve at genealogical scales and the inappropriate use of deep fossil calibration points that reflect phylogenetic time-scales can lead to misleading, usually overestimated, divergence times (Ho et al. 2008).

Additionally, Bayesian Skyline Plots (BSPs) were calculated for some lineages (those with > 20 samples) and continental groups using BEAST. The BSP estimates the posterior distribution of effective population size through time from a sample of gene sequences, given a specified evolution model, using a standard MCMC (Drummond et al. 2005). The analyses for each lineage were run for at least 60 million generations, sampling every 1000, using a piecewise linear BSP model (which assumes that effective population size is constant between coalescent

events but may change at different coalescent event times) with the appropriate evolutionary model (estimated with jModelTest), adjusting the operators and visualizing the results in Tracer. The 95% Highest Posterior Density (HPD) was included in the TMRCA and BSPs estimations.

The nuclear marker data (Y-chromosome introns and BRCA1 gene) were not used to estimate historical demographic parameters of populations because of the low number of informative sites and lack of variation in comparison to the mitochondrial data.

2.3 Results

2.3.1 Sequence polymorphism

The *cyt b* was the most informative of the markers analysed in this study, while the concatenated Y-chromosome introns showed more variation than the autosomal nuclear gene, BRCA1, which was the least informative.

A partial sequence of 1110 bp for the *cyt b* gene was obtained. I found 319 *S. minutus* haplotypes in the 541 sequences analysed (plus 3 haplotypes of *S. volnuchini*), from which 286 have been described in previous studies and 33 are newly described here (Appendix 3). The full dataset presented a total of 412 mutations, 736 invariable sites and 374 polymorphic sites, from which 266 were parsimony informative and 108 were singleton mutations. There were 277 synonymous and 67 non-synonymous changes for the full sample (while excluding the outgroup). No internal stop codons were found and there were no insertion/deletions that could change the reading frame of the gene, enough evidence to presume that the sequences obtained were not pseudogenes.

The MK test was not significant between *S. minutus* and the outgroup ($G = 1.0290$, $p = 0.3103$); therefore, I assumed that the *cyt b* gene is selectively neutral

for *S. minutus*, and that the genetic structure observed here was the result of demographic and historical processes.

For the Y-chromosome introns, I obtained a concatenated sequence of 1143 bp. There were only 26 variants in the 127 sequences analysed (including the outgroup), but there were only 21 variants when not considering the sites with alignment gaps (Appendix 3). Six sequence variants are newly described in this study. There were 30 sites with alignment gaps, most present in a single intronic region in two samples from Austria (AUT1 and ATDo1611), 1078 invariant sites and 35 polymorphic sites, from which 23 were parsimony informative and 12 were singleton mutations.

The sequence length of the partial BRCA1 autosomal gene was 750 bp. In the 37 sequenced samples (Appendix 3), there were 27 sequences with no ambiguous nucleotide sites, nine sequences with one ambiguous nucleotide site and one sequence with two ambiguous nucleotide sites. The ambiguous nucleotide sites were interpreted as heterozygous individuals. Each homozygous individual contributes one haplotype, each heterozygous individual contributes two haplotypes, and the individual with two ambiguous nucleotide sites contributes four haplotypes because I cannot determine the phase. This gave a total of 14 different haplotypes, characterized by 11 polymorphic sites, only 6 of which were parsimony informative, and there were four synonymous and seven non-synonymous substitutions.

2.3.2 Phylogenetic analyses

The molecular markers used in this study had different degrees of sequence information and gave different phylogenetic resolutions of the tree topologies. The phylogenetic methods (NJ, MP, ML and BA) were consistent, because they produced similar trees for each molecular marker. *Sorex minutus* formed a separate

monophyletic clade from *S. volnuchini* with any molecular marker and phylogenetic method, as expected. When considering the main branches only, the phylogenetic methods produced comparable, but not identical, tree topologies between *cyt b* and Y-chromosome introns, but the BRCA1 gene data was poorly informative and did not resolve a similar topology. The lack of a strong phylogeographic structure with nuclear markers does not contradict the mitochondrial findings, but show that the selected Y-chromosome introns and nuclear gene are not adequate for these kinds of intraspecific studies because of the very low genetic variation that they contain.

With the *cyt b* data, the phylogenetic reconstructions showed similar tree topologies and phylogroups as previously found with a more restricted number of samples (Bilton et al. 1998, Mascheretti et al. 2003) and another mitochondrial marker (McDevitt et al. 2010). This means that the *cyt b* gene contains a strong evolutionary signature that supports several distinct phylogenetic lineages. For this marker, I defined the ingroup (composed of all the *S. minutus* samples) as the 'Eurasian' clade, within which I detected several other well supported branches that corresponded to distinct phylogenetic groups or 'phylogroups'. I defined these phylogroups by the geographical origin of the samples as follows (Fig. 2.1, Fig. 2.2, and see Appendix 3 for the allocation of samples into phylogroups): 1) 'North-Central European', the most widespread phylogroup; it included samples from Central France and Britain, extended across Central and Northern Europe to Lake Baikal, Siberia, but did not include samples from Southern Europe. 2) 'North-Central Italian', this lineage was mostly restricted to the Italian peninsula; it included samples from the Apennines and the Alps in Italy, but also from Switzerland, Slovenia, Southern and Eastern France near the border with Italy, Czech Republic and one distant sample from Germany. 3) 'Pyrenean', with a widespread geographic distribution; it included samples from the Pyrenees in Southern France and Andorra, and from the Pyrenean and Cantabrian Mountains in Northern Spain, but also

samples from Western France, Ireland, the Orkney islands, several islands on the western coast of Britain and a few samples from the British mainland. 4) 'South Italian', geographically restricted to La Sila, Calabria in Southern Italy (four samples) and also distinguished with the Y-chromosome introns and BRCA1 gene datasets. 5) 'Iberian', geographically restricted to the Iberian peninsula; it included samples from Rascafría, Central Spain (Sierra de Guadarrama) and Picos de Europa, Northern Spain. 6) 'Balkan', that included samples from the Balkan peninsula, belonging to the European part of Turkey, Serbia, Montenegro, Macedonia and Bosnia Herzegovina, and samples from further north in Slovakia, Czech Republic, Austria and Switzerland; a similar lineage was found with the nuclear markers. There was a basal polytomy including the clade containing the 'Pyrenean', 'South Italian' and 'North-Central Italian' phylogroups, and the 'Balkan' and 'Iberian' phylogroups, and low bootstrap support for the clade containing those lineages.

Besides the previously defined main phylogroups, I also created the 'continental Eurasian', 'continental North-Central European' and 'continental Pyrenean' phylogroups extracting the island samples from the Eurasian, North-Central European and Pyrenean phylogroups, respectively. Also, within the North-Central European phylogroup I distinguished a phylogroup from 'Britain' (Fig. 2.2) composed of samples from England, Scotland and Wales, and islands off the coast of mainland Britain (excluding the Orkney islands and other island samples that belonged to the Pyrenean phylogroup). Within the Pyrenean phylogroup I distinguished three island groups based on geographical isolation and proximity (Fig. 2.2): the 'Ireland' phylogroup (a monophyletic clade), the 'Orkney' group (a genetically heterogeneous group of samples composed of Mainland Orkney, South Ronaldsay and Westray), and a 'Celtic fringe' group (composed of samples from islands off the coast of Western Britain and a small number of samples from mainland Britain that did not cluster with the North-Central European phylogroup;

Searle et al. 2009). These continental and island samples were analysed as separate groups because there could be a noticeable effect of the island samples on the estimation of some phylogeographic results.

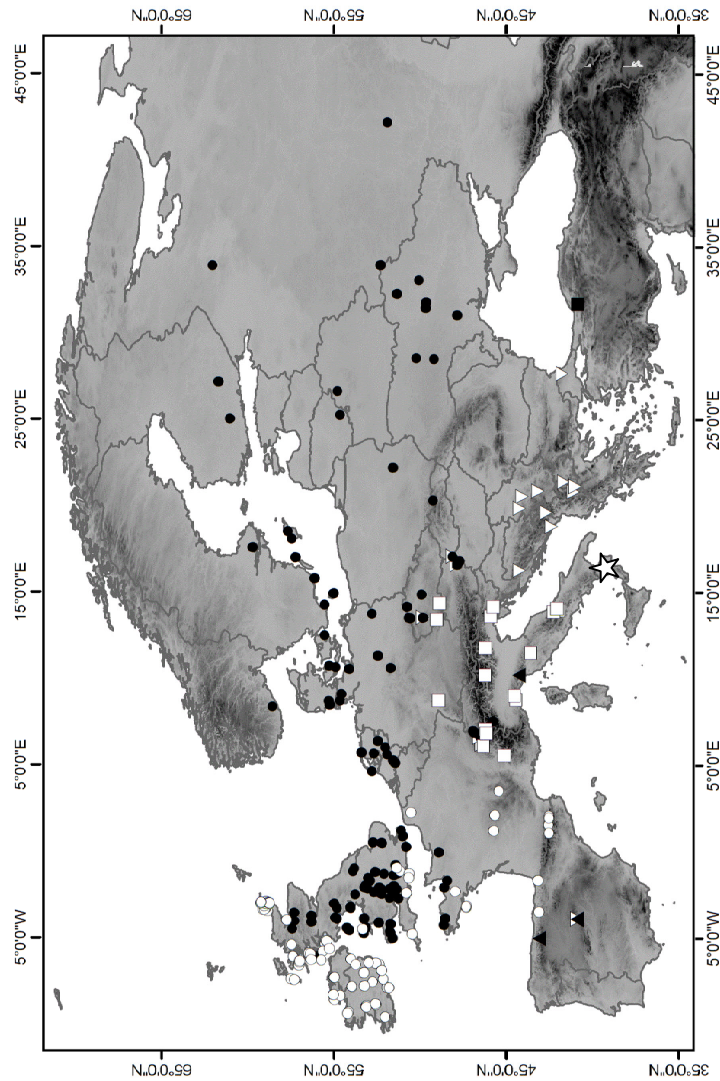


Figure 2.1. Sample localities of *Sorex minutus* from Europe divided into cytochrome *b* phylogroups: ● North-Central European (three Russian samples from Siberia are not shown in map), ○ Pyrenean, ☆ South Italian, □ North-Central Italian, ▽ Balkan and ▲ Iberian; ■ *S. volnuchini* (outgroup). Relief illustrated in grey tones.

The MJ network also resolved six main phylogroups separated by several mutational steps (Fig. 2.3A). The Iberian, Pyrenean, Balkan and Northern-Central European groups were separated by >10 mutational steps and *S. volnuchini* samples were distantly connected to the Eurasian clade through the North-Central European phylogroup (44 steps).

The North-Central European phylogroup had a star-like pattern with three central haplotypes from where all other haplotypes derived (Fig. 2.3B): the most internal one ('A') was a haplotype with one sample from Central Ukraine (UATi0266), connected by one mutational step to the second central haplotype ('B') formed by two samples from the Netherlands (NLBo0001 and NLZV0044), which was connected by one mutational step to the third central haplotype ('C') formed by four samples from Britain (GBAn0042, GBD0459, GBKk0100 and GBNo0002) plus three sequences from the Netherlands (NLDi0001, NLFr0017 and NLFr0040). There was an apparent geographical subdivision within this North-Central European sub-network, where samples from Siberia, Eastern and Northern Europe were derived or most closely connected to 'A', samples from Central Europe were derived or most closely connected to 'B', and all samples from Britain were derived or most closely connected to 'C', than to the other central haplotypes. However, this geographical subdivision was weak because there were several loops among the three central haplotypes in the inner part of the North-Central European network, and only the British and Dutch samples that connected to the central haplotype 'C' formed a well supported group in the phylogenetic analyses. Loops in the networks represent alternative, equally parsimonious explanations of the relationships among haplotypes. Moreover, there were some highly divergent sequences from Russia (Lake Baikal in Siberia), Poland and Ukraine with more than 8 nucleotide differences separating them from 'A'.

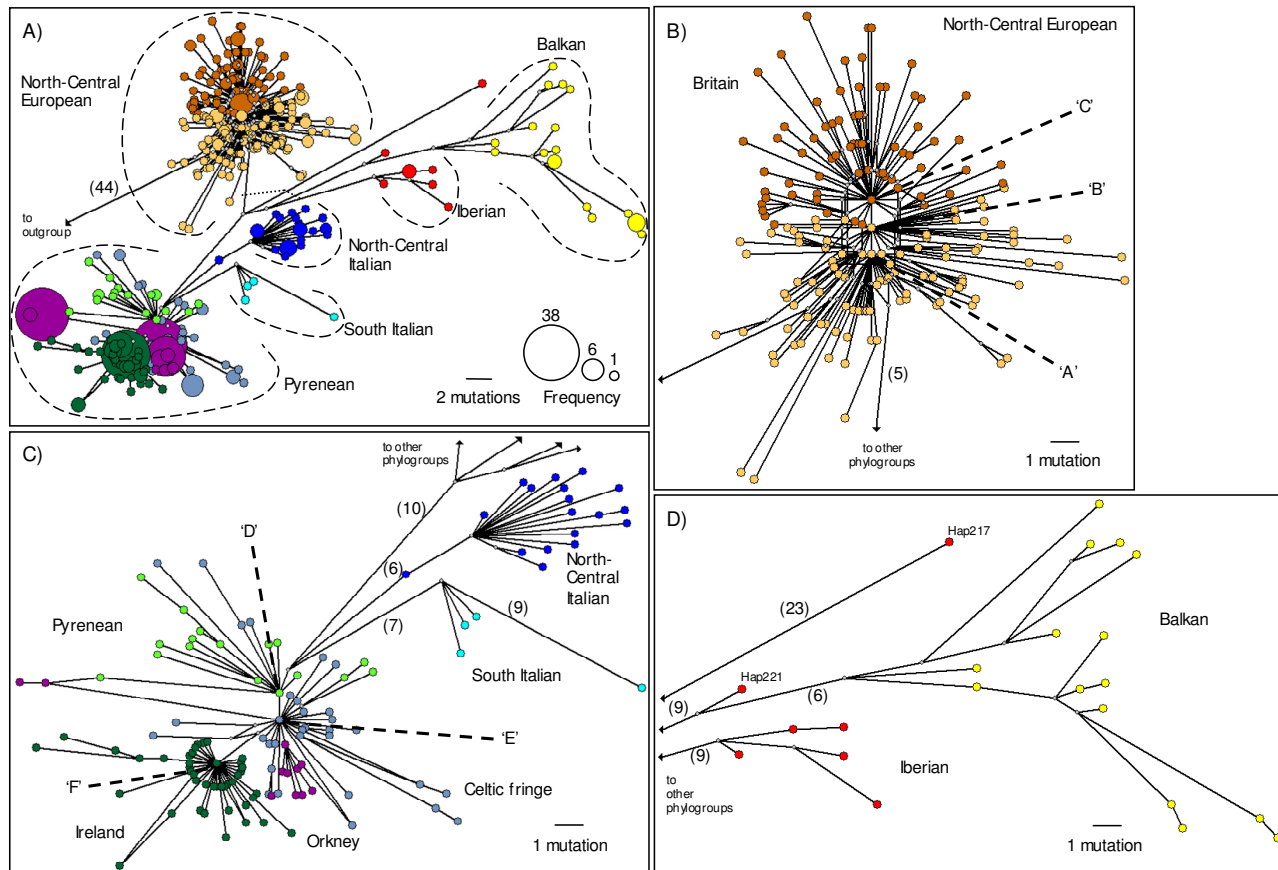


Figure 2.3. Median-Joining network of cytochrome *b* data showing the relationships among *Sorex minutus* haplotypes. A) Full network showing the main phylogroups (dashed lines). B) The North-Central European phylogroup (with British group). C) The Pyrean (with Ireland, Orkney and Celtic fringe groups), North-Central Italian and South Italian phylogroups. D) The Balkan and Iberian phylogroups. Ancestral (central) haplotypes from where all other haplotypes derive from are marked with letters 'A – F' (see text for explanation). Numbers in parentheses represent mutation steps. Dotted line in centre of A) shows where the network was cut.

The Pyrenean phylogroup also had a star like pattern, but it was more complex than the North-Central European clade (Fig. 2.3C). The Pyrenean haplotype ESBa9709 was the most basal of this part of the network ('D'), and all other Pyrenean and some British samples (from the Celtic fringe) were derived from it by one or more mutational steps. Two island samples from the west coast of Britain (GBAr0002 and GBMu0858), sharing the same haplotype ('E'), were central to several other British island samples connected to them by one or more mutational steps, and all belonged to the Celtic fringe group. Notably, two samples from Navarra, Northern Spain plus 29 Irish samples formed a central haplotype ('F') for all Irish sequences, most of them connected by one mutational step only.

The North-Central Italian and South Italian phylogroups were most closely connected to the Pyrenean clade in the MJ network (Fig. 2.3C), in agreement with the phylogenetic trees. The North-Central Italian phylogroup showed no apparent geographical substructure within it and haplotypes were connected among each other by several mutational steps through one hypothetical vector. A sample from North-Western Italy (ITGe0003) was separated by a few steps from the rest of the Italian samples. More samples from Southern Italy are needed for a better comprehension of the genetic structure there, but the current data showed clear differentiation from the North-Central Italian samples and substantial variation among the specimens from La Sila Mountain, with one sample (ITSi0017) separated by 9 mutational steps from the rest.

The Balkan phylogroup (Fig. 2.3D) showed no star like pattern and the haplotypes from this region formed two highly differentiated groups: one comprised samples from the southern parts of the Balkans (European Turkey, Macedonia, Montenegro and Serbia), and the other one comprised samples from the southern and central parts of the Balkans (Macedonia, Montenegro and Bosnia-Herzegovina) plus Austrian, Slovak, Czech and Swiss samples. This phylogroup displayed the

highest number of mutational steps within a group, i.e., making it the most diverse, in agreement with the phylogenetic trees.

The Iberian sub-network was represented by six haplotypes only (Fig. 2.3D); further sampling in this area is needed to infer the genetic structure there, but these results indicate high genetic diversity and differentiation.

The main phylogroups were geographically distinct but there were areas of overlap with other phylogroups, termed contact zones. For example, samples from Czech Republic and Switzerland belonged to the North-Central Italian, the Balkan or the North-Central European phylogroups, so a contact zone among these phylogroups in Central Europe can be inferred; samples from Central France belonged to the Pyrenean or the North-Central European phylogroups, so a contact zone can also be inferred somewhere in Central France; samples from Austria and Slovakia belonged to the Balkan or the North-Central European phylogroups, showing that there is a contact zone north of the Balkan peninsula (Fig. 2.1, and see Appendix 3 for the allocation of samples into phylogroups).

Several samples had particularly interesting haplotypes. Two samples from Navarra, Northern Spain (ESNa0861 and ESNa1131) clustered with and had the same *cyt b* haplotype as several Irish samples. South Italian samples formed a monophyletic group that clustered with the Pyrenean phylogroup with any phylogenetic method used, but not with the geographically closer North-Central Italian phylogroup. The Iberian and Balkan phylogroups had the most diverse sequences, and the later had two subclades, as explained in the network results, with an apparent distinction of southern and northern samples from the Balkan peninsula.

There were three problematic sequences: one sample from Rascafria, Central Spain (ESRa0001) clustered separately from other Iberian samples and it was quite divergent from all other sequences, and another one from the same area

(ESRa3448) clustered within the Balkan phylogroup. One Central Italian sample from Cerreto Laghi (ITLC5646) always clustered within the Iberian phylogroup. Long distance migration events could explain these strange patterns, but this is highly unlikely for *S. minutus*. More likely is that these three samples were either mislabelled or contaminated during collection or during processing. ESRa0001 and ITLC5646 are haplotype sequences obtained from GenBank and I did not have the original samples to verify this. Degraded genomic DNA from ESRa3448 was obtained from brain tissue of a skull sample, but the chromatograms showed a good sequencing signal and I have no reason to believe it could have been contaminated with DNA from Balkan samples, so I suppose that it has been mislabelled. Another possible explanation is that these samples are representative of ancient haplotypes, still present in the Eurasian sample, relating to an older colonisation event. As a precaution, these samples were not included in the phylogroup sequence diversity estimations.

The phylogenetic reconstructions were less resolved with the Y-chromosome introns than with the *cyt b* data because of the low number of parsimony informative sites (Fig. 2.4A, and see Appendix 3 for the allocation of samples into phylogroups). All phylogenetic methods distinguished a 'North-Central Italian' group, represented by one haplotype only (with samples CHBr5421, ITMa0179, IT533, IT56, SWZ47 and SWZ54, but also including sample ITLC5646 which in the *cyt b* phylogeny clustered with the Iberian samples), a 'South Italian' group, represented by one haplotype (samples ITCa5342, ITSi0017, ITSi0021 and IT534) all from Calabria, Southern Italy, and a 'Balkan' group, represented by three haplotypes from the southern Balkan peninsula (samples MEMK0001, RSMK7008 and TUR7). Moreover, the Pyrenean and Iberian lineages found with the *cyt b* data were indistinguishable from each other with the Y-chromosome data, and shared the same sequence or clustered with North-Central European samples, forming the

geographically widespread lineage 'Pyrenean + Iberian + North-Central European'. Also, several North-Central Italian and Balkan samples, which in the *cyt b* data clustered separately, formed an unresolved group with the Y-chromosome intron data named 'North-Central European + North-Central Italian + Balkan'.

For the BRCA1 gene (Fig. 2.4B), the only group that showed bootstrap support was composed of Pyrenean, Orkney and Iberian samples. A South Italian clade was resolved with different phylogenetic methods, but it was poorly supported.

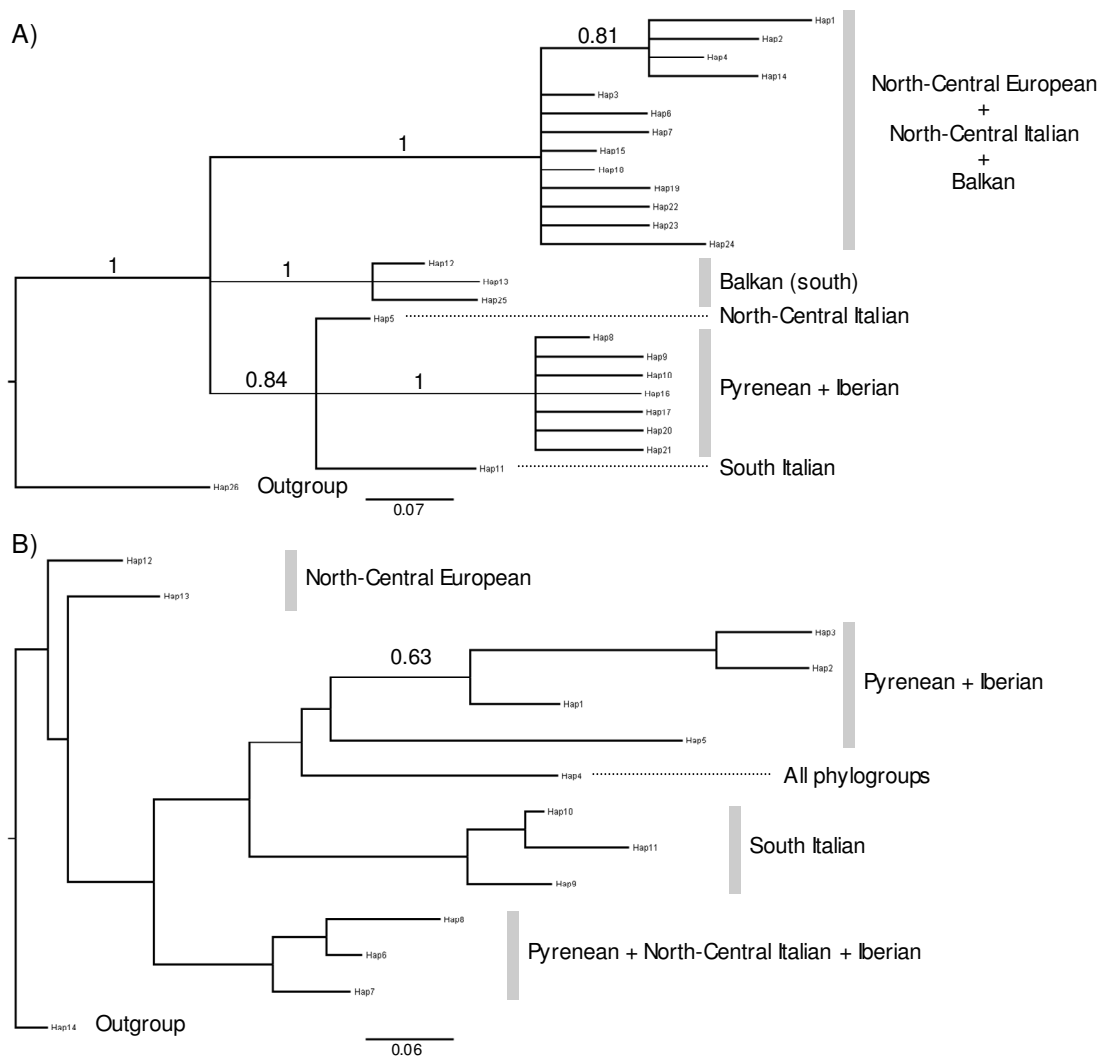


Figure 2.4. Bayesian inference tree of A) Y-chromosome introns and B) BRCA1 gene showing the phylogenetic relationships among *Sorex minutus* sequences. Values on branches represent posterior probability branch support.

2.3.3 Sequence diversity

Nucleotide diversity (π) and haplotype diversity (Hd) for the Eurasian sample and for the phylogroups found with the *cyt b* gene was high and similar to those found in previous studies (Table 2.2). Nucleotide diversity values for the Eurasian and continental Eurasian samples were an order of magnitude higher than for the phylogroups. The phylogroup with the highest nucleotide diversity was the Balkan ($\pi_{\text{Balkan}} = 0.0099$), as expected for the highly divergent sequences there, while the smallest diversity values were found in the island groups, Ireland and the Orkney islands ($\pi_{\text{Ireland}} = 0.0020$, $\pi_{\text{Orkney}} = 0.0027$), as expected for the low number of haplotypes and genetic similarity among samples. There was little effect of island genetic diversity on the total diversity estimations, although the number of haplotypes was rather different, because island samples were usually represented by very similar or identical sequences (Table 2.2). For example, the Eurasian sample had a slightly smaller nucleotide diversity ($\pi_{\text{Eurasian}} = 0.0147$) than the continental Eurasian sample (excluding samples from Britain, Ireland and other islands; $\pi_{\text{cont-Eurasian}} = 0.0171$); likewise, the nucleotide diversities of the North-Central European ($\pi_{\text{NCEuropean}} = 0.0065$) and continental North-Central European ($\pi_{\text{cont-NCEuropean}} = 0.0065$), and those of the Pyrenean ($\pi_{\text{Pyrenean}} = 0.0049$) and continental Pyrenean ($\pi_{\text{cont-Pyrenean}} = 0.0050$) groups were identical. The Celtic fringe group had high diversity values compared to other groups of the Pyrenean phylogroup ($\pi_{\text{Celtic-fringe}} = 0.0057$, $\text{Hd}_{\text{Celtic-fringe}} = 0.9710$), but this was the result of pooling samples from different localities.

Sequence diversity for *S. minutus* Y-chromosome introns and BRCA1 gene was $\pi = 0.0046$ and $\pi = 0.0015$, respectively. Sequence diversity for the main phylogroups of the Y-chromosome introns and nuclear gene was not computed because of the low number of polymorphic sites.

Table 2.2. Cytochrome *b* sequence diversity of phylogroups, island and continental samples of *Sorex minutus*.

Phylogroup	n	Haplotypes	Hd	π	K	S
Eurasian	541	319	0.9847	0.0147	16.1190	362
Continental Eurasian	177	148	0.9974	0.0171	18.6990	252
North-Central European	198	172	0.9977	0.0065	7.1800	253
Continental North-Central European	102	90	0.9970	0.0065	7.1440	170
Britain	80	69	0.9950	0.0054	5.9510	132
Pyrenean	283	102	0.9458	0.0049	5.4400	147
Continental Pyrenean	15	13	0.9810	0.0050	5.5430	28
Ireland	96	42	0.8840	0.0020	2.1730	53
Orkney	119	11	0.7720	0.0027	3.0140	17
Celtic fringe	50	33	0.9710	0.0057	6.2600	71
North-Central Italian	26	18	0.9600	0.0061	6.7720	51
South Italian	4	4	1.0000	0.0073	8.0000	16
Balkan	21	16	0.9570	0.0099	10.9050	53
Iberian	7	5	0.8570	0.0052	5.7140	15

n = Number of sequences.

Hd = Haplotype diversity.

π = Nucleotide diversity (Jukes and Cantor 1969).

K = Average number of nucleotide differences.

S = Number of polymorphic (segregating) sites.

2.3.4 Divergence and genetic structure of populations

In general, there were small pairwise sequence divergence (D_a) values among phylogroups with the *cyt b* data, consistent with intraspecific studies (Table 2.3). The smallest divergence was between the Pyrenean and the South Italian phylogroups ($D_a = 0.7\%$), followed by the divergence between the Pyrenean and the North-Central Italian phylogroups ($D_a = 0.9\%$). Interestingly, the South Italian and North-Central Italian phylogroups presented a larger divergence ($D_a = 1.0\%$) despite the geographical proximity in the Italian peninsula, in accordance with the phylogenetic tree and MJ network. The largest divergences were found among the Balkan and the other phylogroups (D_a values between 1.7% and 2.4%), followed by the divergences among the Iberian and the other phylogroups (D_a values between

1.7% and 2.2%). About 5.2% sequence divergence, on average, was found between the ingroup and the outgroup (average $D_a = 0.0519$) as expected for interspecific sequence divergence.

Pairwise genetic differentiation values among phylogroups based on F_{ST} were large and significant (Table 2.4). Again, the smallest differentiation value was between the Pyrenean and the South Italian phylogroups ($F_{ST} = 0.5922$). The greatest differentiation was between the Pyrenean and the Balkan phylogroups ($F_{ST} = 0.8120$), and between the Pyrenean and the Iberian phylogroups ($F_{ST} = 0.8081$). However, I found no correlation between genetic divergence and geographic distances ($R = 0.3871$, $p = 0.1313$), or between genetic differentiation and geographic distances among phylogroups ($R = 0.0618$, $p = 0.4061$); therefore, there was no evidence of isolation by distance at the level of phylogroups.

Table 2.3. Pairwise sequence divergence values D_a (SD), below diagonal, and pairwise geographic distances (in Km), above diagonal, among cytochrome *b* phylogroups of *Sorex minutus*.

	Pyrenean	South Italian	North-Central Italian	North-Central European	Iberian	Balkan	Outgroup
Pyrenean	-	2385	1616	843	1554	2043	3103
South Italian	0.0069 (0.0018)	-	773	1698	1764	621	1307
North-Central Italian	0.0090 (0.0008)	0.0102 (0.0029)	-	942	1350	553	1695
North-Central European	0.0142 (0.0004)	0.0148 (0.0016)	0.0153 (0.0007)	-	1597	1250	2265
Iberian	0.0206 (0.0028)	0.0213 (0.0080)	0.0223 (0.0041)	0.0168 (0.0014)	-	1884	2987
Balkan	0.0225 (0.0018)	0.0239 (0.0059)	0.0235 (0.0027)	0.0187 (0.0010)	0.0174 (0.0040)	-	1145
Outgroup	0.0524 (0.0127)	0.0524 (0.0262)	0.0508 (0.0150)	0.0486 (0.0093)	0.0529 (0.0238)	0.0540 (0.0168)	-

Table 2.4. Pairwise F_{ST} values (below diagonal) among cytochrome *b* phylogroups and phylogroup specific F_{ST} values (diagonal) of *Sorex minutus*.

	Pyrenean	South Italian	North-Central Italian	North-Central European	Iberian	Balkan
Pyrenean	0.7210					
South Italian	0.5922	0.7206				
North-Central Italian	0.6446	0.6235	0.7202			
North-Central European	0.7191	0.6964	0.7047	0.7198		
Iberian	0.8081	0.7721	0.7869	0.7213	0.7211	
Balkan	0.8120	0.7132	0.7517	0.7352	0.6559	0.7175

The overall pattern of intraspecific genetic differentiation was also strong and highly significant ($p < 0.0001$), about 72% of the variation was found among phylogroups (Table 2.5).

Table 2.5. Analysis of Molecular Variance (AMOVA) among cytochrome *b* phylogroups of *Sorex minutus* and phylogroup F_{ST} .

Source of variation	DF	Sum of squares	Variance components	Percentage of variation
Among populations	5	2595.872	8.2139	72.04
Within populations	532	1696.01	3.1880	27.96
Total	537	4291.881	11.4019	100
Overall (Eurasian) $F_{ST} = 0.7204$ ($p < 0.001$)				

DF = Degrees of Freedom

Using the molecular clock, all intraspecific divergence times fell approximately between 0.2 and 0.6 MYA, within the Middle Pleistocene (Table 2.6). The divergence times among the outgroup and the phylogroups fell between 1.2 and 1.3 MYA, within the Early Pleistocene (Table 2.6), but this divergence time could be underestimated because of substitutional saturation or low sample size for the outgroup. The Balkan and Iberian phylogroups diverged approximately 0.4 MYA, and both had the largest values of divergence time compared to the other phylogroups ranging between 0.4 – 0.6 MYA. As expected from the lower divergence values, the South Italian and Pyrenean phylogroups diverged more recently, about 0.173 MYA, while the North-Central Italian and South Italian split about 0.255 MYA.

Table 2.6. Time of divergence (\pm SD) among cytochrome *b* phylogroups of *Sorex minutus* (in MYA).

	Pyrenean	South Italian	North-Central Italian	North-Central European	Iberian	Balkan	Outgroup
Pyrenean	-						
South Italian	0.173 (0.127-0.218)	-					
North-Central Italian	0.225 (0.205-0.245)	0.255 (0.182-0.328)	-				
North-Central European	0.355 (0.345-0.365)	0.370 (0.331-0.409)	0.383 (0.366-0.399)	-			
Iberian	0.515 (0.446-0.584)	0.533 (0.332-0.733)	0.558 (0.454-0.661)	0.420 (0.385-0.455)	-		
Balkan	0.563 (0.518-0.607)	0.598 (0.450-0.746)	0.588 (0.519-0.656)	0.468 (0.442-0.493)	0.435 (0.335-0.536)	-	
Outgroup	1.310 (0.993-1.627)	1.310 (0.656-1.964)	1.270 (0.896-1.644)	1.215 (0.982-1.448)	1.323 (0.729-1.916)	1.350 (0.931-1.769)	-

The genetic relationships among phylogroups are better visualised in the NJ tree using the pairwise distance values (Fig. 2.5): the Iberian and Balkan formed a divergent clade, separated from the North-Central European, North-Central Italian, South Italian and Pyrenean lineages; the Pyrenean, South Italian and North-Central Italian phylogroups clustered together, separated from North-Central European samples. These results showed a similar topology to the one found with the BA of *cyt b* haplotype sequences, the only difference was in the base of the NJ tree where the North-Central European lineage grouped with the Pyrenean and Italian lineages, and was not basal as in the Bayesian tree.

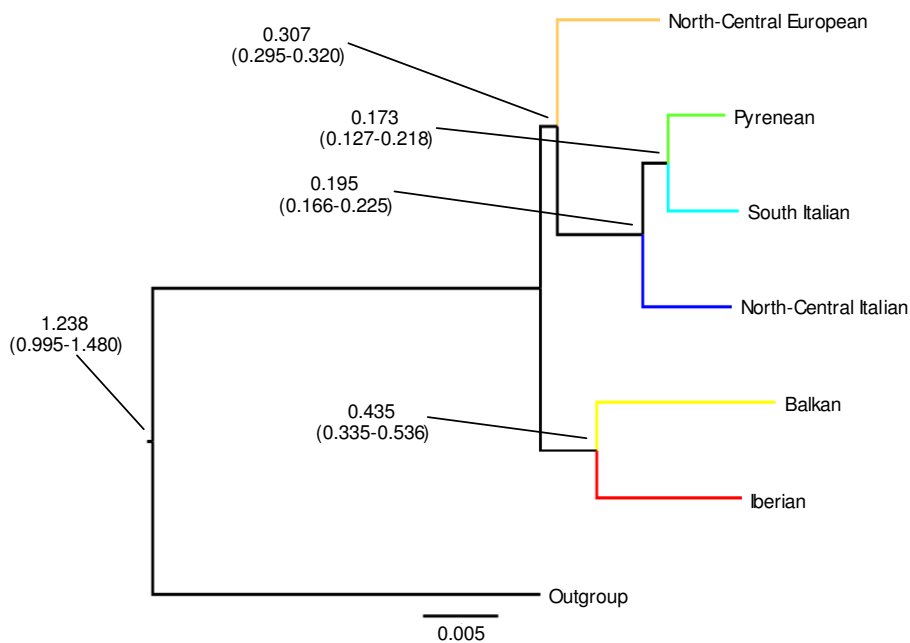


Figure 2.5. Neighbor-Joining tree showing the pairwise distances among cytochrome *b* phylogroups of *Sorex minutus* and estimated divergence times (in MYA) assuming a molecular clock.

I also calculated the genetic divergence and divergence times between the main clades observed on the NJ tree (Fig. 2.5). The genetic divergence between the 'Pyrenean + South Italian' and 'North-Central Italian' lineages was 0.8% ($D_a = 0.0078$, divergence time = 0.195 MYA), between the 'Pyrenean + Italian peninsula'

and 'North-Central European' was 1.2% ($D_a = 0.0123$, divergence time = 0.307 MYA), and between the 'Pyrenean + Italian peninsula + North-Central European' and 'Balkan + Iberian' was 1.4% ($D_a = 0.0136$, divergence time = 0.340 MYA).

The TMRCA for each lineage are shown in Fig. 2.6. The values differed from the time of divergence estimates assuming a molecular clock, as expected from the different methodologies. The root of the Bayesian tree had a mean value of 8.039 MYA (95% HPD: 4.734 – 12.624 MYA), which marked the evolution of *S. minutus* from its ancestral population and split from its sister species *S. volnuchini*. The deepest node for *S. minutus* had an estimated TMRCA of 5.139 MYA (95% HPD: 4.532 – 5.312), in the Early Pliocene, congruent with the fossil calibration.

For each phylogroup the TMRCA ranged between 0.7 – 1.7 MYA. The TMRCA involving multiple phylogroups tended to be much higher, ranging from 1.4 MYA (Pyrenean and South Italian phylogroups) to 5.1 MYA (North-Central European phylogroup and the clade formed by all other phylogroups). Because of the large 95% HPD in the Bayesian analysis, I was not able to estimate with confidence the TMRCA for the island groups.

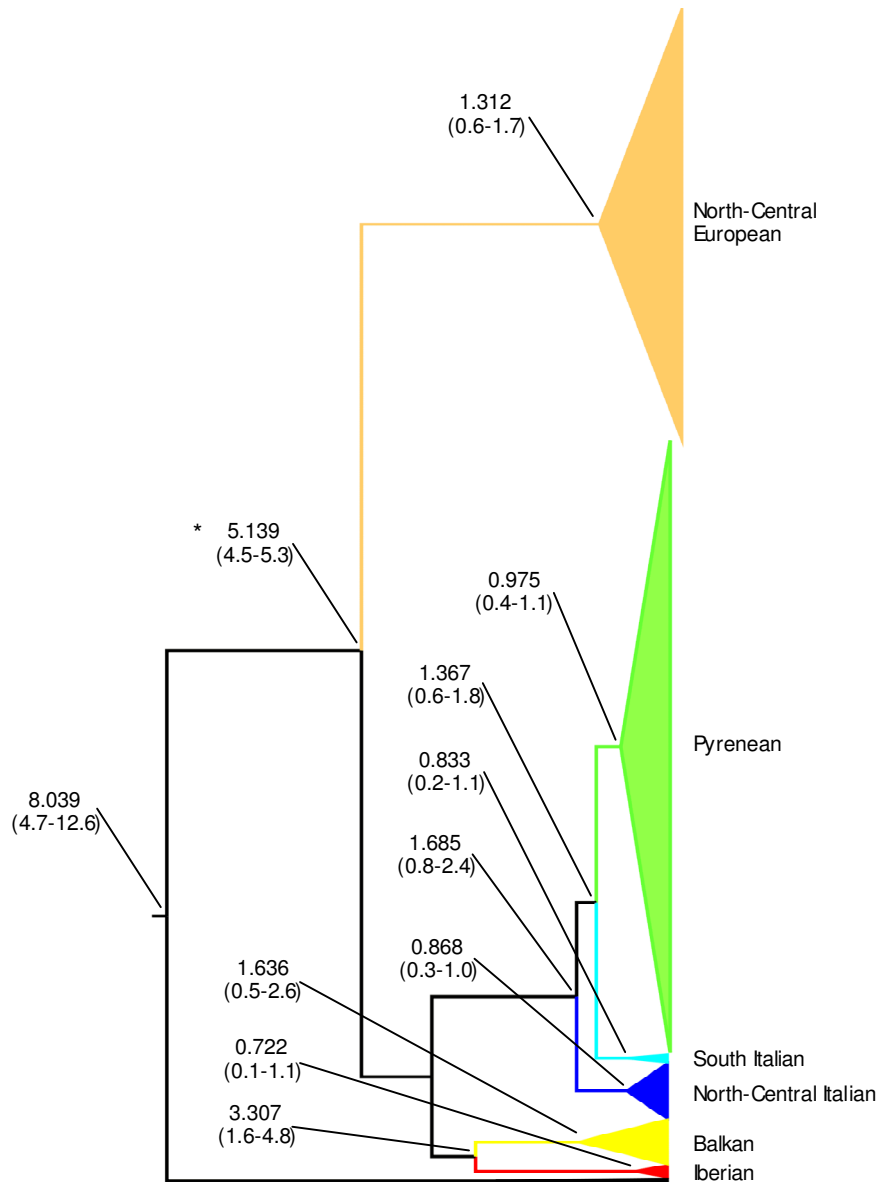


Figure 2.6. Bayesian inference tree of cytochrome *b* data showing the genetic relationships among phylogroups of *Sorex minutus*. Values on nodes correspond to Times to the Most Recent Common Ancestor with 95% Highest Probability Density confidence intervals (in MYA). The ingroup (*) was calibrated with the oldest known fossil record of *S. minutus* (5 MYA, SD = 0.2).

2.3.5 Historical demography

The mismatch distributions for the Eurasian and continental Eurasian samples were multimodal, but related to pairwise differences within and between phylogroups and not to an historically constant population size (Fig. 2.7). The

Pyrenean, North-Central European, North-Central Italian, continental Pyrenean, continental North-Central European, Ireland and Britain groups all had distinctly unimodal mismatch distributions with an almost perfect fit between observed and expected pairwise differences of a sudden population expansion model (Fig. 2.7).

Population expansion tests performed on the main phylogroups, continental and island groups are presented in Table 2.7. Because of low sample size, the population expansion tests were not performed on the South Italian and outgroup lineages ($n < 5$). The Eurasian and continental Eurasian samples had significant R_2 values and showed significant departures from neutrality with highly negative F_u 's F_s and Tajima's D values.

There was consistency among the significant population expansion tests and unimodal mismatch distributions: the Pyrenean, North-Central European, North-Central Italian, continental Pyrenean, continental North-Central European, Ireland and Britain groups also had significant p values for R_2 , F_u 's F_s and Tajima's D statistics. The Balkan and Iberian phylogroups had non-significant p values for R_2 , F_u 's F_s and Tajima's D population expansion statistics, consistent with the multimodal mismatch distributions and the lack of fit between observed and expected pairwise difference distributions for a sudden population expansion model (Fig. 2.7). With the SSD test, all phylogroups showed non-significant differences from the modelled distribution under a sudden population expansion, likely reflecting the low statistical power of this test.

Interestingly, samples from the Orkney islands displayed a skewed mismatch distribution (Fig. 2.7), with a high frequency of zero pairwise differences (23%), because of the low number of nucleotide polymorphisms regardless of the large number of sequences obtained from there. This related to no evidence for population expansion based on the p values for F_u 's F_s , Tajima's D and R_2 statistics (Table 2.7).

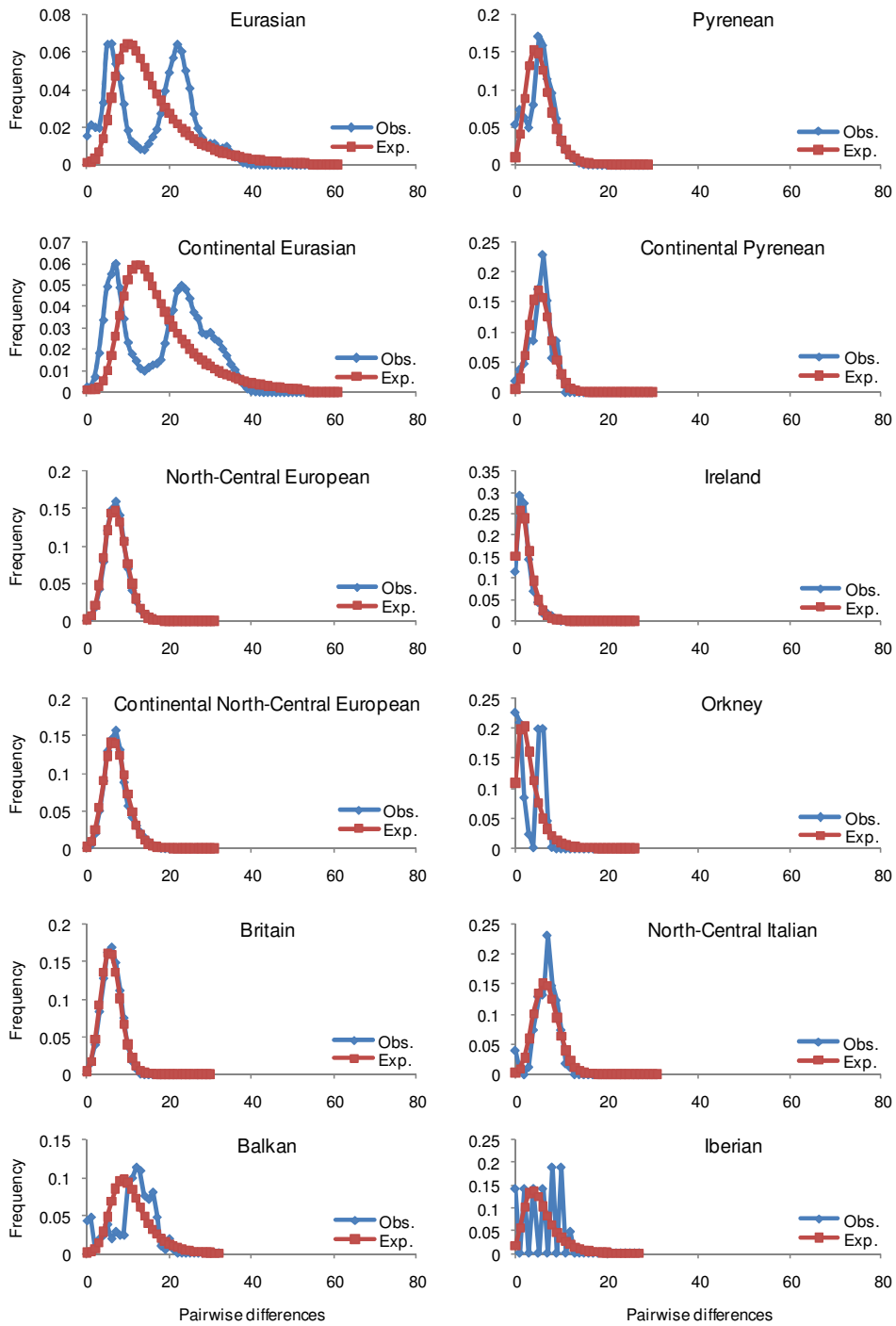


Figure 2.7. Mismatch distribution (frequency of pairwise nucleotide differences) of cytochrome *b* phylogroups of *Sorex minutus*.

Table 2.7. Population expansion analyses for the whole cytochrome *b* dataset (Eurasian) and phylogroups of *Sorex minutus* (*p* values are given between parentheses).

Phylogroup	n	R ₂	Fu's Fs	Tajima's D	SSD
Eurasian	538	0.0218 (< 0.01)	-457.6680 (< 0.01)	-2.1505 (< 0.01)	0.0127 (0.3309)
Continental Eurasian	174	0.0354 (< 0.01)	-159.6300 (< 0.01)	-1.9354 (< 0.01)	0.0067 (0.5640)
North-Central European	198	0.0123 (< 0.01)	-34.1384 (< 0.01)	-2.6878 (< 0.01)	0.0004 (0.3119)
Continental North-Central European	101	0.0172 (< 0.01)	-132.5150 (< 0.01)	-2.6491 (< 0.01)	0.0005 (0.4694)
Britain	92	0.0169 (< 0.01)	-97.6109 (< 0.01)	-2.6501 (< 0.01)	0.0008 (0.3758)
Pyrenean	283	0.0175 (< 0.01)	-114.6990 (< 0.01)	-2.3760 (< 0.01)	0.0056 (0.2807)
Continental Pyrenean	15	0.0793 (< 0.01)	-6.0342 (< 0.01)	-1.4937 (0.0596)	0.0098 (0.4469)
Ireland	96	0.0184 (< 0.01)	-52.7758 (< 0.01)	-2.5291 (< 0.01)	0.0030 (0.1694)
Orkney	119	0.0880 (0.5090)	0.6044 (0.6515)	-0.1417 (0.5090)	0.0548 (0.1518)
North-Central Italian	26	0.0521 (< 0.01)	-5.8766 (0.0159)	-1.8871 (0.0149)	0.0119 (0.0744)
South Italian	4	NA	NA	NA	NA
Balkan	21	0.0880 (0.0777)	-2.9944 (0.1050)	-1.0372 (0.1467)	0.0067 (0.6385)
Iberian	7	0.1396 (0.0847)	0.5529 (0.5539)	-0.3685 (0.3779)	0.0767 (0.3097)
Outgroup	3	NA	NA	NA	NA

n = Number of samples

NA = Non-applicable (low sample size).

SSD = Sum of Square Deviations test.

The population expansion times calculated for those groups with a unimodal mismatch distribution and significant *p* values for R₂ and Fu's Fs statistics were older than the LGM (Table 2.8). However, for the Irish group the time of population expansion dated to 14 or 22 KYA (17 – 27 KYA), depending on the method used, close to the LGM. The North-Central European, Pyrenean and North-Central Italian phylogroups (and the continental and island counterparts) had expansion times between 41 and 81 KYA, all dated in the Late Pleistocene. Usually, the τ values (with confidence intervals) and expansion times obtained with Schneider and Excoffier's (1999) approach were similar to those obtained with Rogers' (1995) method; however, considerable differences in the estimation of τ and population

expansion times were found on the continental Eurasian and Pyrenean phylogroups (Table 2.8).

Table 2.8. Time of expansion parameters for the whole cytochrome *b* dataset (Eurasian) and phylogroups of *Sorex minutus*.

Phylogroup	τ^1	Time	τ^2	Time
Eurasian	7.4810	0.084	3.4 (1.107-23.873)	0.038 (0.012-0.269)
Continental Eurasian	9.3210	0.105	25.0 (14.336-32.381)	0.282 (0.161-0.365)
North-Central European	6.9730	0.079	7.2 (6.555-7.607)	0.081 (0.074-0.086)
Continental North-Central European	6.0930	0.069	6.6 (6.008-7.885)	0.074 (0.068-0.089)
Britain	5.9510	0.067	6.3 (5.379-6.885)	0.071 (0.060-1.078)
Pyrenean	3.6660	0.041	6.5 (3.723-8.676)	0.073 (0.042-0.098)
Continental Pyrenean	5.5430	0.062	6.1 (3.678-7.936)	0.069 (0.041-0.089)
Ireland	1.2420	0.014	2.0 (1.508-2.393)	0.023 (0.017-0.027)
North-Central Italian	6.7720	0.076	7.2 (5.715-8.494-)	0.081 (0.064-0.096)

¹ Based on Rogers (1995).

² Based on Schneider and Excoffier (1999).

95% confidence intervals are given between parentheses.

The traces of the BSPs converged, but had large variations of the posterior probability values and large 95% HPD, diminishing the confidence of this analysis. Figure 2.8 shows the results of the BSP of several lineages. Only the Pyrenean and Ireland groups had a notable increase of effective population size through time, while the other groups had more stable effective population sizes. The North-Central European had a relatively recent increase of population size, but the 95% HPD also increased. The group from Britain showed a stable population size, contrary to what was expected from the population expansion tests. However, the Balkan phylogroup had a stable, flat, effective population size through time, consistent with the non-significant results to the population expansion tests.

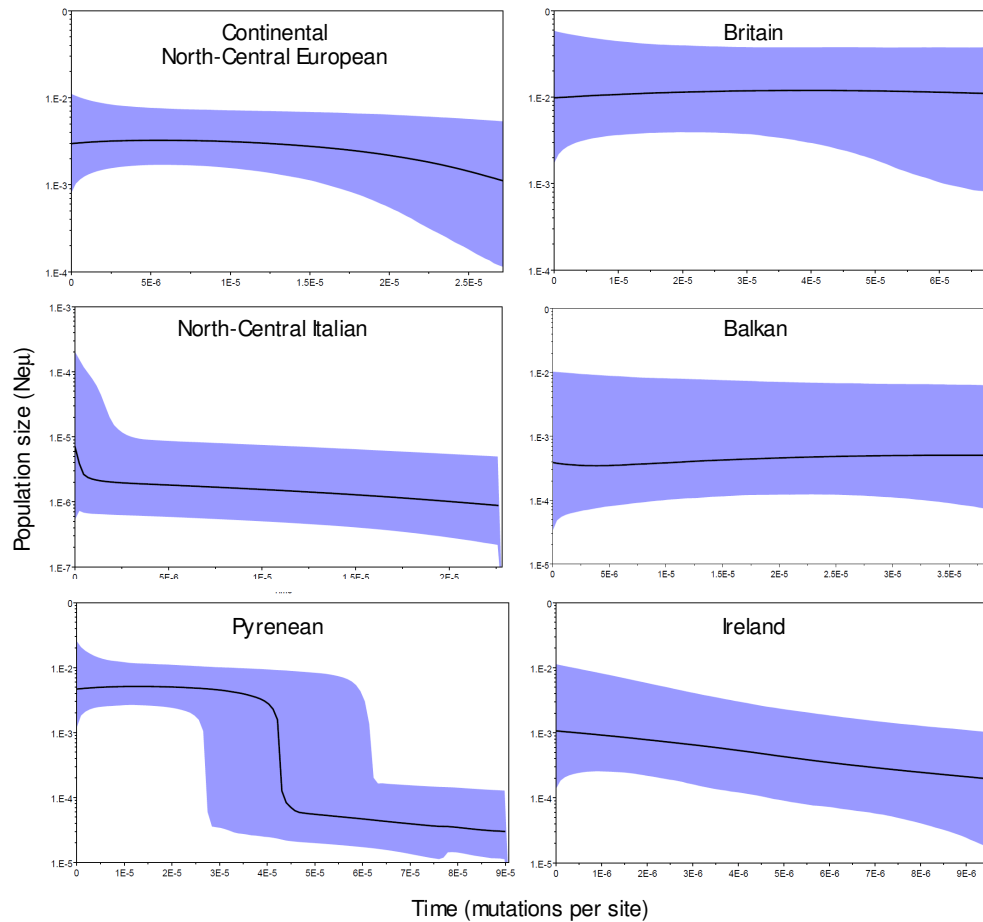


Figure 2.8. Bayesian Skyline Plots of cytochrome *b* phylogroups of *Sorex minutus* showing the historical demographic trends. The solid lines are median estimates and the shaded areas represent 95% Highest Probability Densities (confidence intervals).

2.4 Discussion and conclusions

The phylogeographic study that I present here notably expands previous findings on *S. minutus*, giving a more precise population genetic structure and demographic history, and contributing to the understanding of the patterns and processes during the Quaternary ice ages that shaped the European biota.

2.4.1 Phylogenetic findings and genetic population structure

The genetic lineages detected with *cyt b* data were similar to those previously found, either with fewer samples (Bilton et al. 1998, Mascheretti et al.

2003) or with different molecular markers (McDevitt et al. 2010). The Iberian, Balkan, North-Central Italian and South Italian phylogroups were geographically restricted to the Southern European peninsulas, consistent with the traditional Mediterranean glacial refugia; however, the North-Central European and Pyrenean phylogroups were distributed further north and represent evidence of northern refugia. The high genetic and haplotype diversities in southern and northern refugia reflect long term isolation and differentiation during the Pleistocene and Holocene, and the significant genetic structure illustrate a complicated history of European colonisation, not a simple case of isolation by distance and colonisation of Northern and Central Europe from expanding populations from the south.

It is interesting that the contact zones among phylogroups were detected at the northern extremes of the southern peninsulas. During the LGM, glaciers covered most of the Alpine and Pyrenean mountain ranges; therefore, these areas were deprived of fauna and flora, but when climate ameliorated and suitable habitat became available, pygmy shrew populations expanded and colonised previously glaciated areas only to find related populations from other lineages arriving from the other side of the mountain ranges, forming the contact zones among lineages that we observe today.

The poor phylogenetic resolution obtained with Y-chromosome introns and BRCA1 gene was not unexpected. Gündüz et al. (2007) found low divergence values among different species of ground squirrels with three Y-chromosome introns, ranging between 0.2% and 0.7% (compared to 5% – 10% with *cyt b*), and only eight single nucleotide polymorphisms and two insertion/deletions in 13 males analysed. Using the BRCA1 gene, Dubey et al. (2006) inferred the genetic relationships within the *Crocidura suaveolens* group and found several clades with low bootstrap support and basal polytomies resulting in partially unresolved phylogenies, but comparable to *cyt b* lineages. Moreover, the grouping of Pyrenean

and Iberian samples within a single clade was also found in another study using four concatenated Y-chromosome introns (McDevitt et al. 2010), and this could be related to the lower levels of nucleotide diversity in mammalian Y chromosomes caused by lower mutation rates compared to mtDNA (Hellborg and Ellegren 2004).

2.4.2 Insights on the colonisation routes into Europe

The origin of *S. minutus* from its proposed (extinct) ancestor, *S. minutoides*, has been estimated at the end of the Late Miocene in China (5.3 – 11.6 MYA; Storch et al. 1998, Rzebik-Kowalska 2005, 2008). The estimated time of evolution of *S. minutus* based on the Bayesian analysis with BEAST was consistent with this (estimated root at 8 MYA, ranging between 4.7 and 12.6 MYA). The oldest fossils of *S. minutus* were found in Podlesice and Mała Cave, Poland dated to the Early Pliocene between 4 and 5.3 MYA (Rzebik-Kowalska 1998), and an early widespread colonisation of Europe might have been possible because *S. minutus* was one of the first species of the genus *Sorex* in the continent (based on fossil records; Rzebik-Kowalska 1998, 2008). However, the very early separation of the different phylogroups from the Bayesian analysis with BEAST seems unrealistic compared to the molecular clock dating method I have used. The use of deep calibration points based on fossil records leads to slower observed mutational rates and overestimated evolutionary scenarios (Ho et al. 2008); therefore, these results should be taken with caution. Moreover, the use of a 5 million year calibration point for the earliest occurrence of *S. minutus* may be misleading, because that fossil found in Poland may have been an ancestor of both *S. minutus* and *S. volnuchini*, which are very similar to each other in morphology (see Chapter 4). Morphological analysis of the Polish fossils may be informative on this point.

The highly divergent sequences from Russia (Siberia), Poland and Ukraine, and the connection of *S. volnuchini* to the North-Central European phylogroup in the

MJ network argue in favour of a colonisation route of current *S. minutus* into Europe from the east or the south-east. A similar colonisation scenario before the LGM from Eastern to Western Europe was proposed for the common vole *Microtus arvalis*, which has a south-westward genetic gradient that could be a trace of the original colonisation of Europe (Heckel et al. 2005). A colonisation route originating from the east could also be hypothesised for other species that have the oldest divergence times with Ural phylogroups but have younger European phylogroups. For example, molecular dating suggests that the bank vole *Myodes (Clethrionomys) glareolus* diverged from a Ural phylogroup in the mid-Pliocene (2.98 MYA), but other European phylogroups diverged much more recently (Deffontaine et al. 2005); the North European and Central Asian groups of the root vole *M. oeconomus* diverged three to five glacial periods ago, but the divergence estimates for European groups were more recent (Brunhoff et al. 2003).

2.4.3 Colonisation and historical demography of southern peninsulas

The oldest fossils of *S. minutus* in the Balkans are dated to the Early Pliocene in Romania and Hungary between 4 and 4.5 MYA (Rzebik-Kowalska 1998), where the Balkan lineage is probably distributed, which could indicate the time of arrival of *S. minutus* into this southern peninsula. However, the estimated pairwise divergence times between the Balkan lineage and other phylogroups (within the last 0.6 MYA, Table 2.6) placed the divergence event much later.

The lack of a population expansion signature, high nucleotide and haplotype diversities, highly divergent sequences and apparent structure within the Balkan phylogroup suggest stable population sizes over time and genetic differentiation within the Balkan peninsula. The Balkans are a European hotspot for biodiversity given their environmental stability, topographic and climatic diversity and occasional connectedness with Asia Minor (Kryštufek and Reed 2004), and it could be

expected that some of these factors shaped the genetic diversity of the Balkan lineage there.

In the Iberian peninsula, the earliest fossil records of *S. minutus* are dated to the Early Pleistocene (1.2 – 1.4 MYA) (Cuenca-Bescós et al. 2010, Agustí et al. in press), again reflecting a long presence of *S. minutus* or a similar ancestral form in various part of Europe. Although Iberia is considered a refugial area during the Quaternary ice ages, and stable climate is suggested, it is a topographically diverse region with east-west mountain ranges and other high ground (over 1000 m.a.s.l.), large rivers (which could act as barriers to dispersal), and distinct seasonal precipitation and vegetation types (O'Regan 2008), which could have played an important role in the genetic differentiation of populations. The lack of significant population expansion values for the Iberian lineage may relate to historical stable population sizes; however, the sample size was low and this result should be taken with caution.

It is striking that the Pyrenean and South Italian lineages grouped together in the *cyt b* phylogenies and presented the smallest divergence times despite being geographically separated. This indicates a common history and it can be hypothesised that their common ancestor was more widespread throughout the Italian peninsula, probably displaced later by the North-Central Italian lineage in the Apennines and Western Alps. A similar scenario has been proposed for the water shrew *Neomys fodiens* (Castiglia et al. 2007), Alpine salamander *Salamandra salamandra* (Steinfartz et al. 2000), black pine *Pinus nigra* (Afzal-Rafii and Dodd 2007) and green lizard *Lacerta bilineata bilineata* (Böhme et al. 2007), which showed closely related South Italian and Pyrenean lineages but separated geographically by a North-Central Italian lineage. The Pyrenean phylogroup has significant signatures for population expansion, which suggest that this lineage, north of the traditional southern refugia, expanded during favourable climate

conditions. The expansion signature was not an effect of the island samples that belong to the Pyrenean lineage, because continental samples analysed separately also demonstrate a significant signature of population expansion.

The oldest fossils of the genus *Sorex* from Southern Italy, found in Basilicata region, are dated to the Early-Middle Pleistocene (ca. 0.5 – 1.2 MYA) and belong to an unrelated species, *S. gr. runtonensis-subaraneus* (Masini et al. 2005). Northern Italy also has shrew fossils, including a form classified as *S. minutus*, dated to the Early-Middle Pleistocene ca. 0.5 – 1.2 MYA, from Monte La Mesa near Verona (Masini and Sala 2007). The divergence times between the Pyrenean and South Italian lineages (about 0.173 MYA according to the molecular clock used, i.e., at the Middle-Late Pleistocene) suggest a much later arrival of the current population of *S. minutus* into Southern Italy. This lineage in the Calabria region is genetically and morphologically distinct from Central and North Italian populations, and this could have been a result of isolation and differentiation in an island setting, as hypothesised for other species and lineages in Southern Italy, reflecting island evolution (Vega et al. 2010a). Calabria consists of isolated mountain massifs separated by lowland areas in the southernmost part of the Italian peninsula, which from the Pliocene to the end of the Middle Pleistocene, at times of high sea level, were islands in a chain (Malatesta 1985, Caloi et al. 1989, Bonardi et al. 2001, Bonfiglio et al. 2002).

The finding of two genetic lineages of *S. minutus* in the Italian peninsula gives the impression that the refugial area may have been subdivided into multiple refugia at the LGM, one in the extreme south of Italy and at least one other refugium further north, concordant with the 'refugia within refugia' concept widely recognized for the Iberian peninsula (Gómez and Lunt 2007) and similar to microrefugia in the Balkans (Kryštufek et al. 2007). For the Italian peninsula, a similar 'refugia within refugia' pattern was found in a number of species (Vega et al. 2010a, and

references therein). The widespread North-Central Italian lineage may be presumed to derive from a glacial refugium located somewhere within the vicinity of the Apennine mountain chain. The significant population expansion signature for the North-Central Italian lineage demonstrates that it went through colonisation and expansion phases. However, further sampling and genetic analyses are needed to demonstrate population expansions from two separate refugial areas, and from the current data, it is possible that the North-Central and South Italian phylogroups occupied a single, continuous area at the LGM with the integrity of the groups retained by a hybrid zone (Barton and Hewitt 1985, Vega et al. 2010a).

2.4.4 Northern refugia of the North-Central European phylogroup

The high haplotype and nucleotide diversities and significant population expansion signatures of the North-Central European lineage are congruent with the hypothesis of northern glacial refugia (Bilton et al. 1998, Vega et al. 2010b). The BSP showed that the effective population size of this lineage remained either constant through time or had a steady increase of population size. If Mediterranean peninsulas were the source of northern populations, then the North-Central European phylogroup would not exist, there would be low genetic and haplotype diversities, concordant with a 'southern richness and northern purity' scenario (Hewitt 1996, 2000), and southern haplotypes would be found across Central and Northern Europe. Moreover, the star-like pattern in the phylogenetic network, the three ancestral haplotypes from Central and Eastern Europe identified by their central position from where peripheral, more recent, haplotypes derived, argue in favour of persistence and population expansion in that region (Avice 2000).

The hypothesis of northern refugia is further supported by palaeontological and palynological evidence for other temperate and boreal species (Willis et al. 2000, Willis and van Andel 2004, Magri et al. 2006, Sommer and Nadachowski

2006). Northern refugia have been hypothesised in phylogeographic analyses for a number of small mammal species, including the field vole *M. agrestis* (Jaarola and Searle 2002), bank vole *M. glareolus* (Deffontaine et al. 2005, Kotlík et al. 2006), root vole *M. oeconomus* (Brunhoff et al. 2003), common vole *M. arvalis* (Heckel et al. 2005) and common shrew *S. araneus* (Bilton et al. 1998, Yannic et al. 2008). Most of the phylogeographic studies point to the Carpathians as a likely northern refugial area for the North-Central European lineage, but a refugium in this area could have included broader regions of Hungary, Slovakia, Czech Republic, Moldova and Poland, supported by the occurrence of temperate mammal fossil records in the area (Sommer and Nadachowski 2006). However, for *M. glareolus*, *M. oeconomus*, *M. agrestis* and *M. arvalis*, and recently for *S. minutus*, predictions of their potential LGM distribution based on SDM are also consistent with northern refugia and indicate that the suitable climatic conditions could have been widespread across Central and Eastern Europe (Fløjgaard et al. 2009, Vega et al. 2010b).

Sorex minutus is considered a temperate species, but it is also latitudinally distributed above 60° North (i.e., near the Arctic Circle) and altitudinally above 2000 m.a.s.l. in regions with permafrost and harsh winters (Mitchell-Jones et al. 1999, Hutterer et al. 2008). Species that reach northern non-arctic distributions, like *S. minutus*, could have persisted in high latitude refugia in Europe during the LGM, north of the traditionally recognized Mediterranean refugial areas (Stewart and Lister 2001), as a result of their ecological traits (notably cold tolerance) and biogeographical characteristics that may have determined their response to the glaciations (Bhagwat and Willis 2008). *Sorex minutus* is, therefore, a suitable model organism for exploring the controversial hypothesis of 'northern' glacial refugia. Moreover, *S. minutus* is currently restricted to high altitude areas in Southern Europe, because the dry, hot Mediterranean conditions in the lowlands do not suit it

(Taylor 1998). Therefore, its distribution in southern refugia may actually be more restricted during interglacials than glacials, in line with ideas of 'interglacial refugia' (Hilbert et al. 2007).

2.4.5 Colonisation history of Northern Europe and Britain

Populations of *S. minutus* belonging to the North-Central European lineage apparently colonised Northern Europe from refugia in Eastern-Central Europe. For example, Scandinavian and the Baltic regions were most likely colonised from Eastern Europe; thus, the phylogenetic network shows that sequences from Norway, Finland and Lithuania group closely with the Ukrainian ancestral haplotype. Central European populations likely originated from populations that remained in northern glacial refugia there. The stable population size over time and high genetic diversity indicate that the North-Central European lineage did not suffer from genetic bottlenecks during the glaciations.

From where did the British pygmy shrew populations arrive? The genetic similarity of samples from the Netherlands and Britain suggests that British *S. minutus* belonging to the North-Central European phylogroup originated from populations in the vicinity of the Netherlands (Vega et al. 2010b), reaching Britain over the Doggerland landbridge with continental Europe (Gaffney et al. 2007). Yet, there is a second lineage in Britain which belongs to the Pyrenean phylogroup, represented by individuals found in a few localities in the periphery of mainland Britain and in several British Isles. Compelling evidence indicate that pygmy shrews of the North-Central European lineage, as well as other small mammals, colonised Britain after the LGM and selectively displaced pygmy shrew populations of the Pyrenean lineage, which still remain in uplands and islands in the periphery to the north, west and south of Britain forming a 'Celtic fringe' (Searle et al. 2009), also observed in the sample analysed here.

2.4.6 Northern refugium of the Pyrenean phylogroup?

The significant population expansion signature, increasing population size shown in the BSPs and expansion times suggest that the Pyrenean lineage expanded during the Late Pleistocene. This lineage also may have had a refugium further north than traditionally recognized, separated from the southern refugium of the Iberian phylogroup and the northern refugia of the North-Central European phylogroup; it is restricted to Central, Western and South-Eastern France and North-Western Spain in continental Europe, but it is the only lineage found in Ireland and several islands off the west and north coasts of Britain. The region of the Dordogne in South-Western France was situated outside the LGM permafrost area and has temperate mammal fossil records dated to the end of the LGM; therefore, it has been suggested as another likely refugium north of the traditionally recognized southern refugia (Sommer and Nadachowski 2006). There, the Pyrenean lineage could have persisted and recolonised Western and Central France after the LGM, but SDM studies show that suitable climatic conditions during the LGM for *S. minutus* and other temperate small mammal species could have been more continuous and present further north (Fløjgaard et al. 2009, Vega et al. 2010b).

2.4.7 Origins of the Irish pygmy shrew

There are seven terrestrial small mammals in Ireland: *S. minutus*, *Apodemus sylvaticus*, *M. glareolus*, *Mus musculus*, *Rattus rattus*, *R. norvegicus* and *C. russula*, but only two have been present for a long time, *S. minutus* and *A. sylvaticus* (Martínková et al. 2007). How and when the pygmy shrew arrived and colonised Ireland is still under debate. If *S. minutus* arrived to Ireland on its own legs, then the colonisation would be concordant with the proposed migration route from Iberia and Western France to South-West Britain by an exposed coastline (Yalden 1982), but

this would not explain why other small mammal species did not arrive to Ireland following the same route. A possibility is that cold-tolerant small mammals survived close to the ice sheet at or before the LGM. For example, it was shown that the stoat *Mustela erminea* was present in Ireland before the LGM and spread throughout Ireland and Britain as glaciers retreated (Martínková et al. 2007). However, the pygmy shrew does not reach as far north as the stoat and it appears to be not as cold-tolerant, but a similar scenario cannot be entirely ruled out because the estimated population expansion times pre-date the LGM (although this could be related to the expansion signature found in the continental Pyrenean sample and there is a possibility of error in the molecular clock).

Alternatively, considerable phylogeographic and population genetics evidence for *S. minutus* has been gained favouring human-mediated introductions into Ireland and other islands off Britain from South-Western Europe during the Neolithic period (ca. 4–7 KYA): Mascheretti et al. (2003) showed sequence similarity between Andorran and Irish *S. minutus*; and McDevitt et al. (2009) provided strong evidence based on microsatellite data for a population expansion event for the pygmy shrew in Ireland 6.3 KYA, in the Neolithic, but could not provide a source area. In this study, the central position of samples from Navarra, Spain in the MJ network and the overall similarity of Irish, Pyrenean and Western French samples support the hypothesis that *S. minutus* colonised Ireland from Northern Spain, not from Britain, its closest landmass, or Northern France. The low genetic variability in Ireland in comparison to that in Britain found in this and other studies (McDevitt et al. 2009) also supports a recent human-mediated colonisation, followed by a population expansion event. Nonetheless, there is a clear genetic similarity of Irish, Orkney, Celtic fringe and continental haplotypes, which could potentially indicate a colonisation route from South-Western Britain. Two issues yet need to be resolved: 1) the timing of colonisation, based on Rogers' (1995) τ , does not concur

with a Neolithic colonisation; however, the mutation rate used here might not be suitable over short time frames (Ho et al. 2005, Ho and Larson 2006, but see Bandelt 2008), and 2) it still needs to be explained how a small mammal with high metabolic requirements such as the pygmy shrew survived a long trip and why other shrews, frequent in South-Western Europe, were not introduced the same way.

Further insights into the colonisation, migrations and morphological differences among Pyrenean, Irish, Orkney and the Celtic fringe samples will be discussed in Chapter 4.

2.4.8 Other considerations

The phylogeographic analyses presented here generally support the subspecific status of the genetic lineages described by Hutterer (1990), with distinct lineages in the Balkans, Iberia, Southern Italy and Northern-Central Europe, which roughly correspond to *S. m. gymnurus*, *S. m. carpetanus*, *S. m. lucanius* and *S. m. minutus*, respectively. However, there are no recent morphological analyses of *S. minutus* covering the full European range and there have not been comparisons between phylogeographic and morphometric findings to support this. As far as I know, there has only been one study that explored the morphological variation of *S. minutus* and compared it with molecular findings, but it covered a small part of the range and focused on the morphological and genetic variation within Italy and Northern-Central Europe (Vega et al. 2010a); the authors used a geometric morphometric technique coupled with tree-based phylogeographic analyses and showed that *S. minutus* from Southern Italy is genetically and morphologically distinct from northern populations, in agreement with the subspecific status of *S. m. lucanius*; however, the morphological and genetic differentiation in other regions was not analysed.

In the following chapter, I implement a geometric morphometrics approach and couple it with the phylogeographic findings obtained here to further explore the variation of *S. minutus* throughout its European range.

Chapter 3

Morphological diversity of *Sorex minutus* across Europe

3.1 Introduction

Morphometrics is the quantitative and comparative study of the variation and change of organismal form (Rohlf 1990). In biological studies, the analysis of morphological variation is of special concern for the understanding of ecological and evolutionary patterns and processes, and it is also important because organismal taxonomy is based on morphological traits. Several factors that cause morphological variation have been identified, including disease or injury, ontogenetic development, inbreeding, adaptation to local environments and long-term evolutionary diversification (Zelditch et al. 2004).

In the 1980s, the field of morphometrics was revolutionized (Rohlf and Marcus 1993, Adams et al. 2004) by the invention of coordinate-based methods, the development of the statistical theory of shape and its precise definition, and the computational use of transformation grids to visualize shape variation (Mitteroecker and Gunz 2009). This new morphometric approach was termed 'geometric morphometrics', which is based on the analysis of form (the shape and size of any object) based on Cartesian landmark coordinates, and the geometry of the landmark coordinates are preserved throughout the analysis (Zelditch et al. 2004, Mitteroecker and Gunz 2009).

The methods employed by geometric morphometrics originated from the fusion of geometric (or location) information with data on biological homology, combining geometry with biology (Bookstein 1982). Geometric morphometrics relies on the selection of landmarks, which are discrete anatomical points that should be

present in all specimens in the study, i.e., biologically homologous anatomical loci, also defined as points of correspondence on each object that match between and within populations (Dryden and Mardia 1998). To describe morphological variation properly, the selected landmarks must capture the form (size and shape) of the structure under study (Zelditch et al. 2004). Another characteristic of geometric morphometrics is the precise definition of shape and size, which in total represent the form of an object. Shape is defined as all the geometrical information that remains when scale, location and rotational effects are filtered out of an object (Kendall 1977). Size is defined by the scale of an object, which is mathematically independent of shape because it is filtered out according to Kendall's (1977) definition, and is calculated as the Centroid Size (CS): the square root of the sum of squared distances between each landmark and the centroid (or geometric centre of the object) (Bookstein 1991).

Because most morphological traits are under selection, the study of morphological variation can shed light on the impact of selection in adaptation and speciation processes; however, morphological variation is better understood when comparing it with results obtained from other methods, such as genetic, environmental, physiological or behavioral (Garnier et al. 2005). For example, several studies have used geometric morphometric techniques coupled with phylogenetic data and/or environmental correlates to provide a thorough characterization of species and population divergence with implications for the systematics, taxonomy and conservation of African murids (Fadda and Corti 2001), marmots (Cardini and O'Higgins 2004, Caumul and Polly 2005), spiny rats (Monteiro and dos Reis 2005) and ground squirrels (Gündüz et al. 2007), to evaluate the phylogenetic recoverability of skulls, mandibles and molars for the identification of karyotypic groups of fossils and infer divergence times of common shrew karyotypic races (Polly 2001, 2007), and to assess the correlation between

environmental components and geographical variation of vervet monkeys (Cardini et al. 2007) and punaré rats (Monteiro et al. 2003).

The wide geographic distribution of *Sorex minutus* and the amount of phylogeographic information available for this species makes it ideal for the study of intraspecific morphological variation. In this study I explored the following questions: 1) What is the morphological diversity of *S. minutus* and how is it distributed across Europe? 2) Do mandibles and skulls show the same or distinct patterns of morphological variation? 3) Can a latitudinal and/or longitudinal pattern for size and shape be identified? 4) Is there an allometric effect of size on shape? 5) To what extent does the morphological diversity resemble the phylogeographic structure detected previously with molecular markers? 6) To what extent does the morphological diversity resemble the taxonomical classification of *S. minutus* subspecies? To answer these questions, I employed a geometric morphometrics approach on mandible and skull samples of *S. minutus* obtained throughout its European range, and made use of the phylogeographic information obtained in the previous chapter. As far as I am aware, this is the first study that has analysed the morphological variation of *S. minutus* across its full European range based on a geometric morphometrics approach.

3.2 Materials and methods

3.2.1 Collection and preparation of samples

I acquired *S. minutus* and *S. volnuchini* skull and mandible samples during fieldwork and from museum or private collections. In total, I analysed 576 (left and right) mandibles and 385 skulls from Europe, including eight mandibles and skulls of *S. volnuchini* from the Anatolian peninsula, which were used as an outgroup where appropriate (Fig. 3.1A, B, Appendix 4). The sex was known for 254 mandible samples, of which 127 were males and 127 were females. For the skull sample,

there were 133 known males and 126 known females. Skulls and mandibles from specimens obtained during fieldwork were cleaned using a Papain method (White 2007) or using *Dermestes* sp. beetles. Some of the samples (mainly those from France) were obtained from owl pellets and were carefully cleaned using a small brush.

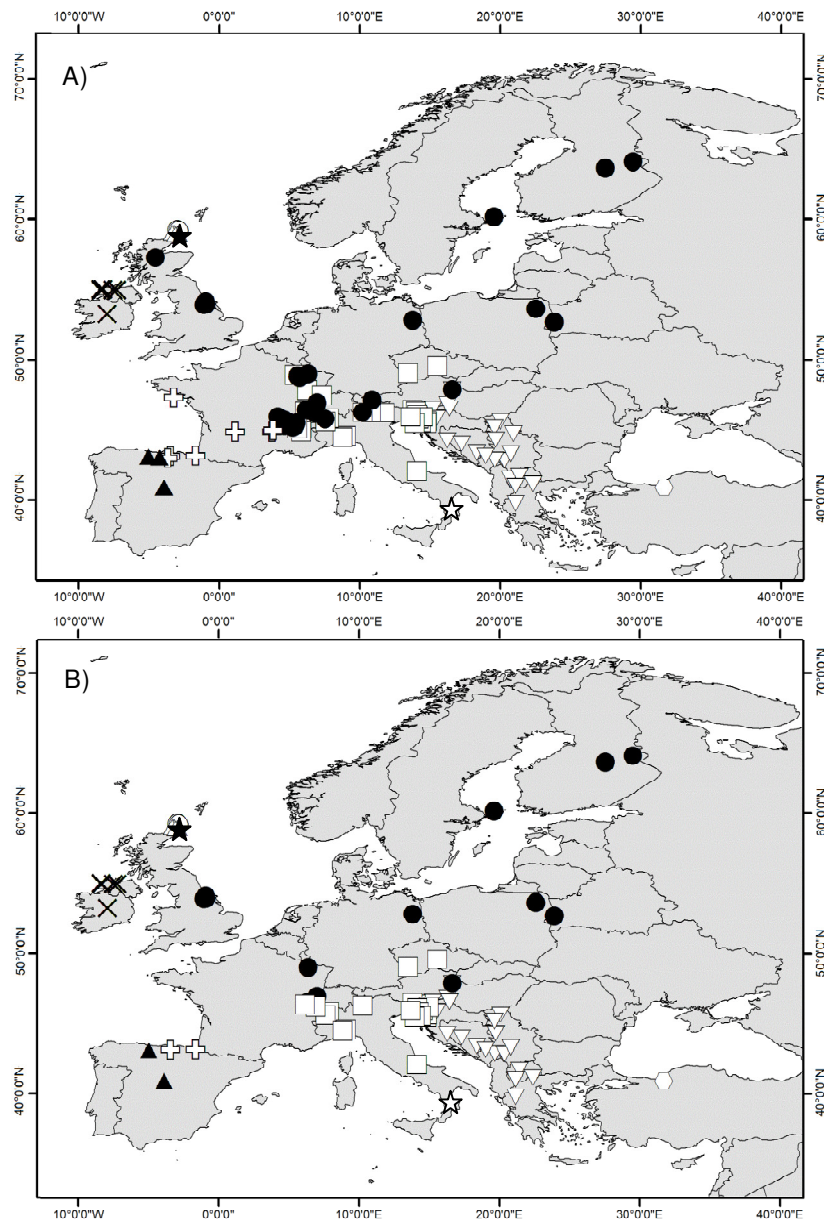


Figure 3.1. Samples of *Sorex minutus* for morphological analysis. A) Mandible dataset. B) Skull dataset. The symbols correspond to the different lineages detected previously with mtDNA. ● North-Central European, □ North-Central Italian, ▽ Balkan, ☆ South Italian, ▲ Iberian, ⊕ Pyrenean (continental and Belle Île, France), △ Orkney Mainland, ○ Westray, ★ South Ronaldsay, X Ireland, ⬡ *S. volnuchini* (outgroup).

3.2.2 Digitization of mandibles and skulls

Photographic images of the external side of left and right mandibles and the ventral side of skulls were taken using a Canon EOS 350D camera (8 million pixels resolution) equipped with a macro lens and extension tubes at a fixed distance of 33 cm (for mandibles) and 34 cm (for skulls). Mandibles were placed on top of an inverted glass Petri dish (to avoid shadows surrounding the mandible) under the camera lens. Skull samples were placed on a purpose-built polystyrene and plasticine cradle leaving the ventral side parallel to the lens, judged by eye (Jones 2009). In each photograph, a small piece of graph paper was included as a scale and the sample was placed in the middle of the image area to avoid parallax.

Morphological analyses were carried out using the 'tps-Series' software (by FJ Rohlf, available at <http://life.bio.sunysb.edu/morph/>). Eighteen landmarks were placed on the external side of each mandible and 19 landmarks were placed on the right and left sides of the ventral cranium using tpsDig2 (Fig. 3.2A, B). The sample images were randomly ordered in tpsUtil before digitizing the landmarks to avoid any bias by repeatedly placing landmarks on samples from the same locality. The selected landmarks provided a comprehensive sampling of the morphology of the biological structures under study (Zelditch et al. 2004).

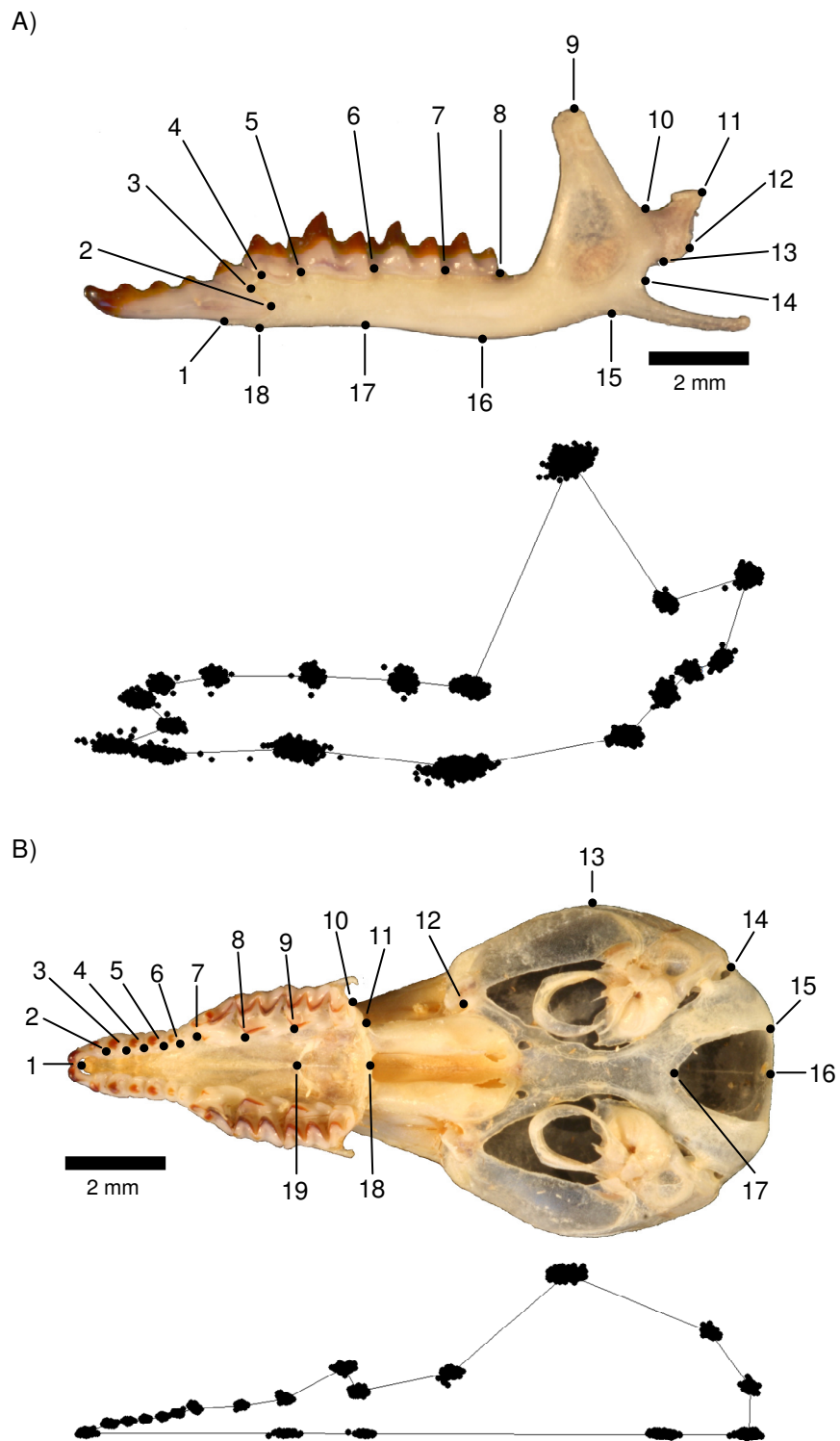


Figure 3.2. Landmarks placed on A) mandibles and B) skulls of *Sorex minutus*. For simplicity, only the left sides are shown. The diagrams show the observed dispersion of landmarks for all the aligned specimens.

3.2.3 Statistical analysis of landmark coordinates data

The statistical analyses were performed with SPSS/PASW Statistics version 17 (IBM), PAST version 1.97 (Hammer et al. 2001) or directly with the tps-Series software.

The size of each mandible and skull was estimated using the CS, obtained by tpsRelw and was transformed with natural logarithms. The landmark configurations were scaled to unit CS, translated and rotated using the Generalised Procrustes Analysis (GPA), which minimizes the differences between configurations by minimizing the Procrustes distances between corresponding landmarks and gives the average landmark configuration (Rohlf and Slice 1990). The Procrustes distance is the shortest distance between corresponding landmarks, and it is computed as the square root of the sum of squared distances between two centred, scaled and optimally rotated configurations of landmarks (Zelditch et al. 2004).

The Procrustes distance is an angle expressed in radians, which gives the geodesic distance between two points in Kendall's shape space, and it corresponds to the distance along the surface of a sphere (Kendall 1977). Because all shapes are in non-Euclidean shape space (i.e., lie in Kendall's shape space), the shortest distance between two points is a curve (Zelditch et al. 2004). To perform statistical analyses, the Procrustes distances have to be approximated to an Euclidean space using, in this case, an orthogonal projection. The average configuration is the point of tangency between shape space and Euclidean shape space. Then, I used tpsSmall to test if shape variation in the mandible and skull samples was small enough to allow an approximation to Euclidean tangent space. A strong positive correlation ($R = 0.9999$) was found between tangent space distances and Procrustes distances among samples; therefore, the orthogonal tangent space approximation for shape analysis was validated.

A weight matrix (W) incorporating Uniform ($n = 2$ for mandibles and skulls) and non-Uniform ($n = 30$ for mandibles and $n = 32$ for skulls) components was extracted using the GPA (Bookstein 1996). Both components were interpreted and pooled together as shape variables ($n = 32$ for mandibles and $n = 34$ for skulls). The Uniform components of shape deformation do not require bending energy to shift from the average configuration to the observed shape, including transformations such as translation, rotation and scaling, which do not alter shape, and compression, dilation and shear, which do alter shape. The non-Uniform components do require bending energy to alter shape, have a location and a spatial extent, and describe the patterns of relative landmark displacements in relation to the average configuration (Zelditch et al. 2004).

First, to check for landmark placement repeatability, I photographed and digitized 23 mandibles and 28 skulls five times each, to give a total of 115 and 140 photographs, respectively. Digital images were randomized with tpsUtil and the appropriate landmarks were placed on each mandible and skull in tpsDig2. The CS values of mandibles and skulls among photographs were subjected to Analysis of Variance (ANOVA) and the W matrices among photographs were analysed with Multivariate Analysis of Variance (MANOVA) (only the landmark configurations on left mandibles and the left side of skulls were analysed). Second, the X coordinates of right mandibles and the Y coordinates of the right side of skulls were multiplied by -1 to create mirror images for both sides of the bilateral structures. Then, left and right mandibles and the left and right sides of skulls were compared by ANOVA for CS, and by MANOVA or non-parametric MANOVA (Anderson 2001) for W to check for asymmetry. Third, male and female samples were compared by ANOVA for CS, and by MANOVA or non-parametric MANOVA for W to check for sexual dimorphism.

The pattern of shape variation related to mandible and skull size change (allometry) was compared for the *S. minutus* data set (excluding the outgroup) using tpsRegr. The optimal measure of allometry is the regression of shape on the logarithm of CS (Mitteroecker and Gunz 2009). Multiple regressions of shape variables on latitude and longitude for the *S. minutus* data set (excluding the outgroup) were also performed with tpsRegr to estimate and visualise their effects on shape.

Because of the relatively small number of individuals from each location, and for the purpose of this study, I pooled the samples into 11 mutually exclusive groups according to their cytochrome (*cyt*) *b* phylogroup membership, designated as Iberian, Balkan, North-Central Italian, North-Central European, South Italian, Pyrenean (including the samples from the continent and Belle Île, France) and outgroup (*S. volnuchini* samples), and to their island origin, designated as Ireland, Orkney Mainland, Westray and South Ronaldsay groups. Normality tests were performed for the CS of all groups. The mandible CS distributions of Balkan, Iberian and South Italian groups, and skull CS distributions of Iberian, Orkney Mainland and South Italian groups were significantly different from a normal distribution, but for the purpose of this study were not excluded from the analysis; quantile-quantile plots only showed small deviations of the observed CS from the expected normal distributions (data not presented).

Mandible and skull size differences among groups were evaluated by ANOVAs and visualised with box plots. I performed a Tukey–Kramer post-hoc test on CS as it allows for unequal sample size (Sokal and Rohlf 1995). Levene's test was performed to detect heteroscedasticity (non-equality of error of variances across groups). Although ANOVAs are relatively robust to heteroscedasticity (Zelditch et al. 2004), if Levene's test gave significant results, I also performed the conservative non-parametric Kruskal-Wallis test for the analysis of CS variance and

a Tamhane non-parametric post-hoc test, both of which do not assume equal variances. A linear regression was performed to assess how group mean CS for mandibles and skulls varied with latitude and longitude (in decimals) treated as independent variables.

Mandible and skull shape differences among groups were evaluated with MANOVAs on W (i.e., shape variables), followed by Hotelling T^2 tests for multivariate comparisons performed in PAST. Levene's tests were also performed for each shape variable among groups in SPSS and, if significant deviations from the assumption of homogeneity of variances were found, non-parametric MANOVAs among groups were performed in PAST.

Ordination of the samples was carried out through Principal Component Analysis, i.e., Relative Warp (RW) Analysis (Rohlf 1993), on the shape variables using *tpsRelw* for the mandible and skull data sets. RW Analysis was also conducted on the average (consensus) configurations of the 11 groups for the mandible and skull data sets. RW Analysis replaces the original shape variables (the W matrix) with Principal Components, which are linear combinations of the original variables but independent from each other (Zelditch et al. 2004). Shape changes in the RW space were visualised as thin-plate spline (TPS) transformation grids (Bookstein 1989) obtained with *tpsSpline*. The TPS is a continuous interpolating function that extends between the landmarks and describes the shape variation as a deformation from the average configuration, which can be visualized as transformation grids (Zelditch et al. 2004).

The Procrustes distances among the average configurations of the groups, for the mandible and skull data sets, were then computed by the program *tpsSmall* and entered into PAST to produce a distance tree using the Neighbor-Joining (NJ) method (discussed in Chapter 2) to evaluate the morphological relationships. The support of the branches was assessed using 10,000 bootstraps.

The geographic midpoints for the 11 groups, using the coordinates of the sampling localities, were calculated with the Geographic Midpoint Calculator (available at <http://www.geomidpoint.com/>). The geographic midpoints were then used to obtain the pairwise geographic distances among groups with the Geographic Distance Matrix Calculator version 1.2.3 (by PJ Ersts, available at http://biodiversityinformatics.amnh.org/open_source/gdmg). A Mantel test was performed in PAST to examine the correlation between the pairwise Procrustes distances and the pairwise geographic distances among groups. Also, Mantel tests were performed between pairwise Procrustes distances and pairwise genetic differentiation (F_{ST}) and genetic divergence (D_a) values of the *cyt b* phylogroups (obtained in Chapter 2). The significance of the test was obtained through a permutation procedure (10,000 bootstraps) used to create an empirical null distribution. The overall shape diversity for mandibles and skulls was visualised as TPS deformations and plotted next to the NJ trees of Procrustes distances among the groups.

A Discriminant Analysis (DA) was performed to predict group membership and to differentiate among the groups by a Canonical Variates Analysis (CVA), using the shape variables as predictors for mandible and skull data sets. The first two functions were used to graph the samples separated by group membership. The DA builds a model to predict the group membership of samples using linear combinations of the predictor variables that best discriminate between the groups. The functions are generated from a selection of samples for which group membership is known and then applied to samples with unknown group membership. I used a cross-validation method in SPSS, repeatedly treating $n - 1$ out of n samples as the 'validating' dataset to determine the discrimination rule and using the rule to classify the one observation left out. I also implemented a pre-validation method in SPSS to predict group membership, selecting those samples

with 'known' group membership for 'training' the model (i.e., using the samples for which I could be absolutely confident about group membership, such as island samples or morphological samples with genetic data) and leaving other samples aside, then applying the trained model to predict group membership of the unused samples.

3.3 Results

3.3.1 Landmark placing error

There were no significant differences with respect to CS or *W* among the five repeated photographs of mandibles ($F_{4, 110} = 0.0050$, $p > 0.05$; Wilks' $\lambda = 0.5117$, $F_{128, 316.9} = 0.4499$, $p > 0.05$) and skulls ($F_{4, 135} = 0.0700$, $p > 0.05$; Wilks' $\lambda = 0.5666$, $F_{136, 408.7} = 0.4610$, $p > 0.05$); therefore, landmarks were placed accurately in each sample and the variation found in this study was not related to the misplacement of landmarks.

3.3.2 Asymmetry and sex differences

There were no significant differences with respect to CS between left and right mandibles ($F_{1, 1150} = 1.7770$, $p = 0.1830$) or the right and left sides of skulls ($F_{1, 768} = 0.1490$, $p = 0.6990$). However, there were significant shape differences for the same comparisons of mandibles (Wilks' $\lambda = 0.6197$, $F_{32, 1119} = 21.4600$, $p < 0.0001$) and skulls (Wilks' $\lambda = 0.4434$, $F_{34, 735} = 27.1400$, $p < 0.0001$). The assumption of homogeneity of variance for *W* of mandibles and skulls was violated, but non-parametric MANOVAs also revealed significant differences between left and right mandibles ($F_{32, 1119} = 21.4600$, $p < 0.0001$) and the right and left sides of skulls ($F_{34, 735}$, $p < 0.0001$). To avoid the effects of asymmetry, I averaged both sides of mandibles and skulls in all subsequent analyses.

There were no significant differences between male and female mandibles for CS ($F_{1, 148} = 0.4840$, $p = 0.4870$) and W (Wilks' $\lambda = 0.8123$, $F_{34, 117} = 0.8447$, $p = 0.7030$; non-parametric MANOVA $F_{34, 117} = 1.4250$, $p = 0.1710$). Similarly, there were no significant differences between male and female skulls for CS ($F_{1, 516} = 0.0320$, $p = 0.8580$) and W (Wilks' $\lambda = 0.9220$, $F_{34, 483} = 1.206$, $p = 0.2010$; non-parametric MANOVA $F_{34, 483} = 1.1290$, $p = 0.3105$). All subsequent analyses on mandibles and skulls were performed pooling all samples irrespective of sex.

3.3.3 Morphometric analysis of mandibles

Mandible CS decreased notably with increasing latitude (Table 3.1), as shown by box plots (Fig. 3.3). The South Italian, Iberian and Balkan groups, as well as the outgroup, had the biggest mandibles with quartile boxes well above the sample average. The median CS of Pyrenean and North-Central Italian mandibles were also bigger than the sample average, while the other groups (North-Central European, Ireland, Orkney Mainland, South Ronaldsay and Westray) had median values below the sample average. Nevertheless, the group ranges were very widespread and overlapping, especially for the Balkan, Pyrenean and North-Central Italian groups.

Table 3.1. Centroid size statistics for *Sorex minutus* mandibles.

Phylogroup	n	Mean	Median	SD	SE
Balkan	51	2.4065	2.4097	0.0303	0.0042
Iberian	13	2.3997	2.4028	0.0220	0.0061
Ireland	63	2.3486	2.3505	0.0232	0.0029
North-Central European	150	2.3359	2.3388	0.0279	0.0023
North-Central Italian	79	2.3803	2.3798	0.0279	0.0023
Orkney Mainland	52	2.3575	2.3606	0.0231	0.0032
Orkney South Ronaldsay	40	2.3390	2.3392	0.0141	0.0022
Orkney Westray	40	2.3590	2.3567	0.0231	0.0032
Pyrenean	77	2.3719	2.3730	0.0353	0.0040
South Italian	3	2.4053	2.4065	0.0289	0.0167
Outgroup	8	2.4165	2.4114	0.0214	0.0076

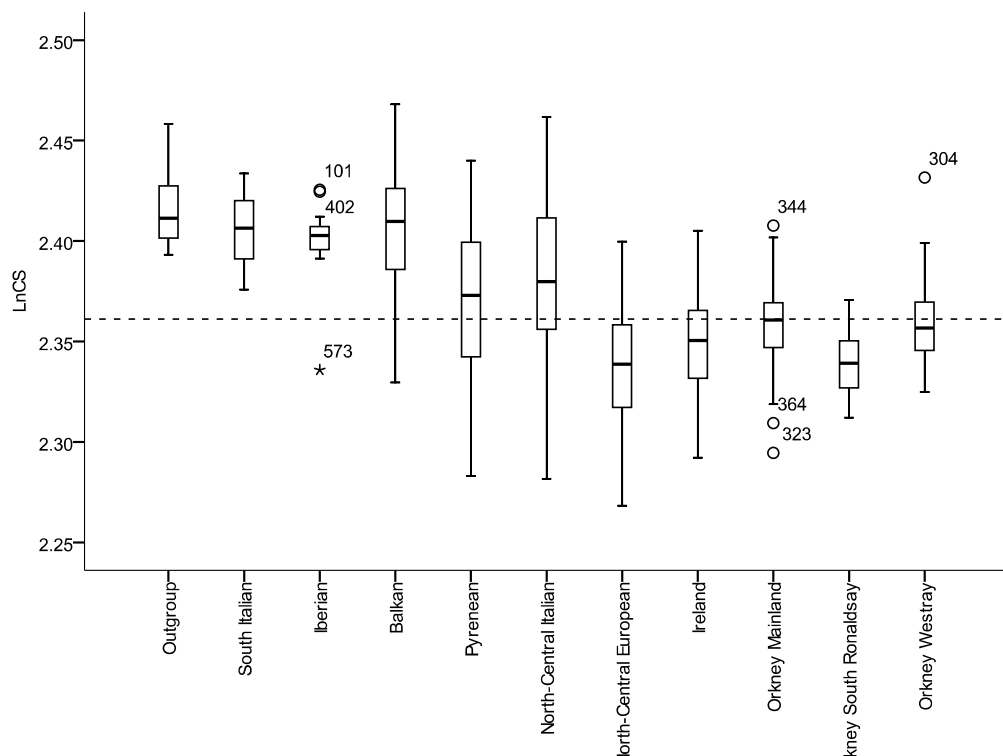


Figure 3.3. Box plots of mandible Centroid Size (CS; transformed with natural logarithms) of *Sorex minutus*. There is a decrease of CS from Southern (left) to Northern (right) latitudes. The horizontal dashed line corresponds to the sample mean. The outgroup (*S. volnuchini*) is shown for purposes of comparison.

The ANOVA revealed that there were significant CS differences among the *S. minutus* groups ($F_{9, 558} = 38.8850$, $p < 0.0001$); however, because the assumption of homogeneity of variances was violated (Levene's statistic $_{9, 558} = 8.5210$, $p < 0.0001$), a non-parametric test was performed and it was also significant ($H_9 = 205.5730$, $p < 0.0001$). Parametric (Tukey–Kramer) and non-parametric (Tamhane T2) post-hoc tests showed that nearly 57% of the pairwise comparisons were significantly different (Appendix 5). In the non-parametric post-hoc tests, the South Italian, Iberian and Balkan groups were not significantly different from each other, having similar and large mandible size. Notably, the mandibles CS of the Pyrenean

and Ireland groups were significantly different, but Ireland was not significantly different from any of the Orkney islands, and only South Ronaldsay was significantly different from the Pyrenean group and the other two Orkney islands.

The linear regressions showed different and significant tendencies of CS with latitude and longitude (Fig. 3.4A, B); I found decreasing CS with increasing latitude, as expected from the box plots, but also an increasing CS with increasing longitude. There was a relatively stronger relationship and higher proportion of CS variation explained by latitude ($R_{\text{Latitude}} = -0.4580$, $R^2_{\text{Latitude}} = 0.2096$, $p < 0.0001$) than longitude ($R_{\text{Longitude}} = 0.2230$, $R^2_{\text{Longitude}} = 0.0499$, $p < 0.0001$).

There was a highly significant allometric effect of CS on mandible shape (Goodall's $F_{32, 18112} = 11.1718$, $p < 0.0001$), but it explained a small percentage of shape variation among individuals (about 2%). In larger mandibles, there was an apparent forward movement of the landmarks on the lower part of the mandible (landmarks 1 and 16 – 18), in relation to the landmarks between teeth alveoli (landmarks 3 – 8), and there was some variation in the position of the condyloid process (landmarks 10 – 14) in relation to other landmarks (Fig. 3.5A).

Latitude and longitude had highly significant effects on mandible shape (Latitude Goodall's $F_{32, 18112} = 30.5923$, $p < 0.0001$; Longitude Goodall's $F_{32, 18112} = 18.8495$, $p < 0.0001$) and explained a higher percentage of shape variation than CS variation (5.13% and 3.22%, respectively). In individuals from southern latitudes there was a relative forward shift of the coronoid process, plus a backward movement of landmarks 3 – 8 between teeth alveoli and forward movement of landmarks 1, 16 – 18 (Fig. 3.5B). Individuals in eastern longitudes also showed a relative forward shift of the coronoid process, backward movement of landmarks between teeth alveoli and forward movement of landmarks on the lower side of the mandible, but these changes were less obvious than with latitude (Fig. 3.5C).

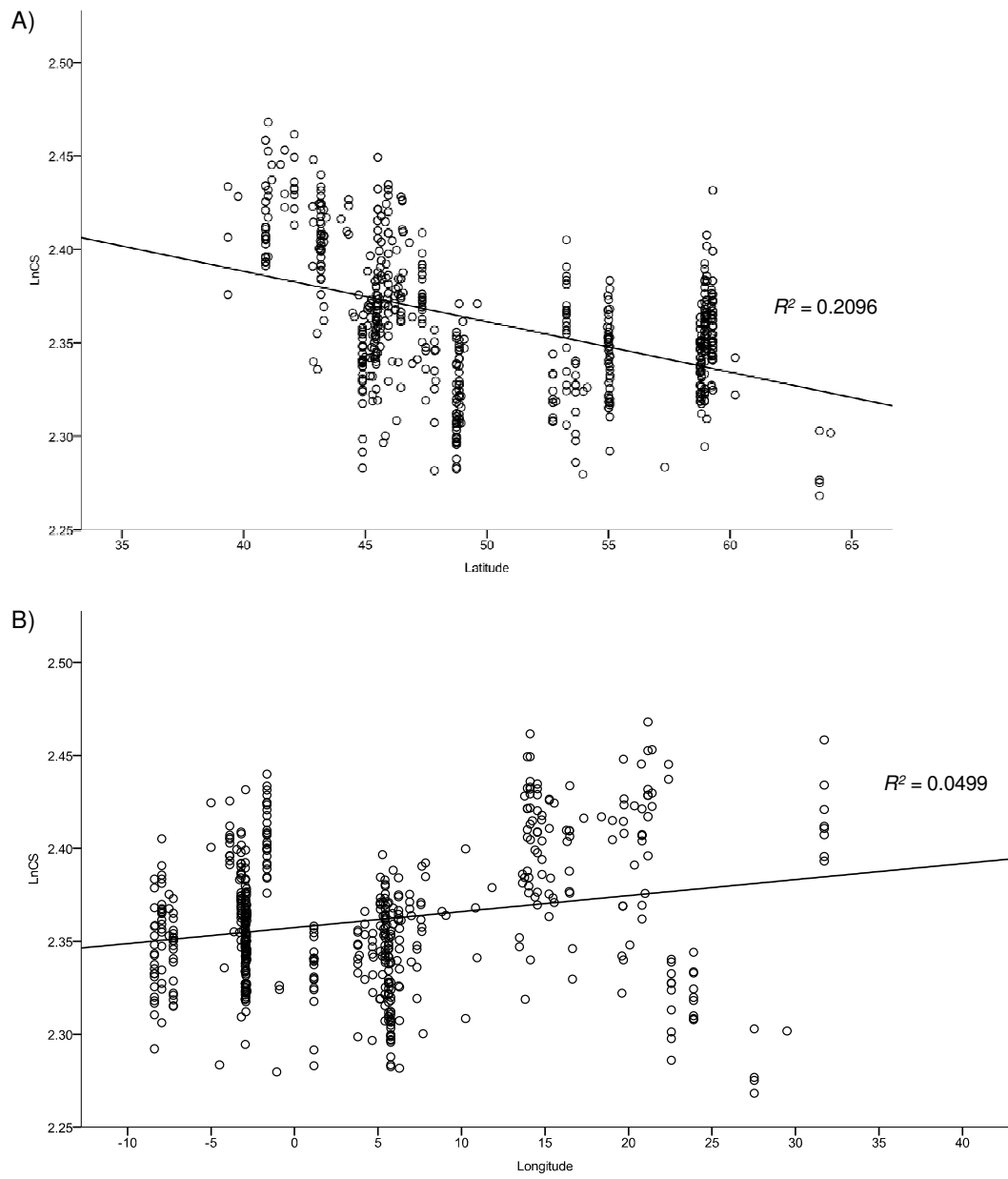


Figure 3.4. Linear regressions of Centroid Size (CS; natural log-transformed) on A) latitude and B) longitude for *Sorex minutus* mandible samples.

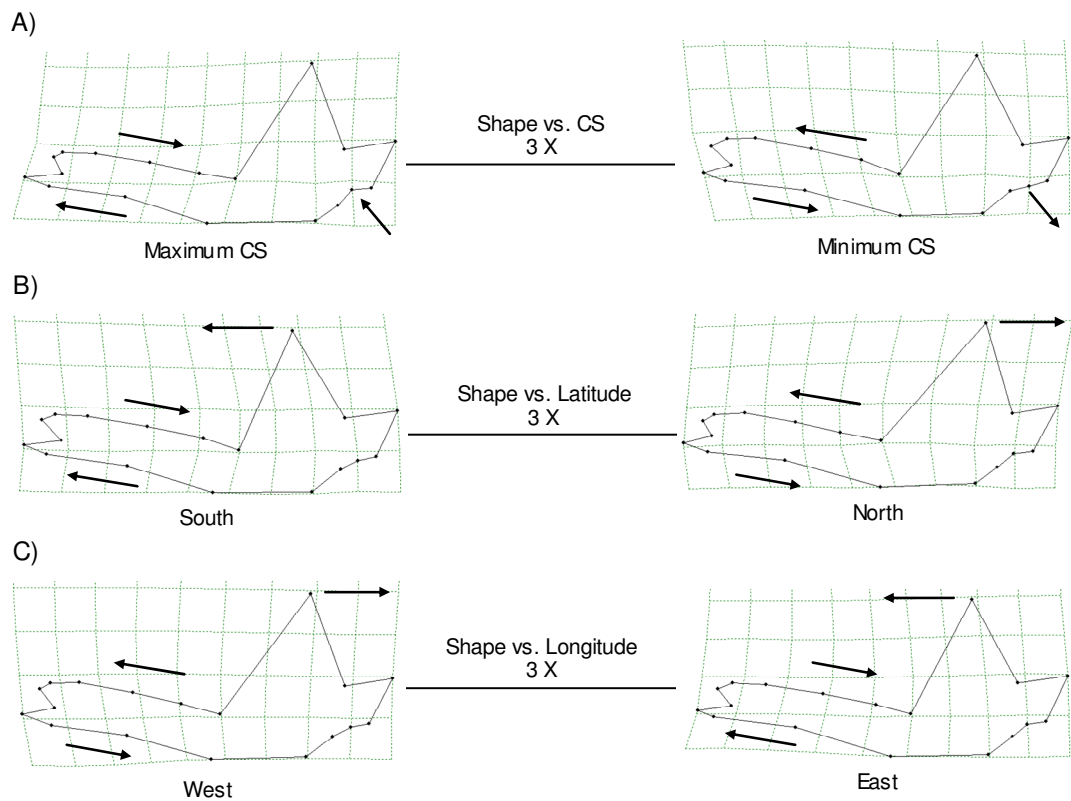


Figure 3.5. Multiple regressions of shape on A) Centroid Size (CS), B) latitude and C) longitude for *Sorex minutus* mandibles. Transformation grids were exaggerated 3 times for purposes of visualisation. Arrows help to evaluate the relative movements of landmarks.

The RW Analysis showed that shape variation was not subdivided in any systematic way. There was a nearly uniform ordination of the samples around the average configuration (Fig. 3.6). The first three RWs explained cumulatively 48.26% of the total variance (20.21%, 14.52% and 13.53%, respectively). There was little shape deviation from the average configuration, but the landmark movements along RW1 seem to follow the latitudinal pattern described previously.

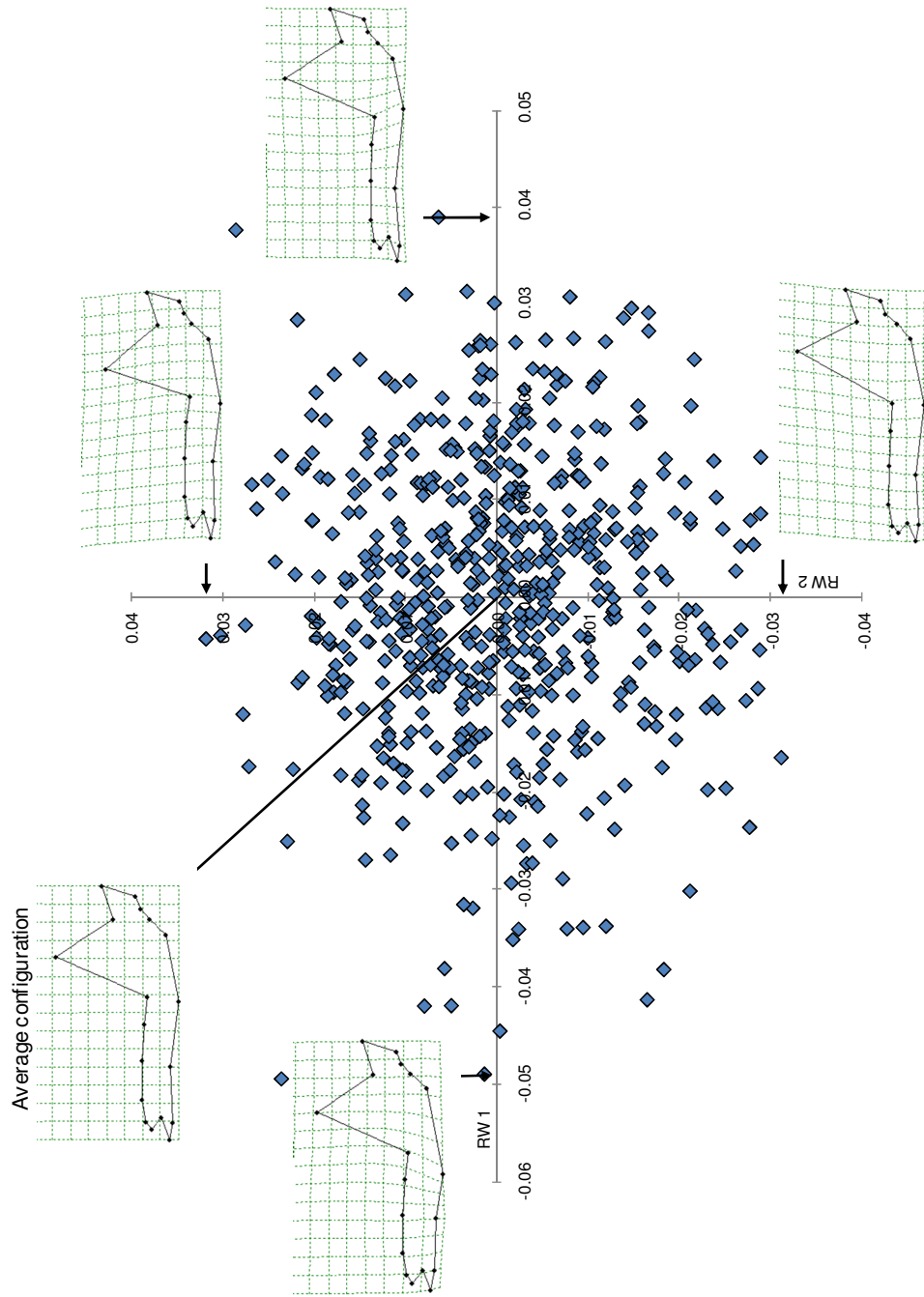


Figure 3.6. Relative Warp Analysis of shape variables of *Sorex minutus* mandibles. The maximum and minimum transformation grids on the first two Relative Warps (RW1 and RW2), and the average configuration are shown for purposes of visualisation.

The parametric and non-parametric MANOVAs, in contrast, revealed significant differences among groups (Wilks' $\lambda = 6.3 \times 10^{-5}$, $F_{320, 5136} = 28.02$, $p < 0.0001$; non-parametric MANOVA $F_{320, 5136} = 10$, $p < 0.0001$), and the post-hoc tests showed that nearly 70% of all pairwise comparisons were significant (Appendix 6). Most of the non-significant differences involved comparisons with the South Italian and Iberian groups, likely a reflection of the small sample size. Including the CS as a covariate of shape variables or including the outgroup in the MANOVA made no differences to the outcome.

The discriminant function analysis allowed further exploration of the differences in mandible shape among groups (separated into phylogroups and island groups, accordingly). This analysis correctly classified 67.7% of the individuals to their predefined group, but using a cross-validation method only 55.4% were properly classified, a matter of chance rather than clear shape differences among groups. Using a pre-validation method, training the classification method with those samples with 'known' group membership, the discriminant function analysis correctly classified 86.9% of selected individuals, and it decreased to 67.3% with the cross-validation method.

For purposes of visualisation, a scatter plot of the first two canonical variates is presented with group memberships and their group centroids (Fig. 3.7): the shape distribution of the North-Central European, Pyrenean, North-Central Italian, South Italian, Balkan and Iberian groups mostly overlapped; however, island samples were more easily discriminated from the rest, especially those from Westray, suggesting that there were shape differences between island and continental samples.

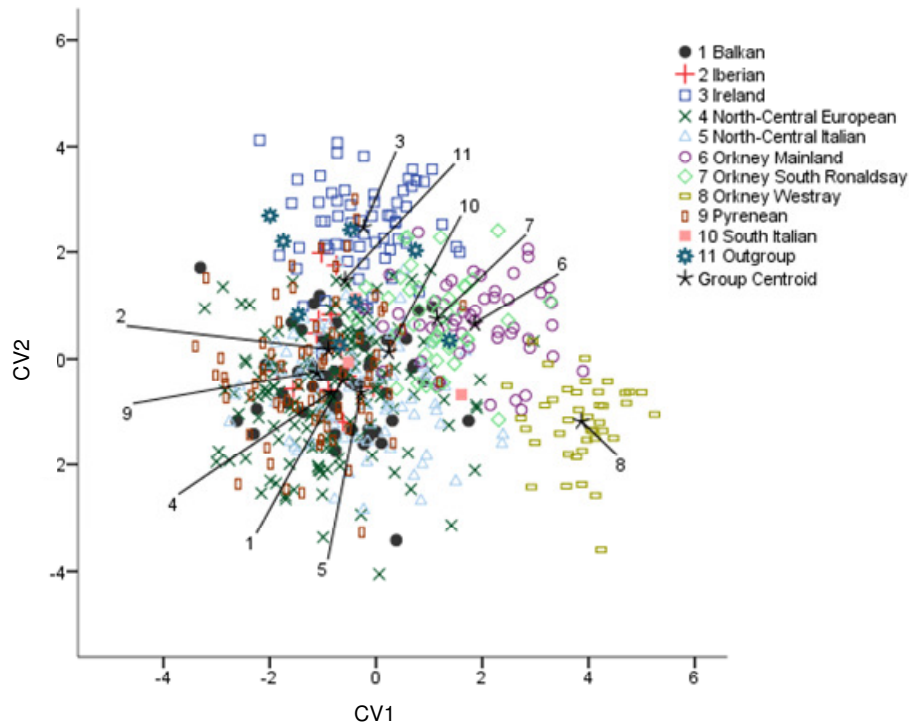


Figure 3.7. Canonical Variate Analysis of shape variables of *Sorex minutus* mandibles showing group differences. The first two canonical variates (CV) were used to describe variation among groups.

Similarly, the unrooted NJ tree of Procrustes distances among groups revealed that island samples clustered separately from continental ones, with the Orkney islands clustering with the South Italian group and the Outgroup, but separate from the Pyrenean, Iberian, Balkan, North-Central European and North-Central Italian groups (Fig. 3.8A). The South Italian, Westray and Outgroup groups were morphologically very distinct from any other groups, with large Procrustes distances, while the Orkney Mainland and South Ronaldsay groups clustered together (Fig. 3.8A). The rooted tree showed a slightly different topology, with Ireland closer to continental groups than to the Orkney islands, and the continental

groups clustering together (Fig. 3.8B). Rooting the tree still showed that Orkney Mainland and South Ronaldsay, and the North-Central Italian and North-Central European groups formed supported groups, and that the South Italian and Westray groups were the most morphologically divergent (Fig. 3.8B).

The transformation grids revealed that the three Orkney islands had notable backward shifts of the coronoid process in comparison to other groups, with Westray also showing pronounced variation in the frontal part of the mandible, whereas in the Iberian and Balkan groups the coronoid process moved slightly forward (Fig. 3.8A, B). The shape variation corresponded to the latitudinal shape change described previously. The South Italian group also had marked landmark variation and had a wider mandible (Fig. 3.8A, B); however, the relatively high pairwise Procrustes distances could be a result of small sample size.

There was no similarity between the NJ trees of Procrustes distances and the phylogenetic tree, and the amount of morphological variation did not seem to parallel the observed genetic distances (Fig. 3.8). Moreover, the Mantel tests revealed that there were significant correlations between Procrustes distances and geographic distances ($R = 0.3706$, $p = 0.0252$), but not with genetic differentiation (F_{ST} ; $R = -0.0509$, $p = 0.6144$) or genetic divergence (D_a ; $R = 0.0645$, $p = 0.2610$) among groups. These results were consistent with the correlations of shape with latitude and longitude.

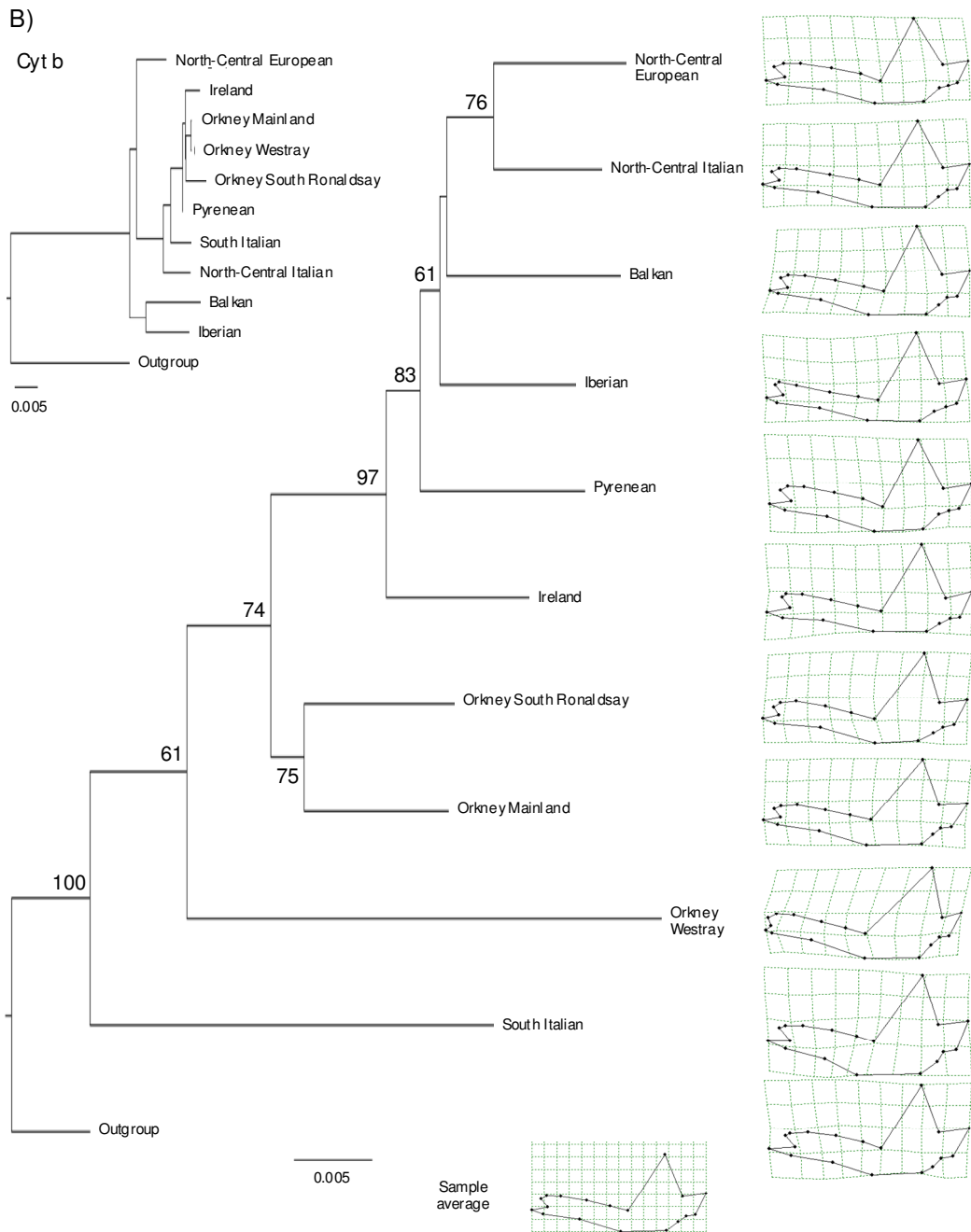


Figure 3.8. A) Unrooted and B) rooted Neighbor-Joining (NJ) trees constructed using mandible Procrustes distances among *Sorex minutus* groups. Branch support is shown as bootstrap values (10,000 replications). The grids on the right correspond to shape deformation per group from the average configuration. Inset: NJ trees based on genetic distances obtained in Chapter 2, shown for purposes of comparison.

3.3.4 Morphometric analysis of skulls

Skull CS showed less variation than mandible size among European regions, and had no apparent decreasing or increasing tendency with latitude (Table 3.2), as shown by the box plots (Fig. 3.9). The Iberian group had the biggest skulls, while the North-Central European had the smallest skulls on average but with a large variability. The median CS for the rest of the groups was similar to the sample average.

Table 3.2. Centroid size statistics for *Sorex minutus* skulls.

Phylogroup	n	Mean	Median	SD	SE
Balkan	46	3.0928	3.0949	0.0276	0.0041
Iberian	12	3.1270	3.1366	0.0354	0.0102
Ireland	60	3.0901	3.0897	0.0388	0.0058
North-Central European	45	3.0688	3.0654	0.0388	0.0058
North-Central Italian	57	3.0949	3.0943	0.0221	0.0029
Orkney Mainland	50	3.0983	3.0951	0.0280	0.0040
Orkney South Ronaldsay	37	3.0983	3.0997	0.0127	0.0021
Orkney Westray	39	3.1044	3.1048	0.0131	0.0021
Pyrenean	28	3.0947	3.0951	0.0174	0.0033
South Italian	3	3.0929	3.1002	0.0177	0.0102
Outgroup	8	3.0946	3.1012	0.0198	0.0070

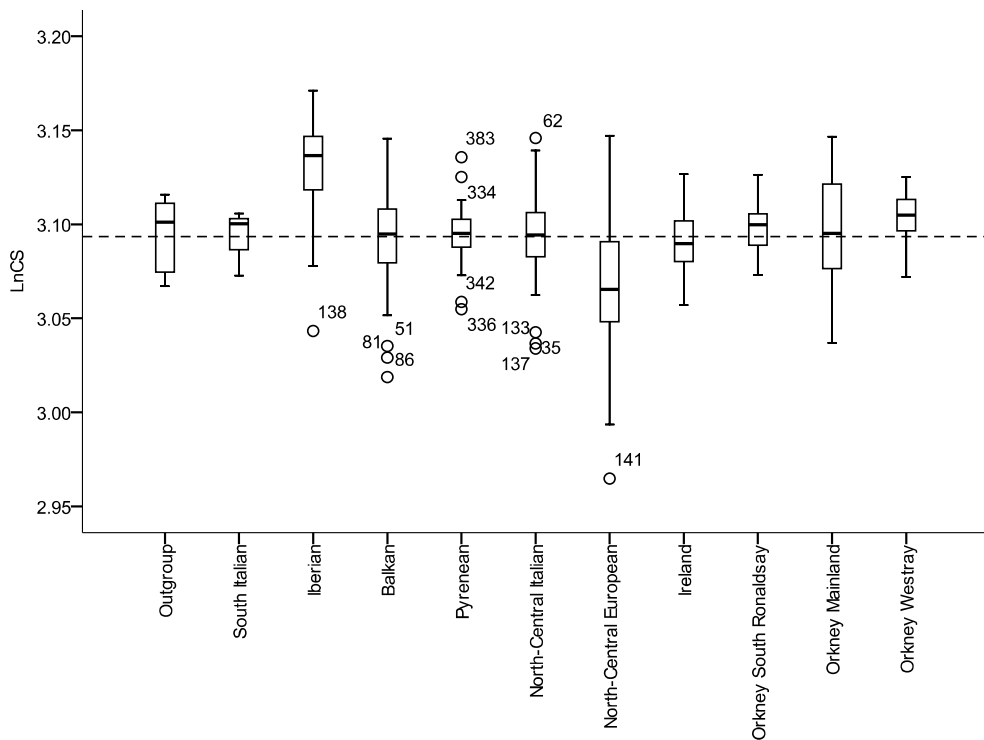


Figure 3.9. Box plots of skull Centroid Size (CS; natural log-transformed) of *Sorex minutus*. There is no apparent tendency from Southern (left) to Northern (right) latitudes. The horizontal dashed line corresponds to the sample mean. The outgroup (*S. volnuchini*) is shown for purposes of comparison.

The ANOVA on skull CS also revealed, as with mandibles, that there were significant differences among groups ($F_{9,367} = 9.1040$, $p < 0.0001$); however, the assumption of homogeneity of variances was violated (Levene's statistic $_{9,367} = 7.9060$, $p < 0.0001$), but the non-parametric test was also significant ($H_9 = 53.1750$, $p < 0.0001$). Parametric (Tukey–Kramer) and non-parametric (Tamhane T2) post-hoc tests revealed that nearly 31% and 20% pairwise comparisons were significantly different, respectively, a lower number of significant differences with respect to CS of skulls than for mandibles. In the parametric post-hoc tests all the significant pairwise comparisons involved the Iberian and North-Central European groups, but in the non-parametric tests the significant values only involved the

North-Central European group, except for a significant value between Ireland and Westray groups (Appendix 7).

Skull CS showed a minor decreasing tendency with increasing latitude and longitude. The linear regression of skull CS on latitude (Fig. 3.10A) was significant but less strong than that previously found in mandibles ($R_{\text{Latitude}} = -0.1090$, $R^2_{\text{Latitude}} = 0.0120$, $p = 0.0320$). The linear regression of skull CS on longitude (Fig. 3.10B) was significant and stronger than latitude, and it was as strong as that previously found with mandibles but it was negatively correlated ($R_{\text{Longitude}} = -0.2220$, $R^2_{\text{Longitude}} = 0.0490$, $p < 0.0001$).

There was a highly significant allometric effect of CS on skull shape (Goodall's $F_{34, 12750} = 4.7488$, $p < 0.0001$), but it only explained a small percentage of shape variation among individuals (1.25 %), in a similar fashion as found for mandibles. In bigger skulls, there was an apparent outward movement of landmark 7 in relation to other landmarks between teeth alveoli (landmarks 2 – 6, 8 and 9) resulting in a wider separation of the upper premolars, there was an inward relative movement of landmark 2 resulting in narrower and more pointed snouts, and there were backward movements of landmarks 18 and 19 resulting in the lengthening of the maxilla and pre-maxilla (Fig. 3.11A).

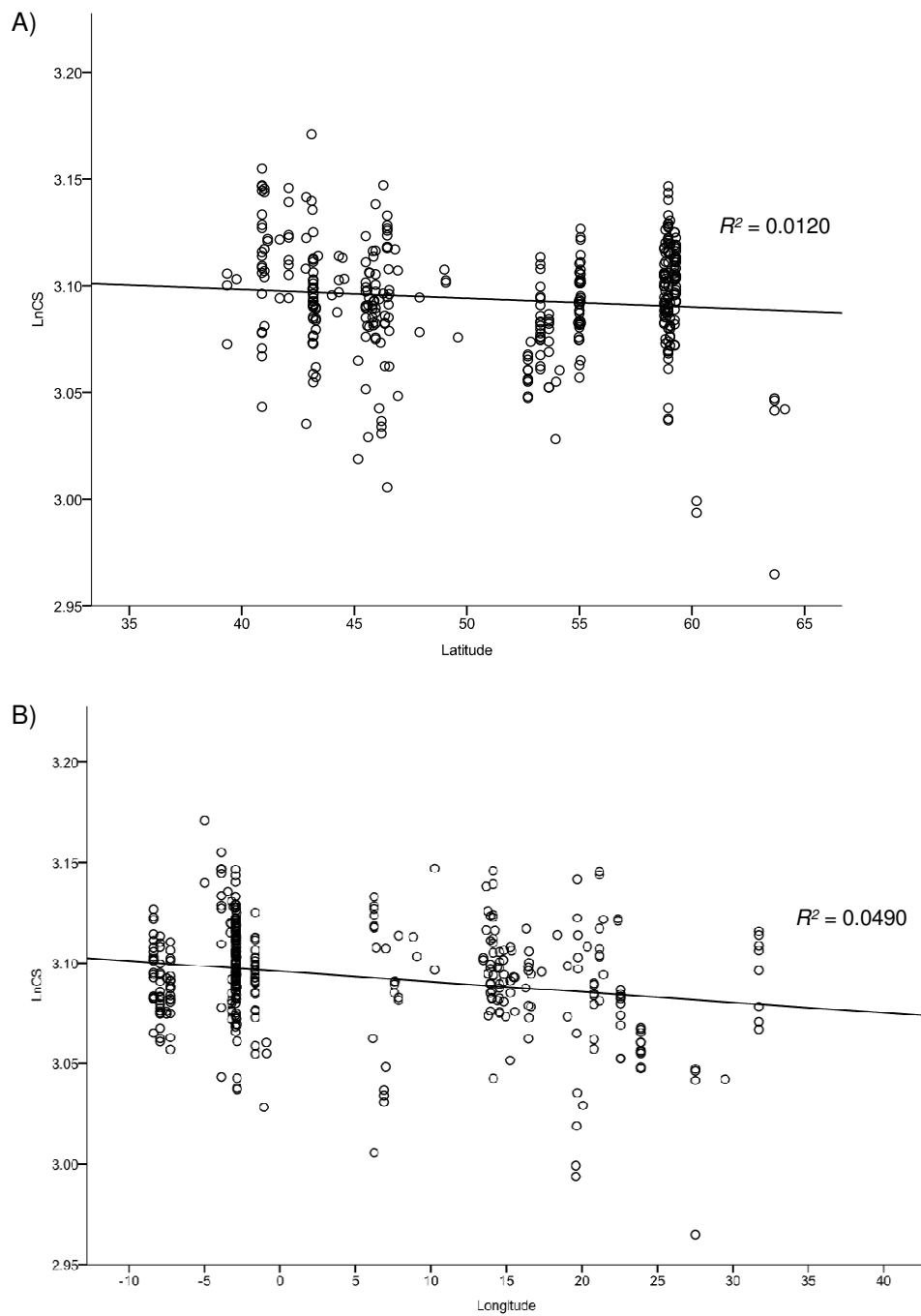


Figure 3.10. Linear regressions of Centroid Size (CS; transformed with natural logarithms) on A) latitude and B) longitude for *Sorex minutus* skull samples.

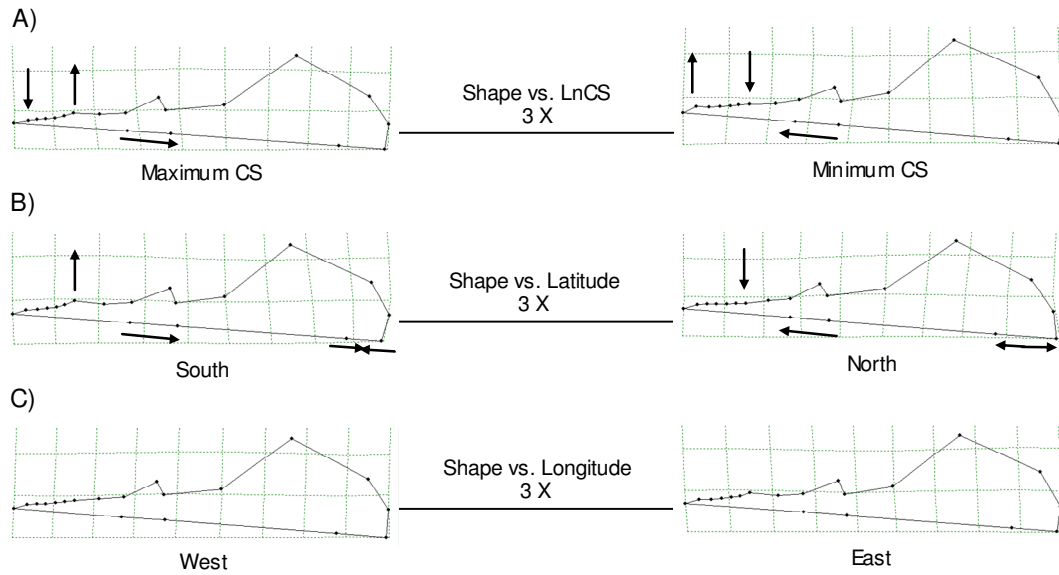


Figure 3.11. Multiple regressions of shape on A) Centroid Size (CS), B) latitude and C) longitude for *Sorex minutus* skulls. Transformation grids were exaggerated 3 times for purposes of visualisation. Arrows help to evaluate the relative movements of landmarks.

Latitude had a highly significant effect on skull shape and it explained a higher percentage of shape variation than CS (Latitude Goodall's $F_{34, 12750} = 52.6744$, $p < 0.0001$, 12.31% explained). Individuals from southern latitudes had skulls of a similar shape but bigger than those from the north, with an outward movement of landmark 7 and backward movements of landmarks 18 and 19 resulting in a wider separation of upper premolars and longer maxilla and pre-maxilla, respectively, plus opposite movements of landmarks 16 and 17 resulting in a smaller foramen magnum compared to skulls from northern latitudes (Fig. 3.11B). Longitude, in contrast, had weaker effects on skull shape variation than latitude, but had stronger effects than size (Longitude Goodall's $F_{32, 18112} = 18.8495$, $p < 0.0001$) and explained 3.8 % of shape variation (Fig. 3.11C).

The RW Analysis of skull data, as in the mandible data, showed that shape variation was not subdivided in any systematic way and there was a nearly uniform ordination of the samples around the average configuration (Fig. 3.12). However,

the first three RWs explained cumulatively 60.82% of the total variance (31.76%, 18.67% and 10.38%, respectively), about 12% more than the first three RWs of mandible data. There was little shape variation from the average configuration, but the apparent landmark movements along RW1 seem to follow the latitudinal pattern described previously. It is interesting that the first two RWs of skull data explained more variation than the first two RWs of mandible data, and that in both cases RW1 reflected the latitudinal pattern of shape variation.

The parametric and non-parametric MANOVAs revealed significant differences among groups (Wilks' $\lambda = 0.0001$, $F_{340, 3306} = 14.24$, $p < 0.0001$; non-parametric MANOVA $F_{340, 3306} = 12.05$, $p < 0.0001$), and the post-hoc tests showed that 60% and 78%, respectively, of all pairwise comparisons were significant (Appendix 8). Again, most of the non-significant differences involved comparisons with the South Italian and Iberian groups, likely a reflection of the small sample size. Including the CS as a covariate of shape variables or including *S. volnuchini* in the MANOVA made no differences to the outcome.

The discriminant function analysis of skull variation correctly classified 79.2% of the individuals to their predefined group, but using a cross-validation method only 63.1% were properly classified. With the pre-validation model, using samples with 'known' group membership, the discriminant function analysis correctly classified 90.3% of selected individuals, and with the cross-validation method it decreased to 77.3%. The first two canonical variates showed that the continental groups mostly overlapped with each other and that the island samples were more easily discriminated from the rest, especially Westray, suggesting that there were shape differences between island and continental samples (Fig. 3.13). This result was very similar to that obtained for the mandible data, where island samples could also be differentiated from continental ones.

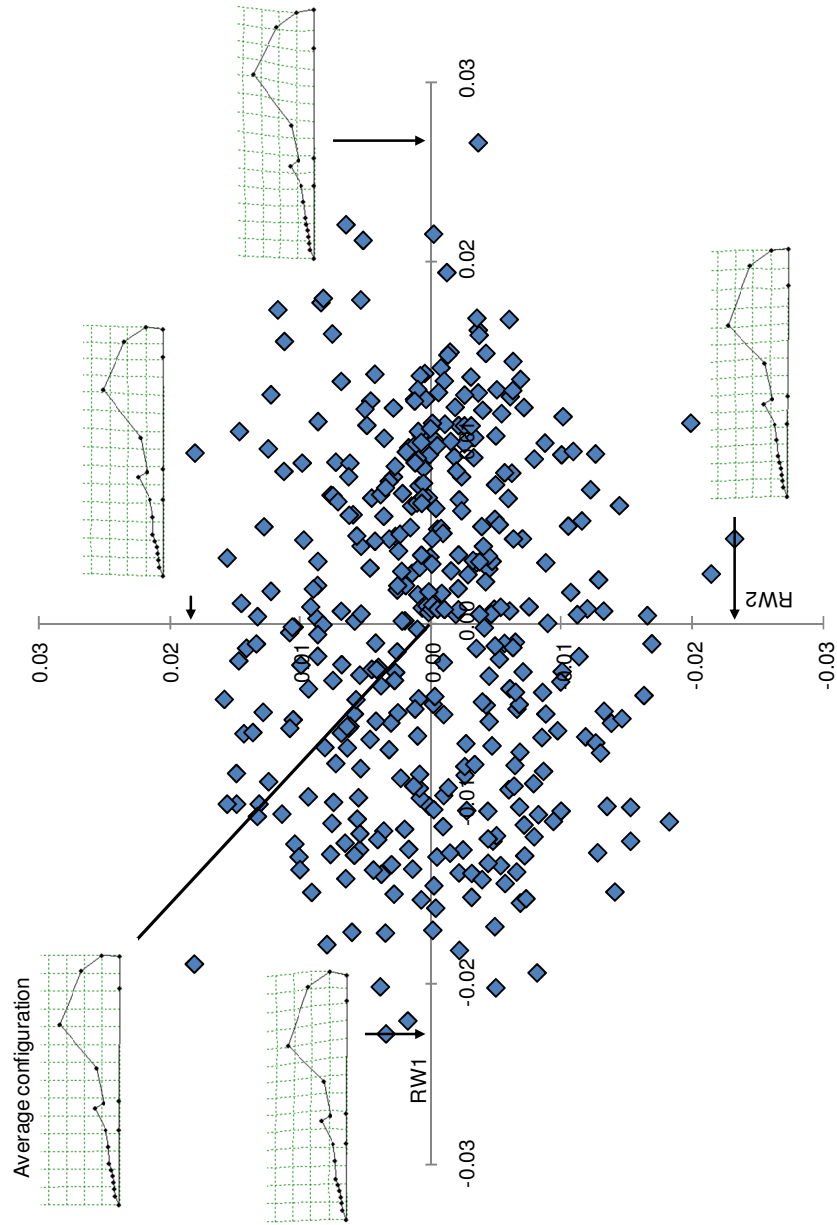


Figure 3.12. Relative Warp Analysis of shape variables of *Sorex minutus* skulls. The maximum and minimum transformation grids on the first two Relative Warps (RW1 and RW2), and the average configuration are shown for purposes of visualisation.

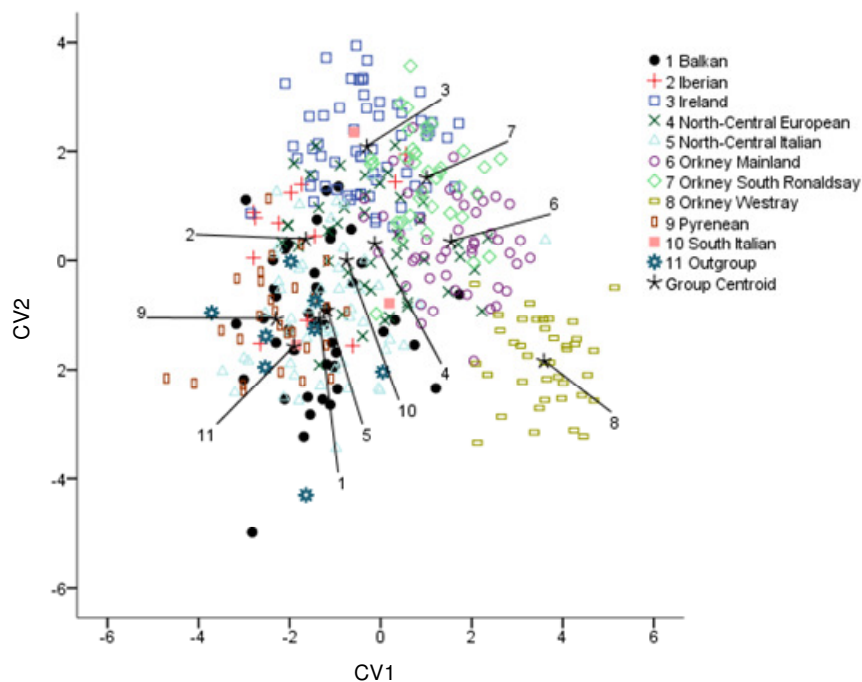
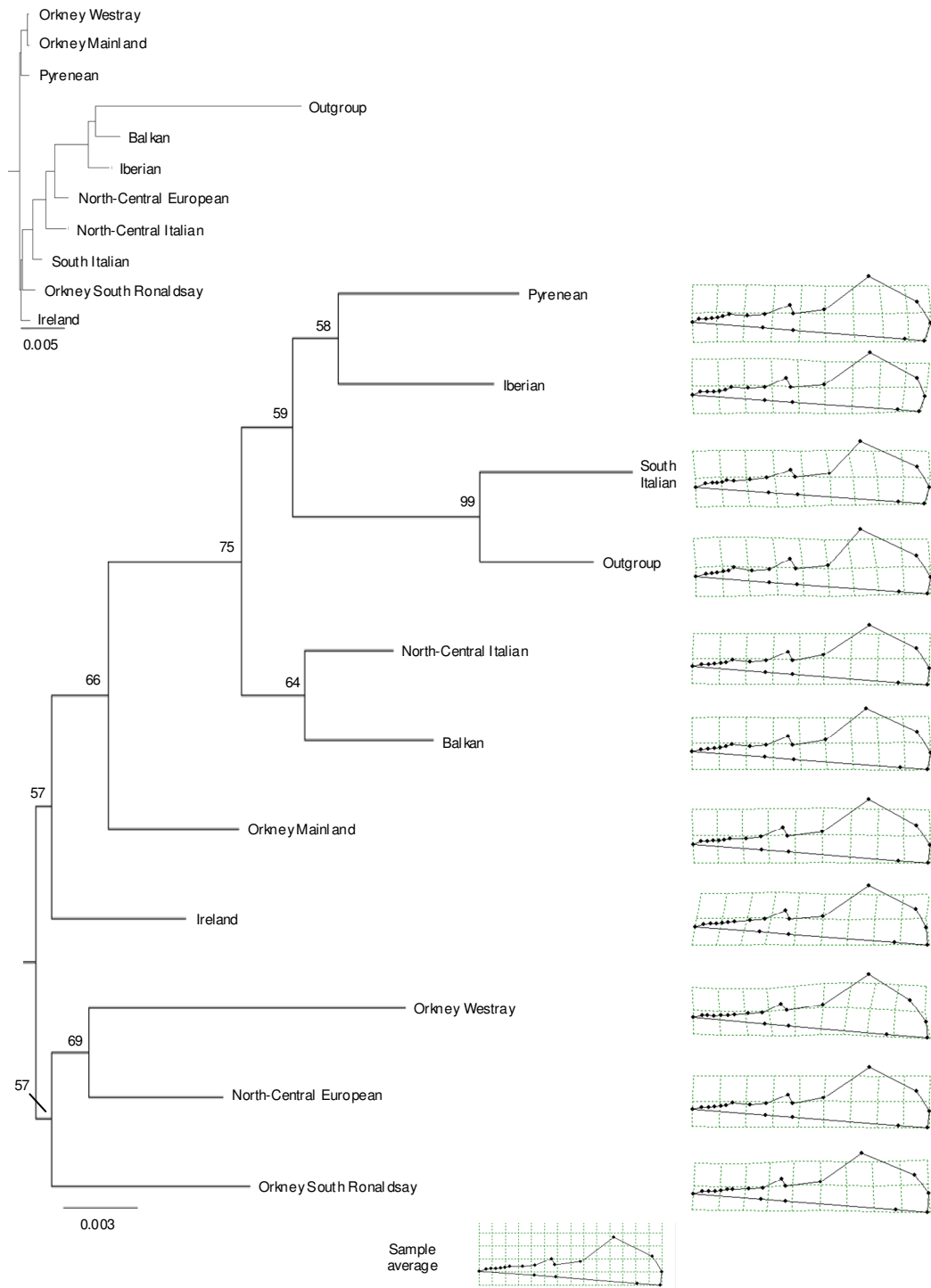


Figure 3.13. Canonical Variate Analysis of shape variables of *Sorex minutus* skulls showing group differences. The first two canonical variates (CV) were used to describe variation among groups.

The unrooted NJ tree of Procrustes distances among groups showed that the island groups clustered separately, with Orkney Mainland more close to other groups than to Westray and South Ronaldsay (Fig. 3.14A). Westray was again the group with the largest pairwise Procrustes distances, as with the mandible dataset. The rooted tree showed a very different topology, with a well supported cluster including all island groups, plus the North-Central European group (Fig. 3.14B). In unrooted and rooted trees, the Iberian and Pyrenean, and the Balkan and North-Central Italian groups formed two separate clusters. As with the mandible data, there was no similarity between the Procrustes and genetic NJ trees, and the amount of morphological variation did not seem to parallel the observed genetic distances (Fig. 3.14A, B).

A)

Cyt b



(Continued)

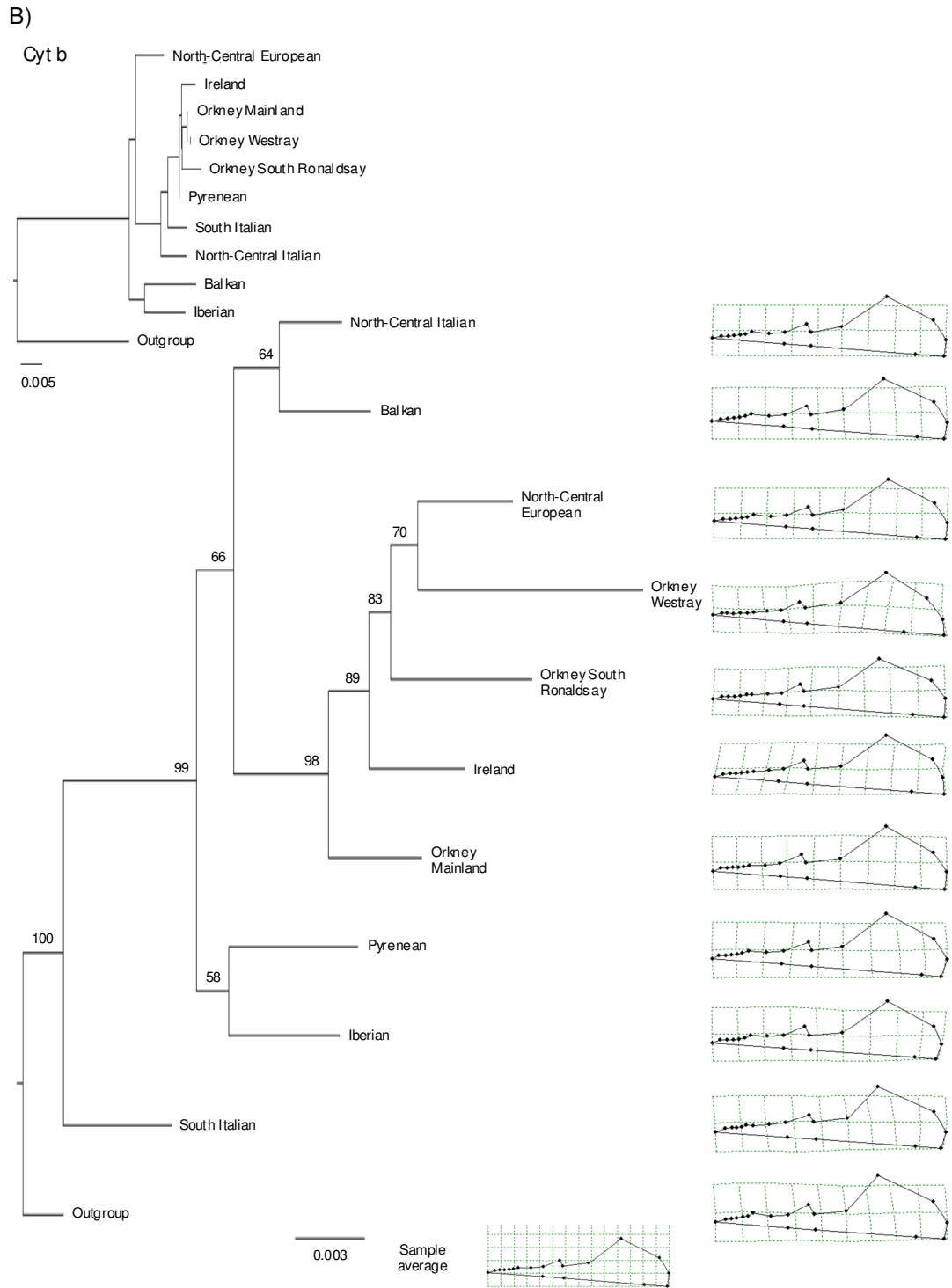


Figure 3.14. A) Unrooted and B) rooted Neighbor-Joining (NJ) trees constructed using skull Procrustes distances among *Sorex minutus* groups. Branch support is shown as bootstrap values (10,000 replications). The grids on the right correspond to shape deformation per group from the average configuration. Inset: NJ trees based on genetic distances obtained in Chapter 2, shown for purposes of comparison.

The Mantel tests for skull data revealed that there was a significant correlation between Procrustes distances and geographic distances ($R = 0.5099$, $p = 0.0021$), stronger than that found with the mandible data, and there were no correlations with genetic differentiation (F_{ST} ; $R = -0.0955$, $p = 0.6916$) or genetic divergence (Da ; $R = 0.0604$, $p = 0.4159$) among groups.

3.4 Discussion and conclusions.

3.4.1 Mandible and skull size variation in *Sorex minutus*

Sorex minutus CS had significant decreasing trends with increasing latitude, more evident for mandibles than for skulls. Southern peninsular samples, including South Italian, Iberian and Balkan groups, and the outgroup, had the biggest mandible size.

This result was contrary to that expected under Bergmann's rule, an ecogeographical rule that states that races from cooler climates tend to be larger in warm-blooded vertebrate species than races of the same species living in warmer climates (Mayr 1963). Other studies have shown a similar pattern to the one described here. For example, the condylobasal length of the skull of *S. araneus*, *S. caecutiens*, *S. tundrensis* and *S. minutus* is negatively correlated with latitude, and the strongest trend with latitude and temperature is found in *S. minutus* (Ochocińska and Taylor 2003). Ashton et al. (2000) showed that several small mammal species have significant and negative size correlations with latitude, including some species of voles (*Microtus*), kangaroo rats (*Dipodomys*) and bats (*Scotorepens*), but they only analysed a single species of shrew, *Blarina brevicauda*, which also had a negative but non-significant correlation of size with latitude. Similarly, three mainland populations of *S. trowbridgii* have decreasing cranial and mandibular dimensions with increasing latitude (Carraway and Verts 2005). Therefore, a smaller

mandible size at higher latitudes in *S. minutus* is a common trend shared with other species.

Why are shrews smaller in northern latitudes than those at southern latitudes? Lower food availability in northern/colder habitats could be the selection factor acting on small mammals, combined with lower absolute food requirements and inferior competitive ability in less productive habitats (Ochocińska and Taylor 2003). At least for *Dipodomys* and *Microtus*, seasonality and food availability appear to be the factors affecting body size (Ashton et al. 2000). Populations of *S. araneus* in Finland are up to 13% smaller on inland locations than coastal locations, where the main differences are lower winter temperatures and less snow cover at inland sites, factors associated with lower habitat productivity, which could favour selectively smaller shrews (Frafjord 2008). Moreover, bigger mandibles could reflect stronger bite force or higher mechanical potential for mastication, which could be an adaptation to more arid conditions and prey with harder exoskeletons (Strait 1993, Carraway and Verts 1994, Monteiro et al. 2003, Vega et al. 2010a). Size and shape variations of the mandible can affect the biomechanics of mastication by modifying the sites of attachment of mandible muscles (Monteiro et al. 2003).

3.4.2 Mandible and skull shape variation in *Sorex minutus*

Mandible and skull samples of *S. minutus* were not clearly differentiated by shape variation across Europe. The RW Analyses, represented graphically with the first two RWs, showed that there was no obvious differentiation of the mandible or skull samples into discrete groups. Although the first three RWs for mandibles and skulls explained 48% and 61% of the total shape variation, respectively, there was still a large amount of unexplained variation which could account for the lack of differentiation into more discrete groups of samples. The mandible and skull shape deformations along the first RW (Fig. 3.6 and Fig. 3.12) were similar to the

transformation grids obtained for the regression of shape variables on latitude and CS (Fig. 3.5 and Fig. 3.11); therefore, RW1 represented the latitudinal and allometric effects, where negative values on RW1 were equivalent to southern latitudes and larger mandible and skull size.

Dividing the sample into groups allowed me to explore the morphological differentiation under a phylogeographic scenario. MANOVAs on shape variables resulted in significantly differentiated groups. However, the CVA and classification results on mandible and skull data showed that the groups could not be differentiated or classified with confidence based on shape variables. Skulls were classified 10% better with shape variables than mandibles. This indicates that mandibles are more affected by ecophysiological factors than the ventral side of skulls (Monteiro et al. 2003, Caumul and Polly 2005). In this study, no morphological structure recovered the phylogenetic relationships detected with the *cyt b* analysis, and the morphological variation among the groups increased with geographic distance, not with genetic distance or differentiation for mandible and skull data. As expected from intra-specific studies such as this, the molecular differentiation was more pronounced than the morphological differentiation. Contrary to this, Carraway and Verts (2005) found, with a traditional morphometric analysis using linear measurements, that cranial and mandible characters recover relatedness within *S. trowbridgii*, and that mandibles alone classify specimens correctly to their groups selected a priori; although they also distinguish mainland from insular taxa.

Interestingly, island samples of *S. minutus* grouped somewhat separately from the rest in the CVA. Moreover, island samples tended to cluster together in NJ trees based on Procrustes distances. Latitudinal and allometric effects could explain this pattern: all the island samples were obtained from higher latitudes than continental ones, and specifically Westray samples, with the highest latitude (59° north latitude), showed the strongest shape differentiation. A more localized study of

the genetic and morphological differentiation of island and continental samples is presented in Chapter 4.

Size, not shape, was the principal and most obvious difference in mandibles and skulls among the European regions. In general, there appeared to be isotropic shape variation for mandibles and skulls, most evident in landmarks 2 to 15 of mandibles and landmarks 2 to 12, 14 and 15 of skulls (e.g., see the distribution of landmark coordinates in Fig. 3.2). Isotropic shape variation occurs when the variation at each landmark is the same in all directions and independent among landmarks, meaning that the scatter of landmark positions around the average is circular and has the same spread at each landmark (Klingenberg and Monteiro 2005). However, the shape variation among regions is of interest to compare with patterns of genetic variation.

The evidence provided here supports the conclusion that latitude and island evolution are the driving factors of size and shape variation in *S. minutus* mandibles and skulls, probably reflecting selection forces or size and shape adaptations to different habitats, food availability and environmental conditions (Fadda and Corti 2001). Overall, both datasets showed similar patterns of shape variation, but latitudinal and size effects were more evident with mandibles than skulls. This is not unexpected because mandibles usually show more ecophenotypic variation than the ventral side of the skull. A detailed analysis of size and shape variation in an island setting is presented in Chapter 4.

3.4.3 Taxonomic implications

In the previous chapter (Chapter 2), I described four phylogroups based on *cyt b*, including the Balkan, Iberian, South Italian and North-Central European, which roughly matched the geographic distribution of four subspecies of *S. minutus* described by Hutterer (1990): *S. m. gymnurus* (Greece), *S. m. carpetanus* (Iberia),

S. m. lucanius (Southern Italy) and *S. m. minutus* (Northern-Central Europe and Siberia), respectively.

The geometric morphometric analyses presented here did not parallel the phylogeographic groupings, but there was important size and shape variation. Populations in southern peninsulas had significantly bigger mandibles than those from Northern-Central Europe, and there were also significantly different groups despite the small amount of shape variation. Similarly, the three subspecies from the southern peninsulas described by Hutterer (1990) are bigger than *S. m. minutus* from Northern-Central Europe. Therefore, this study provided morphological and genetic evidence that support the subspecific status for a Balkan group (equivalent to *S. m. gymnurus*), an Iberian group (equivalent to *S. m. carpetanus*) and a South Italian group (equivalent to *S. m. lucanius*), and a morphologically smaller and genetically distinct North-Central European-Siberian group (equivalent to *S. m. minutus*), all of which could have evolved allopatrically during the glacial/interglacial periods.

The subspecific status of the North-Central Italian and Pyrenean groups is uncertain, however. These two groups were closely related in the *cyt b* analysis and diverged 0.225 MYA according to the molecular clock applied in section 2.3.4, and had a similar average mandible and skull size, but were significantly bigger than the North-Central European group. It is expected that recently separated species/subspecies may be genetically different but not well-differentiated morphologically. This is evident from the observed size and shape similarities between *S. volnuchini* and *S. minutus* samples, which are genetically very distinct. It is possible that the North-Central Italian and Pyrenean groups correspond to two distinct subspecies, one equivalent to *S. m. becki* (Alps) and the other one not yet described.

Chapter 4

Island phylogeography and morphometrics of *Sorex minutus*

4.1 Introduction

During the Last Glacial Maximum (LGM; 23 – 18 KYA), the coldest stage of the Devensian (Weichselian) glaciation, ice sheets covered most of Britain and Ireland, while only the southern-most regions were unglaciated, but presented tundra and permafrost conditions unsuitable for most of the present mammal fauna (Yalden 1982, 2007). The timing of the migration of small mammals from continental Europe into Britain must have coincided then with the presence of an exposed landbridge between Northern France and Southern Britain; however, the natural colonisation of Ireland and other outer islands of the British Isles from source populations in mainland Britain might have not been possible because of the absence of a landbridge interconnecting them (Yalden 1982, Stuart 1995, Lambeck and Purcell 2001). Thus, the presence of the Eurasian pygmy shrew *Sorex minutus* on Britain, Ireland and other outer islands of the British Isles makes it an interesting model for understanding natural and human-mediated island colonisation and evolution.

Previous work on *S. minutus* based on microsatellite data provided evidence for a population expansion and colonisation event in Ireland ca. 6 KYA (7 – 4 KYA), in the Neolithic (McDevitt et al. 2009). The results provided in Chapter 2 indicate a source area for the Irish pygmy shrew in Northern Spain, given the haplotype similarity between Navarra, Spain and those from Ireland, all of which belong to a widespread Pyrenean lineage distributed in Northern Spain, Western and Southern France. Searle et al. (2009) showed that there are individuals of *S. minutus* in

mainland Britain and islands off the coast of Britain, which also belong to the Pyrenean lineage, and represent a 'Celtic fringe' only found in the western and northern regions of mainland Britain and in some offshore islands. Archaeological evidence indicates that Neolithic people travelled by boat between mainland Britain and nearby islands, and also among the Orkney islands (Phillips 2004), and the same applies to more recent human occupants. Therefore; it is expected that small mammals, including *S. minutus*, were sometimes accidentally carried from one region to another by boat, probably hiding in livestock fodder.

It is not only colonisation history of islands that has impacted the genetic and morphological diversity seen on them; island size, selective pressures and geographical isolation are also important (Lomolino 2005). Several studies indicate that mammal populations on islands usually show lower population size, inbreeding and lower levels of genetic diversity than continental populations (Frankham 1998), and morphological traits evolve more rapidly compared to continental counterparts, from a few decades to several thousand years (Millien 2006). For example, White and Searle (2007, 2008a) showed that island populations of *S. araneus* have lower microsatellite expected heterozygosity and lower mean cytochrome (*cyt b*) nucleotide diversity than mainland populations, and that there is morphological differentiation of island populations with variation of mandibles between islands strongly predicted by climate (White and Searle 2009). A meta-analysis of rodents indicates that microevolution and selection cause rapid substantial shifts in morphology among insular rodents shortly after island colonisation (Pergams and Ashley 2001), although other have argued the importance of founder events (Berry 1996). *Marmota vancouverensis*, the only insular species of the genus *Marmota*, has low genetic divergence but strong morphological differences from continental species that evolved rapidly following its isolation after the LGM (Nagorsen and Cardini 2009).

Here, I analyse the genetic and morphological diversity of pygmy shrews within Ireland, the Orkney islands and the periphery of mainland Britain, all belonging to a Pyrenean mitochondrial lineage described previously, and compare it with a continental European population belonging to the same lineage. In this way, island colonisation history and evolution can be examined within a defined genetic lineage. In particular, the objectives are: 1) to investigate the genetic diversity, origin and migration rates among the continental Pyrenean and the Orkney, Ireland and British Celtic fringe populations from the viewpoint of island colonisation and evolution, 2) to evaluate the morphological variation among and within the islands in comparison to the continental population of a phylogenetically related sample, and 3) to evaluate the specific influence of island size on the morphology of *S. minutus*.

4.2 Materials and methods

4.2.1 Samples for genetic and morphological analysis

For the genetic analysis, I used the samples and available sequences that clustered in the full *cyt b* Pyrenean lineage described in Chapter 2. This geographically widespread lineage included samples from the Cantabrian mountain range in Northern Spain, the Pyrenees in North-Eastern Spain and Southern France, Western and Central France, and from the island of Belle Île en Mer (off the coast of Western France), plus all samples that formed the 'Ireland', 'Orkney islands' and British 'Celtic fringe' groups.

I divided the full *cyt b* Pyrenean lineage into four main groups (Fig. 4.1): the 'Continental Pyrenean' (for simplicity now named as 'Continental', but also including the few samples from the island of Belle Île), 'Ireland', 'Orkney islands' and the British 'Celtic fringe'. The samples from Orkney belong to the Celtic fringe described by Searle et al. (2009), but for the purpose of this study they were considered as a separate group.

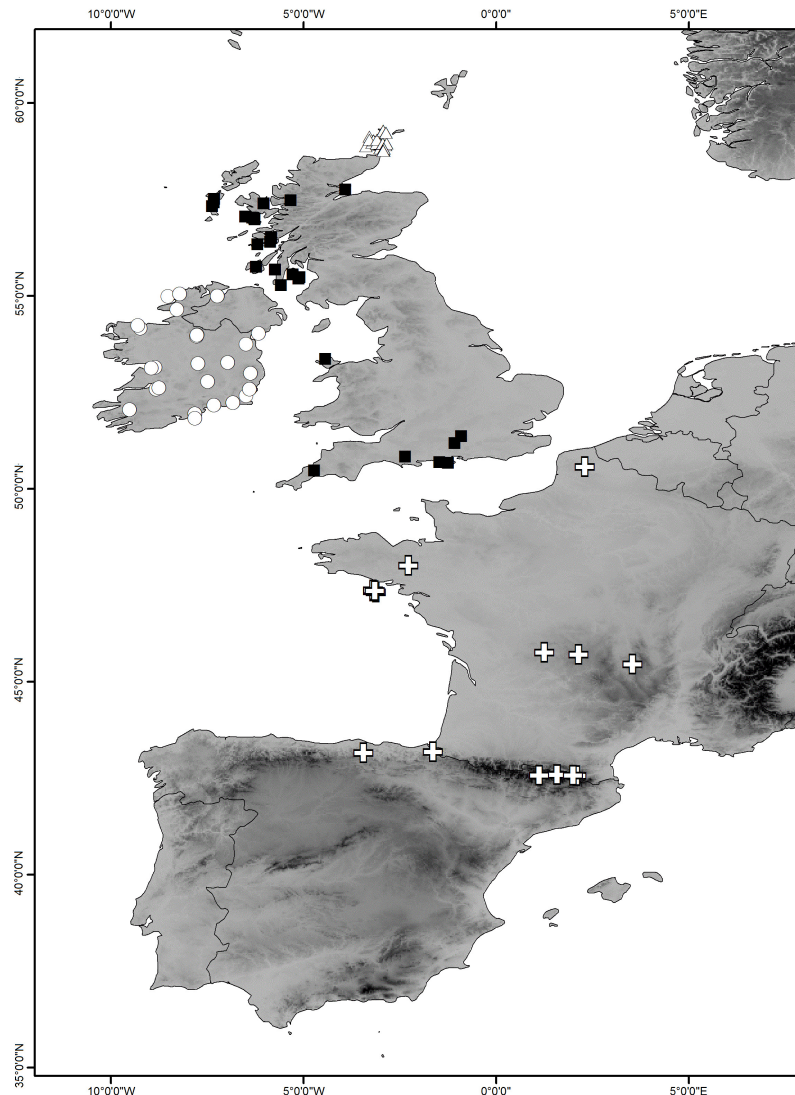


Figure 4.1. Samples of *Sorex minutus* for genetic analysis. ⊕ Continental, ■ British Celtic fringe, ○ Ireland and △ Orkney islands.

The genetic sample from Ireland was subdivided into nine regions: Cork, Derry, Gweedore, Limerick, Wexford, Galway, Kerry, Cloghan and Kildare. The Orkney sample was subdivided into: Orkney Mainland, Westray, South Ronaldsay and Hoy, and into regions or localities within these islands, including three regions within Orkney Mainland (named Mainland 1, Mainland 2 and Mainland 3), two

localities within Westray (Loch of Swartmill and Ness), two localities within South Ronaldsay (Grimness and Windwick), and only one locality for Hoy.

For the geometric morphometrics analysis, I included the mandible and skull samples that formed the 'Pyrenean', 'Ireland', 'Orkney Mainland', 'Westray' and 'South Ronaldsay' morphological groups described in Chapter 3 (see also Fig. 3.1). The Pyrenean sample was divided into 'Navarra' (Northern Spain), 'continental France' (mostly from Central France) and 'Belle Île' (from the island of Belle Île en Mer, off the coast of Western France). Ireland was subdivided into three regions: Cloghan, Derry and Gweedore. The Orkney islands were further subdivided into regions or localities: Orkney Mainland was divided into Mainland 1 and Mainland 2, Westray was divided into Ness and Loch of Swartmill, and South Ronaldsay was divided into Grimness and Windwick.

To investigate island size as a factor affecting the morphology of *S. minutus*, I explored size and shape variation dividing the mandible and skull datasets into four different categories: 1) 'Continental' (grouping samples from Northern Spain and France), 2) 'Large' size islands (Ireland), 3) 'Medium' size islands (Orkney Mainland), and 4) 'Small' size islands (grouping samples from South Ronaldsay, Westray and Belle Île).

4.2.2 Sequence diversity, divergence and differentiation

Sequence diversity, divergence and genetic differentiation parameters were calculated in DnaSP version 5.10 (Librado and Rozas 2009), as explained in Chapter 2. I calculated the genetic (π) and haplotype (H_d) diversity values for the Continental group, and for the islands and regions within islands. Then, I obtained the genetic divergence (D_a) among the main groups (Continental, Orkney Mainland, Westray, South Ronaldsay, Hoy and Ireland), and among the regions within the main groups.

The pairwise geographic distances (in Km) were calculated among the main continental-island groups, and among the regions within islands and the Continental group. Mantel tests were performed in Arlequin version 3.1 (Excoffier et al. 2005) to test the significance of the correlation between the pairwise Da values with the pairwise geographic distances among groups and among regions within groups separately. The significance was obtained through a permutation procedure (10,000 replications) used to create an empirical null distribution.

The structure of the genetic diversity was evaluated using Arlequin with an Analysis of Molecular Variance (AMOVA). I implemented a hierarchical analysis dividing the total variance into three groups (Continental, Orkney and Ireland), and into regions within groups (Mainland 1, Mainland 2, Mainland 3, Loch of Swartmill, Ness, Grimness and Windwick for the Orkney archipelago, and Cork, Derry, Gweedore, Limerick, Wexford, Galway, Kerry and Kildare for Ireland).

Finally, I used the Median-Joining (MJ) phylogenetic network presented in Chapter 2 (Fig. 2.3C) to represent the genetic relationships among continental and island haplotypes that formed the full Pyrenean phylogroup.

4.2.3 Estimation of migration routes

The population parameter 'theta' ($\theta = 2Neu$) and the migration rates between the Continental, Celtic fringe, Ireland and Orkney groups were calculated using Lamarc version 2.1.3 (Likelihood Analysis with Metropolis Algorithm using Random Coalescence), which implements a coalescent method (Kuhner 2006). The effective population size (N_e) was calculated solving for θ , where $u = 2\mu k$, μ is the mutation rate per nucleotide (assuming a mutation rate per nucleotide of 2% per million years, Wilson et al. 1985) per generation (considering one generation per year for *S. minutus*) and k is the number of nucleotide sites (1110 bp for *cyt b* data) (Rogers 1995). In this program, the genealogical relationships among all pair of individuals

are estimated revealing coalescent-based information on the genealogies, and a random effect is incorporated using the Metropolis-Hastings Markov Chain Monte Carlo (MCMC) sampling. The method gives an approximation to the actual value being estimated, but an error range around the Most Probable Estimate (MPE) is generated, which is equivalent to a confidence interval (Kuhner 2006).

For running the program, I selected 10 initial runs of 10,000 generations sampled every 20 generations and a burn-in of 250, followed by two final runs of one million generations sampled every 100 generations with a burn-in of 2500. The results were averaged over three replicates (using the same parameters) and convergence was visualised in Tracer version 1.4.1 (Drummond and Rambaut 2007). I kept default values for the Bayesian start parameters, but set the evolutionary model to the General Time Reversible (GTR).

4.2.4 Geometric morphometric analysis

The mandible and skull samples were statistically analysed in SPSS/PASW Statistics version 17 (IBM), PAST version 1.97 (Hammer et al. 2001) and the 'tps-series' software (by FJ Rohlf, available at <http://life.bio.sunysb.edu/morph/>). The landmarks used in this study were the same as in Chapter 3. The landmark configurations were scaled to unit Centroid Size (CS; natural log-transformed), translated and rotated using the Generalised Procrustes Analysis (GPA). CS was used for the analysis of size variation and the weight matrix (W) was used for the analysis of shape variation. Descriptive statistics were obtained for the mandible and skull samples.

Mandible and skull size differences among continental and island groups were evaluated by an Analysis of Variance (ANOVA) and visualized with box plots. Levene's tests were conducted to detect heteroscedasticity, but the ANOVA is robust to this (Zelditch et al. 2004). I performed a Tukey–Kramer post-hoc test on

CS as it allows for unequal sample size (Sokal and Rohlf 1995). In the case of a significant departure from homogeneity of variances, I performed a non-parametric Kruskal–Wallis test and a Tamhane T2 non-parametric post-hoc test for the analysis of CS variation.

Mandible and skull shape differences among continental and island groups were evaluated with a Multivariate Analysis of Variance (MANOVA) on W , followed by Hotelling T^2 tests. Levene's tests were also performed for each shape variable among groups and, if significant deviations from the assumption of homogeneity of variances were found, non-parametric MANOVAs among groups were also performed.

The Procrustes distances among the average configurations of the groups were then computed with the program tpsSmall. I performed Mantel tests in PAST to test the significance of the correlation between pairwise Procrustes distances and geographic distances and D_a among groups (the significance was obtained with 10,000 permutations).

A Discriminant Analysis (DA) was performed in SPSS to predict group membership using a cross-validation method and to differentiate among the groups by a Canonical Variates Analysis (CVA), as explained in Chapter 3. The first two canonical variates were used to graph the samples separated by group membership. A similar approach was used to discriminate and classify the mandible and skull samples divided into island size categories.

4.3 Results

4.3.1 Genetic diversity and structure

The Continental ($n = 20$) and Ireland groups ($n = 94$) had high cyt b haplotype diversities ($H_d = 0.9840$ and $H_d = 0.8920$, respectively) compared to the full Orkney islands sample ($n = 119$, $H_d = 0.7720$), or to any of the individual Orkney

islands with adequate sample sizes (Table 4.1). However, nucleotide diversity was always low for island samples compared to the Continental group (Table 4.1). The largest island of the Orkney archipelago, Orkney Mainland, had the highest nucleotide and haplotype diversity values. Interestingly, South Ronaldsay had very low genetic diversity and there were only two haplotypes in a sample of 40 individuals, while Westray, the northern-most island sampled, had only one haplotype in 33 sampled individuals.

Table 4.1. Cytochrome *b* sequence diversity of *Sorex minutus* groups of the Pyrenean lineage.

Groups	n	Haplotypes	Hd	π	K	S
Continental	20	17	0.9840	0.0054	5.9370	33
Orkney islands	119	11	0.7720	0.0027	3.0140	17
Orkney Mainland	44	8	0.7550	0.0013	1.4790	9
Orkney Mainland1	29	5	0.5120	0.0010	1.0940	6
Orkney Mainland2	10	4	0.8000	0.0012	1.3330	4
Orkney Mainland3	5	2	0.4000	0.0004	0.4000	1
South Ronaldsay	40	2	0.1420	0.0001	0.1420	1
Grimness	21	2	0.0950	0.0001	0.0950	1
Windwick	19	2	0.1990	0.0002	0.1990	1
Westray	33	1	0.0000	0.0000	0.0000	0
Loch of Swartmill	19	1	0.0000	0.0000	0.0000	0
Ness	14	1	0.0000	0.0000	0.0000	0
Hoy	2	2	1.0000	0.0018	2.0000	2
Ireland	94	42	0.8920	0.0020	2.2180	53
Cork	10	7	0.8670	0.0043	4.7560	15
Derry	11	2	0.3270	0.0003	0.3270	1
Gweedore	6	3	0.6000	0.0011	1.2000	3
Limerick	7	5	0.8570	0.0013	1.4290	5
Wexford	11	4	0.6730	0.0012	1.3090	4
Galway	5	5	1.0000	0.0025	2.8000	7
Kerry	5	3	0.7000	0.0007	0.8000	2
Kildare	5	3	0.7000	0.0013	1.4000	3
Cloghan	3	2	0.6667	0.0006	0.6667	1

n = Number of sequences, Hd = Haplotype diversity, π = Nucleotide diversity (Jukes and Cantor 1969), K = Average number of nucleotide differences, S = Number of polymorphic (segregating) sites.

There was no evidence of isolation by distance for the whole dataset ($R = 0.0204$, $p = 0.3933$), because of the weak and non-significant correlation of geographic distances and genetic divergence values among the Continental and island samples, as expected for populations evolving in an island setting. Moreover, there were very small divergence values, as expected, and no evidence of isolation by distance among localities within Ireland ($R = 0.3597$, $p = 0.0736$) or among localities of the Orkney islands ($R = 0.2105$, $p = 0.0809$).

The genetic diversity of the whole dataset was significantly structured ($p = 0.0001$), with most of the variation found among the Continental and island groups (43%), followed by the variation among localities within the groups (34%) and within localities (22%). For the Orkney archipelago, there was a strong and significant genetic structure ($p < 0.0001$), with more variation found among islands (87%) than within (13%). In contrast, there was less variation among localities (26%) than within localities (74%) in Ireland, but there was also a significant structure ($p < 0.0001$). The genetic structure for the Continental group was not calculated because of low sample size per locality. These results showed that populations of *S. minutus* within Ireland and the Orkney islands are subdivided, especially so on the Orkney islands, although there were small values of genetic diversity there.

The MJ network showed that the haplotype ESBa9709 (from near Barcelona, Spain), was the most basal of the Pyrenean haplotypes to the full network and connected the Pyrenean lineage to the other Eurasian phylogroups. From this haplotype, the other more derived Continental, Orcadian, Irish and Celtic fringe haplotypes extended with one or more mutational steps (Fig. 4.2).

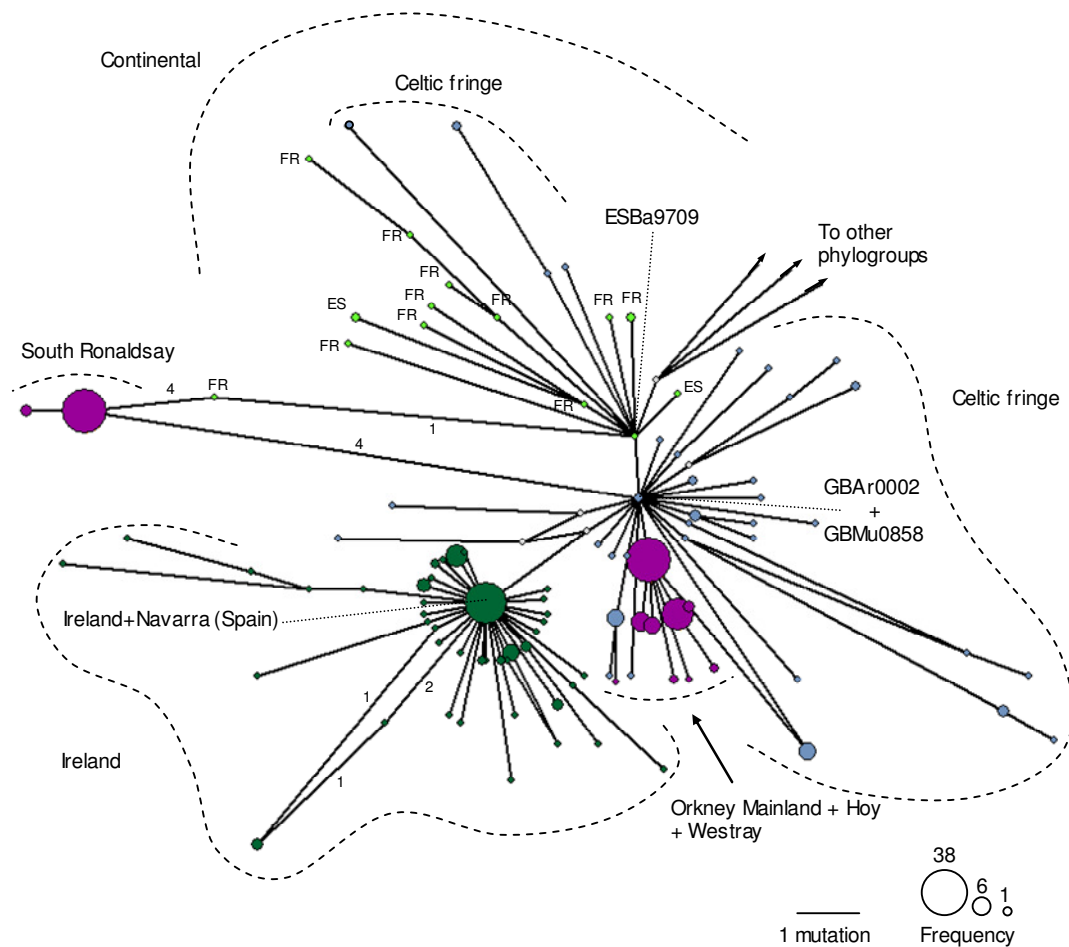


Figure 4.2. Median-Joining network of cytochrome *b* data showing the relationships among *Sorex minutus* haplotypes belonging to the Pyrenean lineage. The Pyrenean lineage is divided into a ‘Continental’ group (light green), a ‘Celtic fringe’ group distributed on Britain and some islands off the coast of Britain (light blue), excluding the Orkney islands, ‘Ireland’ (dark green) and ‘Orkney islands’ groups (purple). Pointed lines indicate the central (ancestral) haplotypes from where all other haplotypes derive from (see text for explanation). Some loops in the network are not in scale and mutations are shown with numbers. For the ‘Continental’ group, the country of origin for the haplotypes is shown (FR = France, ES = Spain).

All haplotypes from the Orkney islands were most closely connected to a central haplotype from the Celtic fringe (GBAr0002 and GBMu0858); therefore, *S. minutus* from the Orkney islands can be considered part of the Celtic fringe. Orkney Mainland, the largest island of the Orkney archipelago, was represented by eight haplotypes (n = 44). There were only two haplotypes in South Ronaldsay (n = 40)

separated by four mutations, and Westray had only one haplotype ($n = 33$), identical to a highly frequent haplotype from Orkney Mainland. All haplotypes from Ireland derived from one Irish central haplotype, which included two Spanish samples (from Navarra, Northern Spain) and 29 Irish samples (from several localities). All the other haplotypes from Navarra, Spain were directly connected with the haplotype ESBa9709. The Irish and Celtic fringe central haplotypes were connected to each other by three mutational steps and one hypothetical haplotype. No Irish haplotype connected directly to the Celtic fringe or to other Continental haplotypes; however, three Celtic fringe haplotypes were directly connected to ESBa9709, showing a close relationship between Continental and Celtic fringe haplotypes. There were several divergent Irish haplotypes without any obvious geographical distribution.

4.3.2 Migration routes

The MPEs for effective population size, θ values and migration rates among the Continental, Celtic fringe, Ireland and Orkney islands groups showed convergence of the three replicates after several runs, but the 95% confidence intervals were wide so these results have to be taken with caution (Table 4.2). The *cyt b* sequences did not contain enough information to provide adequate estimates; therefore, the MPEs should be interpreted as general tendencies or trends, not as precise values.

The Continental group had the highest θ values and effective population size, as expected from a genetically diverse continental source, followed by the Celtic fringe group. The Celtic fringe group was composed of samples from different localities from Britain and offshore islands, so the high θ and effective population size values found there likely resulted because of pooling genetically distinct populations into one single group; however, this grouping likely reflects the genetic diversity of what was once a more widespread lineage in mainland Britain. Ireland

had intermediate θ and effective population size values, compared to the Continental and Orkney islands groups, as expected for a population on a large island and genetically differentiated into subpopulations. The Orkney islands group had the smallest θ and effective population size values. Considering that *S. minutus* is abundant on the Orkney islands, these estimates resulted from the low diversity of the molecular marker used, likely a reflection of a relatively recent colonisation event by a small number of founders.

Table 4.2. Demographic parameters obtained for *Sorex minutus* Pyrenean groups based on cytochrome *b* data.

		Continental	Celtic fringe	Ireland	Orkney
θ	MPE	0.0137	0.0105	0.0065	0.0014
	Lower	0.0075	0.0057	0.0032	0.0004
	Upper	0.0262	0.0217	0.0128	0.0032
Ne	MPE	154.0428	117.7928	73.1531	15.7545
	Lower	84.5158	64.2004	35.8559	5.0338
	Upper	295.6306	244.6622	144.0090	36.4865

MPE = Most Probable Estimate, Lower corresponds to lower 95% CI, Upper corresponds to upper 95% CI, $\theta = 2Neu$ ($u = 2\mu k$).

The migration rates showed a trend from continental to island regions and from larger islands to smaller islands (Fig 4.3). Continental Europe appeared as a source area for the Ireland, Celtic fringe and Orkney islands groups because of the higher migration rates from the continent to islands. However, the migration rates between the Celtic fringe and the Continental groups were almost equal, slightly favouring the Continental group as a source area. The migration rates between the Celtic fringe and Ireland groups were almost equal, showing a slight tendency of the former as a source area for the later. The Celtic fringe had the strongest migration rate onto the Orkney islands, which could be explained by the geographical proximity, and represent the most likely source for the Orkney pygmy shrew.

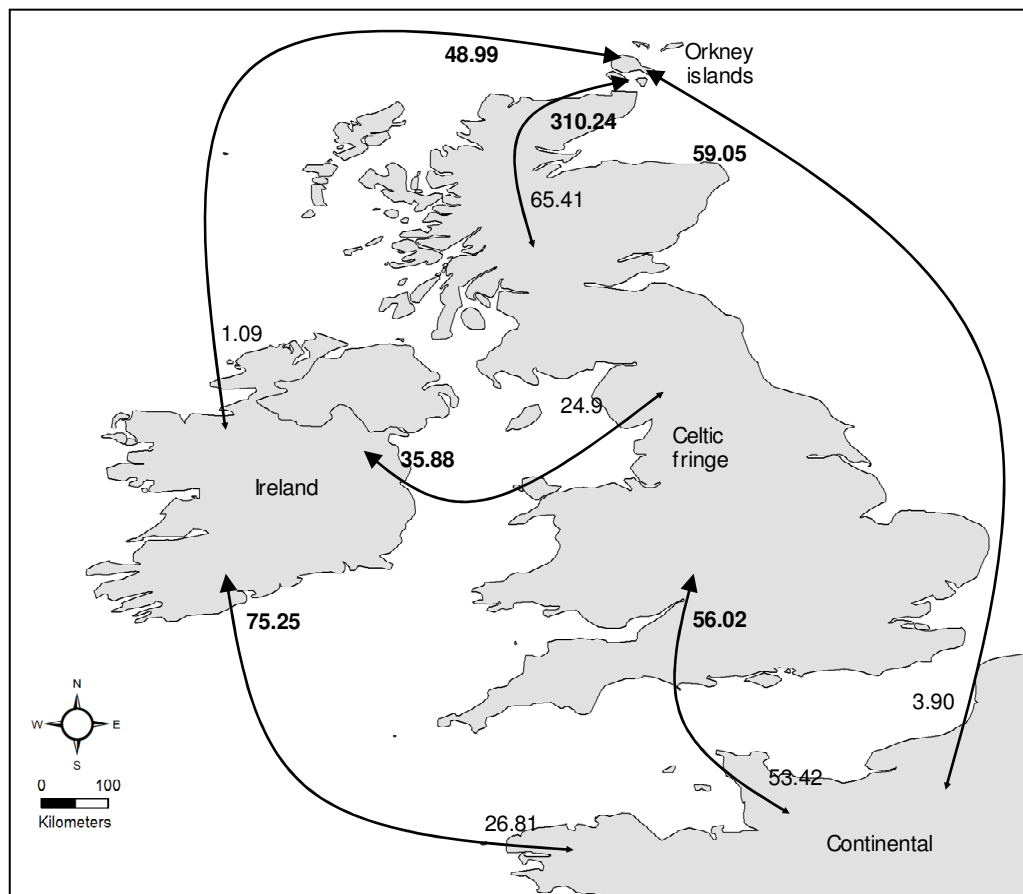


Figure 4.3. Migration rates and routes of *Sorex minutus* among the Continental, Celtic fringe, Ireland and Orkney islands groups estimated from cytochrome *b* data. Values next to arrows are the estimated migration rates from one group to the other. Larger arrow heads and bold numbers represent the migration rate trends, mainly from continent to island and from larger island to smaller island.

4.3.3 Geometric morphometrics findings

The decreasing trend of CS with increasing latitude, as detected for the full Eurasian sample (Chapter 3), was not reflected convincingly in the reduced dataset examined here, although two of the more southerly samples included here (Navarra and Belle Île) did have the highest values (Table 4.3, Fig. 4.4A). Levene's test was not significant for the mandible dataset (Levene's statistic_{11, 260} = 0.8090, $p = 0.6310$), and the ANOVA ($F_{11, 260} = 27.2100$, $p < 0.0001$) and parametric post-hoc tests showed that 47% of the pairwise comparisons of mandible CS were significant

(Appendix 9). Among the populations from the Orkney islands, Westray Ness was the only one that was not significantly different from any other island group.

The CS of skull groups showed no apparent trend with latitude (Table 4.4, Fig. 4.4B), as expected from the full European sample analysed in Chapter 3. Mainland Orkney had the largest skull size variation and the two groups from Westray had the biggest skull CS. The test of homogeneity of variances for skull CS was significant (Levene's statistic_{9, 204} = 7.4460, $p < 0.0001$), so a non-parametric ANOVA was performed and it was significant ($H_9 = 28.7680$, $p < 0.0001$). The only significant post-hoc comparisons were among Westray Ness, Cloghan and Derry (Appendix 10).

Table 4.3. Centroid Size statistics for *Sorex minutus* mandibles of the Pyrenean lineage.

Group	n	mean	median	Lower	Upper	SD	SE
Navarra	28	2.4058	2.4052	2.3984	2.4132	0.0192	0.0036
Continental France	30	2.3361	2.3406	2.3292	2.3430	0.0192	0.0036
Belle Île	19	2.3784	2.3745	2.3715	2.3853	0.0143	0.0033
Ireland Cloghan	20	2.3610	2.3654	2.3497	2.3722	0.0241	0.0054
Ireland Derry	23	2.3459	2.3504	2.3380	2.3537	0.0182	0.0038
Ireland Gweedore	20	2.3393	2.3364	2.3285	2.3501	0.0231	0.0052
O SR Windwick	20	2.3415	2.3442	2.3353	2.3478	0.0133	0.0030
O SR Grimness	20	2.3366	2.3368	2.3297	2.3434	0.0147	0.0033
O Mainland 2	39	2.3538	2.3564	2.3468	2.3608	0.0215	0.0034
O Mainland 1	13	2.3687	2.3664	2.3537	2.3837	0.0248	0.0069
O W Ness	20	2.3551	2.3533	2.3479	2.3623	0.0154	0.0034
O W Swartmill	20	2.3629	2.3590	2.3521	2.3737	0.0231	0.0052

O = Orkney, SR = South Ronaldsay, W = Westray, Lower = Lower 95% CI, Upper = Upper 95% CI, SD = Standard deviation, SE = Standard error.

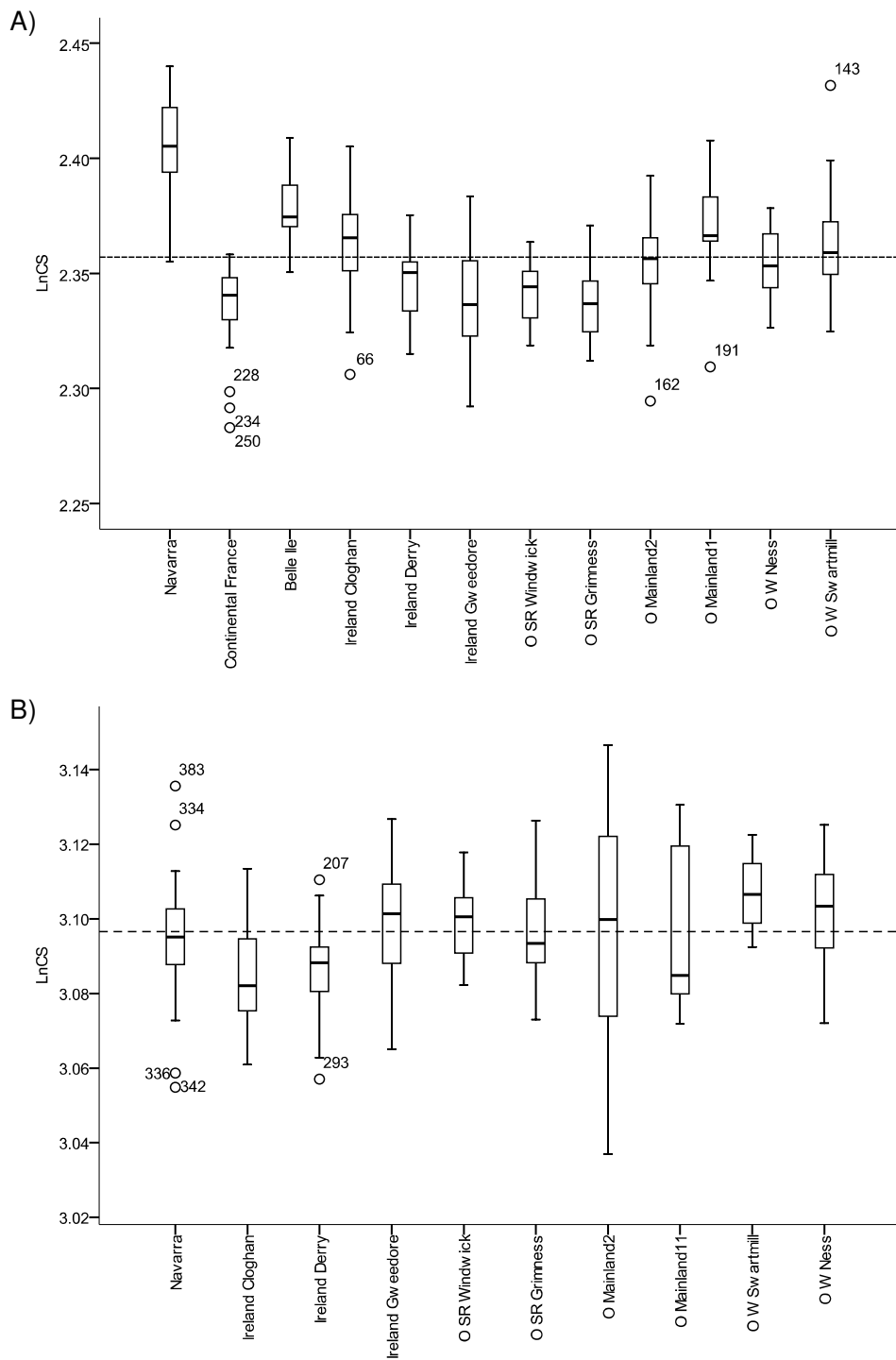


Figure 4.4. Box plots of A) mandible and B) skull Centroid Size (CS; natural log-transformed) of *Sorex minutus* samples ordered latitudinally (with south to the left).

Table 4.4. Centroid Size statistics for *Sorex minutus* skulls of the Pyrenean lineage.

Group	n	mean	median	Lower	Upper	SD	SE
Navarra	28	3.0947	3.0951	3.0879	3.1014	0.0174	0.0033
Ireland Cloghan	20	3.0847	3.0821	3.0777	3.0917	0.0150	0.0034
Ireland Derry	21	3.0865	3.0883	3.0805	3.0925	0.0132	0.0029
Ireland Gweedore	19	3.0998	3.1014	3.0920	3.1075	0.0161	0.0037
O SR Windwick	18	3.0994	3.1006	3.0941	3.1048	0.0108	0.0025
O SR Grimness	19	3.0972	3.0934	3.0902	3.1041	0.0144	0.0033
O Mainland 2	37	3.0989	3.0999	3.0889	3.1090	0.0300	0.0049
O Mainland 1	13	3.0966	3.0849	3.0833	3.1100	0.0222	0.0061
O W Swartmill	20	3.1070	3.1065	3.1025	3.1115	0.0095	0.0021
O W Ness	19	3.1016	3.1034	3.0939	3.1092	0.0158	0.0036

O = Orkney, SR = South Ronaldsay, W = Westray, Lower = Lower 95% CI, Upper = Upper 95% CI, SD = Standard deviation, SE = Standard error.

Parametric and non-parametric MANOVAs showed significant differences among mandible groups (Wilks' $\lambda = 0.0006$, $F_{352, 2421} = 7.0860$, $p < 0.0001$; non-parametric MANOVA $F = 8.2320$, $p < 0.0001$, Appendix 11) and skull groups (Wilks' $\lambda = 0.0006$, $F_{306, 1513} = 6.4670$, $p < 0.0001$; non-parametric MANOVA $F = 10.25$, $p < 0.0001$, Appendix 12).

For the mandible and skull groups, there were no correlations between Procrustes and genetic distances (for mandibles: $R = -0.0823$, $p = 0.6803$; for skulls $R = 0.0617$, $p = 0.3688$), but there were significant correlations between geographic and Procrustes distances (for mandibles: $R = 0.3568$, $p = 0.0363$; for skulls $R = 0.6855$, $p = 0.0046$).

The classification of mandible and skull samples into their respective groups with the DA gave similar results, with 86.8% mandibles correctly classified (69.5% with the cross-validation method) and 84.6% skulls correctly classified (65.4% with the cross-validation method). The CVAs showed that the Continental and island groups were somewhat different (Fig. 4.5A, B). The groups from Navarra for the

mandible and skull datasets were easily distinguishable from the Ireland and Orkney islands groups, while the mandible samples from Belle Île clustered within the range of other continental samples and island groups. The two localities from Westray (Ness and Loch of Swartmill) showed pronounced differences and clustered separately from other island groups in the mandible and skull datasets, similarly to what was found in Chapter 3. Other island groups and localities showed no distinction, either in the mandible or skull datasets.

Dividing the mandible and skull datasets by island size categories gave a very different perspective on shape variation. In general, there was a higher classification percentage: 84.2% of mandibles were correctly classified (74.6% with the cross-validation method), and 93.9% of skulls were correctly classified (86.4% with the cross-validation method) to their original island size categories. The CVA plots showed a clear discrimination of island size categories for the mandible and skull datasets (Fig. 4.6A, B). The continental category was easily distinguishable from all the other categories, the large island size category was separated from medium and small island size categories, but the medium and small island size categories were somewhat mixed. The differentiation by island size category was more evident with the skull than with the mandible dataset.

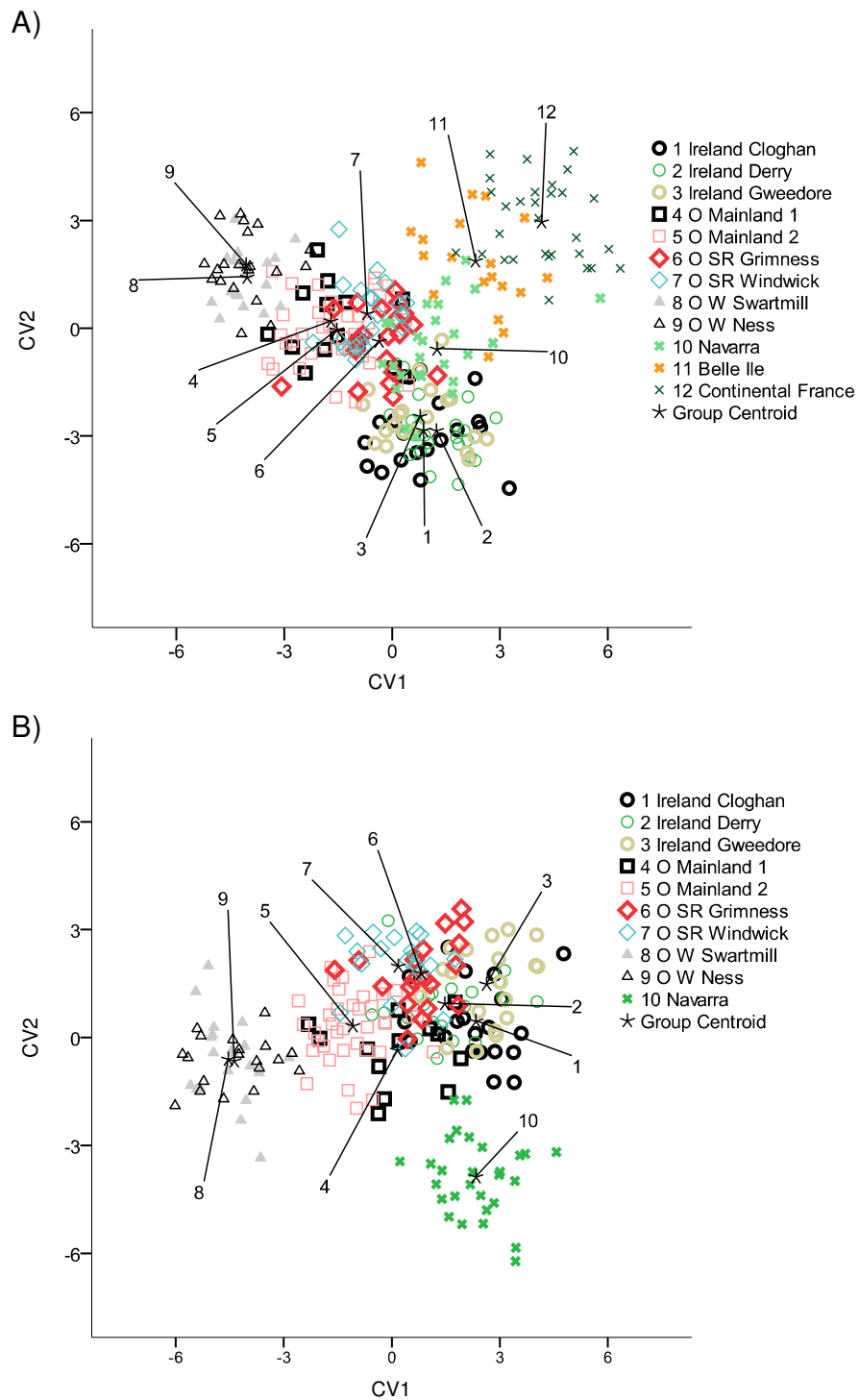


Figure 4.5. Canonical Variate Analysis of shape variables of A) mandibles and B) skulls of *Sorex minutus* from the Pyrenean lineage showing group differences. The first two canonical variates (CV) were used to describe variation among groups. O = Orkney, SR = South Ronaldsay, W = Westray.

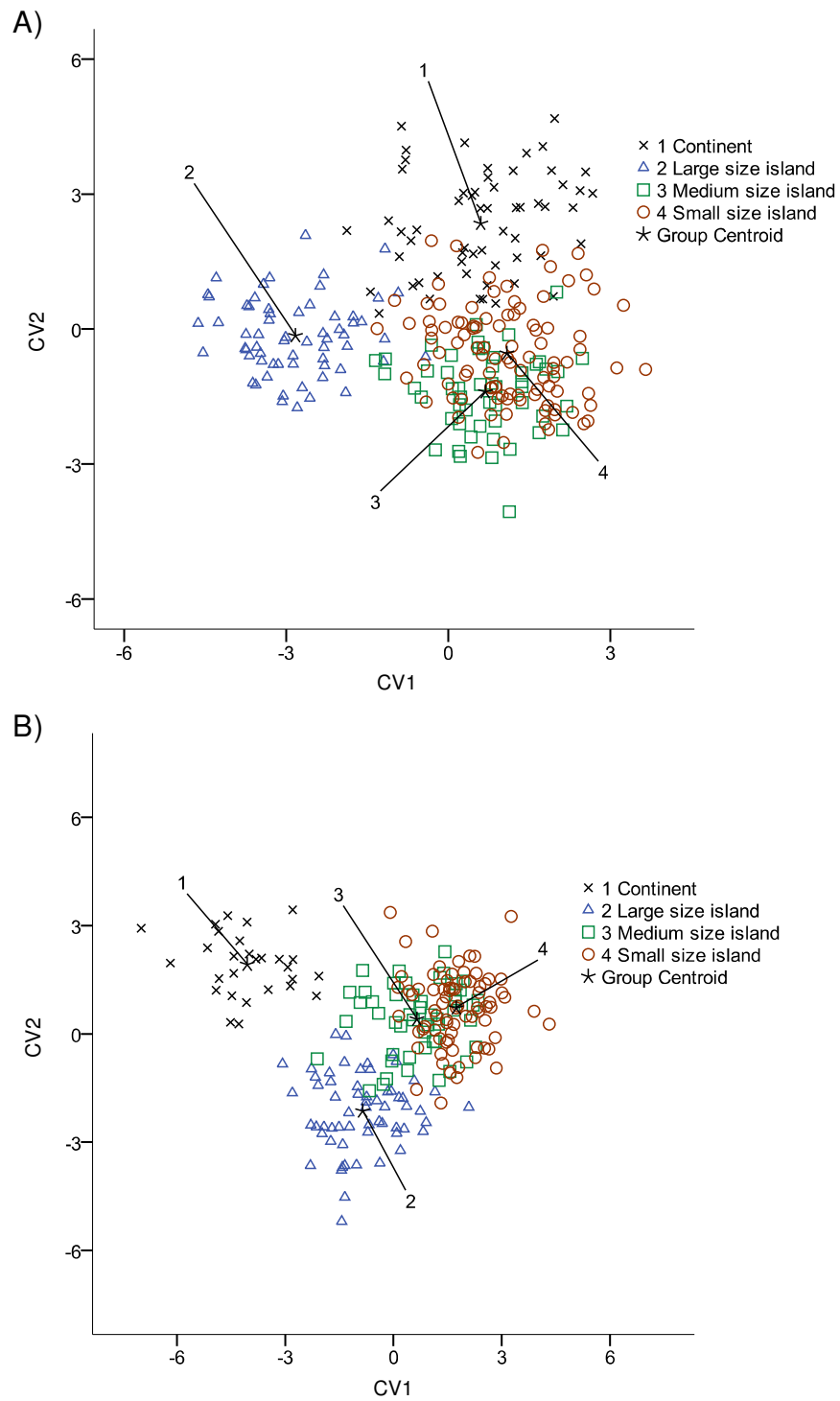


Figure 4.6. Canonical Variate Analysis of shape variables of A) mandibles and B) skulls of *Sorex minutus* from the Pyrenean lineage showing island size differences. The first two canonical variates (CV) were used to describe variations among groups. Continent = Continental European samples, Large size island = Ireland, Medium size island = Orkney Mainland, Small size island = South Ronaldsay, Westray and Belle Île.

4.4 Discussion and conclusions

Within the Pyrenean lineage, the Continental, Ireland, Orkney islands and Celtic fringe groups are closely related and share an intricate colonisation and migration history; however, they are geographically separated and currently isolated, aspects that could have affected their genetic and morphological diversity, and which I explored here.

The migration rates between the Continental and Celtic fringe groups were almost equal, showing a slight tendency of the former as a source area for the later. The phylogenetic network also supported a migration route from continental Europe to Britain, where the most internal haplotype for the full network was found in the Pyrenean group and some Celtic fringe haplotypes expanded from it. This is as expected; at the LGM, Britain would not have been occupied by pygmy shrews (Yalden 1982, 2007) and colonisation would have been from continental Europe over a landbridge that existed until 8.5 KYA (Weninger et al. 2008).

It is interesting that all samples from the Orkney islands also belong to a Celtic fringe described by Searle et al. (2009). The Celtic fringe is the vernacular name given for the culturally and genetically distinct human occupants of the western and northern periphery of Britain, reflecting the scenario that the Celts spread and occupied these regions 2 – 3 KYA and replaced earlier inhabitants (Forster and Toth 2003, Forster et al. 2004, Oppenheimer 2006, Searle et al. 2009). Other small mammals such as the common shrew *Sorex araneus*, bank voles *Myodes glareolus*, water voles *Arvicola terrestris* and field voles *Microtus agrestis*, show a similar peripheral distribution for genetic lineages; however, these species colonised the British Isles soon after the LGM and arrived there before the Celts (Searle et al. 2009).

The presence of an identical haplotype in Northern Spain (Navarra, close to the Pyrenees) and Ireland suggests a direct and long distance human-mediated migration event of *S. minutus* across the sea. However, it is possible that this haplotype was more widespread in continental Europe or it was present in a hypothetical population occupying the landmass between continental Europe and Britain, in which case the migration event would have been across a shorter distance. In the Eurasian phylogeographic study (Chapter 2), I found a few cases of identical haplotypes shared by individuals from distant localities, for example in Britain and the Netherlands (in the North-Central European lineage) or in Serbia and Macedonia (in the Balkan lineage); therefore, it is possible that shared haplotypes of the Pyrenean lineage between continental Europe and Britain exist.

The Celtic fringe hypothesis considers a two-phase colonisation pattern, with one genetic type colonising mainland Britain, then taken by humans to many of the other surrounding islands, but later partially replaced on mainland Britain by a second invading genetic type arriving from the east, generating the peripheral distribution of the first type in the British Isles (Searle et al. 2009). The genetic similarity of the haplotypes of *S. minutus* from South-Western Europe and those from Ireland, the Orkney islands and other Celtic fringe populations can be explained as a first colonisation wave of the 'Pyrenean' lineage from the continent into the British Isles, while the widespread distribution of *S. minutus* in mainland Britain and the genetic similarity with the 'North-Central European' lineage correspond to a second colonisation wave into Britain.

The low genetic diversity found in Ireland and the Orkney islands reflects colonisation of these islands by a restricted number of founders. Similarly, low mean *cyt b* nucleotide diversity values for *S. araneus* are present on islands of the Inner Hebrides off the west coast of Scotland (mean = 0.00105), with nucleotide diversity values ranging between 0 and 0.00316 (White and Searle 2008a); however, the

overall genetic diversity levels there were larger than the ones found in this study. Because Ireland and the Orkney islands have apparently not been connected to mainland Britain during low sea level and natural colonisation to these islands is unlikely (Yalden 1982, Stuart 1995, Lambeck and Purcell 2001), human-mediated colonisation could explain the presence of *S. minutus* on those islands, most likely transported accidentally during the Neolithic. Archaeological evidence indicates that the Neolithic people on Orkney could have easily travelled between islands, and that transportation by sea was easy and more convenient than travelling by land through the rugged interior (Phillips 2004). Spanish and French populations of the common vole *M. arvalis* are closely related to the Orkney vole, showing a comparable pattern to *S. minutus*, so an introduction by Neolithic people from South-Western Europe onto Orkney is plausible, and the high nucleotide diversity there even suggests multiple introductions (Haynes et al. 2003), but rodents may survive longer than shrews on a boat.

The high estimated migration rate between the Celtic fringe and Orkney islands groups indicates that the Orkney pygmy shrew likely originated from a source population in Northern Scotland; however, I did not find shared haplotypes between Orkney and the Celtic fringe or the continent, but most haplotypes from Orkney were directly connected to Celtic fringe haplotypes by only one mutational step, and not to continental haplotypes. Similarly, *S. araneus* *cyt b* haplotypes found on the islands of the Inner Hebrides were generally not found on the Scottish mainland, but most appear to have arisen from one of the haplotypes found on the mainland (White and Searle 2008a). Further sampling along the shores of Northern Scotland may provide haplotypes of *S. minutus* identical to those from the Orkney islands.

It is unlikely that the colonisation of Ireland and Orkney by *S. minutus* was more recent, in historical times (i.e., in the last hundreds of years), because the

island populations show some level of divergence in the *cyt b* gene. Moreover, the AMOVAs indicate that the little genetic variability in the sample was significantly structured among the islands and the Pyrenean group, and within the islands. However, the significant morphological variation observed here, mainly between islands and continental groups, cannot be used to distinguish a recent from an old colonisation event because morphological traits in mammals can evolve quickly on islands, in a matter of a few decades after colonisation (Pergams and Ashley 2001, Millien 2006).

Mandibles and skulls from the Orkney islands did not show the latitudinal trend observed with the full dataset (discussed in Chapter 3), as expected from a dataset more restricted latitudinally and closely related. Both datasets also showed distinct patterns of size variation. Most of the significant differences of mandible CS involved comparisons with the continental populations, while the only significant differences of skull CS involved comparisons with the Westray populations.

The multivariate analysis on shape showed significant differences for mandibles and skulls. There were also some apparent shape differences in the CVA when I divided the sample into groups based on phylogeny and/or geographical origin: Belle Île and continental France, and the Westray groups were differentiated from the other samples from Navarra, Ireland and Orkney in terms of mandible shape. The CVA on skull shape showed that Westray and Navarra were both distinct and separate from other groups from Orkney and Ireland. Unfortunately, I did not have skulls samples from Belle Île and continental France to compare with the mandible pattern of shape variation. However, these results indicated a similar pattern of shape variation for both mandibles and skulls overall, with Westray and Continental samples distinct from samples from Ireland and other Orkney islands.

Island size was a better discriminator of shape variation, because there were marked shape differences when I divided the mandible and skull datasets into island

size categories. For the mandible and skull datasets there were similar patterns of shape variation: The Continental and Large island groups were distinct from each other and from the Small and Medium sized islands, while the Small and Medium sized islands were very similar to each other. Westray, a small size island, had large pairwise Procrustes distances from other islands and the continent, and grouped separately in the CVA. This island also had zero nucleotide and haplotype diversity (only one haplotype was found), although a large number of individuals were sequenced, and it shared its haplotype with Orkney Mainland, likely presenting inbreeding effects.

Populations on small islands are usually smaller and more isolated than populations on larger islands or in the mainland, making them susceptible to extinction and stochastic demographic processes affecting genetic diversity (Frankham 1998), which can have an effect on the developmental stability and fluctuating asymmetry. In *S. araneus*, the significant correlation between heterozygosity and fluctuating asymmetry among the Inner Hebrides Islands were driven by the effects of the smallest island in that study (White and Searle 2008b). In this study, however, I did not assess the fluctuating asymmetry of the Orkney pygmy shrew, but I would expect to find the strongest effects on smaller islands with smaller genetic diversity values.

The results shown and discussed here represent the first analysis of genetic and morphological diversity of *S. minutus* on the Orkney islands, and it is the first study of morphological variation within Ireland in comparison to continental populations.

Chapter 5

General discussion and conclusions

5.1 Phylogeographic structure of *Sorex minutus* in Europe

It has long been recognized that the climatic oscillations during the Quaternary had profound effects on species ranges and the process of speciation (Haffer 1969, Hewitt 1996, Davis and Shaw 2001). The range shifts varied with latitude and topography, depended on individual species responses of migration and adaptations, and resulted in demographic changes that affected the genetic diversity and the geographical distribution of the genealogical lineages (i.e., the phylogeographic structure) of species (Hewitt 2000, 2004). Quaternary refugia represent the geographical regions that species inhabit during periods of glacial and interglacial cycles when there is the maximum contraction in geographical range (Stewart et al. 2010). Traditionally, it has been hypothesised that boreal and temperate species were restricted to Mediterranean refuge areas during glacial maxima in the Southern European peninsulas of Iberia, Italy and the Balkans. This glacial refugia hypothesis is supported by palynological studies, but also by phylogeographical studies on the meadow grasshopper *Chorthippus parallelus*, hedgehog *Erinaceus europeus/concolor* and brown bear *Ursus arctos*, which became the three paradigms to explain the colonisations of northern regions from Southern Europe by temperate species (Taberlet et al. 1998, Hewitt 2000). More recently, palaeontological, palynological, phylogeographic and species distribution modelling indicate that Quaternary refugia in Europe were more complex than currently believed with some temperate refugia further north (Bilton et al. 1998, Stewart and Lister 2001, Kotlík et al. 2006, Provan and Bennett 2008, Fløjgaard 2009, Vega et al. 2010b).

In this study, the phylogeographic analysis on the Eurasian pygmy shrew *Sorex minutus* revealed six cytochrome (cyt) *b* lineages, including an Iberian, North-Central Italian, South Italian, Balkan, Pyrenean and North-Central European, which apparently showed allopatric evolution in southern and northern glacial refugia, followed by population expansions and the establishment of contact zones. The genetic variability of this mitochondrial gene makes it a useful molecular marker for phylogenetic analysis and has been the marker of choice due to the lack of recombination, putative neutrality, smaller effective population size and shorter time for reciprocal monophyly between populations (Hickerson et al. 2010).

The cyt *b* genetic lineages found in the Mediterranean peninsulas are geographically restricted and did not contribute to the northward colonisation of Europe, a pattern first described by Bilton et al. (1998) but later criticised by Michaux et al. (2003) because of the restricted number of samples. Here, I corroborate previous findings on *S. minutus* with a more extensive sampling and comprehensive analysis, and show that, at least for this species, the Southern European peninsulas were refugial areas, while Northern and Central Europe were colonised by expanding populations located further north than the traditional southern glacial refugia.

The high genetic and haplotype diversities found within all the cyt *b* lineages, whether the purely northern lineages or the relatively limited southern forms, indicate that populations have not suffered recent genetic bottlenecks, further supporting the hypothesis of both southern and northern glacial refugia in Europe. Other phylogeographic studies have shown a similar pattern for small mammals, but *S. minutus* is one of the few species that is widely distributed in the three Mediterranean peninsulas, and Central and Northern Europe; therefore, it is an excellent model for understanding the effects of the glaciations in Europe and the colonisation history during the Pleistocene and the postglacial.

Considering the biogeographical traits of *S. minutus*, namely cold tolerance, present-day northerly distribution, habitat generalist, short generation times and small body size (Bhagwat and Willis 2008), it is possible that *S. minutus* populations were more widely dispersed during colder times than currently appreciated. Several cold tolerant species, such as the arctic fox, lemmings, reindeer, ptarmigan, etc., had larger geographical ranges during the glacials than during interglacials (Stewart and Dalén 2008, Stewart et al. 2010), and while this is probably not true for *S. minutus*, the species need not have been as restricted as implied by the grasshopper/hedgehog/bear paradigm for temperate species. Ecological niche models for *S. minutus* and other small mammals for which northern refugia have been hypothesised show relatively widespread distributions at the Last Glacial Maximum (LGM), mostly restricted to the north by the ice sheets, so it is possible that temperate but cold tolerant species were able maintain a wide range in Central Europe during the glacial periods (Fløjgaard 2009, Vega et al. 2010b). Moreover, *S. minutus* is currently found at higher altitudes in the Mediterranean peninsulas (usually higher than 500 m.a.s.l.; Madureira and Magalhães 1980, MacDonald and Barrett 1993), likely because the high temperatures in the lowlands does not suit it (Taylor 1998), which suggests that in the present time populations there could be in interglacial refugia (Hilbert et al. 2007, Bennett and Provan 2008, Stewart et al. 2010).

For the nuclear markers (two concatenated Y-chromosome introns and the BRCA1 autosomal gene) there was very low sequence polymorphism resulting in phylogenetic reconstructions with low power and poor resolution, so further phylogeographic inferences with these markers were not performed and could not be compared with the mitochondrial (mt) DNA findings. Nonetheless, the use of molecular markers with different modes of inheritance provides a better chance to reconstruct the evolutionary history, and it also avoids the over-interpretation of

results with single trees, which can be affected by stochastic processes (Brito and Edwards 2009).

The concatenated Y-chromosome introns showed equivalent clades to the *cyt b* phylogroups, with distinct North-Central Italian, South Italian and Southern Balkan groups, plus a clade including all Pyrenean and Iberian samples, and a clade including all North-Central European, Northern Balkan and some samples from the northernmost distribution of the North-Central Italian phylogroup. This result provided additional evidence for a geographical structure in Europe below the species level of *S. minutus*. The differences between the *cyt b* and concatenated Y-chromosome introns trees, and the clustering of the Pyrenean with Iberian, Balkan with North-Central European and North-Central European with North-Central Italian clades could be due to sex biased dispersal near the contact zones (Prugnolle and de Meeus 2002); however, I consider that this is more likely the result of the lower genetic polymorphism and, thus, lower phylogenetic resolution of the Y-chromosome introns compared to the *cyt b*.

The BRCA1 nuclear gene had very little genetic variation and did not resolve distinct phylogroups, except for a South Italian and a Pyrenean plus Iberian clades. This result was not unexpected because other studies have also shown that the number of informative sites in nuclear genes is small and the phylogenetic resolution is poor, a problem that can be resolved by concatenating multiple genes together (Brito and Edwards 2009).

5.2 Historical demography and colonisation routes

One important result in this study was the finding that Northern and Central Europe, including the British Isles, have been colonised by two lineages, the Pyrenean and the North-Central European. These two lineages show a characteristic signature of a population expansion, strongly supported by the

mismatch distributions, the significant neutrality and R_2 tests, and the star-like pattern of the haplotype network (Fig. 2.3). These results were also characteristic of continental populations only, i.e., excluding the populations on the British Isles. Furthermore, the North-Central European lineage had the most widespread geographical distribution and showed a subtle geographical differentiation among Eastern Europe, Central Europe and Britain, which argues in favour of relatively isolated populations; however, a more detailed analysis with a faster evolving molecular marker would provide a better understanding of the population genetic structure of the North-Central European phylogroup.

The North-Central Italian lineage also showed a significant population expansion signature, likely a result of the colonisation of previously glaciated areas in the Alps, and forms a long contact zone with the Pyrenean, North-Central European and Balkan lineages in Central Europe. The Balkan lineage, in contrast, showed a stable population size through time and no evidence of a recent population expansion. It is possible that in the Balkans, populations were able to maintain relatively constant size in the heterogenic landscape there, but it is also possible that the multimodal mismatch distribution is a result of mixing very distinct populations into a single group. Actually, the *cyt b* phylogenetic trees showed two distinct and divergent sub-lineages in the Balkan peninsula that deserve further attention (see Fig. 2.2). Martino's vole (Dinaric snow vole) *Dinaromys bogdanovi* is a Balkan endemic genus and species with three highly divergent lineages in the North-Western, Central and South-Eastern Balkans, with the first two lineages showing multimodal mismatch distributions, supporting a multirefugia scenario in the Balkans and stable population sizes during the glaciations (Kryštufek et al. 2007, Bužan et al. in press). In Iberia, however, the lack of a significant population expansion signature for *S. minutus* is likely a result of low sample size. Nonetheless, the Iberian peninsula is considered an important and complex refugial

area with several microrefugia and endemics for temperate species of fish, amphibians, reptiles, mammals, invertebrates and plants (Gómez and Lunt 2007). Future studies on *S. minutus* from the Iberian peninsula might be able to show significantly differentiated populations and independent demographic histories in the Sistema Central and Cantabrian mountain ranges.

Searle et al. (2009) described a Celtic fringe in the British Isles composed of samples from the western periphery of Britain, which in this study belonged to the Pyrenean lineage. They hypothesised a selective sweep (or recent adaptive substitution) coming from the east to explain the western and northern peripheral distribution of the Celtic fringe samples and the widespread distribution of the North-Central European phylogroup in mainland Britain. The patterns of an expanding population and a selective sweep can be similar and difficult to distinguish from each other, because the synonymous and segregating sites in the *cyt b* gene used in the population expansion tests can be genetically linked to sites under selection (Ballard and Whitlock 2004). For example, a mtDNA haplotype, characterized with a non-synonymous mutation resulting in a transition between Leucine/Serine aminoacids of the protein encoded by the ATP6 gene, has been implicated in the non-shivering thermogenesis and differences in respiratory and winter survival of the white-toothed shrew *Crocidura russula* (Fontanillas et al. 2005). Similarly, it is possible that natural selection favoured individuals of the North-Central European *cyt b* lineage on Britain, replacing the Pyrenean lineage and originating the Celtic fringe. If this is so, the population expansion pattern observed there could have been a result of a selective sweep. However, the colonisation and spread of *S. minutus* over favourable habitat in Britain most likely produced a population expansion pattern that could have been amplified by a selective sweep effect. There were very few non-synonymous substitutions in the *cyt b* gene, no evidence of selection based on the McDonald-Kreitman test and no violation of the neutrality

hypothesis compared to an external group, so it is possible that within *S. minutus* there are no selection forces acting on the *cyt b* gene. Unfortunately, this test is not suitable for detecting very recent selective sweeps because non-synonymous and synonymous mutations, linked to the beneficial mutation, will be similarly affected by the selective sweep (Nielsen 2005), and a significant signature could also result from a combination of many slightly deleterious non-synonymous mutations and population expansions (McDonald and Krietman 1991).

Contrary to most phylogeographic studies in Europe, the timings of the population expansions in *S. minutus* pre-date the LGM. Other studies have also shown population expansion events pre-dating the LGM, for example for the weasel *Mustela nivalis* in the Western-Palaeartic region (Lebarbenchon et al. in press) and for the Asian clade of the *Crocidura suaveolens* group (Dubey et al. 2006). However, the timing of the population expansion was calculated assuming a molecular clock and a standard 2% substitution rate per million years, which could give problematic results. If I had used a higher substitution rate as molecular clock, the divergence and population expansion times would have been more recent. Different substitution rates for small mammals and shrews are commonly used in phylogeographic studies, for example Ratkiewicz et al. (2002) used a mutation rate of 2.5% per million years for studying the evolutionary history of karyotypic groups of the common shrew *S. araneus* (but originally used for cichlid fish); Haynes et al. (2003) used a 6-10% mutation rate for *Microtus arvalis*; and Yannic et al. (2008) used a divergence rate of 7.1% per million years with a confidence interval between 5.7 and 8.5% based on Maximum Likelihood distances for studying the evolutionary history of the western *S. araneus* group. Another problem with the molecular clock is known as the exponential decay law, which states that the divergence and population expansion times of a lineage can be overestimated when making the erroneous assumption of a linear relationship between genetic differences and time

(Ho et al. 2005, Ho and Larson 2006); but Bandelt (2008) pointed out that there are problems with the way the decay law was modelled originally. Therefore, the timing of events in this and other studies have to be taken with caution because they depend on the chosen mutation rates, but also on other factors such as the time of the fossil calibration for Bayesian estimates of TMRCA, the number of generations per year assumed for the species under study (accurate in the case of the pygmy shrew, Corbet and Harris 1991) and the rate heterogeneity among lineages.

5.3 An emerging pattern of northern glacial refugia

The comparison of the results obtained here with those elsewhere shows an emerging pattern of glacial refugia in Mediterranean peninsulas and further north in Central Europe for several species (Fig. 5.1A–D).

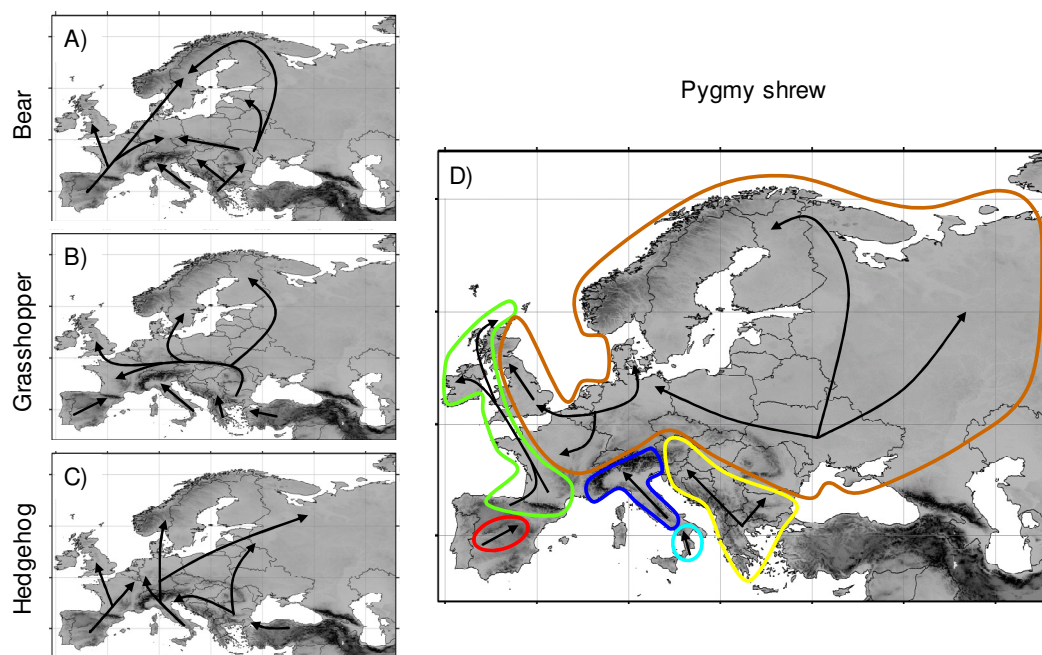


Figure 5.1. Three paradigms of postglacial colonisation routes from Southern Europe: A) the bear, B) the grasshopper and C) the hedgehog (Hewitt 2000). The addition of D) the pygmy shrew gives a more complete picture and exemplifies an emerging pattern of northern refugia. Arrows represent general colonisation routes. Coloured areas are an approximation of the geographical distribution of the cytochrome *b* lineages obtained in this study (see Fig. 2.2 for lineages).

The bank vole *Myodes (Clethrionomys) glareolus* has a phylogeographic pattern very similar to that found with *S. minutus*: there are three Mediterranean (Iberian, Italian and Balkan) and three northern phylogroups (Eastern, Western and the Ural Mountains) significantly differentiated, with heterogeneous mismatch distributions and population expansion signatures in the northern phylogroups but long-term stability for the Mediterranean populations, and most of the genetic structure distributed among lineages (Deffontaine et al. 2005). Furthermore, the bank vole has a northern glacial refugium in the Carpathians from where it expanded at the end of the last glaciation and from where it recolonised northern latitudes (Kotlík et al. 2006, Wójcik et al. 2010). The field vole *Microtus agrestis* has three lineages that derived from separate refugia, one or two in the Iberian peninsula, one in Western Europe and another one in Eastern Europe (Jaarola and Searle 2002). The Iberian and Western lineages have a contact zone in Southern France and Switzerland, while the Western and Eastern lineages have a contact zone in Fennoscandia, likely originating from different colonisation routes (Jaarola and Searle 2002). The common vole *M. arvalis* has significantly differentiated lineages in the Iberian and Italian peninsulas, distinct from the lineages further north in Western, Central and Eastern Europe, which indicate a limited effect of southern refugia in shaping the current patterns of genetic diversity (Haynes et al. 2003, Heckel et al. 2005). Interestingly, the *Sorex araneus* group also shows divergence of Southern Mediterranean populations from Central and Eastern European groups, with *S. granarius* in Iberia, *S. coronatus* in the Pyrenees, France, Western Germany and Switzerland, *S. antinorii* in Italy and other *S. araneus* chromosomal races in Central and Eastern Europe, plus *S. samniticus* (endemic to Southern Italy) as a sister species (Yannic et al. 2008). Moreover, several mammal species show a genetic distinction in Southern Italy, including *M. glareolus* (Amori et al. 2008), *M.*

brachycercus (Castiglia et al. 2008), *Talpa romana* (Ungaro et al. 2001), *Lepus corsicanus* (Pierpaoli et al. 1999) and *Sciurus vulgaris* (Grill et al. 2009), plus other vertebrate species, denoting the importance of the Calabrian arc as a hotspot for European biodiversity (Vega et al. 2010a).

5.4 Natural and human-mediated colonisation

The widespread European distribution of *S. minutus* is a mixture of natural and human-mediated colonisation events. The fossil record of *S. minutus* suggests an old and natural colonisation of the European continent since the Early Pleistocene, originating from the East. The current genetic structure suggests more recent divergence events leading to a variety of phylogroups that attained their present distribution through natural colonisation and (in parts of the British Isles) through human introductions.

The *cyt b* analysis indicates that Britain was colonised naturally by two distinct lineages, the Pyrenean and the North-Central European. Sea level changes during the LGM indicate the presence of a landbridge between mainland Europe and Britain (Yalden 1982, Stuart 1995), which could have been a temporal and suitable land corridor for *S. minutus* and allowed this and other species to colonise Britain by their own means (Yalden 1982). The genetic similarity of continental European and British samples supports this view. The presence of *S. minutus* and other small mammals in Ireland, however, is puzzling and has been the focus of much research.

The close genetic relationship of the haplotypes from the Orkney islands, Ireland and other Celtic fringe samples from Britain with South-Western Europe suggests a geographical origin there. In particular, the occurrence of exactly the same haplotype in Northern Spain and Ireland (where it is the most common haplotype) is striking. However, the direct colonisation of Ireland from Northern

Spain with people seems unlikely given the geographical distance (about 1000 Km); therefore, it seems more plausible that populations in Britain sharing the haplotype now found in Northern Spain were the source for the Irish lineage. It should be noted that haplotypes separated by only one mutation from haplotypes in Northern Spain have been found in France and Britain (Fig. 4.2), and it would not be surprising if some Pyrenean lineage haplotypes identical to haplotypes currently found in Spain managed to colonise Britain and subsequently make their way to Ireland. It is likely that it was humans that transported the shrews from Britain to Ireland, given the lack of evidence of a landbridge (Searle et al. 2009). In support of this model, it is notable that there is currently a wide diversity of haplotypes in the Celtic fringe (Fig. 4.2), which could easily have included the haplotype that started off the colonisation of Ireland. Further sampling of the Celtic fringe on Britain could shed more light onto this. There is particularly poor representation of the Pyrenean lineage in Wales and South-Western England (Fig. 4.1), and it may be that this was the source area of the Irish colonisation. I have provided strong evidence that the Orkney pygmy shrew originated from populations in mainland Britain belonging to the Pyrenean lineage, detected by the genetic similarity to other Celtic fringe haplotypes and by the migration analysis. The pygmy shrew was most likely taken to the Orkney islands by boat during the Neolithic through trade routes among nearby coastal areas widely established by that time (Phillips 2004, Zvelebil 2006) rather than by natural processes like rafting, swimming or migration over ice. The closest island of the archipelago to the mainland (South Ronaldsay) is about 10 Km away from the coast, and the Orkney islands were not connected to the mainland during lower sea levels in the postglacial (Yalden 1982). Furthermore, the pygmy shrew from Westray seems to have originated directly from Orkney Mainland, about 16 Km away, because Westray has only one haplotype shared with Orkney Mainland. Human-mediated colonisation of the islands surrounding Britain and

Ireland does not seem implausible, because other species of small mammals on islands in the Mediterranean, Canary Islands, Madeira archipelago and the British Isles were also transported there by humans, including house mice, white-toothed shrews (*Crocidura* spp.) and *A. sylvaticus* (Delany and Healy 1966, Gündüz et al. 2001, Renaud and Michaux 2007, Michaux et al. 2007).

For several islands separated by short distances or close to the coast, it is possible that *S. minutus* colonised by its own means. At least for *S. araneus* and *S. minutus*, natural island colonisation less than 500 m from the mainland is possible in the cold waters of Lake Koitere in Finland (Hanski 1986). Hoy and Orkney Mainland share the same haplotypes and are geographically proximal, so it is possible that the two islands maintained gene flow in the past when the sea level was lower. Similarly, White and Searle (2008a) hypothesised that Jura and Islay remained in contact until recently, and that gene flow still occurs at a low rate between mainland populations and Skye and Seil in the Inner Hebrides given the high level of microsatellite diversity and low genetic differentiation. Moreover, the haplotypes from South Ronaldsay likely originated from a different source population in Northern Scotland, because they are different from the haplotypes found on the other Orkney islands. Further studies with microsatellites would provide a better understanding of gene flow between the mainland and the Orkney islands.

5.5 Morphological diversity of *Sorex minutus* in Europe

Morphological differentiation of *S. minutus* in Europe is much less evident than genetic differentiation. Without an a priori grouping of the mandible and skull samples, there were no consistent shape differences between samples in the Relative Warp (RW) analyses; however, dividing the mandible and skull samples into the phylogroups detected with *cyt b* revealed small but significant shape variation among the groups with the Canonical Variates Analysis. Multivariate

analyses of variance detected morphologically different phylogroups, but the shape differences did not recover the phylogenetic relationships among them. There are several stochastic, developmental, environmental and genetic factors affecting mandible and skull structures (Klingenberg 2001, Monteiro et al. 2003, Caumul and Polly 2005, Cardini et al. 2007); therefore, it is not surprising that the genetic relationships were not properly recovered. Other studies have shown disagreement between morphological and phylogenetic findings. For example, a three-dimensional geometric morphometric study of *Arvicanthis* (an African murid) showed a close relationship of morphology with environmental background, but only a partial agreement with phylogeny, possibly as a result of repeated, convergent evolution of similar morphology and adaptation to local climatic conditions (Fadda and Corti 2001); and the trends in shape variation of spiny rats of the genus *Trichomys* disagreed with the expected phylogenetic pattern (Monteiro and dos Reis 2005).

There are few detailed intraspecific geometric morphometric studies of wild mammals, although geometric morphometrics is a good method for studying shape variation below the species level (Loy 1996). Inter- and intraspecific studies have shown that marmots, *Trichomys apereoides*, vervet monkeys, phyllostomid bats, etc. have notable shape differences, which are usually correlated with environment, geography, phylogeny and feeding habits (Corti et al. 2001, Cardini 2003, Caumul and Polly 2005, Monteiro et al. 2003, Cardini and O'Higgins 2004, Nogueira et al. 2009). *Sorex minutus* is considered a food generalist because of the high diversity of prey it feeds on. Thus, it is possible that the shape of mandibles and skulls of *S. minutus* responds weakly to habitat changes, because the selection pressures on anatomical structures involved in mastication might be very similar and there is no prey specialization in different geographical regions (Casti n and Gos lbez 1999).

Size, however, showed a marked latitudinal trend on the pygmy shrew mandible across Europe with an increasing size with decreasing latitude, contrary to Bergmann's rule. It is possible that prey in southern latitudes have harder exoskeletons, so selection pressures could have favoured bigger mandibles and a stronger bite force, without affecting overall shape, as shown for South Italian pygmy shrews (Vega et al. 2010a). There was a strong allometric effect on mandibles, so most of the shape variation observed among continental samples was strongly correlated with size and latitude. The skull sample showed a weak but still significant latitudinal pattern of size, but the skull is less involved in the mastication process than the mandible. Ochocińska and Taylor (2003) found a stronger latitudinal pattern on *S. minutus* skulls than in this study, using samples from across Eurasia but with a smaller sample size per locality. They did not use a geometric morphometrics approach; instead they measured the size of the skull as the distance from the condylus occipitalis to the front edge of the praemaxillare, a good indicator of overall body size. Nevertheless, the interpretation of their results was equivalent to the one presented here for mandibles and skulls using a geometric morphometric approach and also support a latitudinal pattern.

5.6 Insights into island evolution of *Sorex minutus*

Besides the evident latitudinal trend of mandible and skull size and the little shape variation of continental samples, it seems that island evolution rather than phylogenetic differentiation in southern and northern refugia played an important role in morphological shape variation of *S. minutus*.

Insular populations of mammals appear to follow an 'island rule' (Van Valen 1973), which predicts an increase of body size for small mammals (gigantism) and a decrease of body size for large mammals (dwarfism) on island populations compared to mainland populations, probably as a result of limited insular resources,

less intraspecific competition and predation (Lomolino 2005). In addition, it is possible that morphological variation is a result of an 'island syndrome', traditionally described as the systematic differences in demography, reproduction, behaviour and morphology (including the island rule discussed previously) in island populations when compared to mainland populations (Adler and Levins 1994). These differences may evolve as a result of microevolutionary processes and after many generations of directional selection following colonisation and isolation, generating locally adapted island populations (Adler and Levins 1994). The effects of genetic variability on the morphological divergence of island populations and speciation have been widely explored in the past (Berry 1986); however, most of the factors involved in island differentiation depend on the genetic composition of the founding population (Berry 1996).

In this study, island pygmy shrews from Ireland and the Orkney archipelago were not bigger than continental populations, inconsistent with the island rule sensu Van Valen (1973), but the size of mandibles and skulls was consistent with the latitudinal pattern described for the full dataset. In contrast, populations in Ireland and the Orkney islands showed a marked shape distinction from continental counterparts, while continental samples showed an extensive overlap of shape variation as illustrated by the RW Analysis. Actually, samples of a genetically divergent *S. volnuchini* sample (with about 5% *cyt b* sequence divergence) showed little morphological variation from the continental groups of *S. minutus*.

It is interesting that the strong pattern of shape divergence between continent and islands evolved in just a few thousand years after the colonisation of Ireland and the Orkney islands. Mandible and skull shape from island populations was easily discriminated by island size and was easily distinguished from continental populations, regardless of the high genetic similarity. Founder effects, genetic bottlenecks, genetic drift due to small population size and geographical

isolation could have affected the morphological variation of *S. minutus* in Ireland and the Orkney islands. Samples from Westray were significantly different from other island populations in terms of mandible and skull size and shape, and the population there had the lowest genetic diversity values, whereas Orkney Mainland and Ireland populations had more heterogeneous shape variation and higher genetic diversity values. The continental population from the Pyrenees, genetically related to the island populations analysed here, was significantly different in mandible and skull shape, had the most heterogeneous shape variation and had the highest genetic diversity values.

The shape and size variation on Westray and other small sized islands could be related to genetic bottlenecks and colonisation events from a low number of founders, while Orkney Mainland and Ireland, much larger islands, could have been colonised in several occasions and can maintain larger populations. In agreement with these results, other studies have also shown morphological divergence of recently colonised island populations. For example, the house mouse on the Canary Islands reflects some degree of differentiation and bigger molars than continental populations, which evolved in a matter of five centuries after the first introduction, although it is unclear if this is an adaptive or a random effect (Michaux et al. 2007). The mandible of the wood mouse *Apodemus sylvaticus* shows significant divergence on islands of the Mediterranean Sea correlated with remoteness from the continent and island size; moreover, there is a latitudinal mainland gradient in size and shape of mandibles and molars, but different individual patterns of differentiation on islands (Renaud and Michaux 2007). Apparently, the large-scale clinal pattern of morphological variation on the mainland populations of *A. sylvaticus* is favoured over adaptation to small-scale environmental variations, buffered by gene flow. Island populations, instead, show a mosaic pattern of evolution because

gene flow is disrupted due to geographic isolation and populations adapt differently to local environmental conditions (Renaud and Michaux 2007).

5.7 Conservation implications

One of the aims of this study was to provide a better understanding of European biodiversity, which could have implications for conservation. Although *S. minutus* is considered as a least concern species by the IUCN (IUCN 2008; <http://www.iucnredlist.org/details/29667>), the distinct lineages deserve more attention than this implies. Local and/or country based conservation efforts are highly valued (for example, on Britain and Ireland the pygmy shrew is protected by law), and genetic diversity is now considered an important aspect of global biodiversity (McNeely et al. 1990). Moreover, as the refugial areas in Southern Europe are often found in mountain ranges at the low-latitude margins of the present-day distribution ranges of species, they are most likely to contain rear-edge populations where selection for local adaptations could have resulted in the evolution of distinct ecotypes (Cook 1961, Hampe and Petit 2005). It has been argued that the populations that inhabit latitudinal margins deserve investigation and high conservation priority because they are important to determine the responses of species to modern climate change (Petit et al. 2003, Hampe & Petit, 2005). Clearly, the genetically divergent lineages of *S. minutus* found in this study should be considered as Evolutionarily Significant Units (ESUs), defined as genetically differentiated and reciprocally monophyletic lineages with a unique geographic distribution, which contain the evolutionary potential of the species (Moritz 1994).

5.8 Future directions

This study opens the door for further investigations. Population genetic studies in Mediterranean peninsulas and further sampling there would provide a

better understanding of the gene flow and structure of the genetic lineages, and would allow further investigation of the concept of 'refugia within refugia'.

In Southern Italy, it is possible that there are very distinct populations in the Calabrian arc. The Aspromonte and Serre Massifs in Calabria contain the southern-most populations of *S. minutus*, which were not described genetically or morphologically in this study, and could contain highly differentiated populations due to geographical isolation. Also, populations in Monte Pollino, Basilicata and in Catena Costiera, Calabria could hold the southern-most populations of the North-Central Italian lineage, separated from the South Italian lineage by the Crati Valley but relatively contiguous with the populations from the Apennines.

In the Balkans, it is likely that there are two highly divergent groups, as explained above. The high genetic divergence of this lineage indicates that it is one of the oldest lineages of *S. minutus* and highlights the importance of the Balkans as a biodiversity hotspot. Because of the historical, political, linguistic and topographic complexity of this peninsula, the scientific studies have accumulated slowly in comparison to other European regions and much remains to be investigated there (Kryštufek and Reed 2004).

Further sampling in Iberia would provide a better delimitation of the Iberian and Pyrenean lineages, and it is possible that both have a contact zone in the Cantabrian mountain range. I encountered one haplotype that clustered with the Balkan lineage and another one quite divergent from all the rest, which were eliminated from the analysis because of the uncertainty of locality data and contamination issues; however, this deserves more attention because they could represent relics of an old colonisation event. Regions in North-Western and Central Spain and Portugal have not been characterised in this or other studies, and samples from there could show other divergent lineages that could add to the refugia within refugia hypothesis of the Iberian peninsula.

Siberia and Eastern Europe were undersampled, and it would be interesting to obtain samples from there to study the phylogeographic structure. The highly divergent haplotypes from Ukraine, Russia and Poland could belong to a cryptic lineage in Siberia.

The mixing of *S. volnuchini* within the shape variation of *S. minutus* was unexpected, and it would be interesting to add other *Sorex* species to the geometric morphometrics analysis, as well as other Soricidae species with terrestrial, aquatic and fossorial habits. Instead of expecting to find a strong phylogenetic component of shape variation, I would expect to find an ecogeographical grouping of Soricidae species. Moreover, further sampling of *S. volnuchini* would provide a better understanding of the genetic relationship between these sister species.

Fluctuating asymmetry could be analysed in the context of different environmental correlates and population genetic diversity on the Orkney islands and other islands off the coast of Britain. There are several microsatellites developed for *Sorex*, and the genetic diversity values and asymmetry could be correlated with island size. For this, other islands of the Orkney archipelago should be sampled to give a more comprehensive picture of island evolution.

Finally, this is an interesting time for phylogeography and population genetics (Brito and Edwards 2009). The way molecular data is collected and analysed has been revolutionised by new genomic tools developed on model organisms and applied to evolutionary and ecological studies, research areas currently named as 'genomic phylogeography' and 'population genomics' (Brito and Edwards 2009). The transition from single to multiple loci in phylogeographic analyses is taking place fast. Larger datasets include more informative sites and increased nodal support, and more loci that sample whole genomes allow the inference of species trees rather than gene trees, and provide a more comprehensible understanding of population history and speciation processes.

Although I used *cyt b*, two Y-chromosome introns and an autosomal gene, this study is not different from a traditional phylogeographic study, because each molecular marker was analysed separately. mtDNA phylogeography has been essential for the development of the field, has provided the basic research and will not be abandoned soon given the relative simplicity of analysis and lower economic costs, and genome-informed studies will gain from traditional phylogeographic findings (Brito and Edwards 2009).

5.9 Conclusions

The Eurasian pygmy shrew *Sorex minutus* is a good model for understanding biological diversity, colonisation patterns and the effects of past climate change on biological diversity.

There is a mosaic of genetic lineages across continental Europe, characterised by different demographic histories and natural colonisation patterns, while island populations are characterised by recent natural and human-mediated colonisations. It is interesting that the pygmy shrew readily colonises islands as a transient stowaway of people despite its high metabolic requirements. Moreover, *S. minutus* also shows varying degrees of morphological variation. There is a latitudinal trend of size variation, contrary to one of the best known biogeographic rules, Bergmann's rule, with increasing size with decreasing latitude, a trend found to be common in other species of shrews. There is little shape variation among continental populations, but the differences are significant. Shape variation is strongly correlated with size, latitude and longitude, not with genetic divergence; therefore, environmental factors played a more important role than genetic differentiation in the morphological diversification of the species. Island evolution has been another factor strongly influencing shape variation, probably because of founder effects, genetic bottlenecks and inbreeding on small islands, but *S. minutus*

on islands does not seem to have been affected by an island syndrome of increasing body size.

This study has notably expanded previous findings on *S. minutus*, with a more precise statistical phylogeographic analysis of the genetic variability, colonisation routes, historical demography and structure across Europe. I have shown more clearly than before that the North-Central European lineage emerged from a northern glacial refugium, both through better characterisation of that lineage and better characterisation of populations in the Mediterranean peninsulas. A Pyrenean lineage is also very likely to have existed north of the traditional southern refugial areas. These studies are helping to develop *S. minutus* as a major model to study northern glacial refugia. *Sorex minutus* is not an easy species to obtain in large numbers, and the sampling described here represents a very substantial effort. However, it is a species that is unusually widespread and genetically subdivided and therefore can inform better than almost any other about the relative importance of southern and glacial refugia. This is important because the characteristics of species within a given area may reflect (in terms of genetic variability, adaptations) the nature of the refugial area from which they derived.

The study of island populations of *S. minutus* has not only been of interest with regards island evolution, but also with regards island colonisation. Although previous studies have investigated *S. minutus* in Ireland, my work has provided the level of sampling that has been necessary to develop a realistic colonisation scenario. It has also been possible to do the same for the Orkney islands. These studies add considerably to our understanding of how even prehistoric (Neolithic) humans can shape the genetic architecture of a species by moving particular forms around.

In summary, this has been (a) the first large-scale study of the morphological diversity of *S. minutus* across Europe with a geometric morphometrics approach, (b)

a large extension of previous studies considering the phylogeography of *S. minutus* across the same range, particularly focusing on the issue of northern versus southern refugia and human-mediated colonisation of the British Isles, and (c) the first study that has explored the colonisation, genetic variability and morphological diversity of *S. minutus* on small islands (the Orkney archipelago). The results presented here are of importance for the conservation of genetic and morphological diversity in one of the smallest mammals in Europe.

References

- Adams DC, Rohlf FJ, Slice DE. 2004.** Geometric morphometrics: ten years of progress following the 'revolution'. *Italian Journal of Zoology* **71**: 5-16.
- Adler GH, Levins R. 1994.** The island syndrome in rodent populations. *The Quarterly Review of Biology* **69**: 473-490.
- Afzal-Rafii Z, Dodd RS. 2007.** Chloroplast DNA supports a hypothesis of glacial refugia over postglacial recolonization in disjunct populations of black pine (*Pinus nigra*) in Western Europe. *Molecular Ecology* **16**: 723-736.
- Agustí J, Blain H-A, Furió M, De Marfá R, Santos-Cubedo A. In Press.** The early Pleistocene small vertebrate succession from the Orce region (Guadix-Baza Basin, SE Spain) and its bearing on the first human occupation of Europe. *Quaternary International*.
- Amori G, Aloise G, Annesi F, Franceschini P, Colangelo P. 2008.** Filogeografia mitocondriale di Arvicola rossastra *Myodes glareolus* in Italia. *69° Congresso Unione Zoologica Italiana*, Senigallia, September 22–25. Abstracts, 18.
- Anderson MJ. 2001.** A new method for non-parametric multivariate analysis of variance. *Austral Ecology* **26**: 32-46.
- Ashton KG, Tracy MC, Queiroz AD. 2000.** Is Bergmann's rule valid for mammals? *The American Naturalist* **156**: 390-415.
- Avise JC 2000.** *Phylogeography. The History and formation of species*. Harvard University Press. Cambridge, USA.
- Avise JC, Arnold J, Ball RM, Bermingham E, Lamb T, Neigel JE, Reeb CA, Saunders NC. 1987.** Intraspecific phylogeography: the mitochondrial DNA bridge between population genetics and systematics. *Annual Review of Ecology and Systematics* **18**: 489-522.

- Ballard JWO, Whitlock MC. 2004.** The incomplete natural history of mitochondria. *Molecular Ecology* **13**: 729-744.
- Bandelt HJ. 2008.** Clock debate: when times are a-changin': Time dependency of molecular rate estimates: tempest in a teacup. *Heredity* **100**: 1-2.
- Bandelt HJ, Forster P, Rohl A. 1999.** Median-Joining networks for inferring intraspecific phylogenies. *Molecular Biology and Evolution* **16**: 37-48.
- Baquero RA, Tellería JL. 2001.** Species richness, rarity and endemism of European mammals: a biogeographical approach. *Biodiversity and Conservation* **10**: 29-44.
- Barton NH, Hewitt GM. 1985.** Analysis of hybrid zones. *Annual Review of Ecology and Systematics* **16**: 113-148.
- Bennett KD, Provan J. 2008.** What do we mean by 'refugia'? *Quaternary Science Reviews* **27**: 2449-2455.
- Berry RJ. 1986.** Genetics of insular populations of mammals, with particular reference to differentiation and founder effects in British small mammals. *Biological Journal of the Linnean Society* **28**: 205-230.
- Berry RJ. 1996.** Small mammal differentiation on islands. *Philosophical Transactions of the Royal Society of London. Series B: Biological Sciences* **351**: 753-764.
- Bhagwat SA, Willis KJ. 2008.** Species persistence in northerly glacial refugia of Europe: a matter of chance or biogeographical traits? *Journal of Biogeography* **35**: 464-482.
- Bilton DT, Mirol PM, Mascheretti S, Fredga K, Zima J, Searle JB. 1998.** Mediterranean Europe as an area of endemism for small mammals rather than a source for northwards postglacial colonization. *Proceedings of the Royal Society of London, Series B: Biological Sciences* **265**: 1219-1226.

- Böhme MU, Fritz U, Kotenko T, Džukić G, Ljubisavljević K, Tzankov N, Berendonk TU. 2007.** Phylogeography and cryptic variation within the *Lacerta viridis* complex (Lacertidae, Reptilia). *Zoologica Scripta* **36**: 119-131.
- Bonardi G, Cavazza W, Perrone V, Rossi S. 2001.** Calabria-Peloritani terrane and Northern Ionian Sea. In: Vai GB, Martini IP (Eds.). *Anatomy of an orogen: The Apennines and adjacent Mediterranean basins*. Kluwer. Dordrecht, The Netherlands. Pp. 287-306
- Bonfiglio L, Mangano G, Marra AC, Masini F, Pavia M, Petruso D. 2002.** Pleistocene Calabrian and Sicilian bioprovinces. *Geobios* **35**: 29-39.
- Bookstein FL. 1982.** Foundations of morphometrics. *Annual Review of Ecology and Systematics* **13**: 451-470.
- Bookstein FL. 1989.** Principal warps: Thin-Plate Splines and the decomposition of deformations. *IEEE Transactions on Pattern Analysis and Machine Intelligence* **11**: 567-585.
- Bookstein FL. 1991** *Morphometric tools for landmark data. Geometry and biology*. Cambridge University Press. Cambridge, UK.
- Bookstein FL. 1996.** Combining the tools of geometric morphometrics. In: Marcus LF, Corti M, Loy A, Naylor GJP, Slice DE. (Eds). *Advances in morphometrics. NATO ASI Series*. Plenum Press. New York, USA. Pp. 131-152.
- Brito P, Edwards S. 2009.** Multilocus phylogeography and phylogenetics using sequence-based markers. *Genetica* **135**: 439-455.
- Brunhoff C, Galbreath KE, Fedorov VB, Cook JA, Jaarola M. 2003.** Holarctic phylogeography of the root vole (*Microtus oeconomus*): implications for late Quaternary biogeography of high latitudes. *Molecular Ecology* **12**: 957-968.
- Bužan E, Kryštufek B, Bryja J. In press.** Microsatellite markers confirm extensive population fragmentation of the endangered Balkan palaeoendemic Martino's vole (*Dinaromys bogdanovi*). *Conservation Genetics*.

- Caloi L, Malatesta A, Palombo RM. 1989.** Biogeografia della Calabria meridionale durante il Quaternario. *Atti Accademia Peloritana dei Pericolanti Classe I, Scienze Matematiche Fisiche e Naturali* **67**: 261-278.
- Canestrelli D, Cimmaruta R, Nascetti G. 2007.** Phylogeography and historical demography of the Italian treefrog, *Hyla intermedia*, reveals multiple refugia, population expansions and secondary contacts within peninsular Italy. *Molecular Ecology* **16**: 4808-4821.
- Canestrelli D, Cimmaruta R, Nascetti G. 2008.** Population genetic structure and diversity of the Apennine endemic stream frog, *Rana italica*; insights on the Pleistocene evolutionary history of the Italian peninsular biota. *Molecular Ecology* **17**: 3856-3872.
- Cardini A. 2003.** The geometry of the marmot (Rodentia: Sciuridae) mandible: phylogeny and patterns of morphological evolution. *Systematic Biology* **52**: 186-205.
- Cardini A, O'Higgins P. 2004.** Patterns of morphological evolution in *Marmota* (Rodentia, Sciuridae): geometric morphometrics of the cranium in the context of marmot phylogeny, ecology and conservation. *Biological Journal of the Linnean Society* **82**: 385-407.
- Cardini A, Jansson A-U, Elton S. 2007.** A geometric morphometric approach to the study of ecogeographical and clinal variation in vervet monkeys. *Journal of Biogeography* **34**: 1663-1678.
- Carraway LN, Verts BJ. 2005.** Assessment of variation in cranial and mandibular dimensions in geographic races of *Sorex trowbridgii*. In: Merritt JF, Churchfield S, Hutterer R, Sheftel BI (Eds.). *Advances in the biology of shrews II*. Special Publication of the International Society of Shrew Biologists. New York, USA. Pp. 139-154.

- Casti3n E, Gos3lbez J. 1999.** Habitat and food preferences in a guild of insectivorous mammals in the Western Pyrenees. *Acta Theriologica* **44**: 1-13.
- Castiglia R, Annesi F, Aloise G, Amori G. 2007.** Mitochondrial DNA reveals different phylogeographic structures in the water shrews *Neomys anomalus* and *N. fodiens* (Insectivora: Soricidae) in Europe. *Journal of Zoological Systematics and Evolutionary Research* **45**: 255-262.
- Castiglia R, Annesi F, Aloise G, Amori G. 2008.** Systematics of the *Microtus savii* complex (Rodentia, Cricetidae) via mitochondrial DNA analyses: paraphyly and pattern of sex chromosome evolution. *Molecular Phylogenetics and Evolution* **46**: 1157-1164.
- Caumul R, Polly PD. 2005.** Phylogenetic and environmental components of morphological variation: skull, mandible, and molar shape in marmots (*Marmota*, Rodentia). *Evolution* **59**: 2460-2472.
- Churchfield S. 1990.** *The natural history of shrews*. Christopher Helm and A&C Black. London, UK.
- Cook LM. 1961.** The edge effect in population genetics. *The American Naturalist* **95**: 295-307.
- Corbet GB. 1961.** Origin of the British insular races of small mammals and of the 'Lusitanian' fauna. *Nature* **191**: 1037-1040.
- Corbet GB, Harris S. 1991.** *The handbook of British mammals*. Blackwell Science. Oxford, UK.
- Corti M, Aguilera M, Capanna E. 2001.** Size and shape changes in the skull accompanying speciation of South American spiny rats (Rodentia: *Proechimys* spp.). *Journal of Zoology* **253**: 537-547.
- Crowcroft P. 1957.** *The life of the shrew*. Max Reinhardt. London, UK.
- Cuenca-Besc3s G, Rofes J, L3pez-Garc3a JM, Blain H-A, De Marf3a RJ, Galindo-Pellicena MA, Benn3sar-Serra ML, Melero-Rubio M, Arsuaga JL,**

- Bermúdez de Castro JM, Carbonell E. 2010.** Biochronology of Spanish Quaternary small vertebrate faunas. *Quaternary International* **212**: 109-119.
- Davis MB, Shaw RG. 2001.** Range shifts and adaptive responses to Quaternary climate change. *Science* **292**: 673-679.
- Deffontaine V, Libois R, Kotlík P, Sommer R, Nieberding C, Paradis E, Searle JB, Michaux JR. 2005.** Beyond the Mediterranean peninsulas: evidence of Central European glacial refugia for a temperate forest mammal species, the bank vole (*Clethrionomys glareolus*). *Molecular Ecology* **14**: 1727-1739.
- Delany MJ, Healy MJR. 1966.** Variation in the white-toothed shrews (*Crocidura* spp.) in the British Isles. *Proceedings of the Royal Society of London, Series B: Biological Sciences* **164**: 63-74.
- Domínguez-Domínguez O, Vázquez-Domínguez E. 2009.** *Filogeografía: aplicaciones en taxonomía y conservación*. Museo de Zoología: Barcelona, Spain.
- Drummond A, Rambaut A. 2007.** BEAST: Bayesian Evolutionary Analysis by Sampling Trees. *BMC Evolutionary Biology* **7**: 214.
- Drummond AJ, Rambaut A, Shapiro B, Pybus OG. 2005.** Bayesian coalescent inference of past population dynamics from molecular sequences. *Molecular Biology and Evolution* **22**: 1185-1192.
- Drummond AJ, Ho SYW, Phillips MJ, Rambaut A. 2006.** Relaxed phylogenetics and dating with confidence. *PLoS Biology* **4**: e88.
- Dryden IL, Mardia KV. 1998.** *Statistical shape analysis*. John Wiley and Sons. Chichester, UK.
- Dubey S, Zaitsev M, Cosson J-F, Abdukadier A, Vogel P. 2006.** Pliocene and Pleistocene diversification and multiple refugia in a Eurasian shrew (*Crocidura suaveolens* group). *Molecular Phylogenetics and Evolution* **38**: 635-647.

- Dubey S, Salamin N, Ohdachi SD, Barrière P, Vogel P. 2007.** Molecular phylogenetics of shrews (Mammalia: Soricidae) reveal timing of transcontinental colonizations. *Molecular Phylogenetics and Evolution* **44**: 126-137.
- Edwards SV. 1997.** Relevance of microevolutionary processes to higher level molecular systematics. In: Mindell DP (Ed.). *Avian molecular evolution and systematics*. Academic Press. New York, USA. Pp. 251-274.
- Ehlers J. 1996.** *Quaternary and glacial geology*. John Wiley and Sons. New York, USA.
- Ehlers J. and Gibbard PL. 2004.** *Quaternary glaciations. Extent and chronology. Part 1: Europe*. Elsevier. New York, USA.
- Esposti MD, De Vries S, Crimi M, Ghelli A, Patarnello T, Meyer A. 1993.** Mitochondrial cytochrome *b*: evolution and structure of the protein. *Biochimica et Biophysica Acta (BBA) - Bioenergetics* **1143**: 243-271.
- Excoffier L, Smouse PE, Quattro JM. 1992.** Analysis of molecular variance inferred from metric distances among DNA haplotypes: Application to human mitochondrial DNA restriction data. *Genetics* **131**: 479-491.
- Excoffier L, Laval G, Schneider S. 2005.** Arlequin ver. 3.0: An integrated software package for population genetics data analysis. *Evolutionary Bioinformatics* **1**: 47-50.
- Fadda C, Corti M. 2001.** Three-dimensional geometric morphometrics of *Arvicanthis*: implications for systematics and taxonomy. *Journal of Zoological Systematics and Evolutionary Research* **39**: 235-245.
- Felsenstein J. 2004.** *Inferring phylogenies*. Sinauer Associates. Sunderland, USA.
- Fløjgaard C, Normand S, Skov F, Svenning J-C. 2009.** Ice age distributions of European small mammals: insights from species distribution modelling. *Journal of Biogeography* **36**: 1152-1163.

- Fontanillas P, Dépraz A, Giorgi MS, Perrin N. 2005.** Nonshivering thermogenesis capacity associated to mitochondrial DNA haplotypes and gender in the greater white-toothed shrew, *Crocidura russula*. *Molecular Ecology* **14**: 661-670.
- Forster P, Toth A. 2003.** Toward a phylogenetic chronology of ancient Gaulish, Celtic, and Indo-European. *Proceedings of the National Academy of Sciences of the United States of America* **100**: 9079-9084.
- Forster P, Romano V, Cali F, Röhl A, Hurles M. 2004.** MtDNA markers for Celtic and Germanic language areas in the British Isles. In: Jones M. (Ed.) *Traces of ancestry: studies in honour of Colin Renfrew*. McDonald Institute for Archaeological Research. Cambridge, UK. Pp. 99-111.
- Foulds LR, Hendy MD, Penny D. 1979.** A graph theoretic approach to the development of minimal phylogenetic trees. *Journal of Molecular Evolution* **13**: 127-149.
- Frafjord K. 2008.** Can environmental factors explain size variation in the common shrew (*Sorex araneus*)? *Mammalian Biology - Zeitschrift für Säugetierkunde* **73**: 415-422.
- Fu YX. 1997.** Statistical tests of neutrality of mutations against population growth, hitchhiking and background selection. *Genetics* **147**: 915-925.
- Gaffney V, Thomson K, Fitch S. 2007.** *Mapping Doggerland: the Mesolithic landscapes of the southern North Sea*. Archaeopress. Oxford, UK.
- Garnier S, Magniez-Jannin F, Rasplus J-Y, Alibert P. 2005.** When morphometry meets genetics: inferring the phylogeography of *Carabus solieri* using Fourier analyses of pronotum and male genitalia. *Journal of Evolutionary Biology* **18**: 269-280.
- Gascuel O. 1997.** BIONJ: an improved version of the NJ algorithm based on a simple model of sequence data. *Molecular Biology and Evolution* **14**: 685-695.

- Gibbard PL, Head MJ, Walker MJC, The Subcomission of Quaternary Stratigraphy. 2010.** Formal ratification of the Quaternary System/Period and the Pleistocene Series/Epoch with a base at 2.58 Ma. *Journal of Quaternary Science* **25**: 96-102.
- Gómez A, Lunt DH. 2007.** Refugia within refugia: patterns of phylogeographic concordance in the Iberian Peninsula. In: Weiss S, Ferrand N. (Eds). *Phylogeography of southern European refugia*. Springer. Dordrecht, The Netherlands. Pp. 155-188.
- Grill A, Amori G, Aloise G, Lisi I, Tosi G, Wauters LA, Randi E. 2009.** Molecular phylogeography of European *Sciurus vulgaris*: refuge within refugia? *Molecular Ecology* **18**: 2687-2699.
- Gündüz I, Auffray J-C, Britton-Davidian J, Catalan J, Ganem G, Ramalhinho MG, Mathias ML, Searle JB. 2001.** Molecular studies on the colonization of the Madeiran archipelago by house mice. *Molecular Ecology* **10**: 2023-2029.
- Gündüz I, Jaarola M, Tez C, Yenyurt C, Polly PD, Searle JB. 2007.** Multigenic and morphometric differentiation of ground squirrels (*Spermophilus*, Scuridae, Rodentia) in Turkey, with a description of a new species. *Molecular Phylogenetics and Evolution* **43**: 916-935.
- Haffer J. 1969.** Speciation in Amazonian forest birds. *Science* **165**: 131-137.
- Hall TA. 1999.** BioEdit: a user-friendly biological sequence alignment editor and analysis program for Windows 95/98/NT. *Nucleic Acids Symposium Series* **41**: 95-98.
- Hammer Ø, Harper DAT, Ryan PD. 2001.** PAST: Paleontological statistics software package for education and data analysis. *Palaeontologia Electronica* **4**: 9 pp.
- Hampe A, Petit RJ. 2005.** Conserving biodiversity under climate change: the rear edge matters. *Ecology Letters* **8**: 461-467.

- Hanski I. 1986.** Population dynamics of shrews on small islands accord with the equilibrium model. *Biological Journal of the Linnean Society* **28**: 23-36.
- Hasegawa M, Kishino H, Yano T-A. 1985.** Dating of the human-ape splitting by a molecular clock of mitochondrial DNA. *Journal of Molecular Evolution* **22**: 160-174.
- Hastings WK. 1970.** Monte Carlo sampling methods using Markov chains and their applications. *Biometrika* **57**: 97-109.
- Haynes S, Jaarola M, Searle JB. 2003.** Phylogeography of the common vole (*Microtus arvalis*) with particular emphasis on the colonization of the Orkney archipelago. *Molecular Ecology* **12**: 951-956.
- Heckel G, Burri R, Fink S, Desmet J-F, Excoffier L. 2005.** Genetic structure and colonization processes in European populations of the common vole, *Microtus arvalis*. *Evolution* **59**: 2231-2242.
- Hellborg L, Ellegren H. 2003.** Y chromosome conserved anchored tagged sequences (YCATS) for the analysis of mammalian male-specific DNA. *Molecular Ecology* **12**: 283-291.
- Hewitt GM. 1996.** Some genetic consequences of ice ages, and their role, in divergence and speciation. *Biological Journal of the Linnean Society* **58**: 247-276.
- Hewitt GM. 2000.** The genetic legacy of the Quaternary ice ages. *Nature* **405**: 907-913.
- Hewitt GM. 2004.** Genetic consequences of climatic oscillations in the Quaternary. *Philosophical Transactions of the Royal Society of London. Series B: Biological Sciences* **359**: 183-195.
- Hickerson MJ, Carstens BC, Cavender-Bares J, Crandall KA, Graham CH, Johnson JB, Rissler L, Victoriano PF, Yoder AD. 2010.** Phylogeography's

- past, present, and future: 10 years after Avise, 2000. *Molecular Phylogenetics and Evolution* **54**: 291-301.
- Hilbert DW, Graham A, Hopkins MS. 2007.** Glacial and interglacial refugia within a long-term rainforest refugium: The wet tropics bioregion of NE Queensland, Australia. *Palaeogeography, Palaeoclimatology, Palaeoecology* **251**: 104-118.
- Ho SYW, Larson G. 2006.** Molecular clocks: when times are a-changin'. *Trends in Genetics* **22**: 79-83.
- Ho SYW, Phillips MJ, Cooper A, Drummond AJ. 2005.** Time dependency of molecular rate estimates and systematic overestimation of recent divergence times. *Molecular Biology and Evolution* **22**: 1561-1568.
- Ho SYW, Saarma U, Barnett R, Haile J, Shapiro B. 2008.** The effect of inappropriate calibration: three case studies in molecular ecology. *PLoS Biology* **3**: e1615.
- Huelsenbeck JP, Ronquist F. 2001.** MrBayes: Bayesian inference of phylogenetic trees. *Bioinformatics* **17**: 754-755.
- Huelsenbeck JP, Ronquist F, Nielsen R, Bollback JP. 2001.** Bayesian inference of phylogeny and its impact on evolutionary biology. *Science* **294**: 2310-2314.
- Hutterer R. 1990.** *Sorex minutus* Linnaeus, 1766. In: Niethammer J, Krapp F. *Handbuch der Säugetiere Europas*, Vol. 3/1: Insektenfresser, Primaten. Aula Verlag. Wiesbaden, Germany. Pp. 183-206.
- Hutterer R. 2005.** Order Soricomorpha. In: Wilson DE, Reeder DM (Eds.). *Mammal species of the world. A taxonomic and geographic reference*. Johns Hopkins University Press. Baltimore, USA. Pp. 220-311.
- Hutterer R, Amori G, Kryštufek B, Fernandes M, Meinig H. 2008.** *Sorex minutus*. IUCN 2009, IUCN Red List of Threatened Species Ver. 2009.2. Available at: www.iucnredlist.org, accessed 12 May 2009.

- Jaarola M, Searle JB. 2002.** Phylogeography of field voles (*Microtus agrestis*) in Eurasia inferred from mitochondrial DNA sequences. *Molecular Ecology* **11**: 2613-2621.
- Johns GC, Avise JC. 1998.** A comparative summary of genetic distances in the vertebrates from the mitochondrial cytochrome *b* gene. *Molecular Biology and Evolution* **15**:1481-1490.
- Jones EP. 2009.** *The house mouse in the North East Atlantic region*. PhD thesis dissertation. The University of York, Department of Biology, UK.
- Jukes TH, Cantor CR. 1969.** Evolution of protein molecules. In: Munro HN (Ed.) *Mammalian protein metabolism*. Academic Press. New York, USA. Pp. 21-132.
- Kendall DG. 1977.** The diffusion of shape. *Advances in Applied Probability* **9**: 428-430.
- Klingenberg CP, Monteiro LR. 2005.** Distances and directions in multidimensional shape spaces: implications for morphometric applications. *Systematic Biology* **54**: 678-688.
- Klingenberg CP, Leamy LJ, Routman EJ, Cheverud JM. 2001.** Genetic architecture of mandible shape in mice: effects of quantitative trait loci analyzed by geometric morphometrics. *Genetics* **157**: 785-802.
- Knowles LL. 2009.** Statistical phylogeography. *Annual Review of Ecology, Evolution, and Systematics* **40**: 593-612.
- Knowles LL, Maddison WP. 2002.** Statistical phylogeography. *Molecular Ecology* **11**: 2623-2635.
- Kotlík P, Deffontaine V, Mascheretti S, Zima J, Michaux JR, Searle JB. 2006.** A northern glacial refugium for bank voles (*Clethrionomys glareolus*). *Proceedings of the National Academy of Sciences of the United States of America* **103**: 14860-14864.

- Kryštufek B, Reed JM. 2004.** Pattern and process in Balkan biodiversity - an overview. In: Griffiths HI, Kryštufek B, Reed JM (Eds.). *Balkan biodiversity. Pattern and process in the European hotspot*. Kluwer Academic Publishers. Dordrecht, The Netherlands. Pp. 1-8.
- Kryštufek B, Bužan EV, Hutchinson WF, Hänfling B. 2007.** Phylogeography of the rare Balkan endemic Martino's vole, *Dinaromys bogdanovi*, reveals strong differentiation within the Western Balkan Peninsula. *Molecular Ecology* **16**: 1221-1232.
- Kuhner MK. 2006.** LAMARC 2.0: maximum likelihood and Bayesian estimation of population parameters. *Bioinformatics* **22**: 768-770.
- Lambeck K, Purcell AP. 2001.** Sea-level change in the Irish Sea since the Last Glacial Maximum: constraints from isostatic modelling. *Journal of Quaternary Science* **16**: 497-506.
- Lanave C, Preparata G, Saccone C, Serio G. 1984.** A new method for calculating evolutionary substitution rates. *Journal of Molecular Evolution* **20**: 86-93.
- Larkin MA, Blackshields G, Brown NP, Chenna R, McGettigan PA, McWilliam H, Valentin F, Wallace IM, Wilm A, Lopez R, Thompson JD, Gibson TJ, Higgins DG. 2007.** Clustal W and Clustal X version 2.0. *Bioinformatics* **23**: 2947-2948.
- Lebarbenchon C, Poitevin F, Arnal V, Montgelard C. In press.** Phylogeography of the weasel (*Mustela nivalis*) in the western-Palaeartic region: combined effects of glacial events and human movements. *Heredity*.
- Librado P, Rozas J. 2009.** DnaSP v5: a software for comprehensive analysis of DNA polymorphism data. *Bioinformatics* **25**: 1451-1452.
- Lomolino MV. 2005.** Body size evolution in insular vertebrates: generality of the island rule. *Journal of Biogeography* **32**: 1683-1699.

- Loy A. 1996.** An introduction to geometric morphometrics and intraspecific variation: a fascinating adventure. In: Marcus LF, Corti M, Loy A, Naylor GJP, Slice DE (Eds.). *Advances in morphometrics*. Plenum Press. New York, USA. Pp. 271-273.
- Lynch M, Crease T. 1990.** The analysis of population survey data on DNA sequence variation. *Molecular Biology and Evolution* **7**: 377-394.
- MacDonald D, Barrett P. 1993.** *Mammals of Britain and Europe*. Harper Collins Publishers. New York, USA.
- Madureira ML, Magalhães CMP. 1980.** *Small mammals of Portugal*. Museo Bocage Arq. 7 (13) (2.s). Lisboa, Portugal.
- Magri D, Vendramin GG, Comps B, Dupanloup I, Geburek T, Gömöry D, Latałowa M, Litt T, Paule L, Roure JM, Tantau I, van der Knaap WO, Petit RJ, de Beaulieu J-L. 2006.** A new scenario for the Quaternary history of European beech populations: palaeobotanical evidence and genetic consequences. *New Phytologist* **171**: 199-221.
- Malatesta A. 1985.** *Geologia e paleobiologia dell'era glaciale*. La Nuova Italia Scientifica, Roma, Italy.
- Maridet O, Escarguel G, Costeur L, Mein P, Hugueney M, Legendre S. 2007.** Small mammal (rodents and lagomorphs) European biogeography from the Late Oligocene to the mid Pliocene. *Global Ecology and Biogeography* **16**: 529-544.
- Martínková N, McDonald RA, Searle JB. 2007.** Stoats (*Mustela erminea*) provide evidence of natural overland colonization of Ireland. *Proceedings of the Royal Society B: Biological Sciences* **274**: 1387-1393.
- Mascheretti S, Rogatcheva MB, Gündüz İ, Fredga K, Searle JB. 2003.** How did pygmy shrews colonize Ireland? Clues from a phylogenetic analysis of mitochondrial cytochrome *b* sequences. *Proceedings of the Royal Society B: Biological Sciences* **270**: 1593-1599.

- Masini F, Sala B. 2007.** Large- and small-mammal distribution patterns and chronostratigraphic boundaries from the Late Pliocene to the Middle Pleistocene of the Italian peninsula. *Quaternary International* **160**: 43-56.
- Masini F, Giannini T, Abbazzi L, Fanfani F, Delfino M, Christian Maul L, Torre D. 2005.** A latest Biharian small vertebrate fauna from the lacustrine succession of San Lorenzo (Sant'Arcangelo Basin, Basilicata, Italy). *Quaternary International* **131**: 79-93.
- Mayr E. 1963.** *Animal species and evolution*. Harvard University Press. Cambridge, USA.
- McDevitt AD, Rambau RV, O'Brien J, McDevitt CD, Hayden TJ, Searle JB. 2009.** Genetic variation in Irish pygmy shrews *Sorex minutus* (Soricomorpha: Soricidae): implications for colonization history. *Biological Journal of the Linnean Society* **97**: 918-927.
- McDevitt AD, Yannic G, Rambau RV, Hayden TJ, Searle JB. 2010.** Postglacial recolonization of continental Europe by the pygmy shrew (*Sorex minutus*) inferred from mitochondrial and Y chromosomal DNA sequences. In: Habel JC, Assmann T (Eds.). *Relict species: phylogeography and conservation biology*. Springer-Verlag. Berlin, Germany. Pp. 217-236.
- McDonald JH, Kreitman M. 1991.** Adaptive protein evolution at the Adh locus in *Drosophila*. *Nature* **351**: 652-654.
- McNeely J A, Miller KR, Reid WV, Mittermeier RA, Werner TB. 1990.** *Conserving the world's biological diversity*. World Conservation Union, World Resources Institute, Conservation International, World Wildlife Fund–US, and the World Bank. Washington, DC, USA.
- Metropolis N, Rosenbluth AW, Rosenbluth MN, Teller AH, Teller E. 1953.** Equation of state calculations by fast computing machines. *The Journal of Chemical Physics* **21**: 1087-1092.

- Michaux JR, Magnanou E, Paradis E, Nieberding C, Libois R. 2003.** Mitochondrial phylogeography of the woodmouse (*Apodemus sylvaticus*) in the Western Palearctic region. *Molecular Ecology* **12**: 685-697.
- Michaux J, Cucchi T, Renaud S, Garcia-Talavera F, Hutterer R. 2007.** Evolution of an invasive rodent on an archipelago as revealed by molar shape analysis: the house mouse in the Canary Islands. *Journal of Biogeography* **34**: 1412-1425.
- Millien V. 2006.** Morphological evolution is accelerated among island mammals. *PLoS Biology* **4**: e321.
- Mitchell-Jones AJ, Amori G, Bogdanowicz W, Kryštufek B, Reijnders PJH, Spitzenberger F, Stubble M, Thissen JBM, Vohralik V, Zima J. 1999.** *The atlas of European mammals*. Academic Press. London, UK.
- Mitteroecker P, Gunz P. 2009.** Advances in geometric morphometrics. *Evolutionary Biology* **36**: 235-247.
- Monteiro LR, dos Reis SF. 2005.** Morphological evolution in the mandible of spiny rats, genus *Trinomys* (Rodentia: Echimyidae). *Journal of Zoological Systematics and Evolutionary Research* **43**: 332-338.
- Monteiro LR, Duarte LC, dos Reis SF. 2003.** Environmental correlates of geographical variation in skull and mandible shape of the punaré rat *Thrichomys apereoides* (Rodentia: Echimyidae). *Journal of Zoology* **261**: 47-57.
- Moritz C. 1994.** Applications of mitochondrial DNA analysis in conservation: a critical review. *Molecular Ecology Notes* **3**: 401-411.
- Myers N, Mittermeier RA, Mittermeier CG, da Fonseca GAB, Kent J. 2000.** Biodiversity hotspots for conservation priorities. *Nature* **403**: 853-858.
- Nagorsen DW, Cardini A. 2009.** Tempo and mode of evolutionary divergence in modern and Holocene Vancouver Island marmots (*Marmota vancouverensis*) (Mammalia, Rodentia). *Journal of Zoological Systematics and Evolutionary Research* **47**: 258-267.

- Nei M. 1987.** *Molecular evolutionary genetics*. Columbia University Press. New York, USA.
- Nei M, Li WH. 1979.** Mathematical model for studying genetic variation in terms of restriction endonucleases. *Proceedings of the National Academy of Sciences of the United States of America* **76**: 5269-5273.
- Nielsen R. 2005.** Molecular signatures of natural selection. *Annual Review of Genetics* **39**: 197-218.
- Nogueira MR, Peracchi AL, Monteiro LR. 2009.** Morphological correlates of bite force and diet in the skull and mandible of phyllostomid bats. *Functional Ecology* **23**: 715-723.
- Ochocińska D, Taylor JRE. 2003.** Bergmann's rule in shrews: geographical variation of body size in Palearctic *Sorex* species. *Biological Journal of the Linnean Society* **78**: 365-381.
- Ohdachi SD, Hasegawa M, Iwasa MA, Vogel P, Oshida T, Lin L-K, Abe H. 2006.** Molecular phylogenetics of soricid shrews (Mammalia) based on mitochondrial cytochrome *b* gene sequences: with special reference to the Soricinae. *Journal of Zoology* **270**: 199-200.
- Oppenheimer S. 2006.** *The origins of the British: a genetic detective story*. Constable and Robinson. London, UK.
- O'Regan HJ. 2008.** The Iberian Peninsula - corridor or cul-de-sac? Mammalian faunal change and possible routes of dispersal in the last 2 million years. *Quaternary Science Reviews* **27**: 2136-2144.
- Pergams ORW, Ashley MV. 2001.** Microevolution in island rodents. *Genetica* **112-113**: 245-256.
- Petit RJ, Aguinagalde I, de Beaulieu J-L, Bittkau C, Brewer S, Cheddadi R, Ennos R, Fineschi S, Grivet D, Lascoux M, Mohanty A, Muller-Starck G, Demesure-Musch B, Palme A, Martin JP, Rendell S, Vendramin GG. 2003.**

- Glacial refugia: hotspots but not melting pots of genetic diversity. *Science* **300**: 1563-1565.
- Phillips T. 2004.** Seascapes and landscapes in Orkney and Northern Scotland. *World Archaeology* **35**: 371-384.
- Pierpaoli M, Riga F, Trocchi V, Randi E. 1999.** Species distinction and evolutionary relationships of the Italian hare (*Lepus corsicanus*) as described by mitochondrial DNA sequencing. *Molecular Ecology* **8**: 1805-1817.
- Polly PD. 2001.** On morphological clocks and paleophylogeography: towards a timescale for *Sorex* hybrid zones. *Genetica* **112-113**: 339-357.
- Polly PD. 2007.** Phylogeographic differentiation in *Sorex araneus*: morphology in relation to geography and karyotype. *Russian Journal of Theriology* **6**: 73-84.
- Posada D. 2008.** jModelTest: phylogenetic model averaging. *Molecular Biology and Evolution* **25**: 1253-1256.
- Posada D, Crandall KA. 2001.** Selecting the best-fit model of nucleotide substitution. *Systematic Biology* **50**: 580-601.
- Provan J, Bennett KD. 2008.** Phylogeographic insights into cryptic glacial refugia. *Trends in Ecology and Evolution* **23**: 564-571.
- Prugnolle F, de Meeus T. 2002.** Inferring sex-biased dispersal from population genetic tools: a review. *Heredity* **88**: 161-165.
- Ramos-Onsins SE, Rozas J. 2002.** Statistical properties of new neutrality tests against population growth. *Molecular Biology and Evolution* **19**: 2092-2100.
- Ratkiewicz M, Fedyk S, Banaszek A, Gielly L, Chetnicki W, Jadwiszczak K, Taberlet P. 2002.** The evolutionary history of the two karyotypic groups of the common shrew, *Sorex araneus*, in Poland. *Heredity* **88**: 235-242.
- Renaud S, Michaux JR. 2007.** Mandibles and molars of the wood mouse, *Apodemus sylvaticus* (L.): integrated latitudinal pattern and mosaic insular evolution. *Journal of Biogeography* **34**: 339-355.

- Reumer JWF. 1998.** A classification of the fossil and recent shrews. In: Wójcik JM, Wolsan M. (Eds.). *Evolution of shrews*. Mammal Research Institute, Polish Academy of Sciences. Białowieża, Poland. Pp. 5-21.
- Rogers AR. 1995.** Genetic evidence for a Pleistocene population explosion. *Evolution* **49**: 608-615.
- Rogers AR, Harpending H. 1992.** Population growth makes waves in the distribution of pairwise genetic differences. *Molecular Biology and Evolution* **9**: 552-569.
- Rohlf FJ. 1990.** Morphometrics. *Annual Review of Ecology and Systematics* **21**: 299-316.
- Rohlf FJ. 1993.** Relative warp analysis and an example of its application to mosquito wings. In: Marcus LF, Bello E, Garcia-Valdecasas A (Eds.). *Contributions to morphometrics*. Museo Nacional de Ciencias Naturales (CSIC), Vol. 8. Madrid, Spain. Pp. 131-159.
- Rohlf FJ, Marcus LF. 1993.** A revolution in morphometrics. *Trends in Ecology and Evolution* **8**:129-132.
- Rohlf FJ, Slice D. 1990.** Extensions of the Procrustes method for the optimal superimposition of landmarks. *Systematic Biology* **39**: 40-59.
- Rzebik-Kowalska B. 1998.** Fossil history of shrews in Europe. In: Wójcik J, Wolsan M. (Eds.). *Evolution of shrews*. Mammal Research Institute, Polish Academy of Sciences. Białowieża, Poland. Pp. 23-71.
- Rzebik-Kowalska B. 2005.** Paleontological relationships of European *Sorex*. In: Merritt JF, Churchfield S, Hutterer R, Sheftel BI (Eds.). *Advances in the Biology of Shrews II*, Special Publication of the International Society of Shrew Biologists. New York, USA. Pp. 1-8.

- Rzebik-Kowalska B. 2008.** Insectivores (Soricomorpha, Mammalia) from the Pliocene and Pleistocene of Transbaikalia and Irkutsk region (Russia). *Quaternary International* **179**: 96-100. Pp. 23-92.
- Schneider S, Excoffier L. 1999.** Estimation of past demographic parameters from the distribution of pairwise differences when the mutation rates vary among sites: application to human mitochondrial DNA. *Genetics* **152**: 1079-1089.
- Searle JB, Kotlík P, Rambau RV, Marková S, Herman JS, McDevitt AD. 2009.** The Celtic fringe of Britain: insights from small mammal phylogeography. *Proceedings of the Royal Society B: Biological Sciences* **276**: 4287-4294.
- Slatkin M. 1995.** A measure of population subdivision based on microsatellite allele frequencies. *Genetics* **139**: 457-462.
- Slatkin M, Hudson RR. 1991.** Pairwise comparisons of mitochondrial DNA sequences in stable and exponentially growing populations. *Genetics* **129**: 555-562.
- Sokal RR, Rohlf FJ. 1995.** *Biometry: the principles and practice of statistics in biological research*. 3rd. edition. WH Freeman and Co. New York, USA.
- Sommer RS, Nadachowski A. 2006.** Glacial refugia of mammals in Europe: evidence from fossil records. *Mammal Review* **36**: 251-265.
- Sparti A, Genoud M. 1989.** Basal rate metabolism and temperature regulation in *Sorex coronatus* and *S. minutus* (Soricidae: Mammalia). *Comparative Biochemistry and Physiology* **92A**: 359-363.
- Stamatakis A. 2006.** RAxML-VI-HPC: maximum likelihood-based phylogenetic analyses with thousands of taxa and mixed models. *Bioinformatics* **22**: 2688-2690.
- Stanhope MJ, Waddell VG, Madsen O, de Jong W, Hedges SB, Cleven GC, Kao D, Springer MS. 1998.** Molecular evidence for multiple origins of Insectivora and

- for a new order of endemic African insectivore mammals. *Proceedings of the National Academy of Sciences of the United States of America* **95**: 9967-9972.
- Steinfartz S, Veith M, Tautz D. 2000.** Mitochondrial sequence analysis of *Salamandra* taxa suggests old splits of major lineages and postglacial recolonizations of Central Europe from distinct source populations of *Salamandra salamandra*. *Molecular Ecology* **9**: 397-410.
- Stewart JR, Dalén L. 2008.** Is the glacial refugium concept relevant for northern species? A comment on Pruett and Winker 2005. *Climatic Change* **86**: 19-22.
- Stewart JR, Lister AM. 2001.** Cryptic northern refugia and the origins of the modern biota. *Trends in Ecology and Evolution* **16**: 608-613.
- Stewart JR, Lister AM, Barnes I, Dalén L. 2010.** Refugia revisited: individualistic responses of species in space and time. *Proceedings of the Royal Society B: Biological Sciences* **277**: 661-671.
- Storch G, Qiu Zhuding, Zazhigin V. 1998.** Fossil history of shrews in Europe. In: Wójcik J, Wolsan M. (Eds.). *Evolution of shrews*. Mammal Research Institute, Polish Academy of Sciences. Białowieża, Poland. Pp. 93-120.
- Strait G. 1993.** Molar morphology and food texture among small-bodied insectivorous mammals. *Journal of Mammalogy* **74**: 391-401.
- Stuart AJ. 1995.** Insularity and Quaternary vertebrate faunas in Britain and Ireland. *Geological Society, London, Special Publications* **96**: 111-125.
- Svenning J-C, Normand S, Kageyama M. 2008.** Glacial refugia of temperate trees in Europe: insights from species distribution modelling. *Journal of Ecology* **96**: 1117-1127.
- Swofford DL. 2000.** PAUP*. Phylogenetic Analysis Using Parsimony (*and other methods). Version 4. Sinauer Associates. Sunderland, USA.

- Taberlet P, Fumagalli L, Wust-Saucy A-G, Cosson J-F. 1998.** Comparative phylogeography and postglacial colonization routes in Europe. *Molecular Ecology* **7**: 453-464.
- Tajima F. 1989.** Statistical method for testing the neutral mutation hypothesis by DNA polymorphism. *Genetics* **123**: 585-595.
- Taylor, JRE. 1998.** Evolution of energetic strategies in shrews. In: Wójcik J, Wolsan M. (Eds.). *Evolution of shrews*. Mammal Research Institute, Polish Academy of Sciences. Białowieża, Poland. Pp. 309-346.
- Temple HJ, Terry A (Eds.). 2007.** *The status and distribution of European mammals*. Office for Official Publications of the European Communities. Luxembourg, Luxembourg.
- Ungaro A, Cecchetti S, Aloise G, Nascetti G. 2001.** *Paleogeographic events in Southern Italy and the genetic structure of Talpa romana*. 8th Congress European Society Evolutionary Biology, Aarhus, Denmark 20-26 August 2001. Abstracts: 88.
- Van Valen L. 1973.** Pattern and the balance of nature. *Evolutionary Theory*, 1: 31–49.
- Vega R, Amori G, Aloise G, Cellini S, Loy A, Searle JB. 2010a.** Genetic and morphological variation in a Mediterranean glacial refugium: evidence from Italian pygmy shrews (*Sorex minutus*, Mammalia, Soricomorpha). *Biological Journal of the Linnean Society* **100**: 774-787.
- Vega R, Fløjgaard C, Lira-Noriega A, Nakazawa Y, Svenning J-C, Searle JB. 2010b.** Northern glacial refugia for the pygmy shrew *Sorex minutus* in Europe revealed by phylogeographic analyses and species distribution modelling. *Ecography* **33**: 260-271.

- Waddell PJ, Steel MA. 1997.** General Time-Reversible distances with unequal rates across sites: Mixing Γ and inverse Gaussian distributions with invariant sites. *Molecular Phylogenetics and Evolution* **8**: 398-414.
- Weir BS, Cockerham CC. 1984.** Estimating F-statistics for the analysis of population structure. *Evolution* **38**: 1358-1370.
- Weninger B, Schulting R, Bradtmöller M, Clare L, Collard M, Edinborough K, Hilpert J, Jöris O, Niekus M, Rohling EJ, Wagner B. 2008.** The catastrophic final flooding of Doggerland by the Storegga slide tsunami. *Documenta Praehistorica XXXV*: 1-24.
- White TA. 2007.** *The genetics, ecology and evolution of island populations of the common shrew, Sorex araneus*. PhD thesis dissertation. The University of York, Department of Biology, UK.
- White TA, Searle JB. 2007.** Genetic diversity and population size: island populations of the common shrew, *Sorex araneus*. *Molecular Ecology* **16**: 2005-2016.
- White TA, Searle JB. 2008a.** The colonization of Scottish islands by the common shrew, *Sorex araneus* (Eulipotyphla: Soricidae). *Biological Journal of the Linnean Society* **94**: 797-808.
- White TA, Searle JB. 2008b.** Mandible asymmetry and genetic diversity in island populations of the common shrew, *Sorex araneus*. *Journal of Evolutionary Biology* **21**: 636-641.
- White TA, Searle JB. 2009.** Ecomorphometric variation and sexual dimorphism in the common shrew (*Sorex araneus*). *Journal of Evolutionary Biology* **22**: 1163-1171.
- Willis KJ, van Andel TH. 2004.** Trees or no trees? The environments of Central and Eastern Europe during the last glaciation. *Quaternary Science Reviews* **23**: 2369-2387.

- Willis KJ, Rudner E, Sümegi P. 2000.** The full-glacial forests of Central and South-Eastern Europe. *Quaternary Research* **53**: 203-213.
- Wilson AC, Cann RL, Carr SM, George M, Gyllensten UB, Helm-Bychowski KM, Higuchi RG, Palumbi SR, Prager EM, Sage RD, Stoneking M. 1985.** Mitochondrial DNA and two perspectives on evolutionary genetics. *Biological Journal of the Linnean Society* **26**: 375-400.
- Wójcik JM, Kawako A, Marková S, Searle JB, Kotlík P. 2010.** Phylogeographic signatures of northward post-glacial colonization from high-latitude refugia: a case study of bank voles using museum specimens. *Journal of Zoology* **281**: 249-262.
- Wright S. 1969.** *Evolution and the genetics of populations, Vol. II. The theory of gene frequencies.* University of Chicago Press. Chicago, USA.
- Xia X. 1998.** The rate heterogeneity of nonsynonymous substitutions in mammalian mitochondrial genes. *Molecular Biology and Evolution* **15**: 336-344.
- Yalden DW. 1982.** When did the mammal fauna of the British Isles arrive? *Mammal Review* **12**: 1-56.
- Yalden DW. 2007.** Zoological perspectives on the late glacial. In: Pettitt P, Bahn P, Ripoll S (Eds.). *Palaeolithic cave art at Creswell Crags in European context.* Oxford University Press. Oxford, UK. Pp. 53-60.
- Yannic G, Basset P, Hausser J. 2008.** A new perspective on the evolutionary history of western European *Sorex araneus* group revealed by paternal and maternal molecular markers. *Molecular Phylogenetics and Evolution* **47**: 237-250.
- Zelditch ML, Swiderski DL, Sheets HD, Fink WL. 2004.** *Geometric morphometrics for biologists: a primer.* Elsevier Academic Press. London, UK.
- Zvelebil M. 2006.** Mobility, contact, and exchange in the Baltic Sea basin 6000-2000 BC. *Journal of Anthropological Archaeology* **25**: 178-192.



Genetic and morphological variation in a Mediterranean glacial refugium: evidence from Italian pygmy shrews, *Sorex minutus* (Mammalia: Soricomorpha)

RODRIGO VEGA^{1,2}, GIOVANNI AMORI³, GAETANO ALOISE⁴, SIMONETTA CELLINI³,
ANNA LOY⁵ and JEREMY B. SEARLE^{1*}

¹Department of Biology, University of York, PO Box 373, York YO10 5YW, UK

²Department of Entomology, Comstock Hall 5123, Cornell University, Ithaca, NY 14853, USA

³CNR, Institute of Ecosystem Studies, Via A. Borelli 50, 00161 Rome, Italy

⁴Dipartimento di Ecologia, Università della Calabria, Via P. Bucci, s.n., 87036 Rende, Italy

⁵Dipartimento di Scienze e Tecnologie per l'Ambiente e il Territorio, Università del Molise, Via
Mazzini 8, I-86170 Isernia, Italy

Received 29 October 2009; revised 28 February 2010; accepted for publication 28 February 2010

At the Last Glacial Maximum (LGM), the southern European peninsulas were important refugia for temperate species. Current genetic subdivision of species within these peninsulas may reflect past population subdivision at the LGM, as in 'refugia within refugia', and/or at other time periods. In the present study, we assess whether pygmy shrew populations from different regions within Italy are genetically and morphologically distinct. One maternally and two paternally inherited molecular markers (cytochrome *b* and Y-chromosome introns, respectively) were analysed using several phylogenetic methods. A geometric morphometric analysis was performed on mandibles to evaluate size and shape variability between populations. Mandible shape was also explored with a functional approach that considered the mandible as a first-order lever affecting bite force. We found genetically and morphologically distinct European, Italian, and southern Italian groups. Mandible size increased with decreasing latitude and southern Italian pygmy shrews exhibited mandibles with the strongest bite force. It is not clear whether or not the southern Italian and Italian groups of pygmy shrews occupied different refugia within the Italian peninsula at the LGM. It is likely, however, that geographic isolation earlier than the LGM on islands at the site of present-day Calabria was important in generating the distinctive southern Italian group of pygmy shrews, and also the genetic groups in other small vertebrates that we review here. Calabria is an important hotspot for genetic diversity, and is worthy of conservation attention. © 2010 The Linnean Society of London, *Biological Journal of the Linnean Society*, 2010, 100, 774–787.

ADDITIONAL KEYWORDS: Calabria – cytochrome *b* – geometric morphometrics – refugia – Italy – phylogeography – Y-chromosome introns.

INTRODUCTION

The three southern European peninsulas, namely the Iberian, Italian, and Balkan (Fig. 1), acted as refugial areas for many species during the Quaternary ice ages, and are consequently species-rich areas and

current hotspots of intra-specific diversity (Bilton *et al.*, 1998; Hewitt, 2000; Myers *et al.*, 2000; Petit *et al.*, 2003). Traditionally, the southern peninsulas have been considered as single refugial areas at the Last Glacial Maximum (LGM; Bilton *et al.*, 1998; Petit *et al.*, 2003). However, recent studies indicate that species in the southern European peninsulas may have persisted in multiple distinct and separated

*Corresponding author. E-mail: jbs3@york.ac.uk

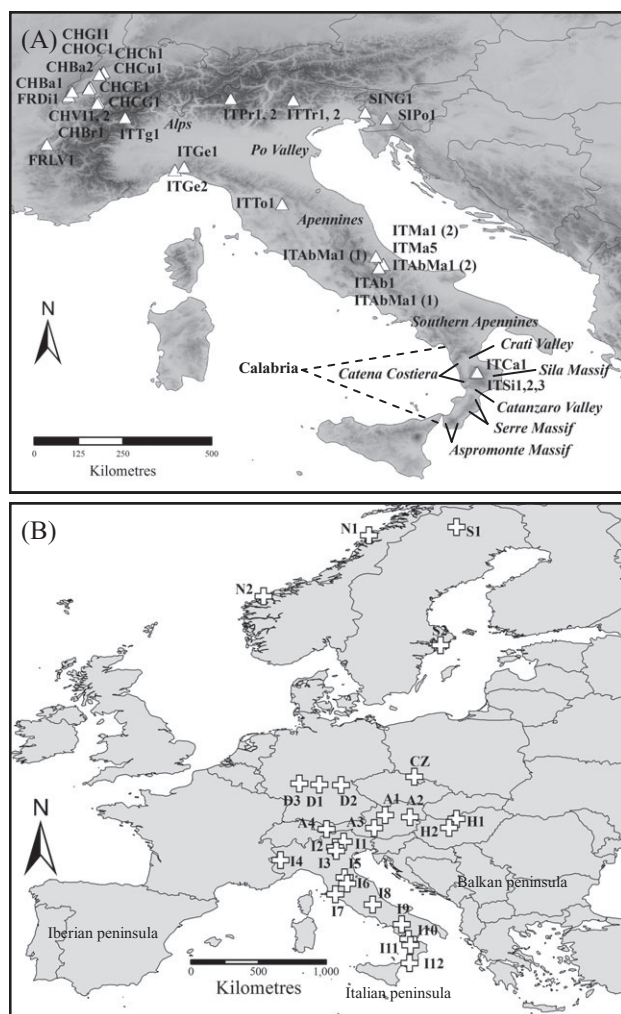


Figure 1. Sample localities for the pygmy shrew in Italy and elsewhere for (A) the cytochrome *b* data, with relief illustrated in grey tones, and (B) the morphometric data (samples from western Siberia are not mapped).

glacial refugia in Iberia (Gómez & Lunt, 2006), Italy (Canestrelli, Cimmaruta & Nascetti, 2007, 2008), and the Balkans (Kryštufek *et al.*, 2007). If this pattern is common, it has important consequences for the interpretation of European phylogeography as well as our understanding of biological diversity.

In the present study, we consider genetic and morphological subdivision in one species of small mammal in the Italian refugial area and compare this with other small vertebrate species from the same area. Our focal species is the pygmy shrew, *Sorex minutus* Linnaeus 1766 (Mammalia, Soricomorpha), which has a wide Palaearctic distribution extending between north-western Spain and Lake Baikal in Siberia (Hutterer, 2005). The distribution of the species becomes patchy and limited to higher altitudes in southern Europe and taxonomists have associated this

trend with differentiation. Hutterer (1990) recognized five valid subspecies: *Sorex minutus minutus* (northern and central Europe to Siberia), *Sorex minutus gymnurus* Chaworth–Musters, 1932 (Greece), *Sorex minutus becki* von Lehmann, 1963 (the Alps), *Sorex minutus carpetanus* Rey, 1971 (Spain), and *Sorex minutus lucanius* Miller, 1909 (the Basilicata and Calabria ridges of southern Italy; Fig. 1A). However, he did not resolve the taxonomic status of the pygmy shrew populations in central Italy.

Phylogeographic analyses of the pygmy shrew using mitochondrial DNA (mtDNA) and Y-chromosome introns have revealed a genetic structure over Eurasia that is considered to reflect isolation and differentiation in different refugia (Bilton *et al.*, 1998; Mascheretti *et al.*, 2003; McDevitt *et al.*, 2010). At least one glacial refugium in Italy has been proposed to explain the genetic distinctiveness of pygmy shrews existing there compared to the rest of Eurasia, and McDevitt *et al.* (2010) described a single individual with distinct mtDNA and Y-chromosome introns from southern Italy.

Thus, studies on the pygmy shrew provide evidence of lineage diversification of Italian populations from the rest of Eurasia and likely genetic and morphological subdivision within Italy. To extend these findings, we used two approaches: First, as previously employed, we implemented a phylogeographic approach, which is useful for exploring the principles and processes that generated the geographic distribution of genealogical lineages (Avise, 2000). The phylogenetic relationships among pygmy shrew populations were determined by an analysis of maternally and paternally inherited markers, adding new samples to the pre-existing data. Additionally, we used a geometric morphometrics approach (Rohlf & Marcus, 1993) on pygmy shrew mandibles from throughout Italy and neighbouring countries. Geometric morphometrics is one of the most powerful techniques for the description and interpretation of patterns of variation below the species level (Loy, 1996; Zelditch *et al.*, 2004). Because populations of pygmy shrews are scattered across a variety of different environments in Italy, adaptation may be a major driving force of recent morphological evolution in this region. Therefore, morphological variability was studied in the context of a functional hypothesis that envisages mandible shape as a first-order lever affecting bite force.

In the present study, we have also considered the genetic and morphological variation in pygmy shrews from Italy in the wider context of European biodiversity. The Italian peninsula hosts a large number of terrestrial species of mammals (74 native species), five of which are endemic, thus accentuating Italy's role and responsibility in European conservation (Gippoliti & Amori, 2002). Our phylogeographic and

morphological study, in conjunction with other data on small mammals that we review here, has important implications for the conservation of Italian mammals.

MATERIAL AND METHODS

PHYLOGEOGRAPHIC ANALYSIS

In total, 35 pygmy shrews were used for the cytochrome *b* (*cyt b*) analysis (Fig. 1A; see also Supporting Information, Table S1). Tissue samples were obtained from 16 individuals from several regions in northern, central, and southern Italy, plus 14 individuals from neighbouring parts of France, Switzerland, and Slovenia. Five published *cyt b* sequences of *S. minutus* (AJ535420–AJ535424) from Italy, France, and Switzerland and a sequence of *Sorex volnuchini* (used as an outgroup; AJ535458) were obtained from GenBank (Mascheretti *et al.*, 2003). Additionally, two Y-chromosome intron sequences (DBY-7 and UTY-11; Hellborg & Ellegren, 2003) were obtained from 15 male *S. minutus* from Italy and neighbouring regions, plus five DBY-7 and UTY-11 *S. minutus* sequences and a sequence of *S. volnuchini* (used as an outgroup) from McDevitt *et al.* (2010) (see Supporting Information, Table S1).

Genomic DNA was extracted using a commercial kit (Qiagen). Partial *cyt b* sequences were obtained by polymerase chain reaction (PCR) amplification either using two primer pairs that amplified approximately 700 bp of overlapping fragments or using five primer pairs (for museum samples with highly degraded DNA) that amplified approximately 250 bp of overlapping fragments (see Supporting Information, Table S2). PCR amplification for *cyt b* was performed in a 50- μ L final volume: 1 \times buffer, 1 μ M each primer, 1 μ M dNTPs, 3 mM MgCl₂ and 0.5 U Platinum *Taq* Polymerase (Invitrogen), with cycling conditions of 94 °C for 4 min, 40 cycles at 94 °C for 30 s, 55 °C for 30 s, and 72 °C for 45 s, and a final elongation step at 72 °C for 7 min. Purification of PCR products was conducted with a commercial kit (Qiagen) and sequenced (Macrogen and Cornell University Core Laboratories Center). Amplification conditions of the Y-chromosome introns are described elsewhere (Hellborg & Ellegren, 2003) and the sequences were concatenated. Known female and male samples were used as controls in all PCR reactions for Y-chromosome introns.

Sequences were edited in BIOEDIT, version 7.0.9.0 (Hall, 1999), aligned in CLUSTALX, version 2.0 (Larkin *et al.*, 2007), and collapsed into haplotypes using DNASP, version 4.90.1 (Rozas *et al.*, 2003). The model of evolution that best fit the molecular data was determined using MODELTEST, version 3.7 (Posada &

Crandall, 1998), using the minimum Akaike's information criterion value. For *cyt b*, the supported substitution model was Hasegawa–Kishino–Yano 1985 with a proportion of invariable sites of 0.5308, a gamma correction of 0.8018, and nucleotide frequencies of $A = 0.2699$, $C = 0.2981$, $G = 0.1417$, and $T = 0.2903$. For the concatenated Y-chromosome introns, the best model was Tamura–Nei 1993 with an equal proportion of invariable sites, no gamma correction, and nucleotide frequencies of $A = 0.3313$, $C = 0.1957$, $G = 0.1901$, and $T = 0.2828$. The phylogenetic relationships among *cyt b* and Y-chromosome intron haplotypes were inferred using different methods in PAUP*, version 4.0b10 (Swofford, 2000), complemented with PAUPu, version 1.0.3.1 (Calendini & Martin, 2005): neighbour-joining (NJ) and maximum likelihood (ML), using the appropriate evolutionary model, and maximum parsimony (MP), using a heuristic search with simple stepwise addition of taxa and branch swapping (tree bisection reconnection, one million rearrangements). Statistical support for the phylogenetic relationships was assessed by 10 000 bootstrap replicates for NJ and 1000 bootstrap replicates for MP and ML. A Bayesian analysis was performed in MrBayes, version 3.1 (Huelsenbeck & Ronquist, 2001), using the appropriate evolutionary model. Two runs were performed with one million generations, a sampling frequency every 100 generations (to give a total of 10 000 samples for each run), a temperature of 0.1 for the heated chain, and checked for convergence. Trees were summarized after a burn-in value of 2500 to obtain the posterior probabilities of each phylogenetic split. A phylogenetic network was constructed using NETWORK, version 4.5.1.0 (Fluxus-Engineering), with a median-joining algorithm and a greedy genetic distance calculation method.

The *cyt b* haplotypes that clustered into major genetic lineages with high bootstrap support (or high posterior probabilities) were considered as distinct phylogroups (Avice, 2000). Genetic diversity values (π , nucleotide diversity of Jukes–Cantor) for each phylogroup and for the total sample were calculated using DNASP. Genetic divergence values between all pairs of phylogroups were estimated as Da (the mean \pm SD number of net nucleotide substitutions per site between phylogroups with Jukes–Cantor correction) using DNASP. Divergence times between *cyt b* phylogroups were estimated as $T = Da/2\mu$, where 2μ is the divergence rate (again given along with the SD). We used the divergence rate of 2% per Myr assuming equal rates of mtDNA sequence divergence among phylogroups (Taberlet *et al.*, 1998). ARLEQUIN, version 3.11 (Excoffier, Laval & Schneider, 2005), was used to estimate the pairwise genetic differentiation values (F_{ST}) between all pairs of phylogroups, for an analysis of molecular variance (AMOVA) among and

within phylogroups, and for a locus-by-locus (per nucleotide site) AMOVA. Ten thousand nonparametric permutations were performed to generate a random distribution to test the significance of the pairwise F_{ST} values and covariance components of the AMOVA, and $\alpha = 0.01$ was set as the threshold for statistical significance. No estimates of genetic diversity or differentiation were made for the Y-chromosome introns because of the low number of males per clade.

GEOMETRIC MORPHOMETRIC ANALYSIS

We examined a total of 277 mandibles of pygmy shrews from 99 different localities in Europe and western Siberia. Because most of the localities were represented by a small number of specimens, samples were pooled on the basis of geographic proximity resulting in 27 operational taxonomic units (OTUs) (Fig. 1B; see also Supporting Information, Table S3). Images of mandibles were collected using a Pixera Professional camera (Pixera Corporation) at a 1.2 million pixel resolution equipped with a Nikkor 210 mm APO MACRO lens, at a fixed distance of 93 cm. Morphological analyses were carried out using the 'tps-Series' software (developed by F.J. Rohlf, Department of Ecology and Evolution, State University of New York at Stony Brook, NY, USA; all software are available at: <http://life.bio.sunysb.edu/morph/>).

Fourteen landmarks were digitized from the internal side of each mandible (Fig. 2A) using tpsDig. The size of each mandible was estimated using the centroid size (CS) (i.e. the square root of the sum of squared distances between each landmark and the centroid) (Bookstein, 1991), obtained by the software tpsRelw and was natural log-transformed. The landmark configurations were scaled, translated, and rotated using generalized Procrustes analysis (GPA; Rohlf & Slice, 1990). A weight matrix (W) incorporating uniform ($N = 2$) and non-uniform ($N = 22$) components was extracted using GPA (Bookstein, 1996). Both components were interpreted as shape variables ($N = 24$) and then reduced through a principal component analysis [namely, relative warp (RW) analysis] using tpsRelw.

Because of the relatively small number of individuals in each OTU, we first tested for size and shape differences between the sexes to justify pooling of sexes in subsequent analyses. We analyzed the effect of sex, OTUs, and their mutual interaction in the OTUs CZ and I9, which had an adequate number of males ($N = 13$ and $N = 12$, respectively) and females ($N = 7$ and $N = 15$, respectively). The effect of sexual dimorphism was examined by analysis of variance (ANOVA) on CS (for size) and by multivariate analysis of variance (MANOVA) on W (for shape).

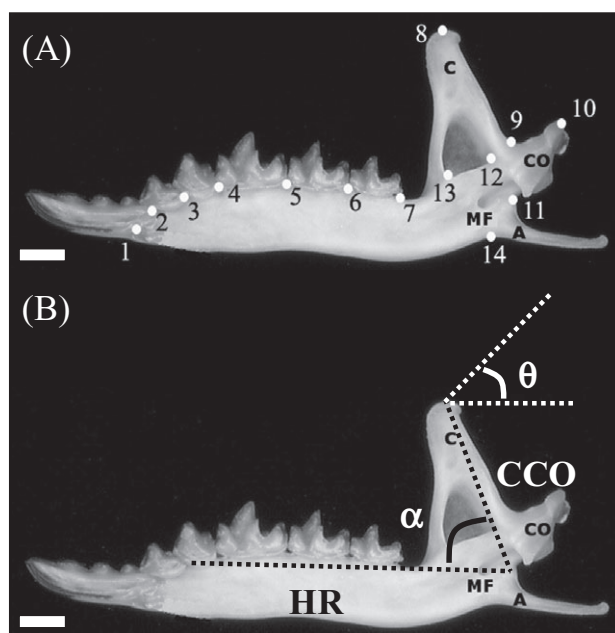


Figure 2. Location of 14 landmarks placed on the internal side of mandibles of the pygmy shrew (A) and measurements for bite force as a first-order lever on pygmy shrew mandibles (B), where coronoid–condyloid length (CCO) is the in-lever and horizontal ramus length (HR) is the out-lever, α is the angle between CCO and HR, and $\theta = 90^\circ - \alpha$. The bite force is measured as $(\cos\theta \times \text{CCO})/\text{HR}$. MF, mandibular fossa; C, coronoid process; CO, condyloid process; A, angular process; white bar = 1 mm.

The pattern of shape variation related to mandible size change (allometry) was compared for the full data set using tpsRegr. A correlation was performed to assess how OTUs mean CS varied with latitude (in decimals). The size differences among OTUs and among phylogroups (dividing the full mandible data set into phylogroups detected by the phylogeographic approach) were evaluated by ANOVAs and visualized with box plots. Levene's tests were performed to detect heteroscedasticity; however, the ANOVA is sufficiently robust to the violation of the assumption of homogeneity of variances (Zelditch *et al.*, 2004). We performed a Tukey–Kramer post-hoc test because it allows for unequal sample size (Sokal & Rohlf, 1995). Shape differences among OTUs and phylogroups were evaluated via MANOVAs on W , followed by a Hotelling T^2 test for multivariate comparisons.

Ordination of the OTUs was obtained through RW analysis (Rohlf, 1993) on the consensus (average) configurations of the 27 OTUs using the software tpsRelw. Shape changes in the RW space were visualized as thin-plate spline deformation grids (Bookstein, 1989). Procrustes distances among the consensus configurations of the OTUs were then

computed using tpsSmall and entered into NTSYS, version 2.2 (Exeter Software), to produce a dendrogram using an unweighted pair group method with arithmetic mean (UPGMA) to evaluate the phenetic relationships.

A functional adaptive hypothesis for shape variation in the mandible (represented as thin-plate spline deformation grids) was investigated by estimating the bite force (BF) in the context of a first-order lever (Fig. 2B; Fearnhead, Shute & Bellairs, 1955; MacDonald & Burns, 1975; Carraway & Verts, 1994), where the in-lever is the coronoid–condyloid length (CCO) measured from the tip of the coronoid process (C; landmark 8) to the base of the condyloid process (CO; landmark 11), and where the out-lever is the horizontal ramus length (HR) measured from CO to the facet-tip of M_1 (landmark 3; Fig. 2B). A stronger bite is given by the increased ratio between the in-lever (CCO) and the out-lever (HR), or by altering the angle (α) between them such that it becomes more obtuse, as described by $BF = (\cos\theta \times CCO)/HR$, where $\theta = 90^\circ - \alpha$. CCO, HR, and α were measured on the deformation grids for the extreme of shape variation along the first RW (RW1) (i.e. the one that explained most of the variation).

RESULTS

PHYLOGEOGRAPHIC ANALYSIS

We analysed a *cyt b* fragment of 1110 bp for the 35 pygmy shrews. There were 31 haplotypes (27 haplotypes first reported in the present study; GenBank accession numbers: GQ272492–GQ272518) with 103 polymorphic sites (105 mutations and one complex codon, with three mutations not included in the analysis) of which 48 were parsimony informative. In total, there were 92 synonymous and ten nonsynonymous changes.

For the Y-chromosome introns, we analysed a concatenated fragment of 1143 bp. We found only five haplotypes that together had 11 polymorphic sites (of which nine were parsimony informative) and one site with an insertion/deletion (GenBank accession numbers: GQ272519–GQ272521 for DBY-7 and GQ272522–GQ272526 for UTY-11). Two of the haplotypes have been reported previously (see Supporting Information, Table S1).

The different phylogenetic methods produced topologically similar trees for the *cyt b* data with high bootstrap and posterior probability support for particular branches (Fig. 3A), classified as: (1) a ‘European’ phylogroup including samples from Switzerland and strictly northern regions of Italy in the Alps (Sondrio, Piemonte and Trento); (2) an ‘Italian’ phylogroup (northern–central Italy) including

samples from central regions (Abruzzo) and north-western regions (Genova) in the Apennines, but also including samples from the north and north-east of Italy (Alps), Switzerland, and neighbouring regions in France and Slovenia; and (3) a ‘southern Italian’ phylogroup with samples strictly from Calabria (La Sila mountain). Of all the phylogroups, the southern Italian had the greatest bootstrap and posterior probability support with the various phylogenetic methods. The sequences from the whole Italian peninsula (including both the ‘Italian’ and ‘southern Italian’ phylogroups) also formed a well supported clade. One sample from Switzerland (CHCE1) clustered separately from all the rest and has been identified as belonging to a distinct Balkans lineage (R. Vega & J. B. Searle, unpublished data), and is not considered further here. The same phylogroups were also seen in the phylogenetic network (data not shown), with the European phylogroup separated from the Italian and southern Italian phylogroups by 18 mutational steps and the southern Italian and Italian phylogroups separated by 12 steps.

Similarly, the phylogenetic analysis of concatenated Y-chromosome introns (Fig. 3B) revealed a distinct ‘southern Italian’ lineage (one haplotype, four samples). This was most closely related to an ‘Italian’ lineage (one haplotype, six samples) composed of northern–central Italian and Swiss samples that in the *cyt b* trees also formed an Italian phylogroup. Additionally, there was a ‘European’ lineage composed of eight Swiss samples, six of which clustered within the *cyt b* European phylogroup, CHV12 that clustered within the *cyt b* Italian phylogroup and CHCE1 that belonged to a *cyt b* Balkans lineage, plus ITPR2 (Prasota, northern Italy) that clustered within the European *cyt b* phylogroup and SIPo1 (Postjoma, Slovenia) that clustered within the Italian *cyt b* phylogroup.

The nucleotide diversity (π) was 0.0157 for the *cyt b* data overall. For the European phylogroup, $\pi = 0.0057$ relating to 11 haplotypes (all nonredundant sequences). For the Italian phylogroup, $\pi = 0.0063$ and there were 15 haplotypes, two occurring in multiple individuals (samples from Abruzzo). For the southern Italian phylogroup, $\pi = 0.0073$, reflecting four different haplotypes, although all samples were caught in the same area (La Sila mountain) and had 14 mutations that were not shared with other phylogroups (six of which were significantly differentiated from the rest of the sample by a locus-by-locus AMOVA and sequence comparison). For the whole Italian phylogroup (Italian plus southern Italian), $\pi = 0.0096$ relating to 19 haplotypes.

The divergence between phylogroups was small, as expected for within species comparisons. For European versus Italian $Da = 1.6\%$ ($\pm 0.3\%$), comparable to

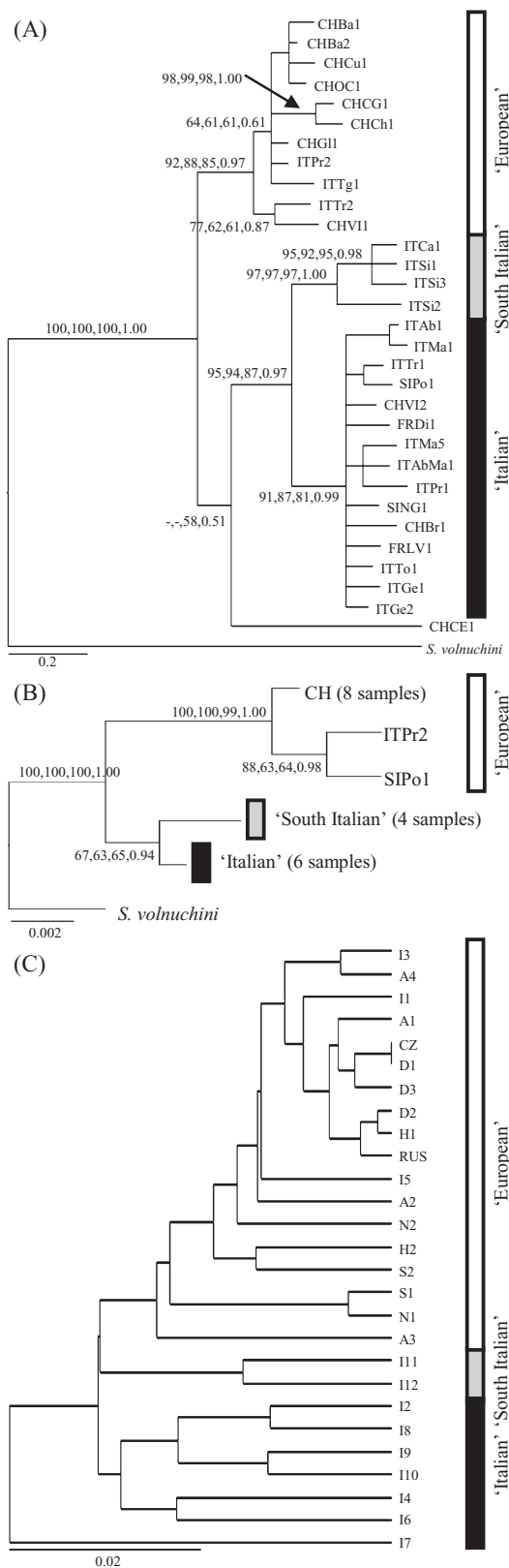


Figure 3. Bayesian analysis of cytochrome *b* data (A) and concatenated Y-chromosome introns DBY-7 and UTY-11 (B) for pygmy shrews with distinct lineages highlighted. C, unweighted pair group method with arithmetic mean phenogram of Procrustes distances among the consensus configurations of 27 operational taxonomic units showing shape differences between ‘European’, ‘Italian’ and ‘southern Italian’ pygmy shrew mandibles. Values on phylogenetic trees correspond to branch support for neighbour-joining, maximum parsimony maximum likelihood and Bayesian analysis, respectively.

European versus southern Italian $Da = 1.5\% (\pm 0.4\%)$, whereas Italian versus southern Italian had the smallest divergence, $Da = 1.0\% (\pm 0.3\%)$. For the European versus whole Italian sample (Italian plus southern Italian) $Da = 1.4\% (\pm 0.2\%)$. All divergence times among phylogroups pre-dated the LGM according to the divergence rate used, where $T_{(\text{European-Italian})} = 0.8 \pm 0.15$ Mya, $T_{(\text{European-southern Italian})} = 0.75 \pm 0.2$ Mya, $T_{(\text{Italian-southern Italian})} = 0.5 \pm 0.15$ Mya, and $T_{(\text{European-whole Italian})} = 0.7 \pm 0.3$ Mya. The AMOVA showed that 71% of the overall genetic variation could be attributed to differences among the three phylogroups and 29% to within-phylogroup variation ($F_{ST} = 0.7101$, $P < 0.001$). Pairwise F_{ST} values were high and significant between phylogroups as a result of the 27 significantly differentiated polymorphic nucleotide sites among populations as determined by the locus-by-locus AMOVA and sequence comparison.

GEOMETRIC MORPHOMETRIC ANALYSIS

The MANOVA on the *W* matrix revealed significant mandible shape differences between the OTUs CZ and I9 but no significant effect of sex and the interaction sex \times OTU. Therefore, all subsequent analyses on shape were performed pooling all samples irrespective of sex.

The regression of shape on size (allometry) was significant ($F_{24, 6600} = 3.03$; $P < 0.001$). The ANOVA on CS among OTUs was significant ($F_{26, 273} = 12.647$, $P < 0.001$); however, Levene’s test was significant and so this result has to be taken with caution and no post-hoc comparisons among OTUs were made. The ANOVA on CS among the mandible sample divided into phylogroups was significant ($F_{2, 271} = 53.212$, $P < 0.001$), and homogeneity of variances supported. Post-hoc tests showed significant CS differences among all pairs of phylogroups, although caution is warranted because of the limited number of mandibles available for the southern Italian phylogroup. There was a significant inverse correlation between mandible size and latitude ($r = -0.661$; $P < 0.001$).

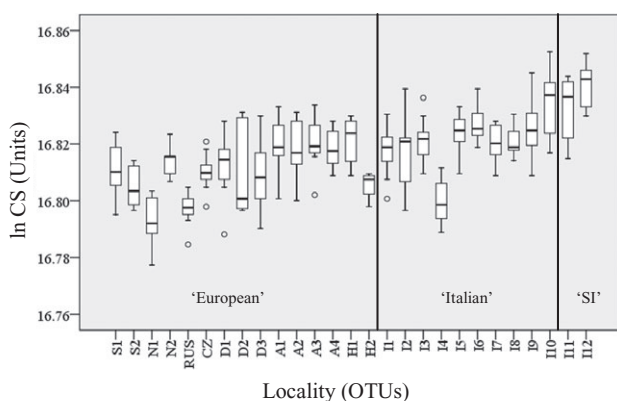


Figure 4. Box-plot showing mandible centroid size (CS) variation (natural log-transformed) of 27 operational taxonomic units of pygmy shrew ordered according to latitude from north (left) to south (right), and by phylogroups (SI, southern Italy).

Mandible size increased progressively from northern to southern European localities (Fig. 4). The only obvious outlier was the north-western Italian locality I4 (Torino), which fell within the range of northern-central European populations.

The MANOVA on W among OTUs were significant (Wilk's $\lambda = 0.008$, $P < 0.001$). The Hotelling T^2 test showed that 51% of the between group comparisons were significant. The highest percentage (80–100%) of significant differences involved comparisons of central-southern Italian OTUs both among themselves and against northern-central European OTUs. The MANOVA on W divided into phylogroups was significant (Wilk's $\lambda = 1.592$; $P = 0.0057$); however, Hotelling's T^2 test showed significant shape differences only between the European and Italian phylogroups ($P = 0.0027$). The southern Italian phylogroup was not different from either of these groups ($P = 0.1467$), most likely as a result of small sample size.

The first three RWs computed on the OTU consensus explained cumulatively 61.75% of the total variance (28.90%, 20.51%, and 12.34%, respectively). There were two groups identifiable based on the geographic origin of the OTUs (Fig. 5A): a European group including all OTUs from northern and central Europe plus north-eastern Italian OTUs I1 and I3 (Trentino, Alps) and central Italian OTU I5 (Foreste Casentinesi, Apennines), and an Italian group with OTUs I2, I4, I6, and I8 to I12. OTU I7 (Grosseto, Tuscany) was an outlier. There was a higher diversity for the mandible within the Italian group along RW2 than within the European group. However, the southern Italian OTUs (I11 and I12) could not be distinguished from the central and northern Italian OTUs based solely on RW analysis.

The main shape differences between the two groups found with RW analysis (Italian and European) are shown, as an example, by the deformation grids taken from the most extreme values along the RW1 axis (the RW that explained most of the variation) from each group (Fig. 5B, C). There was a stronger BF in Italian compared to European pygmy shrews (BF = 0.238 and 0.074, respectively). The mandible of Italian (Fig. 5B) and European shrews (Fig. 5C) was characterized by different slopes of the incisive alveolus (landmark 2), a different HR length, and by notable changes in the posterior portion affecting the relative position of the masseteric fossa (MF) and the angular process (A). The greatest BF in Italian shrews was given by an apparent lengthening of C and a shorter HR length, which increased the ratio between the in-lever and out-lever compared to European pygmy shrew mandibles. However, in Italian shrews, there were relative movements of CO (landmarks 9, 10, and 11) and C in opposite directions causing a forward shift of its tip (landmark 8) and a more acute angle α (between CCO and HR) compared to European pygmy shrew mandibles.

The UPGMA phenogram showed morphological clusters that divided the samples into three main distinct geographical regions (Fig. 3C): (1) a 'European' cluster with northern-central European and north-eastern (Alpine) Italian OTUs (I1 and I3), but which also included OTU I5 (central Italy); (2) an 'Italian' cluster with central Italian OTUs and Italian OTUs from the southern Apennines (Collemeluccio, Muro Lucano and Catena Costiera); and (3) a strictly 'southern Italian' cluster with Calabrian samples (OTUs I11 and I12); OTU I7 (Grosseto, Tuscany) was an outlier.

DISCUSSION

MORPHOLOGICAL AND PHYLOGEOGRAPHICAL CONGRUENCIES

The present study represents the first combined phylogeographic and morphological analysis of the pygmy shrew, and it had a focus on populations of the species in the Italian peninsula. In general, we found congruence between phylogeographic and morphological patterns. Both analyses consistently identified pygmy shrews from the Italian peninsula as being different from northern-central European pygmy shrews, and further distinguished southern Italian pygmy shrews of the Calabria region (Fig. 1A) as being different from Italian populations further north.

We found three main geographically coherent genetic and phenetic clusters (Fig. 3A, B, C). The European morphological group (based on geometric

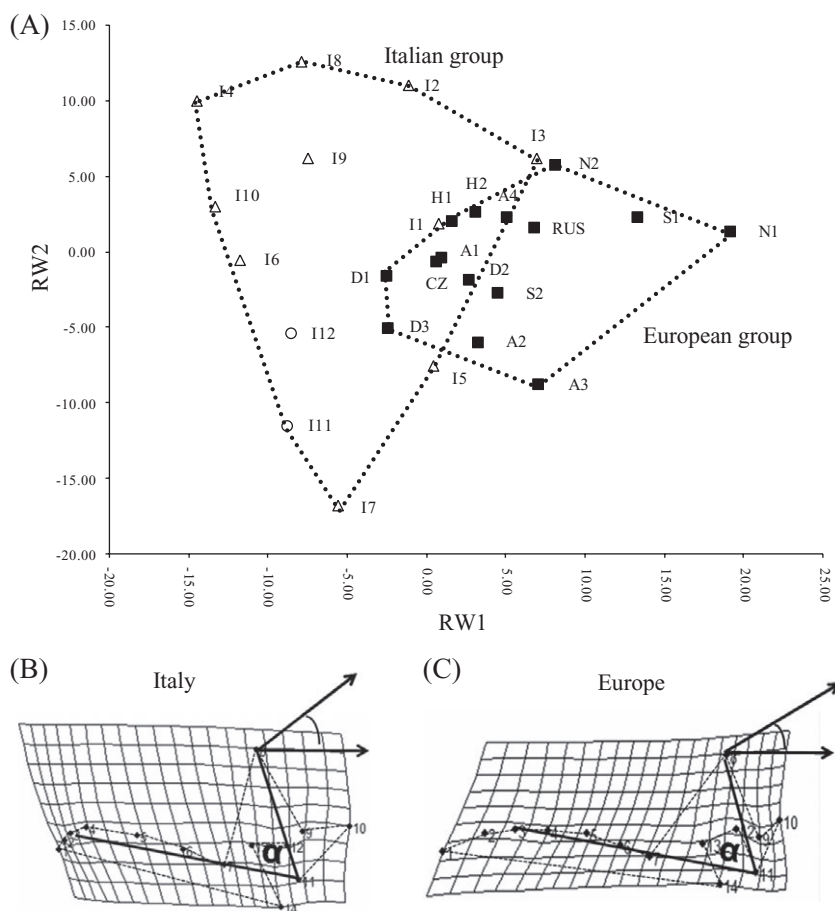


Figure 5. Morphometric analyses of the mandibles of pygmy shrews. Ordination of the consensus configurations (A) of 27 operational taxonomic units (OTUs) along the first two relative warp (RW) axes. ■, Northern-central European OTUs; △, northern-central Italian OTUs; ○, southern Italian OTUs. Shape changes and bite force implied by the variation along RW1 are shown as thin plate spline deformation grids representing the extremes of variation along the axis for (B) an Italian OTU and (C) a European OTU, respectively.

morphometrics) had a widespread distribution in Eurasia (from western Siberia to Norway and Hungary) and included samples from the northern regions of Italy. Previous data show that the European genetic group (based on *cyt b* and the Y-chromosome introns), which we found in central European and north Italian samples, is similarly very widespread (Bilton *et al.*, 1998; McDevitt *et al.*, 2010; Mascheretti *et al.*, 2003). The Italian phenetic cluster included mandible samples from central regions of the peninsula together with OTUs from the Italian Alps and from the southern Apennines. Likewise, the Italian genetic group consisted of north Italian samples from the Alps and central Italian samples from the Apennines. However, more genetic sampling is desirable to determine whether this phylogroup reaches the southern Apennines. The situation in northern parts of Italy is also worth further study. Genetic and morphological samples from

geographically close localities in northern Italy either belonged to the European or to the Italian group (e.g. for the genetic data, samples from Trento and Prasota; for the morphological data, OTUs I1, I2, and I3). Apparently this is a contact area of two lineages.

Interestingly, we found a genetically distinct phylogroup of pygmy shrews from the Calabria region in southern Italy for *cyt b* and Y-chromosome data (all samples from La Sila). We also found a morphologically distinct group of pygmy shrews from this region, specifically from La Sila (I11) and Aspromonte (I12) massifs. When the morphological samples were pooled into the same groupings as the genetic phylogroups, the southern Italian samples had significantly larger mandibles by centroid size than other phylogroups. The southern Italian morphological samples also clustered separately by shape but, when there was no a priori grouping of OTUs, these

samples were not significantly different from northern–central Italian samples by MANOVA and RW analysis. The southern Italian morphological samples from Collemeluccio (I8), Muro Lucano (I9), and Catena Costiera (I10) clustered with northern–central Italian samples and not with those from La Sila and Aspromonte, suggesting that the morphologically and genetically distinct population of pygmy shrews in southern Italy has a very limited distribution (Fig. 1A). More extensive sampling in this southern region (Catena Costiera, other parts of the southern Apennines in Basilicata region, and further south from La Sila in the Serre and Aspromonte massifs) is desirable to obtain a more precise morphological, phylogeographic, and population genetic description. Nevertheless, the genetic results obtained in the present study indicate strongly the distinctiveness of the southern Italian phylogroup. The phylogenetic results were consistent among methods and the phylogroups displayed high branch support and were significantly differentiated. Moreover, in the few samples from southern Italy, there were several fixed and significantly differentiated mutations that were not shared with other phylogroups, and even the less variable Y-chromosome introns revealed a distinct southern Italian lineage. Collectively, the results display the phylogeographic and morphological distinctiveness of pygmy shrew populations from the Italian peninsula and the Calabria within it.

We found some discrepancy between the morphological and genetic analyses. For the morphological data, OTU I5 from central Italy (Foreste Casentinesi) clustered within the European group, whereas, for the genetic data, no central Italian sample clustered within the European lineage. The Italian *cyt b* phylogroup contained several central European samples from Switzerland, Slovenia, and France, whereas no European morphological sample grouped within the Italian cluster. Also, MANOVAs on mandibles among OTUs mainly differentiated European from central–southern Italian samples and the RW analysis discriminated these two main groups only, whereas pairwise F_{ST} on genetic data showed significant differences among European, Italian, and southern Italian lineages.

OTU I7 was an outlier in the cluster and RW analyses and, to further understand this, we need better sampling along the Tyrrhenian coast. Discrepancies among maternally and paternally inherited markers, specifically in northern Italy and Switzerland, may be explained by the larger dispersal rate and activity areas of male versus female pygmy shrews (Shchipanov *et al.*, 2005), as expressed in the contact zone of distinct lineages, and by different mutation rates of the markers examined.

SIZE AND BITE FORCE AMONG MORPHOLOGICAL GROUPS

The mandible of pygmy shrews increases in size from north to south and represents an exception to Bergmann's rule, as reported for other Soricinae in Europe (Ochocinska & Taylor, 2003), where it was suggested that small body size is adaptive under conditions of low resource availability in northern latitudes, especially in winter.

The mandible of shrews may be considered as a first-order lever during bite and mastication (MacDonald & Burns, 1975). This is because the lower condyloid facets act as the fulcrum with the in-lever (CCO) set at an acute angle to the out-lever (HR). The mandible of Italian pygmy shrews, in comparison to other European pygmy shrews, was characterized by a different slope of the incisive alveolus and a bigger ratio of the coronoid process versus the horizontal ramus lengths leading to an increased bite force, and by substantial changes in the posterior portion that created a more acute angle between the condyloid process and the horizontal ramus (Fig. 5B, C). The greater bite force of Italian pygmy shrews compared to other European pygmy shrews is likely a consequence of adaptation to the more arid conditions and prey with harder exoskeletons (Strait, 1993; Carraway & Verts, 1994). An alternative hypothesis is that inter- or intra-specific competition might cause an increase in mandible size and bite strength (Corti & Rohlf, 2001). However, considering the low population densities of pygmy shrews in southern Italy and the similarity of species assemblages throughout the animal's range, this hypothesis appears unlikely.

REFUGIA WITHIN REFUGIA IN THE ITALIAN PENINSULA?

One possible explanation for the current occurrence of two morphologically and genetically distinct clusters of pygmy shrew essentially restricted to Italy is that there were two glacial refugia for this species in this region, and that these distinct groups arose within those refugia during one or more glacial cycles. Thus, for the pygmy shrew, the Italian refugial area may have been subdivided into multiple refugia at the LGM, concordant with the 'refugia within refugia' concept (Gómez & Lunt, 2006). However, genetic subdivision may also arise from population subdivision at times other than glacial maxima.

One of the two groups of pygmy shrews in Italy is very widespread (the Italian group), whereas the other is limited to the extreme south (the southern Italian group). It is apparent that a variety of other small vertebrates are also characterized by a genetic lineage in the extreme south of Italy (Table 1) and, in most of

Table 1. Small vertebrate species with a distinct genetic lineage in the southern part of the Italian peninsula

Class	Species	Distribution range of species	Southern Italian lineage	Reference
Amphibia	<i>Triturus italicus</i>	Central–southern Italy	Calabria	Ragghianti & Wake (1986)
	<i>Rana (Pelophylax) lessonae</i>	Europe	Calabria and Sicily	Santucci <i>et al.</i> (1996); Canestrelli & Nascetti (2008)
	<i>Salamandra salamandra</i>	Europe	Southern Italy	Steinfartz, Veith & Tautz (2000)
	<i>Salamandrina terdigitata</i>	Central–southern Italy	Southern Italy	Mattocchia, Romano & Sbordoni (2005); Nascetti, Zangari & Canestrelli (2005); Canestrelli, Zangari & Nascetti (2006a)
	<i>Bombina pachypus</i>	Peninsular Italy	Calabria	Canestrelli <i>et al.</i> (2006b)
	<i>Hyla intermedia</i>	Peninsular Italy and Sicily	Calabria and Sicily	Canestrelli <i>et al.</i> (2007)
	<i>Rana italica</i>	Peninsular Italy	Calabria	Canestrelli <i>et al.</i> (2008)
Reptilia	<i>Hierophis viridiflavus</i>	Europe	Calabria and Sicily	Nagy <i>et al.</i> (2003)
	<i>Podarcis sicula</i>	Italy & Balkans	Calabria	Podnar, Mayer & Tvrtkovic (2005)
	<i>Vipera aspis</i>	Europe	Southern Italy	Ursenbacher <i>et al.</i> (2006)
	<i>Lacerta bilineata</i>	Europe	Calabria	Böhme <i>et al.</i> (2007)
Mammalia	<i>Lepus corsicanus</i>	Central–southern Italy	Southern Italy and Sicily	Pierpaoli <i>et al.</i> (1999)
	<i>Talpa romana</i>	Central–southern Italy	Calabria	Ungaro <i>et al.</i> (2001)
	<i>Myodes glareolus</i>	Eurasia	Calabria	Amori <i>et al.</i> (2008)
	<i>Microtus brachycercus</i>	Central–southern Italy	Central–southern Italy	Castiglia <i>et al.</i> (2008)
	<i>Sciurus vulgaris</i>	Eurasia	Southern Italy	Grill <i>et al.</i> (2009)
	<i>Sorex minutus</i>	Eurasia	Southern Italy	Present study

these examples, there is at least one more lineage restricted to Italy (a second, Italian-restricted lineage has not been recorded in *Salamandra salamandra*, *Hierophis viridiflavus*, *Lacerta bilineata* or *Sciurus vulgaris*). So, in the pygmy shrew, as in a range of other species, this may be the result of one glacial refugium in the extreme south of Italy, and at least one other refugium further north. In *Rana (Pelophylax) lessonae*, *Vipera aspis* and *Myodes glareolus*, there is a similar situation as in the pygmy shrew, with an Italian lineage that makes contact with one or more other European lineages in the extreme north of Italy (Santucci, Nascetti & Bullini, 1996; Deffontaine *et al.*, 2005; Ursenbacher *et al.*, 2006; Canestrelli & Nascetti, 2008). For each of these species, the widespread Italian lineage may be presumed to derive from a glacial refugium located somewhere within the vicinity of the Apennine mountain chain.

Although the data appear consistent with the ‘refugia within refugia’ concept, a degree of caution is needed for the pygmy shrew, and probably for some other species as well. The concept implies that the species were restricted to particular localized areas at

the LGM, which can be termed ‘refugia’ (Bennett & Provan, 2008; Stewart *et al.*, 2010), and that their distribution expanded on amelioration of the climate. Indeed, the pygmy shrew is currently restricted to high altitude areas in Italy because the dry, hot Mediterranean conditions in the lowlands do not suit it. Therefore, in southern Europe, the distribution of the pygmy shrew may actually be more restricted during interglacials than glacials, in line with ideas of ‘interglacial refugia’ (Hilbert, Graham & Hopkins, 2007).

Further samples are needed to test whether the ‘refugia within refugia’ concept applies to the pygmy shrew in Italy (i.e. genetic analyses are needed to demonstrate population expansions from two separate refugial areas). From the current data, it is possible that the Italian and southern Italian morphological and genetic clusters occupied a single, continuous area at the LGM with the integrity of the groups retained by a hybrid zone (Barton & Hewitt, 1985).

Thus, pygmy shrews from southern Italy are genetically and morphologically distinctive, and may

be restricted to Calabria. The general question that remains is: how did the southern Italian and Italian groups of pygmy shrew become separate entities? Here, comparison with other small vertebrates can be informative. For many of the species with a southern Italian lineage, that lineage is also restricted to the peninsula of Calabria (Fig. 1A, Table 1). Calabria consists of isolated mountain massifs separated by lowland areas. From the Pliocene to the Middle Pleistocene, at times of high sea level, those massifs would have been islands in a chain that stretched between the southernmost part of the Italian peninsula and Sicily (Malatesta, 1985; Caloi, Malatesta & Palombo, 1989; Bonardi *et al.*, 2001; Bonfiglio *et al.*, 2002). Since the Late Pleistocene, uplift has prevented island-formation. Considering all species that have distinct Calabrian lineages, it is reasonable to suggest that the distinction of these Calabrian forms reflects island evolution. On the basis of the molecular clock used in the present study, the separation of the Italian and southern Italian *cyt b* lineages of pygmy shrew from each other and from the European lineage extend back into the Middle Pleistocene.

Over the last glacial cycle, the putative Calabrian island forms have been limited to a mainland distribution. For the pygmy shrew at least, it is likely that the Calabrian form is geographically isolated at the present time because pygmy shrews there are apparently restricted to the Calabrian massifs. The extent to which Calabrian pygmy shrews were isolated during the period extending back to the LGM is less certain, and is of course crucial in relation to the 'refugia within refugia' concept.

Calabria forms part of the 'Calabrian Arc' and includes the separate mountain massifs of Catena Costiera in the north, La Sila in central Calabria, and the Serre and Aspromonte massifs in southern Calabria (Fig. 1A; Bonardi *et al.*, 2001). Catena Costiera makes contact in the north with the southern Apennines (southern Lucania, Basilicata region) but it is separated from La Sila by the Crati Valley depression in the east and from southern Calabria by the Catanzaro Plain in the south. Therefore, pygmy shrews from Catena Costiera in the northern Calabrian Arc might have been able to remain in long-term contact with the southern Apennine populations, thus avoiding differentiation. This could explain why the morphological samples from Catena Costiera (I10) clustered with northern-central Italian and not with the geographically nearby southern Italian samples from La Sila (I11) and Aspromonte (I12). For the southern Italian pygmy shrew, the La Sila and Aspromonte massifs are geographically isolated from each other and from the Apennines.

TAXONOMIC AND LOCAL CONSERVATION IMPLICATIONS FOR SOUTHERN ITALIAN PYGMY SHREWS

The subspecies concept has been widely criticised (Wilson & Brown, 1953), although the use of trinomials can generate interest at a local scale by giving a regional- or country-based value for biodiversity, and the recognition of subspecific levels may stimulate further investigation of those populations (Mayr, 1982; Amori, Angelici & Boitani, 1999). The morphological and genetic differentiation shown in the present study does not justify that Italian and/or southern Italian pygmy shrews be considered as separate species. However, we consider that the trinomial *S. m. lucanius* should be kept as the taxonomic name to describe the southern Italian pygmy shrews, emphasizing that it is an Evolutionarily Significant Unit (ESU; Moritz, 1994). Our data also suggest that Italian pygmy shrews form a different ESU from the European *S. m. minutus*. Given that the Italian and southern Italian pygmy shrews are distinctive forms, do they need protection? Currently, the pygmy shrew overall is characterized as a Least Concern species for conservation purposes (IUCN, 2007; <http://www.iucnredlist.org/details/29667/0>). However, the Italian populations deserve more attention than this implies. In particular, the distinctive Calabrian populations of pygmy shrew surely need specific protection. They occur in a very small area and, on the basis of our field efforts, are very uncommon there (R. Vega & G. Aloise, pers. observ.). Given the range of species and populations that are distinctive in Calabria (Table 1), there needs to be a clear conservation effort to protect plant and animal communities in that region.

CONCLUSIONS

On the basis of the morphological and phylogeographic data presented here, we show three distinguishable and significantly differentiated clusters of pygmy shrews corresponding to European, Italian, and southern Italian groups. The differentiation includes adaptive features, on the basis of our analysis of mandible characteristics. The two Italian groups appear to have arisen as a consequence of geographic isolation before the LGM (one group originating on islands in the location of present-day Calabria), and it is unclear whether they were located in separate glacial refugia at the LGM. Moreover, because studies of several other species have also shown genetic and morphological distinction of populations in Calabria, this region should be a focus for conservation.

ACKNOWLEDGEMENTS

Specimens of pygmy shrews were made available by several museums and we acknowledge the help of the curators from the following institutions: Institute de Zoologie et d'Ecologie Animale (Université de Lausanne, Switzerland), Museo di Storia Naturale 'La Specola' (Firenze, Italy), Museo Civico di Storia Naturale Giacomo Doria (Genova, Italy), and DIVAPRA, Università degli Studi di Torino (Italy), together with those listed in the Supporting Information (Table S3). We are very grateful for the tissue samples provided by Heidi Haufler, Patrick Brunet-Lecomte, and Boris Kryštufek. Two anonymous reviewers made valuable comments and the Zamudio Laboratory (Cornell University) gave a fresh perspective on a previous version of the manuscript. R. Vega received funds from CONACyT (México; Reg. no. 181844). This work is dedicated to the memory of Marco Corti (1950–2007), mammalogist and morphometrician, who contributed substantially to this study during the last years of his life.

REFERENCES

- Amori G, Angelici FM, Boitani L. 1999.** Mammals of Italy: a revised checklist of species and subspecies (Mammalia). *Senckenbergiana Biologica* **79**: 271–286.
- Amori G, Aloise G, Annesi F, Franceschini P, Colangelo P. 2008.** Filogeografia mitocondriale di Arvicola rossastra *Myodes glareolus* in Italia. 69° Congresso Unione Zoologica Italiana, Senigallia, September 22–25. Abstracts, 18.
- Avise JC. 2000.** *Phylogeography: the history and formation of species*. Cambridge, MA: Harvard University Press.
- Barton NH, Hewitt GM. 1985.** Analysis of hybrid zones. *Annual Review of Ecology and Systematics* **16**: 113–148.
- Bennett KD, Provan J. 2008.** What do we mean by 'refugia'? *Quaternary Science Reviews* **27**: 2449–2455.
- Bilton DT, Mirol PM, Mascheretti S, Fredga K, Zima J, Searle JB. 1998.** Mediterranean Europe as an area of endemism for small mammals rather than a source for northwards postglacial colonization. *Proceedings of the Royal Society of London Series B, Biological Sciences* **265**: 1219–1226.
- Böhme MU, Fritz U, Kotenko T, Džukić G, Ljubisavljević K, Tzankov N, Berendonk TU. 2007.** Phylogeography and cryptic variation within the *Lacerta viridis* complex (Lacertidae, Reptilia). *Zoologica Scripta* **36**: 119–131.
- Bonardi G, Cavazza W, Perrone V, Rossi S. 2001.** Calabria-Peloritani terrane and northern Ionian Sea. In: Vai GB, Martini IP, eds. *Anatomy of an orogen: the Apennines and adjacent Mediterranean basins*. Dordrecht: Kluwer, 287–306.
- Bonfiglio L, Mangano G, Marra AC, Masini F, Pavia M, Petruso D. 2002.** Pleistocene Calabrian and Sicilian bioprovinces. *Geobios* **35**: 29–39.
- Bookstein FL. 1989.** Principal warps: thin-plate spline and the decomposition of transformations. *IEEE Transactions on Pattern Analysis and Machine Intelligence* **11**: 567–595.
- Bookstein FL. 1991.** *Morphometric tools for landmark data*. Cambridge: Cambridge University Press.
- Bookstein FL. 1996.** Standard formula for the uniform shape component in landmark data. In: Marcus LF, Corti M, Loy A, Naylor GJP, Slice DE, eds. *Advances in morphometrics*. New York, NY: NATO ASI Series A, Life Sciences, **284**: 153–168.
- Calendini F, Martin JF. 2005.** *PaupUP*, Version 1.0.3.1. A graphical frontend for PAUP* DOS software. Available at: <http://www.agro-montpellier.fr/sppe/Recherche/JFM/PaupUp/main.htm>
- Caloi L, Malatesta A, Palombo RM. 1989.** Biogeografia della Calabria meridionale durante il Quaternario. *Atti Accademia Peloritana dei Pericolanti Classe I, Scienze Matematiche Fisiche e Naturali* **67**: 261–278.
- Canestrelli D, Cimmaruta R, Costantini V, Nascetti G. 2006b.** Genetic diversity and phylogeography of the Apennine yellow-bellied toad *Bombina pachypus*, with implications for conservation. *Molecular Ecology* **15**: 3741–3754.
- Canestrelli D, Cimmaruta R, Nascetti G. 2007.** Phylogeography and historical demography of the Italian tree frog, *Hyla intermedia*, reveals multiple refugia, population expansions and secondary contacts within peninsular Italy. *Molecular Ecology* **16**: 4808–4821.
- Canestrelli D, Cimmaruta R, Nascetti G. 2008.** Population genetic structure and diversity of the Apennine endemic stream frog, *Rana italica* – insights on the Pleistocene evolutionary history of the Italian peninsular biota. *Molecular Ecology* **17**: 3856–3872.
- Canestrelli D, Nascetti G. 2008.** Phylogeography of the pool frog *Rana (Pelophylax) lessonae* in the Italian peninsula and Sicily: multiple refugia, glacial expansions and nuclear-mitochondrial discordance. *Journal of Biogeography* **35**: 1923–1936.
- Canestrelli D, Zangari F, Nascetti G. 2006a.** Genetic evidence for two distinct species within the Italian endemic *Salamandrina terdigitata* Bonnaterra, 1789 (Amphibia: Urodela: Salamandridae). *Herpetological Journal* **16**: 221–227.
- Carraway LN, Verts BJ. 1994.** Relationship of mandibular morphology to relative bite force in some *Sorex* from western North America. In: Merritt JF, Kirkland GL, Rose RK, eds. *Advances in the biology of shrews*. Pittsburgh, PA: Special Publication of the Carnegie Museum of Natural History, 18: 201–210.
- Castiglia R, Annesi F, Aloise G, Amori G. 2008.** Systematics of the *Microtus savii* complex (Rodentia, Cricetidae) via mitochondrial DNA analysis: parapatry and pattern of sex chromosome evolution. *Molecular Phylogenetics and Evolution* **46**: 1157–1164.
- Corti M, Rohlf FJ. 2001.** Chromosomal speciation and phenotypic evolution in the house mouse. *Biological Journal of the Linnean Society* **73**: 99–112.
- Defontaine V, Libois R, Kotlík P, Sommer R, Nieberding C, Paradis E, Searle JB, Michaux JR. 2005.** Beyond

- the Mediterranean peninsulas: evidence of central European glacial refugia for a temperate forest mammal species, the bank vole (*Clethrionomys glareolus*). *Molecular Ecology* **14**: 1727–1739.
- Excoffier L, Laval G, Schneider S. 2005.** Arlequin version 3.0: an integrated software package for population genetics data analysis. *Evolutionary Bioinformatics Online* **1**: 47–50.
- Fearnhead RW, Shute CCD, Bellairs AA. 1955.** The temporo-mandibular joint of shrews. *Proceedings of the Zoological Society of London* **125**: 795–806.
- Gippoliti S, Amori G. 2002.** Mammal diversity and taxonomy in Italy: implications for conservation. *Journal for Nature Conservation* **10**: 133–143.
- Gómez A, Lunt DH. 2006.** Refugia within refugia: patterns of phylogeographic concordance in the Iberian Peninsula. In: Weiss S, Ferrand N, eds. *Phylogeography of southern refugia: evolutionary perspectives on the origins and conservation of European biodiversity*. Dordrecht: Springer Verlag, 155–188.
- Grill A, Amori G, Aloise G, Lisi I, Tosi G, Wauters LA, Randi E. 2009.** Molecular phylogeography of European *Sciurus vulgaris*: refuge within refugia? *Molecular Ecology* **18**: 2687–2699.
- Hall TA. 1999.** BioEdit: a user-friendly biological sequence alignment editor and analysis program for Windows 95/98/NT/XP. *Nucleic Acids Symposium Series* **41**: 95–98.
- Hellborg L, Ellegren H. 2003.** Y-chromosome conserved anchored tagged sequences (YCATS) for the analysis of mammalian male-specific DNA. *Molecular Ecology* **12**: 283–291.
- Hewitt GM. 2000.** The genetic legacy of the Quaternary ice ages. *Nature* **405**: 907–913.
- Hilbert DW, Graham A, Hopkins MS. 2007.** Glacial and interglacial refugia within a long-term rainforest refugium: the Wet Tropics Bioregion of NE Queensland, Australia. *Palaeogeography, Palaeoclimatology, Palaeoecology* **251**: 104–118.
- Huelsenbeck JP, Ronquist F. 2001.** MrBayes: Bayesian inference of phylogeny. *Bioinformatics* **17**: 754–755.
- Hutterer R. 1990.** *Sorex minutus* Linnaeus, 1766. Zwergspitzmaus. In: Niethammer J, Krapp F, eds. *Handbuch der Säugetiere Europas, band 3*. Wiesbaden: Aula-Verlag, 183–206.
- Hutterer R. 2005.** Order Soricomorpha. In: Wilson DE, Reeder DM, eds. *Mammal species of the world: a taxonomic and geographic reference*, 3rd edn, Vol. 1. Baltimore, MD: John Hopkins University Press, 220–311.
- IUCN. 2007.** Temple HJ, Terry A, comp. *The status and distribution of European mammals*. Luxembourg: The World Conservation Union, Office for Official Publications of the European Communities.
- Kryštufek B, Buzan EV, Hutchinson WF, Hänfling B. 2007.** Phylogeography of the rare Balkan endemic Martino's vole, *Dinaromys bogdanovi*, reveals strong differentiation within the western Balkan Peninsula. *Molecular Ecology* **16**: 1221–1232.
- Larkin MA, Blackshields G, Brown NP, Chenna R, McGettigan PA, McWilliam H, Valentin F, Wallace IM, Wilm A, Lopez R, Thompson JD, Gibson TJ, Higgins DG. 2007.** Clustal W and Clustal X version 2.0. *Bioinformatics* **23**: 2947–2948.
- Loy A. 1996.** An introduction to geometric morphometrics and intraspecific variation: a fascinating adventure. In: Marcus LF, Corti M, Loy A, Naylor GJP, Slice DE, eds. *Advances in morphometrics*. New York, NY: Plenum Press, 271–273.
- McDevitt A, Yannic G, Rambau RV, Hayden TJ, Searle JB. 2010.** Postglacial re-colonization of continental Europe by the pygmy shrew (*Sorex minutus*) inferred from mitochondrial and Y chromosomal DNA sequences. In: Habel JC, Assmann T, eds. *Relict species: phylogeography and conservation biology*. Heidelberg: Springer-Verlag, 217–236.
- MacDonald SG, Burns DM. 1975.** *Physics for the life and health sciences*. Reading, PA: Addison-Wesley Publishing Company.
- Malatesta A. 1985.** *Geologia e paleobiologia dell'era glaciale*. Roma: La Nuova Italia Scientifica.
- Mascheretti S, Rogatcheva MB, Gündüz İ, Fredga K, Searle JB. 2003.** How did pygmy shrews colonize Ireland? Clues from a phylogenetic analysis of mitochondrial cytochrome *b* sequences. *Proceedings of the Royal Society of London Series B, Biological Sciences* **270**: 1593–1599.
- Mattoccia M, Romano A, Sbordoni V. 2005.** Mitochondrial DNA sequence analysis of the spectacled salamander, *Salamandrina terdigitata* (Urodela: Salamandridae), supports the existence of two distinct species. *Zootaxa* **995**: 1–19.
- Mayr E. 1982.** Of what use are subspecies? *Auk* **99**: 593–595.
- Moritz C. 1994.** Defining 'evolutionarily significant units' for conservation. *Trends in Ecology and Evolution* **9**: 373–375.
- Myers N, Mittermeier RA, Mittermeier CG, Fonseca GAB, Kent J. 2000.** Biodiversity hotspots for conservation priorities. *Nature* **403**: 853–858.
- Nagy ZT, Joger U, Guicking D, Wink M. 2003.** Phylogeography of the European whip snake *Coluber (Hierophis) viridiflavus* as inferred from nucleotide sequences of the mitochondrial cytochrome *b* gene and ISSR genomic fingerprinting. *Biota* **3**: 109–118.
- Nascetti G, Zangari F, Canestrelli D. 2005.** The spectacled salamanders, *Salamandrina terdigitata* Lacépède, 1788 and *S. perspicillata* Savi, 1821: 1) genetic differentiation and evolutionary history. *Rendiconti Lincei: Scienze Fisiche e Naturali* **16**: 159–169.
- Ochocinska D, Taylor JRE. 2003.** Bergmann's rule in shrews: geographical variation of body size in Palaearctic *Sorex* species. *Biological Journal of the Linnean Society* **78**: 365–381.
- Petit RJ, Aguinagalde I, de Beaulieu JL, Bittkau C, Brewer S, Cheddadi R, Ennos R, Fineschi S, Grivet D, Lascoux M, Mohanty A, Müller-Starck G, Demesure-Musch B, Palmé A, Martín JP, Rendell S, Vendramin GG. 2003.** Glacial refugia: hotspots but not melting pots of genetic diversity. *Science* **300**: 1563–1565.
- Pierpaoli M, Riga F, Trocchi V, Randi E. 1999.** Species distinction and evolutionary relationships of the Italian hare (*Lepus corsicanus*) as described by mitochondrial DNA sequencing. *Molecular Ecology* **8**: 1805–1817.

- Podnar M, Mayer W, Tvrťkovic N. 2005.** Phylogeography of the Italian wall lizard, *Podarcis sicula*, as revealed by mitochondrial DNA sequences. *Molecular Ecology* **14**: 575–588.
- Posada D, Crandall KA. 1998.** Modeltest: testing the model of DNA substitution. *Bioinformatics* **14**: 817–818.
- Ragghianti M, Wake DB. 1986.** Genic variation and its evolutionary implications in the Italian newt, *Triturus italicus*. *Herpetologica* **42**: 206–214.
- Rohlf FJ. 1993.** Relative warp analysis and an example of its application to mosquito wings. In: Marcus LF, Bello E, Garcia-Valdecasas A, eds. *Contributions to morphometrics*. Madrid: Museo Nacional de Ciencias Naturales, 131–159.
- Rohlf FJ, Marcus LF. 1993.** A revolution in morphometrics. *Trends in Ecology and Evolution* **8**: 129–132.
- Rohlf FJ, Slice DE. 1990.** Extensions of the Procrustes method for the optimal superimposition of landmark. *Systematic Zoology* **39**: 40–59.
- Rozas J, Sánchez-Delbarrio JC, Messeguer X, Rozas R. 2003.** DnaSP, DNA polymorphism analyses by the coalescent and other methods. *Bioinformatics* **19**: 2496–2497.
- Santucci F, Nascetti G, Bullini L. 1996.** Hybrid zones between two genetically differentiated forms of the pond frog *Rana lessonae* in southern Italy. *Journal of Evolutionary Biology* **9**: 429–450.
- Shchipanov NA, Kalinin AA, Demidova TB, Oleinichenko VY, Aleksandrov DY, Kouptzov AV. 2005.** Population ecology of red-toothed shrews, *Sorex araneus*, *S. caecutiens*, *S. minutus*, and *S. isodon*, in central Russia. In: Merritt JF, Churchfield S, Hutterer R, Sheftel BI, eds. *Advances in the biology of shrews II*. New York, NY: International Society of Shrew Biologists, 199–214.
- Sokal RR, Rohlf FJ. 1995.** *Biometry: the principles and practice of statistics in biological research*, 3rd edn. New York, NY: Freeman.
- Steinfartz S, Veith M, Tautz D. 2000.** Mitochondrial sequence analysis of *Salamandra* taxa suggests old splits of major lineages and postglacial recolonizations of central Europe from distinct source populations of *Salamandra salamandra*. *Molecular Ecology* **9**: 397–410.
- Stewart JR, Lister AM, Barnes I, Dalén L. 2010.** Refugia revisited: individualistic responses of species in space and time. *Proceedings of the Royal Society B, Biological Sciences* **277**: 661–671.
- Strait G. 1993.** Molar morphology and food texture among small-bodied insectivorous mammals. *Journal of Mammalogy* **74**: 391–402.
- Stofford DL. 2000.** *Paup**. *Phylogenetic analysis using parsimony (*and other methods)*, Version 4. Sunderland, MA: Sinauer.
- Taberlet P, Fumagalli L, Wust-Saucy AG, Cosson JF. 1998.** Comparative phylogeography and postglacial colonization routes in Europe. *Molecular Ecology* **7**: 453–464.
- Ungaro A, Cecchetti S, Aloise G, Nascetti G. 2001.** Paleogeographic events in southern Italy and the genetic structure of *Talpa romana*. *Eighth Congress of the European Society for Evolutionary Biology (ESEB)*. August 20–25. Abstracts, 88. Aarhus.
- Ursenbacher S, Conelli A, Golay P, Monney JC, Zuffi MAL, Thiery G, Durand T, Fumagalli L. 2006.** Phylogeography of the asp viper (*Vipera aspis*) inferred from mitochondrial DNA sequence data: evidence for multiple Mediterranean refugial areas. *Molecular Phylogenetics and Evolution* **38**: 546–552.
- Wilson EO, Brown JW. 1953.** The subspecies concept and its taxonomic application. *Systematic Zoology* **2**: 97–111.
- Zelditch ML, Swiderski DL, Sheets HD, Fink WL. 2004.** *Geometric morphometrics for biologists: a primer*. London: Elsevier Academic Press.

SUPPORTING INFORMATION

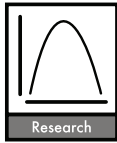
Additional Supporting Information may be found in the online version of this article:

Table S1. Samples and localities for phylogeographic analysis of pygmy shrews.

Table S2. List of primers used for the amplification of cytochrome *b* (cyt *b*) and Y-chromosome introns from pygmy shrews.

Table S3. Samples and localities for morphological analysis of pygmy shrews.

Please note: Wiley-Blackwell is not responsible for the content or functionality of any supporting materials supplied by the authors. Any queries (other than missing material) should be directed to the corresponding author for the article.



Northern glacial refugia for the pygmy shrew *Sorex minutus* in Europe revealed by phylogeographic analyses and species distribution modelling

Rodrigo Vega, Camilla Fløjgaard, Andrés Lira-Noriega, Yoshinori Nakazawa, Jens-Christian Svenning and Jeremy B. Searle

R. Vega (rrv9@cornell.edu) and J. B. Searle, Dept of Biology, Univ. of York, PO Box 373, York YO10 5YW, UK. (Present address of R. V.: Dept of Entomology, Comstock Hall 5123, Cornell Univ., Ithaca, NY 14853, USA.) – C. Fløjgaard, Ecoinformatics and Biodiversity Group, Dept of Biological Sciences, Aarhus Univ., Ny Munkegade 114, DK-8000 Aarhus C., Denmark and Dept of Wildlife Ecology and Biodiversity, National Environmental Research Inst., Aarhus Univ., Grenaaavej 14, DK-8410 Rønde, Denmark. – A. Lira-Noriega and Y. Nakazawa, Natural History Museum and Biodiversity Research Center, The Univ. of Kansas, Lawrence, KS 66045, USA. – J.-C. Svenning, Ecoinformatics and Biodiversity Group, Dept of Biological Sciences, Aarhus Univ., Ny Munkegade 114, DK-8000 Aarhus C., Denmark.

The southern European peninsulas (Iberian, Italian and Balkan) are traditionally recognized as glacial refugia from where many species colonized central and northern Europe after the Last Glacial Maximum (LGM). However, evidence that some species had more northerly refugia is accumulating from phylogeographic, palaeontological and palynological studies, and more recently from species distribution modelling (SDM), but further studies are needed to test the idea of northern refugia in Europe. Here, we take a rarely implemented multidisciplinary approach to assess if the pygmy shrew *Sorex minutus*, a widespread Eurasian mammal species, had northern refugia during the LGM, and if these influenced its postglacial geographic distribution. First, we evaluated the phylogeographic and population expansion patterns using mtDNA sequence data from 123 pygmy shrews. Then, we used SDM to predict present and past (LGM) potential distributions using two different training data sets, two different algorithms (Maxent and GARP) and climate reconstructions for the LGM with two different general circulation models. An LGM distribution in the southern peninsulas was predicted by the SDM approaches, in line with the occurrence of lineages of *S. minutus* in these areas. The phylogeographic analyses also indicated a widespread and strictly northern-central European lineage, not derived from southern peninsulas, and with a postglacial population expansion signature. This was consistent with the SDM predictions of suitable LGM conditions for *S. minutus* occurring across central and eastern Europe, from unglaciated parts of the British Isles to much of the eastern European Plain. Hence, *S. minutus* likely persisted in parts of central and eastern Europe during the LGM, from where it colonized other northern areas during the late-glacial and postglacial periods. Our results provide new insights into the glacial and postglacial colonization history of the European mammal fauna, notably supporting glacial refugia further north than traditionally recognized.

During the Quaternary ice ages substantial areas of northern Europe were covered by ice sheets while permafrost existed in large areas of central Europe, which restricted the distribution of many temperate and warm-adapted species to the three southern European peninsulas of Iberia, Italy and the Balkans at the Last Glacial Maximum (LGM; Hewitt 2000). These species are interpreted to have recolonized central and northern Europe from these traditionally recognized southern glacial refugia in response to the late-glacial and postglacial warming (Taberlet et al. 1998, Hewitt 2000). Therefore, southern glacial refugia and the northward postglacial recolonization of central and northern Europe from these areas has become an established biogeographical paradigm (Hewitt 2000).

Other studies have, however, provided palaeontological, palynological and phylogeographic evidence that glacial refugia for some temperate and boreal species existed further north than the traditionally recognized southern European refugia, implying a more complex pattern of glacial survival and postglacial recolonization: fossils of temperate mammal species dated to the LGM (albeit rarely small mammals) have been described for a number of sites in central Europe, sometimes in co-occurrence with cold-adapted Pleistocene faunal elements (Sommer and Nadachowski 2006). Macrofossil charcoal (organic plant material ≥ 2 mm in diameter) of coniferous and broad-leaved trees dating to the Upper Palaeolithic has been found in several sites in Austria (42–23 Kya), Czech Republic (29–24.5 Kya), Croatia (27.8–10.8 Kya) and Hungary

(31.5–16.5 Kya), suggesting that these regions were also refugial areas for temperate deciduous species (Willis and van Andel 2004, Magri et al. 2006). Palynological records have shown European beech *Fagus sylvatica* pollen in several sites in central Europe between the late glacial and postglacial (15–10 Kya), and have shown that none of the three traditional refugial areas was the source for northern-central European beech populations (Magri et al. 2006). Phylogeographic studies on several small mammals have shown little similarity between Mediterranean and northern populations, and have described genetic clades linking together haplotypes sampled throughout northern-central Europe (Bilton et al. 1998, Kotlík et al. 2006). Furthermore, species distribution modelling (SDM) has shown that suitable climatic conditions existed for temperate and boreal species in northern latitudes supporting more northerly refugial areas in Europe (Svenning et al. 2008, Fløjgaard et al. 2009). However, a more comprehensive understanding of the relative importance of southern versus northern refugia in terms of LGM species' ranges as well as for postglacial recolonization is needed.

Here, we use the pygmy shrew *Sorex minutus* (Mammalia, Soricomorpha), as a model for studying the persistence of populations in northern European refugia during the LGM. *Sorex minutus* is widely distributed in the Palearctic, throughout Europe to Lake Baikal (Siberia), including the three southern European peninsulas (Hutterer et al. 2008). The species occurs at low density in a wide range of terrestrial habitats with adequate ground cover (Churchfield and Searle 2008). In southern Europe the distribution becomes patchy and limited to higher altitudes where it occurs with some degree of geographical isolation and differentiation, while in central and northern parts of Europe and in Siberia it is more abundant and populations are more connected and widespread.

Previous phylogeographic studies on *S. minutus* revealed a very widespread and genetically homogeneous “northern-central European and Siberian” lineage, extending from Britain through central and northern Europe to Siberia (ca 7000 km), but genetically distinct from the southern lineages in Iberia, Italy and the Balkans (Bilton et al. 1998, Mascheretti et al. 2003, McDevitt et al. 2010). These studies suggested that the northern-central European lineage persisted and expanded from one or more central or eastern European refugia located further north than the traditionally recognized southern European refugia. However, the size and locations of the possible northern refugia for *S. minutus* could not be assessed precisely.

Species distribution models combine information about species occurrences with environmental (usually climatic) data found across the study region to estimate the present-day geographical distribution of suitable environmental conditions for the species (Guisan and Zimmermann 2000). Then, the set of environmental conditions can be projected to past conditions to identify areas where there were suitable environmental conditions for the species (hindcasting) (Nogués-Bravo 2009), in this case at the LGM. Such SDM-based hindcasting has not been integrated into the previous phylogeographic studies on *S. minutus*, and the genetic data for central and eastern regions of Europe and in Siberia have been rather incomplete. This

makes it difficult to determine the importance of these regions for the LGM distribution of the species, its postglacial colonization history and its present-day genetic structure. Moreover, the inference of glacial refugia based solely on phylogeographic analyses can be obscured by the extinction of genetic variants, incomplete sampling and large-scale range shifts of the species (Waltari et al. 2007). Hence at this point, although the previous phylogeographic studies suggested the existence of northern glacial refugia for *S. minutus*, the size and geographic spread of these refugia as well as their role in the postglacial range dynamics of the species remain unclear.

The purpose of this study is to assess the distribution of *S. minutus* during the LGM based on a multidisciplinary approach using more detailed mtDNA-based phylogeographic analyses than conducted hitherto and including SDM-based hindcasting. Only a few studies have tried to estimate potential northern refugial areas in this way, despite the stronger inference allowed by these independent and highly complementary approaches (Waltari et al. 2007).

We assessed the following specific study questions: would a more detailed phylogeographic analysis also detect a distinctive “northern-central European and Siberian” lineage as has been previously found? Would this widespread lineage present a genetic signature of population expansion? Would different SDM-based hindcasting approaches predict suitable LGM conditions for *S. minutus* not only in the southern European peninsulas, but also further north, consistent with northern refugia? Would the combined phylogeographic and SDM approach allow us to estimate more precisely the geographic locations of northern refugia for *S. minutus*, as well as determine their potential role for its postglacial range dynamics? From the population expansion characteristics, how did the refugial populations colonize their current ranges? Finally, are the rather scant fossil data for *S. minutus* consistent with our phylogeographic and distributional findings?

This study sheds light on the spatial variation of the genetic diversity within the widespread distribution of *S. minutus*, its postglacial population expansion and colonization of Europe from northern refugia, and contributes towards an emerging new synthesis of the full-glacial distributions of the European biota. The nature of northern refugia also has important implications for the understanding of their biogeographic roles as sources of genetic diversity, areas of speciation, identification of conservation units and preservation of species, particularly in response to future climate change (Kotlík et al. 2006, Provan and Bennett 2008).

Materials and methods

Phylogeographic analyses

Samples and laboratory procedures

In total, 123 individuals of *S. minutus* from Europe and Siberia were used for the phylogeographic analysis of the mitochondrial cytochrome b (cyt b) gene. Sixty-six *S. minutus* cyt b sequences were obtained from Genbank

(AB175132; Ohdachi et al. 2006; AJ535393–AJ535457; Mascheretti et al. 2003). Fifty-seven out of the 123 samples of *S. minutus* were obtained from northern-central Europe during fieldwork and from museum collections (see Acknowledgements) to increase the molecular data and to provide a more detailed analysis of this region. A sequence of *S. volnuchini* was used as outgroup (AJ535458; Mascheretti et al. 2003).

Genomic DNA was extracted using a commercial kit (Qiagen). Partial cyt b sequences were obtained by PCR using two primer pairs that amplified ca 700 bp of overlapping fragments. PCR amplification was performed in a 50 µl final volume: 1X Buffer, 1 µM each primer, 1 µM dNTP's, 3 mM MgCl₂ and 0.5 U Platinum Taq Polymerase (Invitrogen), with cycling conditions: 94°C for 4 min, 40 cycles at 94°C for 30 s, 55°C for 30 s and 72°C for 45 s, and a final elongation step at 72°C for 7 min. Purification of PCR products was done with a commercial kit (Qiagen) and sequenced (Macrogen and Cornell Univ. Core Laboratories Center).

Sequence and phylogenetic analyses

Cyt b sequences were edited in BioEdit 7.0 (Hall 1999) and aligned by eye. For the construction of phylogenetic trees, the model of evolution that best fitted the molecular data was searched using MrModeltest 2.3 (Nylander 2004) using the minimum Akaike information criteria value. The substitution model supported was the General Time Reversible with specified substitution types (A–C = 0.3663, A–G = 17.4110, A–T = 1.0216, C–G = 2.1621, C–T = 13.0604, G–T = 1.0), proportion of invariable sites (0.5332), gamma shape parameter (0.9799) and nucleotide frequencies (A = 0.2750, C = 0.2996, G = 0.1382, T = 0.2872).

The phylogenetic relationships within *S. minutus* were inferred by Neighbour-Joining (NJ), Maximum Likelihood (ML) and Bayesian analysis using PAUP* 4.0b10 (Swofford 2000), PhyML 3.0 (Guindon and Gascuel 2003) and MrBayes 3.1 (Huelsenbeck and Ronquist 2001), respectively. Confidence for the phylogenetic relationships in NJ and ML was assessed by bootstrap replicates (10 000 and 500 replicates, respectively). For the Bayesian analysis, two independent runs were performed with 10 million generations and 5 chains each, a sampling frequency every 1000 generations, a temperature of 0.1 for the heated chain and checking for convergence. Trees were summarized after a burn-in value of 2500 to obtain the posterior probabilities of each phylogenetic branch.

Phylogenetic networks provide an explicit graphic representation of evolutionary history between sequences in which taxa are represented as nodes and their evolutionary relationships are represented by edges. Most internal nodes represent ancestral states from which more recent and peripheral nodes derive (Avisé 2000). A parsimony phylogenetic network of cyt b haplotypes was constructed using the software Network 4.5 (Fluxus-Engineering) with a median-joining algorithm and a greedy FHP genetic distance calculation method. The median joining algorithm identifies groups of haplotypes and introduces hypothetical (non-observed) haplotypes to construct the parsimony network.

Genetic and statistical analyses

Standard sequence polymorphism indices (number of haplotypes, polymorphic sites and parsimony informative sites) and genetic diversity values (π , nucleotide diversity \pm SD; h , haplotype diversity) were estimated using Arlequin 3.11 (Excoffier et al. 2005).

Population expansion was examined for both the full dataset (Eurasia) and for the “northern-central European and Siberian” lineage using DnaSP 5.0 (Librado and Rozas 2009). In each case a mismatch distribution (distribution of the number of differences between pairs of haplotypes) was estimated to compare the demography of the populations with the expectations of a sudden population expansion model (Rogers and Harpending 1992). The raggedness index (rg), which measures the smoothness of the observed distribution, was computed and the statistical validity of the estimated expansion model was tested by a parametric bootstrap approach as a sum of square deviations (SSD) between the observed and the expected mismatch (Schneider and Excoffier 1999) using Arlequin (10 000 replicates). Three other tests for population expansion were performed in DnaSP using coalescent simulations to test for statistical significance (10 000 replicates): R_2 test of neutrality, based on the difference of the number of singleton mutations and the average number of nucleotide differences (Ramos-Onsins and Rozas 2002); Fu's F_s , a statistic based on the infinite-site model without recombination that shows large negative F_s values when there has been a demographic population expansion (Fu 1997); Tajima's D , a test for selective neutrality based on the infinite-site model without recombination where significant values appear from selective effects but also from factors such as population expansion, bottleneck or heterogeneous mutation rates (Tajima 1989).

Species distribution modelling

Important discrepancies in the prediction of the potential distribution of a particular species arise from differences in data sample size (Stockwell and Peterson 2002, Wisz et al. 2008), environmental and/or climatic data (Peterson and Nakazawa 2008), and algorithms (Peterson et al. 2007, but see Phillips 2008). Also, if the occurrence records used to model the distribution do not adequately sample the environmental requirements of the species, the prediction will not truly reflect its potential geographic distribution (Pearson et al. 2007). Therefore, to ensure the robustness of our findings, we modelled the potential distribution of *S. minutus* in the present and at the LGM using two independent training data sets, two algorithms, namely the maximum entropy algorithm (Maxent; Phillips et al. 2006) and the Genetic Algorithm for Rule-set Prediction (GARP; Stockwell and Noble 1992, Stockwell 1999), and using climate reconstructions for the LGM based on two general circulation models (GCMs). All GIS operations were performed using ArcGIS 9.3 (ESRI, Redlands, CA, USA).

Species occurrence data

For the first data set, hereafter termed “data set 1”, we used the species records from fieldwork, from two online sources (Global Biodiversity Information Facility, GBIF,

and Mammal Networked Information System, MaNIS) and from museum specimens obtained for our study (see Acknowledgements). Most of the data were derived from the following sources: the Atlas of Mammals in Britain (Arnold 1993), the European Environment Agency, the UK National Biodiversity Network, the Highland Biological Recording Group – HBRG Mammals data set and the Ministerio de Medio Ambiente y Medio Rural y Marino (Spain). Low precision occurrences, such as presence data taken from the centroids of atlas grids and falsely georeferenced occurrences (i.e. offshore and out-of-range locations), were eliminated from this data set. In total, we collected 536 high-precision unique latitude-longitude localities, but this data set was geographically biased towards western Europe and Britain due to differences in sampling effort across the species' distribution range (i.e. there are few species records from Siberia and southern Europe). In order to correct for sampling bias, we created 25 random subsets from the original data set to limit the number of unique occurrences to ≤ 5 in squares of 5×5 degrees distributed across the extent of the geographical analysis (Wisiz et al. 2008). This procedure yielded a total of 146 unique localities for each subset which were more evenly distributed.

For the second data set, hereafter termed “data set 2”, we used the records from the Atlas of European Mammals (AEM; Mitchell-Jones et al. 1999) which present less geographic bias within Europe, but had a much coarser resolution than data set 1. The AEM uses an approximate equal area grid of 50×50 km based on the Universal Transverse Mercator (UTM) projection and the Military Grid Reference System (MGRS). Records of “species presence” as well as “presence assumed” (i.e. presence was observed before 1970 and no evidence of later extinction) were included in the study and a total of 1178 data points were used.

To ensure transferability of our models, we used a geographically independent test data set. We digitized the Eurasian range map for *S. minutus* (Hutterer et al. 2008) and recorded the species as present in all 50×50 km MGRS grid cells within the outline of the range map. Then, we used the part of the range located east of the European study area (for simplicity referred to hereafter as Siberia) only as a test data set ($n = 3122$ data points). This allowed us to evaluate the performance of the models with both data sets and assess which climatic variables provided the strongest predictive ability in a geographically independent region with relatively LGM-like conditions (Fløjgaard et al. 2009). We used the digitised range map data only for testing, given its much coarser resolution and uncertain quality compared to the occurrence data from data sets 1 and 2.

Climate data

For the present-day SDM we initially considered the 19 bioclimatic variables from the WorldClim dataset at a spatial resolution of 2.5 minutes <www.worldclim.org/>. These climate layers are based on spatially interpolated values of temperature and precipitation gathered from weather stations around the world from 1950–2000 (Hijmans et al. 2005). For the LGM (21 Kya) we used

the climate reconstructions of the same 19 bioclimatic variables based on the CCSM3 (Collins et al. 2006) and MIROC3.2 (Hasumi and Emori 2004) GCMs <<http://bioge.berkeley.edu>> at a spatial resolution of 2.5 minutes.

We used the Jackknife procedure implemented in Maxent with the 19 bioclimatic variables on the two data sets to find the best set of predictor variables. We assessed the performance of the models based on the Area Under the Curve (AUC) values of the Receiver Operating Characteristic (ROC) in the independent test region of Siberia. The worst predictor of the whole set of variables was eliminated, a new model was produced using the remaining variables and the process was repeated until all variables were exhausted. We chose the final set of predictors based on parsimony (i.e. with the fewest number of climatic variables) and with the highest AUC value in the independent test region of Siberia.

The final set of predictors comprised the variables Annual Mean Temperature (AMT) and Precipitation of the Warmest Quarter (PWQ); thus, AMT and PWQ were used for estimating the present and LGM distribution of *S. minutus*. These two variables were not highly correlated ($r = -0.3550$) and models that included only these yielded higher or almost equal AUC values than models that included only one or more variables in combination with AMT and PWQ. In addition, these variables are biologically meaningful for *S. minutus* considering its broad distribution in northern-central Europe and Siberia and habitat preference for damp and temperate areas (Churchfield and Searle 2008, Hutterer et al. 2008). The modelling was performed with data sets 1 and 2 as inputs in Maxent and GARP, and all models were evaluated on the geographically independent (extrinsic) test data from Siberia. For data set 1 we made models with all 25 subsets. Finally, all models were projected onto the two LGM climate reconstructions to identify the potential distribution of *S. minutus*.

Modelling algorithms

To assess the variation in the outcome of model predictions due to differences in modelling algorithms, we used Maxent and GARP. Maxent has been shown to perform very well in comparative studies of species distribution modelling compared to GARP (Elith et al. 2006, Phillips and Dudík 2008, Elith and Graham 2009, but see also Peterson et al. 2008), while GARP has been shown to perform better than Maxent in transferability studies (Peterson et al. 2007, but see also Phillips 2008). Ultimately, the performance of each algorithm may be properly compared using the corresponding thresholding during model evaluation, since their predictions are not given in the same scale (Peterson et al. 2008).

To evaluate the accuracy of our models, the empirical AUC values were compared against the AUC values of 1000 random models, as implemented in Peterson et al. (2008), using the data from the test region. AUC ROC values are expressed as the ratio of the area under the observed curve (i.e. the overall area for which each algorithm predicts as present) to the area under the line that defines a random expectation; consequently, the AUC values are expected to

be larger than one as the model departs from the random expectation (Peterson et al. 2008).

Maxent is a machine-learning technique based on the principle of maximum entropy that fits a probability distribution to the environmental conditions at the locations where a species has been observed (Phillips et al. 2004, 2006). When implemented with ecologically meaningful sets of predictor variables, Maxent produced similar estimates for the locations of glacial refugia as Bioclim, another commonly used, but simpler, modelling technique (Svenning et al. 2008, Fløjgaard et al. 2009). We used the default settings in Maxent 3.2.1 <www.cs.princeton.edu/~schapire/maxent/> with background data limited to Eurasia as described in the species occurrence data section. We converted the continuous logistic output from Maxent into a binary map of predicted suitable environmental conditions for *S. minutus* using the maximum test sensitivity and specificity threshold because it optimized the correct discrimination of presences and pseudoabsences in the test data.

GARP is a genetic algorithm that produces a set of rules that describe the non-random association between environmental variables and occurrence data (Stockwell and Noble 1992, Stockwell 1999). First, the algorithm creates a set of rules based on four basic types (bioclimatic, atomic, negated and logistic regression rules), their individual predictive accuracy is calculated and only those rules with the highest predictive accuracy are retained in the model. The overall performance of the model is evaluated using a subset of presence points. Then, a second generation of rules is produced via the random modification of the previous generation rules, their predictive accuracy is calculated and only those with the highest accuracy are included in the model. Finally, the overall performance of the model is re-evaluated and the process of creation, evaluation and inclusion of rules is repeated until a maximum number of iterations is reached (1000 in this case), or until performance values no longer change appreciably from one iteration to the next (convergence parameter of 1%). We used the version of DesktopGarp as implemented in openModeller ver. 1.0.9 <<http://openmodeller.sf.net>> using the default parameters (Anderson et al. 2003). We converted the continuous output into a binary map of predicted occurrence of the suitable conditions for *S. minutus* by assigning a value of 1 for the model values that corresponded to 10% or more of the testing points.

Results

Phylogeographic analysis

Sequence analysis and phylogenetic reconstructions

A partial sequence of 1110 bp from the *S. minutus* cyt b was analysed. One hundred and twelve haplotypes were obtained, from which 46 were newly described and deposited in GenBank (accession numbers: GQ494305–GQ494350). There were 894 invariable and 216 variable positions, from which 137 were parsimony informative.

All the phylogenetic analyses revealed five distinct lineages (Fig. 1). Samples from the Mediterranean peninsula clustered in three lineages, namely the “Iberian”, “Italian” and “Balkan” groups, corresponding to their

geographical origin. There was also a well supported “Pyrenean” lineage with samples from Andorra and Ireland. Samples from northern-central Europe and Siberia clustered together forming a geographically widespread lineage that did not include any individuals from the southern peninsula, hereafter named as the “northern-central European” lineage. This lineage was composed of 105 sequences (94 haplotypes) with 940 invariable and 170 variable positions, from which 92 were parsimony informative.

The phylogenetic network of the northern-central European lineage presented a star-like pattern with three most central haplotypes, named A, B and C, separated by only one mutational step from each other and from which all other sequences derived (Fig. 2). The other phylogroups from the southern peninsula were much more distantly related and separated by several mutations (data not shown). The central haplotypes A and B were entirely composed of samples from the Netherlands (three and two individuals, respectively), while the third central haplotype (C) belonged to a central Ukrainian specimen from the locality Tishki (50°6.27'N, 33°6.39'E). There was an apparent geographical subdivision of the samples that were connected to these three central haplotypes (Fig. 2). Only haplotypes from Great Britain and the Netherlands were directly connected to A. Several haplotypes from different countries of northern and central Europe were connected to B, also including some haplotypes from Great Britain and the Netherlands, but there were no haplotypes from eastern Europe or Siberia (except for one sample from Ukraine ambiguously connected to B and C). Haplotypes from northern, central and eastern Europe and Siberia were all directly connected to C, but there were no samples from countries further west than Germany. However, the support for these subdivisions was not strong; equally parsimonious explanations (loops) appeared in the central part of the network between B and C, and there was no supported sub-structure within the northern-central European lineage in the phylogenetic trees.

Genetic and statistical analyses

The whole Eurasian sample presented a nucleotide diversity $\pi = 0.0109 \pm 0.0055$, and a haplotype diversity $h = 0.9983$. The northern-central European lineage had a nucleotide diversity $\pi = 0.0067 \pm 0.0035$, and a haplotype diversity $h = 0.9980$. Genetic diversity values were not calculated for the southern European lineages because of small sample size.

The mismatch distribution of the whole dataset (Eurasia) was bimodal, consistent with pairwise differences between sequences belonging to the same and different lineages (Fig. 3a). The mismatch distribution of the northern-central European lineage showed a unimodal distribution that, visually, fitted almost perfectly over the expected values for a population expansion model (Fig. 3b). There was an observed mean of 7.382 pairwise differences with a variance of 8.152. The goodness of fit test showed no significant differences between the observed and expected values under a sudden expansion model for the northern-central European lineage (SSD = 0.0004, $p_{SSD} > 0.05$; $rg = 0.0082$, $p > 0.05$). Negative and significant Tajima's D ($D = -2.5721$, $p < 0.001$) and Fu's F_s ($F_s = -24.8437$,

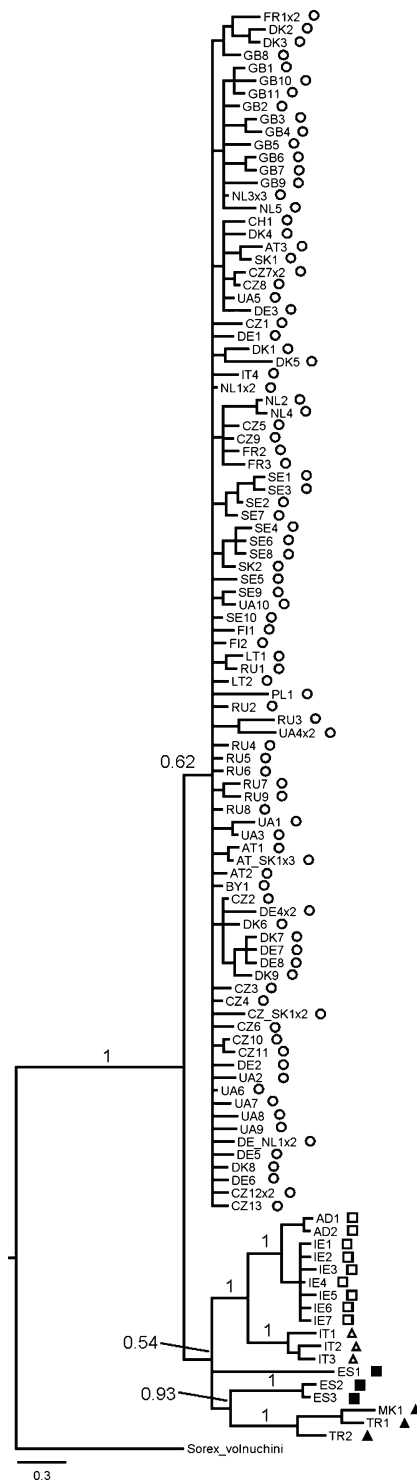


Figure 1. Continued.

$p < 0.001$) showed departures from neutrality also consistent with a sudden population expansion. Moreover, the R_2 test of neutrality also showed that the northern-central European lineage gave a genetic signature consistent with a

sudden population expansion ($R_2 = 0.0180$, $p < 0.001$). The rest of the sequences and lineages that belonged to the more distantly related southern European lineages (Iberian, Italian and Balkan peninsulas) and the Pyrenees were not analysed because of small sample size.

Species distribution modelling

Predicted present distribution

Species distribution models from Maxent matched the reported distribution of the species (Fig. 4a, c). The models also predicted suitable climatic conditions outside the reported distribution of the species especially in two regions, the Asia Minor-Caucasus region and in the Far East (Fig. 4a, c). The predicted present distribution of *S. minutus* with GARP was very similar to that of Maxent, it also matched the reported distribution and the predicted suitable climatic conditions in the Asia Minor-Caucasus region and in the Far East (Fig. 4b, d).

All Maxent and GARP models were accurate in the test region, with AUC values for both data sets higher than null expectations ($p < 0.001$; mean $AUC_{MAXENT} = 1.24 \pm 0.021$ and mean $AUC_{GARP} = 1.049 \pm 0.007$ for data set 1, and mean $AUC_{MAXENT} = 1.249 \pm 0.011$ and mean $AUC_{GARP} = 1.032 \pm 0.005$ for data set 2).

Predicted LGM distribution

With the two data sets and GCMs, Maxent and GARP predicted suitable LGM climatic conditions in the southern European peninsulas (Fig. 4e–l), concordant with southern refugia. In general, suitable LGM conditions with the two data sets, GCMs and algorithms were also predicted north of the southern refugia, particularly throughout central Europe, most of eastern Europe, southern Poland, eastern and southern Ukraine, the Crimea peninsula and the Caucasus. With Maxent, the LGM predictions differed little between data sets or between GCMs, and there were predicted suitable conditions in central and eastern Europe close to the ice sheet (Fig. 4e, g, i, k). With GARP, predictions differed between GCMs: more restricted suitable conditions in central and eastern Europe were predicted with CCSM3 (Fig. 4f, h) than with MIROC3.2 (Fig. 4j, l), but predictions did not differ much between data sets. The most restricted predictions (using GARP with CCSM3) still showed suitable climatic conditions in southern Ireland, central and southern France, western parts

Figure 1. Bayesian inference tree showing the phylogenetic relationships among *Sorex minutus* samples (*S. volnuchini*, out-group). Five lineages were found (\square = Pyrenean-Irish, Δ = Italian, \blacksquare = Iberian, \blacktriangle = Balkan, and \circ = northern-central European). The northern-central European lineage is geographically widespread but has not been found within the southern European peninsulas. Values on branches correspond to Bayesian posterior probabilities. Haplotypes are represented with two-letter country codes followed by an identification number (x2, haplotype frequency = 2 etc.): AD = Andorra, AT = Austria, BY = Belarus, CH = Switzerland, CZ = Czech Republic, DE = Germany, DK = Denmark, ES = Spain, FI = Finland, FR = France, GB = Great Britain, IE = Ireland, IT = Italy, LT = Lithuania, MK = Macedonia, NL = the Netherlands, PL = Poland, RU = Russia, SE = Sweden, SK = Slovakia, TR = Turkey, UA = Ukraine.

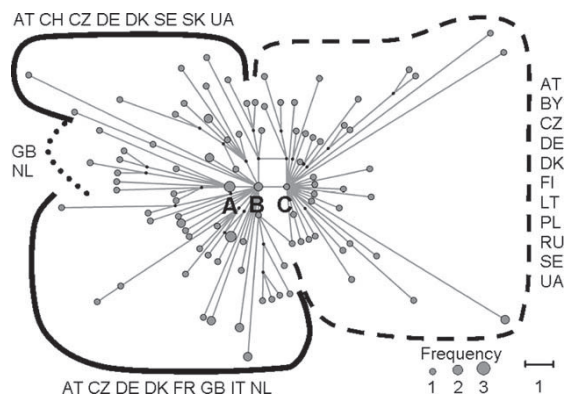


Figure 2. Parsimony median joining haplotype network for the northern-central European lineage of *Sorex minutus*. Observed haplotypes are shown as grey circles (proportional to frequency) and hypothetical haplotypes are shown as black circles. There is a star-like phylogeny with three central (ancestral) haplotypes. A and B are two central haplotypes from the Netherlands, and C is from central Ukraine. The dotted black line encircles haplotypes directly linked to A, black lines encircle haplotypes directly linked to B and the dashed line encircles haplotypes directly linked to C (the country of origin for haplotypes is shown next to clusters; two-letter country codes as in Fig. 1). For simplicity, haplotypes from the more diverged southern European lineages are not shown, but relate to central-European haplotypes by the addition of several hypothetical haplotypes and >10 mutational steps. The scale bar represents one mutational step.

of Switzerland, a few regions north of the Balkans, the Crimea peninsula and the Caucasus.

Discussion

Northern glacial refugia revealed by a combined approach

Sorex minutus is considered a temperate species, but it is also latitudinally distributed above 60°N (i.e. near the Arctic Circle) and altitudinally above 2000 m in regions with permafrost and harsh winters (Mitchell-Jones et al. 1999, Hutterer et al. 2008). Northern non-arctic species like *S. minutus* could have persisted in high latitude refugia in Europe during the LGM, north of the traditionally recognized Mediterranean refugial areas (Stewart and Lister 2001). This could have been a result of their ecological traits (notably cold tolerance) and biogeographical characteristics that may have determined their response to the glaciations (Bhagwat and Willis 2008). *Sorex minutus* is, therefore, a suitable model organism for exploring the controversial hypothesis of “northern” glacial refugia.

The general concordance of the phylogeographic analyses with the predicted LGM distributions based on species distribution modelling and the concordance between models suggest that we have obtained robust results concerning the LGM distribution of *S. minutus*. Our phylogeographic analyses provided evidence for a distinct lineage in northern-central Europe, with additional lineages in the Iberian, Italian and Balkan peninsulas in southern Europe. First, the absence of southern haplotypes in northern-central Europe supports the hypothesis that the

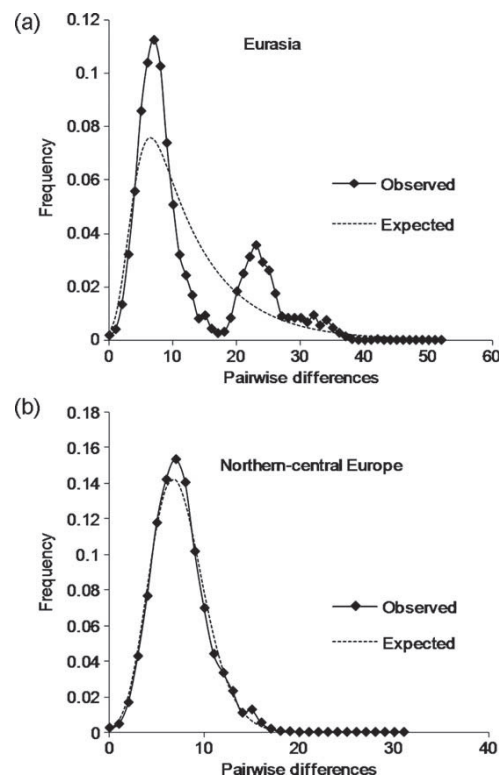


Figure 3. Mismatch distribution for observed (continuous line) and expected (dashed line) pairwise comparisons under a sudden population expansion model among *Sorex minutus* cyt b sequences. (a) Mismatch distribution among Eurasian sequences with a bimodal observed distribution where the first peak corresponds to pairwise comparisons among closely related individuals within lineages, while the second peak corresponds to pairwise comparisons among distantly related individuals from different lineages. (b) Mismatch distribution among sequences from the northern-central European lineage showing a unimodal distribution, a genetic signature which corresponds to the expected distribution for sudden population expansion.

southern peninsulas were areas of endemism and differentiation for *S. minutus*, but not for northward colonization (Bilton et al. 1998), i.e. the current populations in northern-central Europe were not derived from LGM populations in the traditional southern European refugia. Second, the northern-central European lineage showed a strong signature of population expansion supported by the mismatch distribution and population expansion tests. Finally, ancestral haplotypes in a phylogenetic network can be identified by their central or internal position from where the peripheral, more recent, haplotypes are derived, by the number of haplotypes that arise from them and by their abundance (Avice 2000). The phylogenetic network of the northern-central European lineage showed a star-like pattern with three ancestral haplotypes from distant regions in central and eastern Europe (the Netherlands and Ukraine). This pattern was also consistent with a widespread LGM distribution and congruent with the hypothesis of persistence and postglacial expansion from northern glacial refugia.

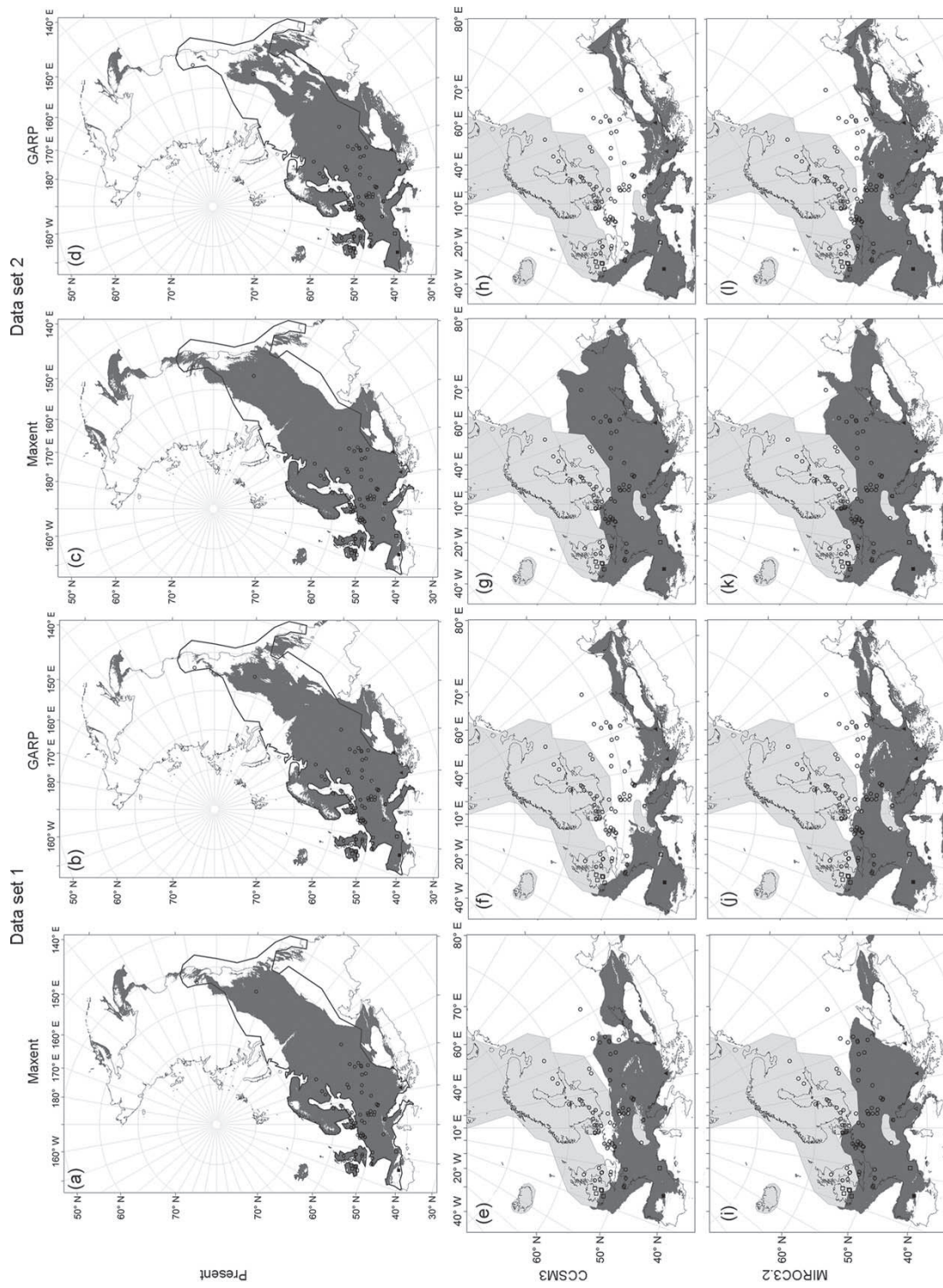


Figure 4. Continued.

The phylogeographic pattern that we observe here did not arise from the low sample size in southern Europe: the few samples from southern peninsulas belonged to lineages differentiated by a large number of mutation steps from the northern-central European lineage; if northern-central Europe had been colonized from southern Europe we would have found northern-central European samples clustering within southern lineages, not forming a separate lineage. Moreover, a phylogeographic study on *S. minutus* using the mitochondrial Control Region and Y-chromosome introns with more samples from southern peninsulas showed a similar pattern (McDevitt et al. 2010). Nevertheless, further sampling in southern regions and the use of other molecular markers is desirable to investigate the genetic variation and population expansion events within Mediterranean peninsulas, and for the determination of contact zones among lineages.

We did not use the mismatch distributions to date the population expansion for the northern-central European lineage because of the lack of a suitable mutation rate for *cyt b* in *S. minutus*. Previous studies on *Sorex* have used mismatch distributions for molecular dating (e.g. Ratkiewicz et al. 2002), but with mutation rates that may not be suitable over short time frames (Ho et al. 2005).

The modelling approaches predicted successfully the wide present-day distribution of *S. minutus* in Eurasia. Therefore, we consider our SDM approaches as giving realistic estimates of the area with suitable climatic conditions for our species and of its potential LGM distribution. A third model using Bioclim with SDM data sets 1 and 2 also resulted in very similar present-day and LGM distributions for *S. minutus* (data not shown). The potential LGM distributions predicted by our SDM approaches not only included the traditionally recognized southern refugia, but also a wide area across central and eastern Europe, from the unglaciated parts of southern Ireland and Britain to most of the central and southeast European (or Russian) Plain. In particular, the predicted LGM distribution throughout central and eastern Europe encompasses suggested northern refugial areas based on palaeontological and palynological data for other temperate and boreal species (Willis et al. 2000, Willis and van Andel 2004, Magri et al. 2006, Sommer and Nadachowski 2006). Thus, the northern-central European lineage could have persisted in various parts of this wide area during the LGM according to the phylogeographic and the SDM approaches.

We note that the central and eastern European LGM distribution was similar with both data sets, particularly when using Maxent (with both GCMs) and when using GARP with MIROC3.2, even though we used very different species records. However, the LGM distributions

when using GARP were more widespread to the north with MIROC3.2 than with CCSM3 GCMs, which could represent variations due to modelling algorithms and GCMs. Also, the predicted present-day suitable climatic conditions outside the reported distribution of *S. minutus* in the Asia Minor-Caucasus region and in the Far East probably reflect competitive or speciation processes rather than an inaccurate estimation of the suitable climatic conditions. In Asia Minor-Caucasus, *S. minutus* is replaced by the closely related sister species *S. volnuchini*, while in the Far East many other *Sorex* species occur including similar-sized species such as *S. gracillimus*.

The predicted LGM distribution of *S. minutus* appears to be continuous throughout Europe; however, lineage diversification is still plausible: First, the present distribution of *S. minutus* also appears to be continuous but it is affected by landscape features, not evident at the geographic resolution given, which could have subdivided the species range. Therefore, it could be expected that landscape features at the LGM also affected the distribution of *S. minutus*. Second, the estimation of the extent of ice sheets in mountainous areas is not precise, so it may be expected that the Iberian and Italian populations remained isolated from the rest of Europe by ice sheets covering the Pyrenees and the Alps, respectively, while the heterogeneous landscape in the Balkans could have been responsible for the limited distribution of the genetic lineage there. Also, different genetic variants could have arisen within regions and could have been maintained there selectively reducing further spread into contiguous regions. Another explanation could be that interspecific competition and/or other non-climatic conditions subdivided the potentially continuous LGM distribution.

Insights into postglacial colonization

The predicted distribution for *S. minutus* in the Iberian, Italian and Balkan peninsulas presumably corresponds to the refugial areas where the southern genetic lineages persisted during the LGM. The Pyrenean lineage, here represented by a limited number of Andorran and Irish samples, could have persisted during the LGM in central and south-western France and even in unglaciated areas in southern Ireland, as shown by our SDM models. However, genetic studies support a more recent origin of the Irish pygmy shrew, transported there by humans during the Holocene (Mascheretti et al. 2003, McDevitt et al. 2009, A. D. McDevitt, V. R. Rambau, R. Vega and J. B. Searle pers. comm.). Further molecular sampling in southern Europe is desirable to determine the extent of the

Figure 4. Species distribution modelling of *Sorex minutus* in the present and at the Last Glacial Maximum (LGM) using different approaches. Two independent data sets, two algorithms, Maximum entropy (Maxent) and Genetic Algorithm for Rule-set prediction (GARP), and climate reconstructions for the LGM based on two general circulation models (CCSM3 and MIROC3.2) were used. Climatic variables were obtained from WorldClim and two were selected as best predictors with a Jackknife procedure: annual mean temperature and precipitation of the warmest quarter. (a–d) Maxent and GARP modelled present distributions with data sets 1 and 2. (e–l) Maxent and GARP modelled LGM distributions with data sets 1 and 2 using CCSM3 and MIROC3.2. The thick lines (a–d) represent the outline of present-day distribution range of the species, the dark shading corresponds to present-day and LGM suitable climatic conditions, and the light gray polygon represents the ice extent at the LGM, about 21 Kya (redrawn from Svendsen et al. 2004). Location of samples used for the phylogeographic analysis is shown (lineages as in Fig. 1: □ = Pyrenean-Irish, Δ = Italian, ■ = Iberian, ▲ = Balkan, and ○ = northern-central European).

geographic distribution of the lineages found there and the contact zones between them.

Considering the phylogenetic network for the northern-central European lineage, the three central (ancestral) haplotypes were located in or near regions where the SDM approaches predicted a potential LGM distribution for *S. minutus*. These results imply that *S. minutus* was not dependent on amelioration of the climate at the end of the last glaciation to colonize northern-central Europe from southern refugia; instead, it was already present. As the ice sheets retreated and the climate improved, the range of *S. minutus* expanded from northern refugia colonizing the rest of northern-central Europe. For example, Scandinavian and the Baltic regions were most likely colonized by pygmy shrews from eastern Europe, not from the west or from southern peninsulas. Thus, the phylogenetic network shows that sequences from Norway, Finland and Lithuania group closely with the Ukrainian central haplotype, which according to the SDM modelling could have survived the LGM in situ on the east European Plain. Likewise, the genetic similarity of samples from the Netherlands and Britain, in comparison to those elsewhere, suggests that the British pygmy shrew originated from populations in the vicinity of the Netherlands, reaching Britain over the landbridge with continental Europe. An alternative explanation is that *S. minutus* persisted in the unglaciated regions of southern Britain (as predicted by several of our SDM approaches) which were geographically connected and genetically similar to populations in continental Europe during the LGM. Whatever the explanation, as ice sheets retreated, *S. minutus* belonging to the northern-central European lineage was able to colonize the northern parts of mainland Britain.

Further support from fossils and phylogeographic analyses

Northern refugia in central Europe and further east, north of the traditional Mediterranean refugia, have been hypothesized in phylogeographic analyses for a number of small mammal species other than the pygmy shrew, including the field vole *Microtus agrestis* (Jaarola and Searle 2002), bank vole *Clethrionomys glareolus* (Deffontaine et al. 2005, Kotlík et al. 2006), root vole *Microtus oeconomus* (Brunhoff et al. 2003), common vole *Microtus arvalis* (Heckel et al. 2005) and the common shrew *Sorex araneus* (Bilton et al. 1998, Yannic et al. 2008). For bank voles, root voles, field voles and common voles, predictions of their potential LGM distribution based on SDM were also consistent with northern refugia (Fløjgaard et al. 2009).

Most of the phylogeographic studies point to the Carpathians as a likely northern refugial area, but a refugium in this area could have included broader regions of Hungary, Slovakia, Czech Republic, Moldova and Poland, supported by the occurrence of temperate mammal fossil records in the area (Sommer and Nadachowski 2006) and by our results. Also, the region of the Dordogne in south-western France was situated outside the LGM permafrost area and has temperate mammal fossil records dated to the end of the LGM. Therefore, it has been suggested as another likely refugium north of

the traditionally recognized southern refugia (Sommer and Nadachowski 2006), further supported by our findings.

In addition, there are a few but important fossil records of *S. minutus* from several localities north of the southern refugia, radiocarbon dated close to the LGM or earlier (S3P Faunal Database <www.esc.cam.ac.uk/research/research-groups/oistage3/stage-three-project-database-downloads>). These fossil remains have been found in sites in France (26 Kya), Belgium (38–40 Kya), Germany (23–29 Kya) and Hungary (20–22 Kya).

In conclusion, a wide northern LGM distribution for *S. minutus* is supported by the combined use of a phylogeographic and species distribution modelling approach. The SDM methodologies provide evidence for a central and eastern European LGM distribution of *S. minutus*, where the northern-central European lineage could have been distributed. Additionally, the SDM approaches reveal potential LGM distributions for *S. minutus* in southern refugia, consistent with the lineages present in those regions. The phylogeographic analyses, however, indicate that the southern refugia were not the postglacial source of the current and widespread northern-central European populations. The other phylogeographic and SDM studies on small mammals, mammal and plant fossil records, and *S. minutus* fossil remains presented here provide additional evidence consistent with or directly supportive of our findings.

Our results contribute to the understanding of persistence and colonization from glacial refugia further north than traditionally recognized. They also provide new insights into the location and importance of refugial areas for the persistence of populations and genetic lineages during climate change. The use of *S. minutus* as a model exemplifies how the combined use of phylogeography and species distribution modelling can be applied to understand present-day biodiversity patterns, and can predict and test the past distribution of species to gain insight into the colonization patterns, differentiation and biogeography of species.

Acknowledgements – Specimens and species records of *Sorex minutus* were made available by several museums and we acknowledge the help of the curators from the following institutions: Dept of Ecology and Evolution (Univ. de Lausanne, Switzerland), Univ. na Primorskem and Research Centre of Koper (Slovenia), Natuurhistorisch Museum (Rotterdam, the Netherlands), Dipartimento di Ecologia (Univ. della Calabria, Italy), Museo di Anatomia Comparata and Museo di Zoologia “La Sapienza” (Univ. di Roma, Italy) and Natuurmuseum Brabant (Tilburg, the Netherlands). We are very grateful for the tissue samples provided by Boris Kryštufec, Allan McDevitt, Glenn Yannic, Jacques Hausser, Jan Zima, Frída Jóhannesdóttir, Holger Bruns, Peter Borkenhagen and Petr Kotlík. We thank David Nogués-Bravo and two anonymous referees for their valuable comments. Bayesian analyses were run at the Computational Biology Service Unit from Cornell Univ. which is partially funded by Microsoft Corporation. We gratefully acknowledge financial support to R. Vega (181844) and A. Lira-Noriega (189216) from CONACyT (México), and to J.-C. Svenning from the Danish Natural Science Research Council (grant 272-07-0242). This work represents the fruits of the discussion of our work presented at the 4th Biennial

Conference of the International Biogeography Society (8–12 January 2009, Mérida, Yucatán, México).

References

- Anderson, R. P. et al. 2003. Evaluating predictive models of species' distributions: criteria for selecting optimal models. – *Ecol. Model.* 162: 211–232.
- Arnold, H. R. 1993. Atlas of mammals of Britain. – Her Majesty's Stationary Office, London.
- Avise, J. C. 2000. Phylogeography: the history and formation of species. – Harvard Univ. Press.
- Bhagwat, S. A. and Willis, K. J. 2008. Species persistence in northerly glacial refugia of Europe: a matter of chance or biogeographical traits? – *J. Biogeogr.* 35: 464–482.
- Bilton, D. T. et al. 1998. Mediterranean Europe as an area of endemism for small mammals rather than a source for northwards postglacial colonization. – *Proc. R. Soc. B* 265: 1219–1226.
- Brunhoff, C. et al. 2003. Holarctic phylogeography of the root vole (*Microtus oeconomus*): implications for late Quaternary biogeography of high latitudes. – *Mol. Ecol.* 12: 957–968.
- Churchfield, S. and Searle, J. B. 2008. Pygmy shrew *Sorex minutus*. – In: Harris, S. and Yalden, D. W. (eds), Mammals of the British Isles: handbook. Mammal Society, pp. 267–271.
- Collins, W. D. et al. 2006. The Community Climate System Model: CCSM3. – *J. Climate* 19: 2122–2143.
- Deffontaine, V. et al. 2005. Beyond the Mediterranean peninsulas: evidence of central European glacial refugia for a temperate forest mammal species, the bank vole (*Clethrionomys glareolus*). – *Mol. Ecol.* 14: 1727–1739.
- Elith, J. and Graham, C. H. 2009. Do they? How do they? WHY do they differ? On finding reasons for differing performances of species distribution models. – *Ecography* 32: 66–77.
- Elith, J. et al. 2006. Novel methods improve prediction of species' distributions from occurrence data. – *Ecography* 29: 129–151.
- Excoffier, L. et al. 2005. Arlequin ver. 3.0: an integrated software package for population genetics data analysis. – *Evol. Bioinform.* Online 1: 47–50.
- Fløjgaard, C. et al. 2009. Ice age distributions of European small mammals: insights from species distribution modelling. – *J. Biogeogr.* 36: 1152–1163.
- Fu, Y. X. 1997. Statistical tests of neutrality of mutations against population growth, hitchhiking and background selection. – *Genetics* 147: 915–925.
- Guindon, S. and Gascuel, O. 2003. A simple, fast, and accurate algorithm to estimate large phylogenies by maximum likelihood. – *Syst. Biol.* 52: 696–704.
- Guisan, A. and Zimmermann, N. E. 2000. Predictive habitat distribution models in ecology. – *Ecol. Model.* 135: 147–186.
- Hall, T. A. 1999. BioEdit: a user-friendly biological sequence alignment editor and analysis program for Windows 95/98/NT/XP. – *Nucleic Acids Symp. Ser.* 41: 95–98.
- Hasumi, H. and Emori, S. 2004. K-1 coupled GCM (MIROC) description. – Center for Climate System Research, Univ. of Tokyo.
- Heckel, G. et al. 2005. Genetic structure and colonization processes in European populations of the common vole, *Microtus arvalis*. – *Evolution* 59: 2231–2242.
- Hewitt, G. M. 2000. The genetic legacy of the Quaternary ice ages. – *Nature* 405: 907–913.
- Hijmans, R. J. et al. 2005. Very high resolution interpolated climate surfaces for global land areas. – *Int. J. Climatol.* 25: 1965–1978.
- Ho, S. Y. W. et al. 2005. Time dependency on molecular rate estimates and systematic overestimation of recent divergence times. – *Mol. Biol. Evol.* 22: 1561–1568.
- Huelsenbeck, J. P. and Ronquist, F. 2001. MrBayes: Bayesian inference of phylogeny. – *Bioinformatics* 17: 754–755.
- Hutterer, R. et al. 2008. *Sorex minutus*. – IUCN 2009, IUCN Red List of Threatened Species, ver. 2009.2 <www.iucnredlist.org>, accessed 12 May 2009.
- Jaarola, M. and Searle, J. B. 2002. Phylogeography of field voles (*Microtus agrestis*) in Eurasia inferred from mitochondrial DNA sequences. – *Mol. Ecol.* 11: 2613–2621.
- Kotlík, P. et al. 2006. A northern glacial refugium for bank voles (*Clethrionomys glareolus*). – *Proc. Nat. Acad. Sci. USA* 103: 14860–14864.
- Librado, P. and Rozas, J. 2009. DnaSP ver. 5: a software for comprehensive analysis of DNA polymorphism data. – *Bioinformatics* 25: 1451–1452.
- Magri, D. et al. 2006. A new scenario for the Quaternary history of European beech populations: palaeobotanical evidence and genetic consequences. – *New Phytol.* 171: 199–221.
- Mascheretti, S. et al. 2003. How did pygmy shrews colonize Ireland? Clues from a phylogenetic analysis of mitochondrial cytochrome b sequences. – *Proc. R. Soc. B* 270: 1593–1599.
- McDevitt, A. D. et al. 2009. Genetic variation in Irish pygmy shrews *Sorex minutus* (Soricomorpha: Soricidae): implications for colonization history. – *Biol. J. Linn. Soc.* 97: 918–927.
- McDevitt, A. D. et al. 2010. Postglacial re-colonization of continental Europe by the pygmy shrew (*Sorex minutus*) inferred from mitochondrial and Y chromosomal DNA sequences. – In: Habel, J. C. and Assman, T. (eds), Relict species – phylogeography and conservation biology. Springer, in press.
- Mitchell-Jones, A. J. et al. 1999. The atlas of European mammals. – Poyser Natural History.
- Nogués-Bravo, D. 2009. Predicting the past distribution of species climatic niches. – *Global Ecol. Biogeogr.* 18: 521–531.
- Nylander, J. A. A. 2004. MrModeltest ver. 2. Program distributed by the author. – Evolutionary Biology Centre, Uppsala Univ.
- Ohdachi, S. D. et al. 2006. Molecular phylogenetics of soricid shrews (Mammalia) based on mitochondrial cytochrome b gene sequences: with special reference to the Soricinae. – *J. Zool.* 270: 177–191.
- Pearson, R. G. et al. 2007. Predicting species distributions from small numbers of occurrence records: a test case using cryptic geckos in Madagascar. – *J. Biogeogr.* 34: 102–117.
- Peterson, A. T. and Nakazawa, Y. 2008. Environmental data sets matter in ecological niche modeling: an example with *Solenopsis invicta* and *Solenopsis richterii*. – *Global Ecol. Biogeogr.* 17: 135–144.
- Peterson, A. T. et al. 2007. Transferability and model evaluation in ecological niche modeling: a comparison of GARP and Maxent. – *Ecography* 30: 550–560.
- Peterson, A. T. et al. 2008. Rethinking receiver operating characteristic analysis applications in ecological niche modeling. – *Ecol. Model.* 213: 63–72.
- Phillips, S. J. 2008. Transferability, sample selection bias and background data in presence-only modelling: a response to Peterson et al. 2007. – *Ecography* 31: 272–278.
- Phillips, S. J. and Dudík, M. 2008. Modeling of species distributions with Maxent: new extensions and a comprehensive evaluation. – *Ecography* 31: 161–175.
- Phillips, S. J. et al. 2004. A maximum entropy approach to species distribution modeling. – In: Greiner, R. and Schuurmans, D. (eds), Proc. 21st Int. Conf. on Machine Learning. ACM Press, pp. 655–662.

- Phillips, S. J. et al. 2006. Maximum entropy modeling of species geographic distributions. – *Ecol. Model.* 190: 231–259.
- Provan, J. and Bennett, K. D. 2008. Phylogeographic insights into cryptic glacial refugia. – *Trends Ecol. Evol.* 23: 564–571.
- Ramos-Onsins, S. E. and Rozas, J. 2002. Statistical properties of new neutrality tests against population growth. – *Mol. Biol. Evol.* 19: 2092–2100.
- Ratkiewicz, M. et al. 2002. The evolutionary history of the two karyotypic groups of the common shrew, *Sorex araneus*, in Poland. – *Heredity* 88: 235–242.
- Rogers, A. R. and Harpending, H. 1992. Population growth makes waves in the distribution of pairwise genetic differences. – *Mol. Biol. Evol.* 9: 552–569.
- Schneider, S. and Excoffier, L. 1999. Estimation of demographic parameters from the distribution of pairwise differences when the mutation rates vary among sites: application to human mitochondrial DNA. – *Genetics* 152: 1079–1089.
- Sommer, R. S. and Nadachowski, A. 2006. Glacial refugia of mammals in Europe: evidence from fossil records. – *Mammal Rev.* 36: 251–265.
- Stewart, J. R. and Lister, A. M. 2001. Cryptic northern refugia and the origins of the modern biota. – *Trends Ecol. Evol.* 16: 608–613.
- Stockwell, D. R. B. 1999. Genetic algorithms II. – In: Fielding, A. H. (ed.), *Machine learning methods for ecological applications*. Kluwer, pp. 123–144.
- Stockwell, D. R. B. and Noble, I. R. 1992. Introduction of sets of rules from animal distribution data: a robust and informative method of data analysis. – *Math. Comput. Simulat.* 33: 385–390.
- Stockwell, D. R. B. and Peterson, A. T. 2002. Effects of sample size on accuracy of species distribution models. – *Ecol. Model.* 148: 1–13.
- Svendsen, J. I. et al. 2004. Late Quaternary ice sheet history of northern Eurasia. – *Quat. Sci. Rev.* 23: 1229–1271.
- Svenning, J.-C. et al. 2008. Glacial refugia of temperate trees in Europe: insights from species distribution modeling. – *J. Ecol.* 96: 1117–1127.
- Swofford, D. L. 2000. PAUP*. Phylogenetic analysis using parsimony (*and other methods), ver. 4. – Sinauer.
- Taberlet, P. et al. 1998. Comparative phylogeography and postglacial colonization routes in Europe. – *Mol. Ecol.* 7: 453–464.
- Tajima, F. 1989. Statistical method for testing the neutral mutation hypothesis by DNA polymorphism. – *Genetics* 123: 585–595.
- Waltari, E. et al. 2007. Locating Pleistocene refugia: comparing phylogeographic and ecological niche model predictions. – *PLoS One* 7: e563.
- Willis, K. J. and van Andel, T. H. 2004. Trees or no trees? The environments of central and eastern Europe during the Last Glaciation. – *Quat. Sci. Rev.* 23: 2369–2387.
- Willis, K. J. et al. 2000. The full-glacial forests of central and south-eastern Europe. – *Quat. Res.* 53: 203–213.
- Wisz, M. S. et al. 2008. Effects of sample size on the performance of species distribution models. – *Divers. Distrib.* 14: 763–773.
- Yannic, G. et al. 2008. A new perspective on the evolutionary history of western European *Sorex araneus* group revealed by paternal and maternal molecular markers. – *Mol. Phylogenet. Evol.* 47: 237–250.

Appendix 3. List of samples of *Sorex minutus* for genetic analysis.

Samples of *Sorex minutus* for genetic analysis of cytochrome (cyt) *b*, Y-chromosome intron (Y) and BRCA1 gene.

Country	Locality	Phylo group	Code	Longitude (Decimal)	Latitude (Decimal)	Cyt <i>b</i> hap	Y	BRCA 1
Andorra	Andorra ¹	Pyr	ADAd0001	1.5833	42.5833	156		
Andorra	Andorra ¹	Pyr	ADAd0002	1.5833	42.5833	157		
Austria	Donnerskirchen ⁵	NCE	ATDo1612	16.6413	47.8957	159		
Austria	Donnerskirchen ⁶	Balk	ATDo1611	16.6413	47.8957	158	1	4
Austria	Illmitz ⁵	NCE	ATII0003	16.8454	47.7647	161		
Austria	Illmitz ⁵	NCE	ATII0004	16.8454	47.7647	162	4	
Austria	Illmitz ⁵	NCE	ATII0005	16.8454	47.7647	163	3	
Austria	Illmitz ⁶	Balk	ATII0001	16.8454	47.7647	160	2	
Austria	Illmitz ⁶	Balk	ATII0002	16.8454	47.7647		3	
Belarusia	Lesnojezero ⁵	NCE	BYLE0026	26.6918	54.8302	165		
Bosnia Herzegovina	Osjecenica ⁶	Balk	BAOs5670	16.2887	44.2397	164		
Britain	Aird, Benbecula ³	Pyr	GBBe0740	-7.3328	57.4278	19		
Britain	Allt Loch an Tairbh, Rum ³	Pyr	GBRu0105	-6.3300	57.0297	26		
Britain	Allt nah Uamha, Rum ³	Pyr	GBRu0104	-6.2692	56.9878	26		
Britain	Ambergate, Derbyshire ³	NCE	GBDe0953	-1.4889	53.0619	37		
Britain	Balintore, Easter Ross ³	Pyr	GBER0408	-3.9175	57.7531	41		
Britain	Balintore, Easter Ross ³	NCE	GBER0410	-3.9175	57.7531	42		
Britain	Beanacre, Wiltshire ³	NCE	GBWi0042	-2.1494	51.3975	108		
Britain	Biggar, Walney ³	NCE	GBWi0669	-3.2275	54.0772	111		
Britain	Biggar, Walney ³	NCE	GBWi0670	-3.2275	54.0772	111		
Britain	Biggar, Walney ³	NCE	GBWi0671	-3.2275	54.0772	111		
Britain	Billington, Lancashire ³	NCE	GBLa1071	-2.4328	53.8122	70		
Britain	Birsay, OM ³	Pyr	GBOM0261	-3.2931	59.1283	84		
Britain	Bislington, Kent ³	NCE	GBKe0010	0.9339	51.0672	66		
Britain	Bodmin, Cornwall ³	NCE	GBCo00C1	-4.7283	50.4753	27		
Britain	Bodmin, Cornwall ³	Pyr	GBCo00C2	-4.7283	50.4753	28		
Britain	Bracknell Forest ³	NCE	GBBF0035	-0.7436	51.4503	20		
Britain	Bracknell Forest ³	NCE	GBBF0036	-0.7436	51.4503	21		
Britain	Bradley Hill, Hampshire ³	Pyr	GBHa0039	-1.0800	51.1872	47		
Britain	Canna ³	Pyr	GBCn0901	-6.5117	57.0594	26		
Britain	Canna ³	Pyr	GBCn0905	-6.5117	57.0594	26		
Britain	Canna ³	Pyr	GBCn0906	-6.5117	57.0594	26		
Britain	Carinish, N. Uist ³	Pyr	GBNU0319	-7.3225	57.5181	19		
Britain	Carinish, N. Uist ³	Pyr	GBNU0325	-7.3225	57.5181	78		
Britain	Carmarthenshire ³	NCE	GBCa0001	-4.1553	51.7603	22		
Britain	Carmarthenshire ³	NCE	GBCa0002	-4.1478	51.7525	23		
Britain	Carmarthenshire ³	NCE	GBCa0003	-4.1478	51.7525	24		
Britain	Carmarthenshire ³	NCE	GBCa0004	-4.5817	51.7922	25		
Britain	Clarach, Cardiganshire ³	NCE	GBCr1100	-4.0611	52.4381	30		
Britain	Craighouse, Jura ³	NCE	GBJu0815	-5.9435	55.8528	64		
Britain	Craighouse, Jura ³	NCE	GBJu0816	-5.9435	55.8528	64		
Britain	Cromdale, Inverness ³	NCE	GBIn0180	-3.4856	57.3411	54		
Britain	Desnage, Suffolk ³	NCE	GBSu0005	0.5189	52.2478	102		
Britain	Desnage, Suffolk ³	NCE	GBSu0006	0.5411	52.2769	103		

Britain	Desnage, Suffolk ³	NCE	GBSu0007	0.5411	52.2769	104	
Britain	Desnage, Suffolk ³	NCE	GBSu0008	0.5411	52.2769	105	
Britain	Dorset ³	NCE	GBDo0458	-2.3633	50.8306	38	
Britain	Dorset ³	NCE	GBDo0459	-2.3633	50.8306	10	
Britain	Dorset ³	NCE	GBDo0460	-2.3633	50.8306	39	
Britain	Dorset ³	Pyr	GBDo0461	-2.3633	50.8306	40	
Britain	Dorset ³	NCE	GBDo0462	-2.3633	50.8306	38	
Britain	Dounby, OM ³	Pyr	GBOM0419	-3.2244	58.9700	50	
Britain	Dover, Kent ³	NCE	GBKe0009	1.2578	51.1269	65	
Britain	East Cottingwith ¹	NCE	GBEC0001	-0.9167	53.8667	233	
Britain	East Harptree, Somerset ³	NCE	GBSo002	-2.6597	51.2856	97	
Britain	East Hendred ¹	NCE	GBEH0001	-1.3333	51.5667	234	
Britain	Easter Ross Balintore ³	Pyr	GBER0177	-3.9175	57.7531	41	
Britain	Fishnish, Mull ⁹	Pyr	GBMu0858	-5.8378	56.5100	14	
Britain	Fishnish, Mull ⁹	Pyr	GBMu0859	-5.8378	56.5100	72	
Britain	Foulney, Cumbria ³	NCE	GBCu0642	-3.1522	54.0661	33	
Britain	Fulford, North Yorkshire ³	NCE	GBNY00F2	-1.0736	53.9364	79	
Britain	Fulford, North Yorkshire ³	NCE	GBNY00F3	-1.0736	53.9364	80	
Britain	Fulford, North Yorkshire ³	NCE	GBNY00Y1	-1.0736	53.9364	81	
Britain	Gask ¹	NCE	GBGa0001	-3.6667	56.3500	235	
Britain	Gask ¹	NCE	GBGa0002	-3.6667	56.3500	236	
Britain	Gayton Thorpe, Norfolk ³	NCE	GBNo0001	0.5919	52.7481	75	
Britain	Gayton Thorpe, Norfolk ³	NCE	GBNo0002	0.5919	52.7481	10	
Britain	Gayton, Norfolk ³	NCE	GBNo0004	0.5706	52.7628	77	
Britain	Gigha ³	Pyr	GBGi0001	-5.7410	55.6833	43	
Britain	Gigha ³	Pyr	GBGi0002	-5.7410	55.6833	43	
Britain	Gigha ³	Pyr	GBGi0003	-5.7410	55.6833	43	
Britain	Gigha ³	Pyr	GBGi0004	-5.7410	55.6833	43	
Britain	Gigha ³	Pyr	GBGi0005	-5.7410	55.6833	43	
Britain	Gigha ³	Pyr	GBGi0006	-5.7410	55.6833	43	
Britain	Glen Artney, Perthshire ³	NCE	GBPr0132	-4.0033	56.3464	90	
Britain	Gloucestershire ³	NCE	GBGI0001	-2.6450	51.7883	44	
Britain	Gloucestershire ³	NCE	GBGI0043	-2.1097	51.6511	45	
Britain	Gloucestershire ³	NCE	GBGI0047	-2.1031	51.8092	46	
Britain	Grimness, OS ⁶	Pyr	OSGr0006	-2.9167	58.8167	98	1
Britain	Grimness, OS ⁶	Pyr	OSGr0007	-2.9167	58.8167	98	
Britain	Grimness, OS ⁶	Pyr	OSGr0008	-2.9167	58.8167	98	
Britain	Grimness, OS ⁶	Pyr	OSGr0009	-2.9167	58.8167	98	
Britain	Grimness, OS ⁶	Pyr	OSGr0010	-2.9167	58.8167	98	
Britain	Grimness, OS ⁶	Pyr	OSGr0011	-2.9167	58.8167	98	
Britain	Grimness, OS ⁶	Pyr	OSGr0012	-2.9167	58.8167	98	
Britain	Grimness, OS ⁶	Pyr	OSGr0013	-2.9167	58.8167	98	
Britain	Grimness, OS ⁶	Pyr	OSGr0014	-2.9167	58.8167	98	
Britain	Grimness, OS ⁶	Pyr	OSGr0015	-2.9167	58.8167	98	8
Britain	Grimness, OS ⁶	Pyr	OSGr0016	-2.9167	58.8167	98	
Britain	Grimness, OS ⁶	Pyr	OSGr0018	-2.9167	58.8167	98	8
Britain	Grimness, OS ⁶	Pyr	OSGr0020	-2.9167	58.8167	98	
Britain	Grimness, OS ⁶	Pyr	OSGr0023	-2.9167	58.8167	98	
Britain	Grimness, OS ⁶	Pyr	OSGr0025	-2.9167	58.8167	98	
Britain	Grimness, OS ⁶	Pyr	OSGr0027	-2.9167	58.8167	98	8
Britain	Grimness, OS ⁶	Pyr	OSGr0028	-2.9167	58.8167	98	
Britain	Grimness, OS ⁶	Pyr	OSGr0029	-2.9167	58.8167	98	
Britain	Grimness, OS ⁶	Pyr	OSGr0039	-2.9167	58.8167	98	
Britain	Grimstone, Norfolk ³	NCE	GBNo0003	0.5561	52.7650	76	

Britain	Grittenham ¹	NCE	GBGr0001	-1.9667	51.5500	237		
Britain	Hardiwick, Staffordshire ³	NCE	GBSt0030	-2.0925	53.0983	101		
Britain	Harray, OM ⁶	Pyr	OMHa0003	-3.1902	59.0337	50		
Britain	Harray, OM ⁶	Pyr	OMHa0004	-3.1902	59.0337	50		
Britain	Harray, OM ⁶	Pyr	OMHa0006	-3.1902	59.0337	318		
Britain	Harray, OM ⁶	Pyr	OMHa0009	-3.1902	59.0337	318		
Britain	Harray, OM ⁶	Pyr	OMHa0011	-3.1902	59.0337	318		
Britain	Havenstreet, Isle of Wight ³	Pyr	GBIW0001	-1.2528	50.6689	62		
Britain	Havenstreet, Isle of Wight ³	Pyr	GBIW0002	-1.2528	50.6689	62		
Britain	Hestwall, OM ³	Pyr	GBOM0001	-2.9131	58.9067	82		
Britain	Hestwall, OM ³	Pyr	GBOM0002	-2.9131	58.9067	82		
Britain	Hestwall, OM ³	Pyr	GBOM0003	-2.9131	58.9067	82		
Britain	Hestwall, OM ³	Pyr	GBOM0004	-2.9131	58.9067	82		
Britain	Hobbister, OM ⁶	Pyr	OMHo0014	-3.0676	58.9464	85	8	
Britain	Hobbister, OM ⁶	Pyr	OMHo0015	-3.0676	58.9464	85		
Britain	Holm, OM ³	Pyr	GBOM0260	-2.9256	58.9186	83		
Britain	Holm, OM ³	Pyr	GBOM0262	-2.8783	58.9044	83		
Britain	Holy Island, Anglesey ³	NCE	GBAn0038	-4.6667	53.3028	9		
Britain	Hoy village, Hoy ³	Pyr	GBHo0001	-3.3333	58.9167	50		
Britain	Islay ³	Pyr	GBIs0001	-6.2333	55.7500	58		
Britain	Islay ³	Pyr	GBIs0002	-6.2333	55.7500	59		
Britain	Islay ³	Pyr	GBIs0003	-6.2333	55.7500	60		
Britain	Islay ³	Pyr	GBIs0004	-6.2333	55.7500	61		
Britain	Isle of Man ¹	NCE	GBIM0001	-4.4833	54.1500	238		
Britain	Isle of Man ¹	NCE	GBIM0002	-4.4833	54.1500	239		
Britain	Isle of Man ³	NCE	GBIM0600	-4.4833	54.1500	52		
Britain	Isle of Man ³	NCE	GBIM0601	-4.3511	54.2914	53		
Britain	Isle of Man ³	NCE	GBIM0602	-4.4517	54.1725	52		
Britain	Kildonan, Arran ³	Pyr	GBAr0004	-5.1281	55.4500	16		
Britain	Kildonan, Arran ³	Pyr	GBAr0006	-5.1281	55.4500	17		
Britain	Kildonan, Arran ³	Pyr	GBAr0007	-5.1281	55.4500	18		
Britain	Kildonan, Arran ³	Pyr	GBAr0008	-5.1281	55.4500	17		
Britain	Kinloch, Rum ³	Pyr	GBRu0127	-6.2803	57.0125	93		
Britain	Kippford, Kirkcudbright ³	NCE	GBKk0099	-3.8233	54.8669	34		
Britain	Kippford, Kirkcudbright ³	NCE	GBKk0100	-3.8233	54.8669	10		
Britain	Kirbister, OM ⁶	Pyr	OMKi0013	-3.1101	58.9500	85		
Britain	Kirkcudbrightshire ³	NCE	GBKk0589	-3.7814	54.9756	69		
Britain	Kirkhill, Inverness ³	NCE	GBIn0181	-4.4169	57.4544	55		
Britain	Kirkhill, Inverness ³	NCE	GBIn0182	-4.4169	57.4544	56		
Britain	Knockan, Mull ³	Pyr	GBMu0861	-6.2006	56.3336	74		
Britain	Lang Taing, OS ³	Pyr	GBSR0274	-2.9214	58.7586	98		
Britain	Leicester, Leicestershire ³	NCE	GBLe0497	-1.1333	52.6333	71		
Britain	Llanbabo, Anglesey ³	Pyr	GBAn0046	-4.4353	53.3617	12		
Britain	Llangaffo, Anglesey ³	NCE	GBAn0044	-4.3300	53.1889	11		
Britain	Loch Swartmill, OW ⁶	Pyr	OWLS0001	-2.9334	59.2833	50		
Britain	Loch Swartmill, OW ⁶	Pyr	OWLS0002	-2.9334	59.2833	50		
Britain	Loch Swartmill, OW ⁶	Pyr	OWLS0003	-2.9334	59.2833	50		
Britain	Loch Swartmill, OW ⁶	Pyr	OWLS0005	-2.9334	59.2833	50		
Britain	Loch Swartmill, OW ⁶	Pyr	OWLS0024	-2.9334	59.2833	50	8	1
Britain	Loch Swartmill, OW ⁶	Pyr	OWLS0025	-2.9334	59.2833	50		

Britain	Loch Swartmill, OW ⁶	Pyr	OWLS0036	-2.9334	59.2833	50	
Britain	Loch Swartmill, OW ⁶	Pyr	OWLS0037	-2.9334	59.2833	50	
Britain	Loch Swartmill, OW ⁶	Pyr	OWLS0038	-2.9334	59.2833	50	
Britain	Loch Swartmill, OW ⁶	Pyr	OWLS0055	-2.9334	59.2833	50	
Britain	Loch Swartmill, OW ⁶	Pyr	OWLS0059	-2.9334	59.2833	50	
Britain	Loch Swartmill, OW ⁶	Pyr	OWLS0060	-2.9334	59.2833	50	
Britain	Loch Swartmill, OW ⁶	Pyr	OWLS0061	-2.9334	59.2833	50	
Britain	Loch Swartmill, OW ⁶	Pyr	OWLS0072	-2.9334	59.2833	50	
Britain	Loch Swartmill, OW ⁶	Pyr	OWLS0073	-2.9334	59.2833	50	
Britain	Loch Swartmill, OW ⁶	Pyr	OWLS0082	-2.9334	59.2833	50	
Britain	Loch Swartmill, OW ⁶	Pyr	OWLS0083	-2.9334	59.2833	50	
Britain	Loch Swartmill, OW ⁶	Pyr	OWLS0084	-2.9334	59.2833	50	
Britain	Loch Swartmill, OW ⁶	Pyr	OWLS0085	-2.9334	59.2833	50	
Britain	Longnor ¹	NCE	GBLo0001	-1.8833	53.1667	242	
Britain	Longtown, Cumbria ³	NCE	GBCu0677	-2.9686	55.0139	34	
Britain	Lyn Conwy ³	NCE	GBCo0139	-3.8333	53.2833	29	
Britain	Lyn Conwy ¹	NCE	GBLC0001	-3.8333	53.2833	240	
Britain	Lyn Conwy ¹	NCE	GBLC0002	-3.8333	53.2833	241	
Britain	Macclesfield ¹	NCE	GBMa0001	-2.0333	53.2500	243	
Britain	Machrie, Arran ³	Pyr	GBAr0001	-5.2856	55.5564	13	
Britain	Machrie, Arran ³	Pyr	GBAr0002	-5.2856	55.5564	14	
Britain	Malltraeth, Anglesey ³	NCE	GBAn0042	-4.3822	53.1928	10	
Britain	Maltraeth, Anglesey ³	NCE	GBAn0001	-4.3403	53.1992	8	
Britain	Mull ³	Pyr	GBMu0860	-5.8611	56.4047	73	
Britain	Ness, OW ⁶	Pyr	OWNe0002	-2.8667	59.2334	50	
Britain	Ness, OW ⁶	Pyr	OWNe0003	-2.8667	59.2334	50	
Britain	Ness, OW ⁶	Pyr	OWNe0004	-2.8667	59.2334	50	
Britain	Ness, OW ⁶	Pyr	OWNe0005	-2.8667	59.2334	50	
Britain	Ness, OW ⁶	Pyr	OWNe0006	-2.8667	59.2334	50	
Britain	Ness, OW ⁶	Pyr	OWNe0007	-2.8667	59.2334	50	
Britain	Ness, OW ⁶	Pyr	OWNe0008	-2.8667	59.2334	50	
Britain	Ness, OW ⁶	Pyr	OWNe0009	-2.8667	59.2334	50	
Britain	Ness, OW ⁶	Pyr	OWNe0026	-2.8667	59.2334	50	1
Britain	Ness, OW ⁶	Pyr	OWNe0028	-2.8667	59.2334	50	
Britain	Ness, OW ⁶	Pyr	OWNe0030	-2.8667	59.2334	50	
Britain	Ness, OW ⁶	Pyr	OWNe0041	-2.8667	59.2334	50	
Britain	Ness, OW ⁶	Pyr	OWNe0062	-2.8667	59.2334	50	8
Britain	Ness, OW ⁶	Pyr	OWNe0103	-2.8667	59.2334	50	
Britain	Orielton, Pembrokeshire ³	NCE	GBPe0026	-4.9539	51.6508	88	
Britain	Orielton, Pembrokeshire ³	NCE	GBPe0042	-4.9539	51.6508	89	
Britain	Orphir, OM ³	Pyr	GBOM0418	-3.0514	58.9444	85	
Britain	Pembrokeshire ³	NCE	GBPe0005	-4.6575	51.7725	86	
Britain	Pembrokeshire ³	NCE	GBPe0006	-4.6575	51.7725	87	
Britain	Plastow, Hampshire ³	NCE	GBHa0040	-1.2258	51.3589	48	
Britain	Plastow, Hampshire ³	NCE	GBHa0041	-1.2258	51.3589	49	
Britain	Raasay ³	Pyr	GBRa0001	-6.0333	57.4000	91	
Britain	Raasay ³	Pyr	GBRa0002	-6.0333	57.4000	92	

Britain	Raasay ³	Pyr	GBRa0003	-6.0333	57.4000	91	
Britain	Raasay ³	Pyr	GBRa0004	-6.0333	57.4000	91	
Britain	Rackwick Road, Hoy ³	Pyr	GBHo0868	-3.3828	58.8803	51	
Britain	Rinigar, OS ³	Pyr	GBSR0612	-3.0217	58.8208	98	
Britain	Rinigar, OS ³	Pyr	GBSR0613	-3.0217	58.8208	99	
Britain	Romney Warren, Kent ³	NCE	GBKe0972	0.9603	50.9953	67	
Britain	Rudge, Shropshire ³	NCE	GBSh0006	-2.2597	52.5742	95	
Britain	Rudge, Shropshire ³	NCE	GBSh0007	-2.2597	52.5742	96	
Britain	Saint Ola, OM ⁶	Pyr	OMSO0006	-2.9500	58.9500	85	1
Britain	Saint Ola, OM ⁶	Pyr	OMSO0007	-2.9500	58.9500	83	
Britain	Saint Ola, OM ⁶	Pyr	OMSO0008	-2.9500	58.9500	83	1
Britain	Saint Ola, OM ⁶	Pyr	OMSO0009	-2.9500	58.9500	83	
Britain	Saint Ola, OM ⁶	Pyr	OMSO0010	-2.9500	58.9500	83	
Britain	Saint Ola, OM ⁶	Pyr	OMSO0011	-2.9500	58.9500	319	
Britain	Saint Ola, OM ⁶	Pyr	OMSO0013	-2.9500	58.9500	83	
Britain	Saint Ola, OM ⁶	Pyr	OMSO0014	-2.9500	58.9500	83	
Britain	Saint Ola, OM ⁶	Pyr	OMSO0015	-2.9500	58.9500	83	
Britain	Saint Ola, OM ⁶	Pyr	OMSO0017	-2.9500	58.9500	319	8
Britain	Saint Ola, OM ⁶	Pyr	OMSO0020	-2.9500	58.9500	277	
Britain	Saint Ola, OM ⁶	Pyr	OMSO0026	-2.9500	58.9500	83	8
Britain	Saint Ola, OM ⁶	Pyr	OMSO0029	-2.9500	58.9500	83	
Britain	Saint Ola, OM ⁶	Pyr	OMSO0036	-2.9500	58.9500	83	
Britain	Sanda Island, Kintyre ³	Pyr	GBKi0795	-5.5828	55.2819	68	
Britain	Sandwick, OM ⁶	Pyr	OMSa0001	-3.2972	59.0483	82	8
Britain	Sandwick, OM ⁶	Pyr	OMSa0002	-3.2972	59.0483	50	8
Britain	Serrigar, OS ³	Pyr	GBSR0273	-2.9747	58.7808	98	
Britain	Settiscarth, OM ⁶	Pyr	OMSe0001	-3.1034	59.0505	82	
Britain	Settiscarth, OM ⁶	Pyr	OMSe0002	-3.1034	59.0505	82	8
Britain	South Gloucestershire ³	NCE	GBSG0044	-2.3317	51.5617	94	
Britain	Staffordshire ³	NCE	GBSt0005	-2.2903	52.7233	100	
Britain	Stilligarry, S. Uist ³	Pyr	GBSU0227	-7.3708	57.3236	19	
Britain	Stilligarry, S. Uist ³	Pyr	GBSU0310	-7.3708	57.3233	106	
Britain	Tankerness, OM ⁶	Pyr	OMTa0001	-2.8500	58.9500	83	
Britain	Tankerness, OM ⁶	Pyr	OMTa0002	-2.8500	58.9500	83	1
Britain	Tankerness, OM ⁶	Pyr	OMTa0003	-2.8500	58.9500	83	
Britain	Tankerness, OM ⁶	Pyr	OMTa0004	-2.8500	58.9500	83	
Britain	Tankerness, OM ⁶	Pyr	OMTa0005	-2.8500	58.9500	83	
Britain	Tankerness, OM ⁶	Pyr	OMTa0006	-2.8500	58.9500	83	
Britain	Tankerness, OM ⁶	Pyr	OMTa0007	-2.8500	58.9500	83	
Britain	Tankerness, OM ⁶	Pyr	OMTa0008	-2.8500	58.9500	277	1
Britain	Tankerness, OM ⁶	Pyr	OMTa0009	-2.8500	58.9500	83	
Britain	Thorley, Isle of Wight ³	Pyr	GBIW0003	-1.4719	50.6889	63	
Britain	Thurvaston, Derbyshire ³	NCE	GBDe0001	-1.6369	52.9442	35	
Britain	Thurvaston, Derbyshire ³	NCE	GBDe0002	-1.6369	52.9442	36	
Britain	Tomatin, Inverness ³	NCE	GBIn0407	-3.9606	57.3364	57	
Britain	Warwickshire ³	NCE	GBWa0050	-1.2431	52.1272	107	
Britain	Warwickshire ³	NCE	GBWa0051	-1.2431	52.1272	107	
Britain	Wedholme Flow, Cumbria ³	NCE	GBCu00B1	-3.2347	54.8678	31	
Britain	Wedholme Flow, Cumbria ³	NCE	GBCu00B2	-3.2347	54.8678	32	
Britain	Wedholme Flow, Cumbria ³	NCE	GBCu00D1	-3.2347	54.8678	32	
Britain	West Sussex ³	NCE	GBWS0011	0.3075	50.8447	117	
Britain	Wester Ross ³	Pyr	GBWR0176	-5.3317	57.4819	115	

Britain	Wester Ross ³	Pyr	GBWR0178	-5.3317	57.4819	116	
Britain	Whiting Bay, Arran ³	Pyr	GBAr0003	-5.0992	55.4858	15	
Britain	Windwick, OS ⁶	Pyr	OSWW0006	-2.9407	58.7668	98	1
Britain	Windwick, OS ⁶	Pyr	OSWW0007	-2.9407	58.7668	98	
Britain	Windwick, OS ⁶	Pyr	OSWW0008	-2.9407	58.7668	98	
Britain	Windwick, OS ⁶	Pyr	OSWW0009	-2.9407	58.7668	98	8
Britain	Windwick, OS ⁶	Pyr	OSWW0010	-2.9407	58.7668	98	
Britain	Windwick, OS ⁶	Pyr	OSWW0011	-2.9407	58.7668	98	
Britain	Windwick, OS ⁶	Pyr	OSWW0012	-2.9407	58.7668	98	
Britain	Windwick, OS ⁶	Pyr	OSWW0013	-2.9407	58.7668	98	
Britain	Windwick, OS ⁶	Pyr	OSWW0014	-2.9407	58.7668	98	
Britain	Windwick, OS ⁶	Pyr	OSWW0015	-2.9407	58.7668	98	
Britain	Windwick, OS ⁶	Pyr	OSWW0017	-2.9407	58.7668	98	
Britain	Windwick, OS ⁶	Pyr	OSWW0018	-2.9407	58.7668	99	
Britain	Windwick, OS ⁶	Pyr	OSWW0019	-2.9407	58.7668	98	
Britain	Windwick, OS ⁶	Pyr	OSWW0020	-2.9407	58.7668	98	
Britain	Windwick, OS ⁶	Pyr	OSWW0021	-2.9407	58.7668	98	
Britain	Windwick, OS ⁶	Pyr	OSWW0024	-2.9407	58.7668	98	
Britain	Windwick, OS ⁶	Pyr	OSWW0025	-2.9407	58.7668	99	
Britain	Wokingham ³	Pyr	GBWk0037	-0.9039	51.3664	109	
Britain	Wokingham ³	Pyr	GBWk0038	-0.9039	51.3664	110	
Britain	Worcestershire ³	NCE	GBWo0009	-2.1247	52.3100	112	
Britain	Worcestershire ³	NCE	GBWo0011	-2.0294	52.4125	113	
Britain	Worcestershire ³	NCE	GBWo0012	-2.4133	52.2667	114	
Czech Republic	Bohemia ⁵	NCE	CZBo0154	13.5695	49.8642	178	
Czech Republic	Bohemia ⁵	NCE	CZBo0155	13.5695	49.8642	179	4,12
Czech Republic	Bohemia ⁵	NCE	CZBo0156	13.5695	49.8642	180	
Czech Republic	Bohemia ⁵	NCE	CZBo0238	13.5695	49.8642		3
Czech Republic	Bohemia ⁶	Balk	CZBo0153	13.5695	49.8642	177	3
Czech Republic	Ceske Jiretin ¹	NCE	CZCJ0001	13.5667	50.6833	181	
Czech Republic	Decin City, Bohemia ⁵	NCE	CZDe0009	14.1988	50.8059	182	
Czech Republic	Decin City, Bohemia ⁵	NCE	CZDe0010	14.1988	50.8059	183	3
Czech Republic	Most district, Bohemia ⁵	NCE	CZMo0794	13.5377	50.6003	184	
Czech Republic	Oleska ⁵	NCE	CZOI0039	14.9096	49.9486	44	3
Czech Republic	Srnin Sumava Mts ⁵	NCE	CZSS0237	13.4755	49.0656	185	
Czech Republic	Srnin Sumava Mts ⁵	NCE	CZSS0238	13.4755	49.0656	186	
Czech Republic	Srnin Sumava Mts ⁶	NCI	CZSS4767	13.4755	49.0656	187	
Czech Republic	Srnin Sumava Mts ⁶	NCI	CZSS4838	13.4755	49.0656	187	
Czech Republic	Vltava River, Bohemia ⁵	NCE	CZVI0001	14.4129	48.9114	188	
Czech Republic	Vltava River, Bohemia ⁵	NCE	CZVI0002	14.4129	48.9114	188	3
Czech Republic	Vltava River, Bohemia ⁵	NCE	CZVI0003	14.4129	48.9114	189	3
Czech Republic	Vltava River, Bohemia ⁵	NCE	CZVI0004	14.4129	48.9114	190	
Czech Republic	Vltava River, Bohemia ⁶	NCE	CZVI0005	14.4190	48.9115	191	3
Czech Republic	Vltava River, Bohemia ⁶	NCI	CZVI0006	14.4190	48.9115	192	
Czech Republic	Vltava River, Bohemia ⁶	NCI	CZVI0007	14.4190	48.9115	192	
Czech	Vltava River,	NCI	CZVI0008	14.4190	48.9115	192	3

Republic	Bohemia ⁶							
Denmark	Amager ¹	NCE	DKAm0001	12.5833	55.5833	203		
Denmark	Bornholm ¹	NCE	DKBo0001	15.0000	55.0333	204		
Denmark	Bornholm ¹	NCE	DKBo0002	15.0000	55.0333	205		
Denmark	Fyn ¹	NCE	DKFy0001	10.8000	55.3167	206		
Denmark	Langeland ¹	NCE	DKLa0001	10.7167	54.9500	207		
Denmark	Mandø ⁵	NCE	DKMa0005	8.5521	55.2772	208	7	
Denmark	Mandø ⁵	NCE	DKMa0006	8.5521	55.2772	209	3	
Denmark	Mandø ⁵	NCE	DKMa0007	8.5521	55.2772	210		
Denmark	Viking centre, Ribe ⁵	NCE	DKRi0003	8.7628	55.3270	211	3	
Finland	Lammi ¹	NCE	FILa0001	25.1167	61.0667	222		
Finland	Saortu ¹	NCE	FISa0001	27.2500	61.7333	223		
France	Belle Île, Brittany ³	Pyr	FRBI0001	-3.1958	47.3375	1		
France	Belle Île, Brittany ³	Pyr	FRBI0002	-3.1958	47.3375	2		
France	Belle Île, Brittany ³	Pyr	FRBI0005	-3.2000	47.3708	3		
France	Belle Île, Brittany ³	Pyr	FRBI0011	-3.1222	47.3083	4		
France	Belle Île, Brittany ³	Pyr	FRBI00LP	-3.1500	47.3500	5		
France	Broualan, Brittany ³	NCE	FRBr2McD	-1.6250	48.4667	6		
France	Cistriere Auvergne ⁶	Pyr	FRCi0003	3.5408	45.4459	224	8	
France	Divonne Les Bains, Ain ⁴	NCI	FRDi3003	6.1432	46.3568	187		
France	Etang des Balceres ⁶	Pyr	FREB0001	2.0802	42.5525	225		1,3
France	Fressenville, Normandie ⁵	NCE	FRFr0139	0.0012	48.9314	226		
France	Lac des Bouillouses ⁶	Pyr	FRLB0066	1.9923	42.5614	228	8	1
France	Lans en Vercors ⁴	NCI	FRLV0002	5.5891	45.1280	227		
France	Limousin ³	Pyr	FRLi3McD	2.1333	45.7000	7		
France	Morlaix ¹	NCE	FRMo0001	-3.8333	48.5833	229		
France	Nexon ⁶	Pyr	FRNe0004	1.2500	45.7500	5	10	
France	Paimpont Broceliande ⁶	Pyr	FRPa0001	-2.2795	48.0013	231		
France	Pas de Calais ⁶	Pyr	FRPC0001	2.3021	50.5660	231		
France	Pont Plancoet, Bretagne ⁵	NCE	FRPP5540	-4.1987	48.6510	229	8	4,6
France	Pont Saint Marco, Nord ⁵	NCE	FRSM0001	-2.0403	48.6144	232		
Germany	Anholt, Saxony ⁵	NCE	DESa0003	11.3955	52.4779	201	6	
Germany	Anholt, Saxony ⁵	NCE	DESa0005	11.3955	52.4779	202		
Germany	Beltingharder Koog ⁵	NCE	DEBK0001	8.7846	54.6756	193		
Germany	Eberswalde ⁵	NCE	DEEb3996	13.8109	52.8331	195	3	4,13
Germany	Entin ⁵	NCE	DEEn0005	10.6038	54.1359	196		
Germany	Hartz Mts ¹	NCE	DEHM0001	10.6667	51.7500	197		
Germany	Norderoo ⁵	NCE	DENN0002	9.1759	54.5896	198	3	
Germany	Norderoo ⁵	NCE	DENN0003	9.1759	54.5896	199	3	
Germany	Oetisheim ⁶	NCI	DEOe0001	8.7915	48.9708	200		
Ireland	Adare, Limerick ³	Pyr	IELi0058	-8.8342	52.5842	141		
Ireland	Adare, Limerick ³	Pyr	IELi0059	-8.8342	52.5842	142		
Ireland	Adare, Limerick ³	Pyr	IELi0060	-8.8342	52.5842	143		
Ireland	Adare, Limerick ³	Pyr	IELi0068	-8.8342	52.5842	127		
Ireland	Adare, Limerick ³	Pyr	IELi0069	-8.7692	52.6175	127		
Ireland	Adare, Limerick ³	Pyr	IELi0080	-8.7692	52.6175	127		
Ireland	Adare, Limerick ³	Pyr	IELi0082	-8.7692	52.6175	144		
Ireland	Aran Island ⁶	Pyr	IEAI0001	-8.5286	54.9934	127	8	
Ireland	Ballinamore, Leitrim ³	Pyr	IELe0001	-7.7861	53.9583	140		
Ireland	Ballinamore, Leitrim ³	Pyr	IELe0007	-7.7861	53.9583	127		
Ireland	Ballinamore, Leitrim ³	Pyr	IELe0008	-7.7689	53.9911	127		
Ireland	Ballinamore, Leitrim ³	Pyr	IELe0018	-7.7733	53.9867	127		

Leitrim ³						
Ireland	Ballinamore, Leitrim ³	Pyr	IELe0019	-7.7733	53.9867	127
Ireland	Ballycastle, Mayo ³	Pyr	IEMa0032	-9.3167	54.2333	147
Ireland	Ballycastle, Mayo ³	Pyr	IEMa0037	-9.3167	54.2333	148
Ireland	Camolin, Wexford ¹	Pyr	IECa0001	-6.4167	52.5833	244
Ireland	Camolin, Wexford ³	Pyr	IEWe0036	-6.4167	52.5833	152
Ireland	Camolin, Wexford ³	Pyr	IEWe0054	-6.4167	52.5833	127
Ireland	Camolin, Wexford ³	Pyr	IEWe0055	-6.4167	52.5833	127
Ireland	Carlingford, Louth ³	Pyr	IELo011a	-6.1833	54.0333	145
Ireland	Carlingford, Louth ³	Pyr	IELo011b	-6.1833	54.0333	145
Ireland	Carlingford, Louth ³	Pyr	IELo011c	-6.1833	54.0333	145
Ireland	Castlebridge ¹	Pyr	IECt0001	-6.5000	52.4167	246
Ireland	Cloghan ¹	Pyr	IECI0001	-7.7500	53.2500	245
Ireland	Durrow, Laois ³	Pyr	IELa0LSa	-7.5000	52.7833	138
Ireland	Durrow, Laois ³	Pyr	IELa0LSb	-7.5000	52.7833	139
Ireland	Durrow, Laois ³	Pyr	IELa0LSc	-7.5000	52.7833	127
Ireland	Glendalough, Wicklow ³	Pyr	IEWi00Qa	-6.3833	53.0000	127
Ireland	Glendalough, Wicklow ³	Pyr	IEWi00Qb	-6.3833	53.0000	154
Ireland	Glendalough, Wicklow ³	Pyr	IEWi00Qc	-6.3833	53.0000	127
Ireland	Greysteel, Derry ³	Pyr	IEDy0001	-7.2500	55.0000	127
Ireland	Greysteel, Derry ³	Pyr	IEDy0003	-7.2500	55.0000	128
Ireland	Greysteel, Derry ³	Pyr	IEDy0004	-7.2500	55.0000	127
Ireland	Greysteel, Derry ³	Pyr	IEDy0005	-7.2500	55.0000	128
Ireland	Greysteel, Derry ³	Pyr	IEDy0006	-7.2500	55.0000	128
Ireland	Greysteel, Derry ³	Pyr	IEDy0007	-7.2500	55.0000	128
Ireland	Greysteel, Derry ³	Pyr	IEDy0008	-7.2500	55.0000	128
Ireland	Greysteel, Derry ³	Pyr	IEDy0009	-7.2500	55.0000	128
Ireland	Greysteel, Derry ³	Pyr	IEDy0010	-7.2500	55.0000	128
Ireland	Greysteel, Derry ³	Pyr	IEDy0011	-7.2500	55.0000	128
Ireland	Greysteel, Derry ³	Pyr	IEDy0012	-7.2500	55.0000	128
Ireland	Gweedore, Donegal ³	Pyr	IEGW0001	-8.2300	55.0500	133
Ireland	Gweedore, Donegal ³	Pyr	IEGW0026	-8.2300	55.0500	133
Ireland	Gweedore, Donegal ³	Pyr	IEGW005a	-8.2300	55.0500	133
Ireland	Gweedore, Donegal ³	Pyr	IEGW005b	-8.2300	55.0500	133
Ireland	Kill, Waterford ³	Pyr	IEWa0001	-7.3333	52.1750	150
Ireland	Kill, Waterford ³	Pyr	IEWa0002	-7.3333	52.1750	127
Ireland	Kill, Waterford ³	Pyr	IEWa0003	-7.3333	52.1750	136
Ireland	Kill, Waterford ³	Pyr	IEWa0004	-7.3333	52.1750	150
Ireland	Kill, Waterford ³	Pyr	IEWa0005	-7.3333	52.1750	136
Ireland	Killala, Mayo ³	Pyr	IEMa0020	-9.2500	54.1667	146
Ireland	Killala, Mayo ³	Pyr	IEMa0025	-9.2500	54.1667	146
Ireland	Killarney, Kerry ³	Pyr	IEKe0001	-9.5333	52.0556	127
Ireland	Killarney, Kerry ³	Pyr	IEKe0002	-9.5333	52.0556	134
Ireland	Killarney, Kerry ³	Pyr	IEKe0004	-9.5333	52.0556	127
Ireland	Killarney, Kerry ³	Pyr	IEKe0005	-9.5333	52.0556	127
Ireland	Killarney, Kerry ³	Pyr	IEKeP3kY	-9.5333	52.0556	135
Ireland	Kinvarra, Galway ³	Pyr	IEGa0039	-8.8667	53.1500	129
Ireland	Kinvarra, Galway ³	Pyr	IEGa0046	-8.8667	53.1500	130
Ireland	Kinvarra, Galway ³	Pyr	IEGa0047	-8.9667	53.1333	127
Ireland	Kinvarra, Galway ³	Pyr	IEGa0050	-8.9667	53.1333	131
Ireland	Kinvarra, Galway ³	Pyr	IEGa0057	-8.9667	53.1333	132
Ireland	Mountcharles, Donegal ³	Pyr	IEDN0001	-8.3000	54.6500	125
Ireland	Mountcharles, Donegal ³	Pyr	IEDN0009	-8.3000	54.6500	126
Ireland	Offaly, Cloghan ³	Pyr	IEOf0019	-7.7500	53.2500	149

Ireland	Offaly, Cloghan ³	Pyr	IEOf0026	-7.7500	53.2500	127		
Ireland	Offaly, Cloghan ³	Pyr	IEOf0048	-7.7500	53.2500	149		
Ireland	Rathangan, Kildare ³	Pyr	IEKi0084	-6.9778	53.2797	127		
Ireland	Rathangan, Kildare ³	Pyr	IEKi0085	-6.9778	53.2797	127		
Ireland	Rathangan, Kildare ³	Pyr	IEKi0086	-6.9778	53.2797	136		
Ireland	Rathangan, Kildare ³	Pyr	IEKi0087	-6.9778	53.2797	127		
Ireland	Rathangan, Kildare ³	Pyr	IEKi0089	-6.9778	53.2797	137		
Ireland	Slane ¹	Pyr	IESI0001	-6.5000	53.7500	127		
Ireland	Tintern Abbey, Wexford ³	Pyr	IEWe0005	-6.8417	52.2333	151		
Ireland	Tintern Abbey, Wexford ³	Pyr	IEWe0008	-6.8417	52.2333	127		
Ireland	Tintern Abbey, Wexford ³	Pyr	IEWe0018	-6.8417	52.2333	151		
Ireland	Tintern Abbey, Wexford ³	Pyr	IEWe0031	-6.8417	52.2333	127		
Ireland	Tintern Abbey, Wexford ³	Pyr	IEWe0033	-6.8417	52.2333	151		
Ireland	Tintern Abbey, Wexford ³	Pyr	IEWe020a	-6.8417	52.2333	127		
Ireland	Tintern Abbey, Wexford ³	Pyr	IEWe023a	-6.8417	52.2333	153		
Ireland	Tintern Abbey, Wexford ³	Pyr	IEWe023b	-6.8417	52.2333	127		
Ireland	Whiting Bay, Cork ¹	Pyr	IEWB0001	-7.8333	51.8333	247		
Ireland	Whiting Bay, Cork ¹	Pyr	IEWB0002	-7.8333	51.8333	248		
Ireland	Whiting Bay, Cork ¹	Pyr	IEWB0003	-7.8333	51.8333	118		
Ireland	Whiting Bay, Cork ³	Pyr	IECo0095	-7.8283	51.9494	118		
Ireland	Whiting Bay, Cork ³	Pyr	IECo0098	-7.8283	51.9494	118		
Ireland	Whiting Bay, Cork ³	Pyr	IECo0099	-7.8283	51.9494	118		
Ireland	Whiting Bay, Cork ³	Pyr	IECo0100	-7.8283	51.9494	119		
Ireland	Whiting Bay, Cork ³	Pyr	IECo0101	-7.8283	51.9494	118		
Ireland	Whiting Bay, Cork ³	Pyr	IECo0102	-7.8283	51.9494	120		
Ireland	Whiting Bay, Cork ³	Pyr	IECo0103	-7.8283	51.9494	121		
Ireland	Whiting Bay, Cork ³	Pyr	IECo0104	-7.8283	51.9494	122		
Ireland	Whiting Bay, Cork ³	Pyr	IECo0105	-7.8283	51.9494	123		
Ireland	Whiting Bay, Cork ³	Pyr	IECo0108	-7.8283	51.9494	124		
Italy	Abruzzo ¹	NCl	ITAb0001	14.0000	42.0000	249		
Italy	Abruzzo ¹	NCl	ITAb0002	14.0000	42.0000	250		
Italy	Camigliatello, Calabria ⁴	Slta	ITCa5342	16.4460	39.3386	251	11	10
Italy	Castelfranco, Toscana ⁴	NCl	ITTo1578	11.5501	43.6176	262		
Italy	La Sila, Calabria ⁴	Slta	ITSi0011	16.4911	39.3522	258		11
Italy	La Sila, Calabria ⁴	Slta	ITSi0017	16.4911	39.3522	259	11	4,9
Italy	La Sila, Calabria ⁴	Slta	ITSi0021	16.4911	39.3522	260	11	4
Italy	Laghi di Ceretto ²	Iber	ITLC0001	10.2426	44.2978	218	5	
Italy	Majella Mts, Abruzzo ⁴	NCl	ITMa00NT	13.9284	42.2854	250		
Italy	Majella Mts, Abruzzo ⁴	NCl	ITMa0175	14.1157	42.0834	254		4,5
Italy	Majella Mts, Abruzzo ⁴	NCl	ITMa0176	14.1157	42.0834	250		4
Italy	Majella Mts, Abruzzo ⁴	NCl	ITMa0177	14.1157	42.0834	255		
Italy	Majella Mts, Abruzzo ⁴	NCl	ITMa0178	14.1157	42.0834	250		
Italy	Majella Mts, Abruzzo ⁴	NCl	ITMa0179	14.1157	42.0834	254	5	
Italy	Prasota, Mazzo ⁴	NCl	ITPr0001	10.2480	46.2870	256		
Italy	Prasota, Mazzo ⁴	NCE	ITPr0004	10.2480	46.2870	257	2	
Italy	San Carlo di Cese ⁴	NCl	ITGe0001	8.8320	44.4773	252		

Italy	Trento ¹	NCI	ITTr0001	11.8333	46.2500	263		
Italy	Trento ¹	NCE	ITTr0002	11.8333	46.2500	264		
Italy	Valbrevenna, Genova ⁴	NCI	ITGe0003	9.0648	44.5553	253		
Italy	Valle Aosta, Torgnon ⁴	NCE	ITTg0049	7.5712	45.8072	261		
Lithuania	Vilnius ¹	NCE	LTVi0001	25.3167	54.6667	265		
Lithuania	Vilnius ¹	NCE	LTVi0002	25.3167	54.6667	266		
Macedonia	Jakupica Mts ⁶	Balk	MKJa1247	21.4189	41.6891	269		
Macedonia	Jakupica Mts ⁶	Balk	MKJa9222	21.4189	41.6891	270		
Macedonia	Mount Galicica ⁶	Balk	MKMG0001	20.8508	41.1015	271		4
Macedonia	Pelister Mts ¹	Balk	MKPe0001	21.1667	41.0000	272		
Montenegro	Lovćen ⁶	Balk	MELo6362	18.8188	42.4058	267		
Montenegro	Mount Komovi ⁶	Balk	MEMK0001	19.6581	42.6947	268	12	4
Netherlands	Ameland, Friesland ⁵	NCE	NLFr0017	5.7960	53.4453	10		
Netherlands	Ameland, Friesland ⁵	NCE	NLFr0040	5.7960	53.4453	10		
Netherlands	Boxtel ¹	NCE	NLBo0001	5.3333	51.6000	273		
Netherlands	Callantsoog ⁵	NCE	NLCa0002	4.6937	52.8303	274		
Netherlands	Dieren, Gelderland ⁵	NCE	NLDi0001	6.0815	52.0479	10		
Netherlands	Diessen ⁵	NCE	NLDi0062	5.1752	51.4748	201		
Netherlands	Overijssel ⁵	NCE	NLOv0042	6.4570	52.4953	275		
Netherlands	Wageningen ¹	NCE	NLWa0001	5.6667	51.9667	276		
Netherlands	Zeeuws Vlaanderen ⁵	NCE	NLZV0044	5.7221	52.7181	273	8	
Norway	Askland ³	NCE	NOAs0301	8.4500	58.6000	155		
Poland	Blizocin ¹	NCE	PLBI0001	22.2667	51.6000	278		
Russia	Brjansk ¹	NCE	RUBr0001	34.0000	52.3333	280		
Russia	Brjansk ¹	NCE	RUBr0002	34.0000	52.3333	281		
Russia	Lake Baikal, Siberia ¹	NCE	RULB0001	108.0000	53.6667	282		
Russia	Novosibirsk, Siberia ¹	NCE	RUNo0002	83.1000	54.8167	284		
Russia	Novosibirsk, Siberia ¹	NCE	RUNo0003	83.1000	54.8167	285		
Russia	Novosibirsk, Siberia ²	NCE	RUNo0001	82.7791	55.2014	283		
Russia	Pertozero ¹	NCE	RUPe0001	34.0000	62.0833	286		
Russia	Tambov ¹	NCE	RUTa0001	42.2500	51.9167	287		
Russia	Tambov ¹	NCE	RUTa0002	42.2500	51.9167	288		
Serbia	Jastrebac ⁶	Balk	RSJa7390	20.5871	44.0936	279		
Serbia	Mount Kopaonik ⁶	Balk	RSMK1078	20.8936	43.1632	270		
Serbia	Mount Kopaonik ⁶	Balk	RSMK7008	20.8936	43.1632	270	13	
Serbia	Valjevo ⁶	Balk	RSVa7855	19.8828	44.2463	270		
Slovakia	Bratislava ⁵	NCE	SKBr5733	17.1077	48.1479	161	3	
Slovakia	Bratislava ⁵	NCE	SKBr5736	17.1077	48.1479	302		
Slovakia	Bratislava ⁵	NCE	SKBr5743	17.1077	48.1479	161	3	
Slovakia	Bratislava ⁶	Balk	SKBr5730	17.1077	48.1479	301		
Slovakia	Bratislava ⁶	Balk	SKBr5734	17.1077	48.1479	301	3	
Slovakia	Bratislava ⁶	Balk	SKBr5735	17.1077	48.1479	301		
Slovakia	Kezmarok, Jezerko ⁵	NCE	SKKe0418	20.3711	49.2887	44	3	
Slovakia	Kezmarok, Jezerko ⁵	NCE	SKKe0419	20.3711	49.2887	97	3	4
Slovenia	Nova Gorica, Anhovo ⁴	NCI	SING0001	13.6571	45.9447	299		4
Slovenia	Postjma ⁴	NCI	SIPo0001	14.2082	45.7811	300	14	4
Spain	Cantabria ⁶	Pyr	ESEM0069	-3.4503	43.1423	213	8	6
Spain	Navarra ⁶	Pyr	ESNa0047	-1.6455	43.1757	214		
Spain	Navarra ⁶	Pyr	ESNa0861	-1.6455	43.1757	127		
Spain	Navarra ⁶	Pyr	ESNa1131	-1.6455	43.1757	127		
Spain	Navarra ⁶	Pyr	ESNa1286	-1.6455	43.1757	214		
Spain	Picos de Europa ⁶	Iber	ESPE0047	-4.9997	43.1049	215	9	4,6

Spain	Picos de Europa ⁶	Iber	ESPE0057	-4.9997	43.1049	216	8	2
Spain	Pyrenees ⁶	Pyr	ESBa9709	1.1136	42.5650	212		
Spain	Rascafria ¹	Iber	ESRa0001	-3.8833	40.9000	217		
Spain	Rascafria ¹	Iber	ESRa0002	-3.8833	40.9000	218		
Spain	Rascafria ¹	Iber	ESRa0003	-3.8833	40.9000	219		
Spain	Rascafria ⁶	Iber	ESRa0640	-3.8794	40.9036	220	8	4,6,7,8
Spain	Rascafria ⁶	Balk	ESRa3448	-3.8794	40.9036	221		
Spain	Rascafria ⁶	Iber	ESRa5939	-3.8794	40.9036	218	8	4
Sweden	Jamj ¹	NCE	SEJa0001	15.8667	56.1667	292		
Sweden	Jamj ¹	NCE	SEJa0002	15.8667	56.1667	293		
Sweden	Oland ¹	NCE	SEOI0001	17.0833	57.2667	294		
Sweden	Oland ¹	NCE	SEOI0002	17.0833	57.2667	295		
Sweden	Revinge ¹	NCE	SERe0001	14.3333	55.5833	296		
Sweden	Revinge ¹	NCE	SERe0002	14.3333	55.5833	297		
Sweden	Tingstade, Gotland ¹	NCE	SEGo0003	18.6000	57.7000	291		
Sweden	Uppsala ¹	NCE	SEUp0001	17.6667	59.7500	298		
Sweden	Vastergarn, Gotland ¹	NCE	SEGo0001	18.1667	57.4667	289		
Sweden	Vastergarn, Gotland ¹	NCE	SEGo0002	18.1667	57.4667	290		
Switzerland	Bassin, Vaud ¹	NCE	CHBa0001	6.6500	46.5333	166		
Switzerland	Bassins, Vaud ⁴	NCE	CHBa5756	6.2311	46.4628	167	3	
Switzerland	Bassins, Vaud ⁶	NCE	CHBa5698	6.2311	46.4628	315		
Switzerland	Bassins, Vaud ⁶	Balk	CHBa5712	6.2311	46.4628	316		
Switzerland	Bretolet, Valais ⁴	NCI	CHBr5421	6.8652	46.1689	168	5	4,6
Switzerland	Chablais Cudrefin ⁴	NCE	CHCu7581	7.0266	46.9593	172		
Switzerland	Chalet a Gobet ⁴	NCE	CHCG5272	6.6927	46.5646	170		
Switzerland	Chalet des Enfants ⁴	Balk	CHCE0889	6.6644	46.5742	169	3	4
Switzerland	Champmartin ⁴	NCE	CHCh7622	6.9974	46.9327	171	3	
Switzerland	Gletterens ⁴	NCE	CHGI7628	6.9361	46.8927	173	3	
Switzerland	Ostende Chevroux ⁴	NCE	CHOC7576	6.9178	46.8943	173	3	
Switzerland	Ostende Chevroux ⁴	NCE	CHOC7583	6.9178	46.8943	174	3	4,12
Switzerland	Pont de Nant, Vaud ⁶	NCI	CHPN5442	7.0943	46.2491	317		
Switzerland	Val d'Illicz ⁴	NCE	CHVI4747	6.8927	46.2043	175		
Switzerland	Val d'Illicz ⁴	NCI	CHVI4748	6.8927	46.2043	176	3	
Turkey	Anatolia ¹	Out	TRAr0001	31.7238	40.8988	322		
Turkey	Anatolia ⁵	Out	TRAr6106	31.7238	40.8988	321		
Turkey	Anatolia ⁵	Out	TRSA6079	31.7238	40.8988	320		
Turkey	Strandzha Mts ¹	Balk	TRSM0001	27.6833	41.7500	303		
Turkey	Strandzha Mts ¹	Balk	TRSM0002	27.6833	41.7500	304		
Ukraine	Cherkassy ¹	NCE	UACh0001	31.5000	49.7167	305		
Ukraine	Jaduty ⁵	NCE	UAJa0043	32.3167	51.3667	306	3	
Ukraine	Kanev ⁵	NCE	UAKa0024	31.8349	49.6928	307		4
Ukraine	Kanev ⁵	NCE	UAKa0025	31.8349	49.6928	308	3	
Ukraine	Kanev ⁵	NCE	UAKa0250	31.8349	49.6928	308		
Ukraine	L'Vov ⁵	NCE	UALV0255	31.0833	47.9000	309	3	
Ukraine	Tishki ⁵	NCE	UATi0266	33.1109	50.1076	310		
Ukraine	Vinnitsa ⁵	NCE	DEBK0020	8.7846	54.6756	194		
Ukraine	Vinnitsa ⁵	NCE	UAVi0253	28.5623	49.2307	311	3	
Ukraine	Vinnitsa ⁵	NCE	UAVi0254	28.5623	49.2307	312	3	
Ukraine	Volyn ⁵	NCE	DEBK0021	8.7846	54.6756	193		
Ukraine	Volyn ⁵	NCE	UAVo0256	24.8567	51.1240	313		
Ukraine	Zhitomer ⁵	NCE	UAZh0257	28.6149	50.2617	314		

¹Mascheretti et al. (2003)

²Ohdachi et al. (2006)

³Searle et al. (2009)

⁴Vega et al. (2010a)

⁵Vega et al. (2010b)

⁶This study

Pyr = Pyrenean

NCE = North-Central European

NCI = North-Central Italian

Balk = Balkan

SIIta = South Italian

Iber = Iberia

Out = Outgroup

OM = Orkney Mainland

OS = Orkney South Ronaldsay

OW = Orkney Westray

Appendix 4. List of mandible and skull samples for geometric morphometric analysis.

Mandible and skull datasets for geometric morphometric analysis.

Country	Code	Phylo group	Longitude (Decimal)	Latitude (Decimal)	Mandible	Skull	Group	Island Size Category
Austria	ATDo1611	Balk	16.6413	47.8957	x	x		
Austria	ATDo1612	NCE	16.6413	47.8957	x	x		
Austria	ATUmA139	NCE	10.9277	47.1361	x			
Bosnia Herzegovina	BAKu2517	Balk	17.3207	44.0022	x	x		
Bosnia Herzegovina	BAOs5670	Balk	16.2887	44.2397	x	x		
Bosnia Herzegovina	BAZe4239	Balk	18.3889	43.3949	x	x		
Britain	GBCa1	NCE	-0.8926	53.9647	x	x		
Britain	GBCH1	NCE	-0.9104	54.1209	x	x		
Britain	GBDrG140	NCE	-4.4893	57.3090	x			
Britain	GBHe1	NCE	-1.0577	53.9432	x	x		
Britain	OMHa10	OM	-3.1902	59.0337	x	x	Main1	Med
Britain	OMHa11	OM	-3.1902	59.0337	x	x	Main1	Med
Britain	OMHa12	OM	-3.1902	59.0337	x	x	Main1	Med
Britain	OMHa3BM	OM	-3.1902	59.0337	x	x	Main1	Med
Britain	OMHa3CM	OM	-3.1902	59.0337	x	x	Main1	Med
Britain	OMHa3M	OM	-3.1902	59.0337	x	x	Main1	Med
Britain	OMHa4	OM	-3.1902	59.0337	x	x	Main1	Med
Britain	OMHa6	OM	-3.1902	59.0337	x	x	Main1	Med
Britain	OMHa9F	OM	-3.1902	59.0337	x	x	Main1	Med
Britain	OMHa9Fb	OM	-3.1902	59.0337	x		Main1	Med
Britain	OMHa9M	OM	-3.1902	59.0337	x	x	Main1	Med
Britain	OMHo15	OM	-3.0676	58.9464	x	x	Main2	Med
Britain	OMSa1	OM	-3.2972	59.0483	x	x	Main1	Med
Britain	OMSa2	OM	-3.2972	59.0483	x	x	Main1	Med
Britain	OMSO1	OM	-2.9500	58.9500	x		Main2	Med
Britain	OMSO10F	OM	-2.9500	58.9500	x	x	Main2	Med
Britain	OMSO11	OM	-2.9500	58.9500	x	x	Main2	Med
Britain	OMSO12	OM	-2.9500	58.9500	x	x	Main2	Med
Britain	OMSO13	OM	-2.9500	58.9500	x	x	Main2	Med
Britain	OMSO15	OM	-2.9500	58.9500	x	x	Main2	Med
Britain	OMSO16	OM	-2.9500	58.9500	x	x	Main2	Med
Britain	OMSO17	OM	-2.9500	58.9500	x	x	Main2	Med
Britain	OMSO18	OM	-2.9500	58.9500	x	x	Main2	Med
Britain	OMSO2	OM	-2.9500	58.9500	x		Main2	Med
Britain	OMSO20	OM	-2.9500	58.9500	x	x	Main2	Med
Britain	OMSO21	OM	-2.9500	58.9500	x	x	Main2	Med
Britain	OMSO24	OM	-2.9500	58.9500	x	x	Main2	Med
Britain	OMSO25	OM	-2.9500	58.9500	x	x	Main2	Med
Britain	OMSO26	OM	-2.9500	58.9500	x	x	Main2	Med
Britain	OMSO28	OM	-2.9500	58.9500	x	x	Main2	Med
Britain	OMSO29	OM	-2.9500	58.9500	x	x	Main2	Med
Britain	OMSO3	OM	-2.9500	58.9500	x	x	Main2	Med
Britain	OMSO30	OM	-2.9500	58.9500	x	x	Main2	Med
Britain	OMSO31	OM	-2.9500	58.9500	x	x	Main2	Med
Britain	OMSO35	OM	-2.9500	58.9500	x	x	Main2	Med
Britain	OMSO36	OM	-2.9500	58.9500	x	x	Main2	Med
Britain	OMSO37	OM	-2.9500	58.9500	x	x	Main2	Med

Britain	OMSO38	OM	-2.9500	58.9500	x	x	Main2	Med
Britain	OMSO4	OM	-2.9500	58.9500	x	x	Main2	Med
Britain	OMSO5	OM	-2.9500	58.9500	x	x	Main2	Med
Britain	OMSO6M	OM	-2.9500	58.9500	x	x	Main2	Med
Britain	OMSO7F	OM	-2.9500	58.9500	x	x	Main2	Med
Britain	OMSO8M	OM	-2.9500	58.9500	x	x	Main2	Med
Britain	OMSO9F	OM	-2.9500	58.9500	x	x	Main2	Med
Britain	OMTa10	OM	-2.8500	58.9500	x	x	Main2	Med
Britain	OMTa2	OM	-2.8500	58.9500	x	x	Main2	Med
Britain	OMTa3	OM	-2.8500	58.9500	x	x	Main2	Med
Britain	OMTa4	OM	-2.8500	58.9500	x	x	Main2	Med
Britain	OMTa5	OM	-2.8500	58.9500	x	x	Main2	Med
Britain	OMTa6	OM	-2.8500	58.9500	x	x	Main2	Med
Britain	OMTa7	OM	-2.8500	58.9500	x	x	Main2	Med
Britain	OMTa8	OM	-2.8500	58.9500	x	x	Main2	Med
Britain	OMTa9	OM	-2.8500	58.9500		x	Main2	Med
Britain	OSGr10	OS	-2.9167	58.8167	x	x	Grimn	Small
Britain	OSGr12	OS	-2.9167	58.8167	x	x	Grimn	Small
Britain	OSGr14	OS	-2.9167	58.8167	x	x	Grimn	Small
Britain	OSGr15	OS	-2.9167	58.8167	x	x	Grimn	Small
Britain	OSGr18	OS	-2.9167	58.8167	x	x	Grimn	Small
Britain	OSGr20	OS	-2.9167	58.8167	x	x	Grimn	Small
Britain	OSGr23	OS	-2.9167	58.8167	x	x	Grimn	Small
Britain	OSGr25	OS	-2.9167	58.8167	x	x	Grimn	Small
Britain	OSGr27	OS	-2.9167	58.8167	x	x	Grimn	Small
Britain	OSGr28	OS	-2.9167	58.8167	x	x	Grimn	Small
Britain	OSGr31	OS	-2.9167	58.8167	x	x	Grimn	Small
Britain	OSGr35	OS	-2.9167	58.8167	x	x	Grimn	Small
Britain	OSGr39	OS	-2.9167	58.8167	x	x	Grimn	Small
Britain	OSGr42	OS	-2.9167	58.8167	x	x	Grimn	Small
Britain	OSGr45	OS	-2.9167	58.8167	x	x	Grimn	Small
Britain	OSGr49	OS	-2.9167	58.8167	x	x	Grimn	Small
Britain	OSGr50	OS	-2.9167	58.8167	x	x	Grimn	Small
Britain	OSGr7	OS	-2.9167	58.8167	x		Grimn	Small
Britain	OSGr8	OS	-2.9167	58.8167	x	x	Grimn	Small
Britain	OSGr9	OS	-2.9167	58.8167	x	x	Grimn	Small
Britain	OSWW11	OS	-2.9407	58.7668	x	x	Wind	Small
Britain	OSWW12	OS	-2.9407	58.7668	x	x	Wind	Small
Britain	OSWW13	OS	-2.9407	58.7668	x	x	Wind	Small
Britain	OSWW14	OS	-2.9407	58.7668	x	x	Wind	Small
Britain	OSWW15	OS	-2.9407	58.7668	x	x	Wind	Small
Britain	OSWW16	OS	-2.9407	58.7668	x		Wind	Small
Britain	OSWW17	OS	-2.9407	58.7668	x	x	Wind	Small
Britain	OSWW18	OS	-2.9407	58.7668	x	x	Wind	Small
Britain	OSWW19	OS	-2.9407	58.7668	x	x	Wind	Small
Britain	OSWW20	OS	-2.9407	58.7668	x	x	Wind	Small
Britain	OSWW21	OS	-2.9407	58.7668	x	x	Wind	Small
Britain	OSWW23	OS	-2.9407	58.7668	x	x	Wind	Small
Britain	OSWW24	OS	-2.9407	58.7668	x	x	Wind	Small
Britain	OSWW25	OS	-2.9407	58.7668	x	x	Wind	Small
Britain	OSWW26	OS	-2.9407	58.7668	x	x	Wind	Small
Britain	OSWW28	OS	-2.9407	58.7668	x	x	Wind	Small
Britain	OSWW6	OS	-2.9407	58.7668	x	x	Wind	Small
Britain	OSWW7	OS	-2.9407	58.7668	x	x	Wind	Small
Britain	OSWW8	OS	-2.9407	58.7668	x	x	Wind	Small
Britain	OSWW9	OS	-2.9407	58.7668	x		Wind	Small
Britain	OWLS1	OW	-2.9334	59.2833	x	x	Swart	Small
Britain	OWLS112	OW	-2.9334	59.2833	x	x	Swart	Small
Britain	OWLS2	OW	-2.9334	59.2833	x	x	Swart	Small
Britain	OWLS24	OW	-2.9334	59.2833	x	x	Swart	Small

Britain	OWLS25	OW	-2.9334	59.2833	x	x	Swart	Small
Britain	OWLS36	OW	-2.9334	59.2833	x	x	Swart	Small
Britain	OWLS37	OW	-2.9334	59.2833	x	x	Swart	Small
Britain	OWLS38	OW	-2.9334	59.2833	x	x	Swart	Small
Britain	OWLS55	OW	-2.9334	59.2833	x	x	Swart	Small
Britain	OWLS59	OW	-2.9334	59.2833	x	x	Swart	Small
Britain	OWLS6	OW	-2.9334	59.2833	x	x	Swart	Small
Britain	OWLS60	OW	-2.9334	59.2833	x	x	Swart	Small
Britain	OWLS61	OW	-2.9334	59.2833	x	x	Swart	Small
Britain	OWLS72	OW	-2.9334	59.2833	x	x	Swart	Small
Britain	OWLS73	OW	-2.9334	59.2833	x	x	Swart	Small
Britain	OWLS82	OW	-2.9334	59.2833	x	x	Swart	Small
Britain	OWLS83	OW	-2.9334	59.2833	x	x	Swart	Small
Britain	OWLS84	OW	-2.9334	59.2833	x	x	Swart	Small
Britain	OWLS85	OW	-2.9334	59.2833	x	x	Swart	Small
Britain	OWLS99	OW	-2.9334	59.2833	x	x	Swart	Small
Britain	OWNe102	OW	-2.8667	59.2334	x	x	Ness	Small
Britain	OWNe103	OW	-2.8667	59.2334	x	x	Ness	Small
Britain	OWNe2	OW	-2.8667	59.2334	x	x	Ness	Small
Britain	OWNe26	OW	-2.8667	59.2334	x	x	Ness	Small
Britain	OWNe28	OW	-2.8667	59.2334	x	x	Ness	Small
Britain	OWNe29	OW	-2.8667	59.2334	x	x	Ness	Small
Britain	OWNe30	OW	-2.8667	59.2334	x	x	Ness	Small
Britain	OWNe31	OW	-2.8667	59.2334	x	x	Ness	Small
Britain	OWNe4	OW	-2.8667	59.2334	x	x	Ness	Small
Britain	OWNe41	OW	-2.8667	59.2334	x	x	Ness	Small
Britain	OWNe42	OW	-2.8667	59.2334	x	x	Ness	Small
Britain	OWNe43	OW	-2.8667	59.2334	x	x	Ness	Small
Britain	OWNe47	OW	-2.8667	59.2334	x		Ness	Small
Britain	OWNe6	OW	-2.8667	59.2334	x	x	Ness	Small
Britain	OWNe62	OW	-2.8667	59.2334	x	x	Ness	Small
Britain	OWNe68	OW	-2.8667	59.2334	x	x	Ness	Small
Britain	OWNe7	OW	-2.8667	59.2334	x	x	Ness	Small
Britain	OWNe75	OW	-2.8667	59.2334	x	x	Ness	Small
Britain	OWNe89	OW	-2.8667	59.2334	x	x	Ness	Small
Britain	OWNe90	OW	-2.8667	59.2334	x	x	Ness	Small
Czech Republic	CZHa9166	NCI	15.5607	49.6048	x	x		
Czech Republic	CZSS4767	NCI	13.4755	49.0656	x	x		
Czech Republic	CZSS4838	NCI	13.4755	49.0656	x	x		
Finland	FIAE1747	NCE	19.6118	60.2037	x	x		
Finland	FIAE1760	NCE	19.6118	60.2037	x	x		
Finland	FIKu2071	NCE	29.4957	64.1254	x	x		
Finland	FISo1773	NCE	27.5296	63.6695	x	x		
Finland	FISo1779	NCE	27.5296	63.6695	x	x		
Finland	FISo1783	NCE	27.5296	63.6695	x	x		
Finland	FISo1785	NCE	27.5296	63.6695	x	x		
France	FRAF174	NCE	5.6397	48.8561	x			
France	FRAF175	NCE	5.6397	48.8561	x			
France	FRAF176	NCE	5.6397	48.8561	x			
France	FRAF179	NCE	5.6397	48.8561	x			
France	FRAF180	NCE	5.6397	48.8561	x			
France	FRAF181	NCE	5.6397	48.8561	x			
France	FRAF182	NCE	5.6397	48.8561	x			
France	FRAF183	NCE	5.6397	48.8561	x			
France	FRAF184	NCE	5.6397	48.8561	x			
France	FRAF185	NCE	5.6397	48.8561	x			
France	FRAF186	NCE	5.6397	48.8561	x			
France	FRAF187	NCE	5.6397	48.8561	x			

France	FRAF188	NCE	5.6397	48.8561	x		
France	FRAF189	NCE	5.6397	48.8561	x		
France	FRAF190	NCE	5.6397	48.8561	x		
France	FRAF192	NCE	5.6397	48.8561	x		
France	FRAF193	NCE	5.6397	48.8561	x		
France	FRAF194	NCE	5.6397	48.8561	x		
France	FRAF195	NCE	5.6397	48.8561	x		
France	FRAF196A	NCE	5.6397	48.8561	x		
France	FRAF196B	NCE	5.6397	48.8561	x		
France	FRAF197	NCE	5.6397	48.8561	x		
France	FRAF198	NCE	5.6397	48.8561	x		
France	FRBe19	NCE	5.2656	45.2033	x		
France	FRBe20	NCE	5.2656	45.2033	x		
France	FRBe21	NCE	5.2656	45.2033	x		
France	FRBI100	Pyr	-3.1958	47.3375	x	B Ile	Small
France	FRBI101	Pyr	-3.1958	47.3375	x	B Ile	Small
France	FRBI102	Pyr	-3.1958	47.3375	x	B Ile	Small
France	FRBI103	Pyr	-3.1958	47.3375	x	B Ile	Small
France	FRBI104	Pyr	-3.1958	47.3375	x	B Ile	Small
France	FRBI105	Pyr	-3.1958	47.3375	x	B Ile	Small
France	FRBI106	Pyr	-3.1958	47.3375	x	B Ile	Small
France	FRBI107	Pyr	-3.1958	47.3375	x	B Ile	Small
France	FRBI108	Pyr	-3.1958	47.3375	x	B Ile	Small
France	FRBI109	Pyr	-3.1958	47.3375	x	B Ile	Small
France	FRBI110	Pyr	-3.1958	47.3375	x	B Ile	Small
France	FRBI111	Pyr	-3.1958	47.3375	x	B Ile	Small
France	FRBI93	Pyr	-3.1958	47.3375	x	B Ile	Small
France	FRBI94	Pyr	-3.1958	47.3375	x	B Ile	Small
France	FRBI95	Pyr	-3.1958	47.3375	x	B Ile	Small
France	FRBI96	Pyr	-3.1958	47.3375	x	B Ile	Small
France	FRBI97	Pyr	-3.1958	47.3375	x	B Ile	Small
France	FRBI98	Pyr	-3.1958	47.3375	x	B Ile	Small
France	FRBI99	Pyr	-3.1958	47.3375	x	B Ile	Small
France	FRBo141	NCE	5.7622	48.7475	x		
France	FRBo142	NCE	5.7622	48.7475	x		
France	FRBo143	NCE	5.7622	48.7475	x		
France	FRBo144	NCE	5.7622	48.7475	x		
France	FRBo145	NCE	5.7622	48.7475	x		
France	FRBo146	NCE	5.7622	48.7475	x		
France	FRBo147	NCE	5.7622	48.7475	x		
France	FRBo148	NCE	5.7622	48.7475	x		
France	FRBo149	NCE	5.7622	48.7475	x		
France	FRBo150	NCE	5.7622	48.7475	x		
France	FRBo151	NCE	5.7622	48.7475	x		
France	FRBo152	NCE	5.7622	48.7475	x		
France	FRBo153	NCE	5.7622	48.7475	x		
France	FRBo154	NCE	5.7622	48.7475	x		
France	FRBo155	NCE	5.7622	48.7475	x		
France	FRBo156	NCE	5.7622	48.7475	x		
France	FRBo157	NCE	5.7622	48.7475	x		
France	FRBo158	NCE	5.7622	48.7475	x		
France	FRBo159	NCE	5.7622	48.7475	x		
France	FRBo160	NCE	5.7622	48.7475	x		
France	FRBo161	NCE	5.7622	48.7475	x		
France	FRBo162	NCE	5.7622	48.7475	x		
France	FRBo163	NCE	5.7622	48.7475	x		
France	FRBo164	NCE	5.7622	48.7475	x		
France	FRBo165	NCE	5.7622	48.7475	x		
France	FRBo166	NCE	5.7622	48.7475	x		
France	FRCh043A	NCE	5.4317	45.4447	x		

France	FRCh38	NCE	5.4317	45.4447	x		
France	FRCh39	NCE	5.4317	45.4447	x		
France	FRCh40	NCE	5.4317	45.4447	x		
France	FRCh41	NCE	5.4317	45.4447	x		
France	FRCh42	NCE	5.4317	45.4447	x		
France	FRCh44	NCE	5.4317	45.4447	x		
France	FRCh45	NCE	5.4317	45.4447	x		
France	FRCh46	NCE	5.4317	45.4447	x		
France	FRCh48	NCE	5.4317	45.4447	x		
France	FRCh49	NCE	5.4317	45.4447	x		
France	FRCh50	NCE	5.4317	45.4447	x		
France	FRCh51	NCE	5.4317	45.4447	x		
France	FRCh52	NCE	5.4317	45.4447	x		
France	FRCh54	NCE	5.4317	45.4447	x		
France	FRCh55	NCE	5.4317	45.4447	x		
France	FRCh56	NCE	5.4317	45.4447	x		
France	FRCh58	NCE	5.4317	45.4447	x		
France	FRCM1	NCE	4.7275	45.3847	x		
France	FRCu136	Pyr	3.8850	44.9894	x	France	Cont
France	FRDi3003	NCI	6.1432	46.3568	x	x	
France	FRFS24	NCE	4.6928	45.2975	x		
France	FRFS25	NCE	4.6928	45.2975	x		
France	FRFS26	NCE	4.6928	45.2975	x		
France	FRFT12	NCE	5.5244	45.5275	x		
France	FRGL035A	NCE	5.4206	45.3992	x		
France	FRGL33	NCE	5.4206	45.3992	x		
France	FRGL34	NCE	5.4206	45.3992	x		
France	FRHa59	NCI	6.2847	47.8436	x		
France	FRHa60	NCI	6.2847	47.8436	x		
France	FRHa61	NCI	6.2847	47.8436	x		
France	FRHa62	NCI	6.2847	47.8436	x		
France	FRHa63	NCI	6.2847	47.8436	x		
France	FRHa64	NCI	6.2847	47.8436	x		
France	FRHa65	NCI	6.2847	47.8436	x		
France	FRLa87	NCI	5.4108	48.9397	x		
France	FRLa88	NCI	5.4108	48.9397	x		
France	FRLa89	NCI	5.4108	48.9397	x		
France	FRLe37	NCE	5.1142	45.3000	x		
France	FRLG003A	NCI	5.9031	45.0919	x		
France	FRLG003B	NCI	5.9031	45.0919	x		
France	FRLG003C	NCI	5.9031	45.0919	x		
France	FRLo13	NCE	5.3483	45.4197	x		
France	FRLo14	NCE	5.3483	45.4197	x		
France	FRLV27	NCI	5.5891	45.1280	x		
France	FRMu16	NCE	5.3158	45.2139	x		
France	FRMu36	NCE	5.3158	45.2139	x		
France	FROR15	NCI	5.8706	44.9219	x		
France	FRPD3082	NCE	6.3818	49.0071	x	x	
France	FRSA079A	Pyr	1.1675	44.8867	x	France	Cont
France	FRSA079B	Pyr	1.1675	44.8867	x	France	Cont
France	FRSA168	Pyr	1.1675	44.8867	x	France	Cont
France	FRSA169	Pyr	1.1675	44.8867	x	France	Cont
France	FRSA171	Pyr	1.1675	44.8867	x	France	Cont
France	FRSA172	Pyr	1.1675	44.8867	x	France	Cont
France	FRSA173	Pyr	1.1675	44.8867	x	France	Cont
France	FRSA68	Pyr	1.1675	44.8867	x	France	Cont
France	FRSA69	Pyr	1.1675	44.8867	x	France	Cont
France	FRSA70	Pyr	1.1675	44.8867	x	France	Cont
France	FRSA71	Pyr	1.1675	44.8867	x	France	Cont
France	FRSA72	Pyr	1.1675	44.8867	x	France	Cont

France	FRSA74	Pyr	1.1675	44.8867	x		France	Cont
France	FRSA75	Pyr	1.1675	44.8867	x		France	Cont
France	FRSA77	Pyr	1.1675	44.8867	x		France	Cont
France	FRSA78	Pyr	1.1675	44.8867	x		France	Cont
France	FRSA81	Pyr	1.1675	44.8867	x		France	Cont
France	FRSA82	Pyr	1.1675	44.8867	x		France	Cont
France	FRSA83	Pyr	1.1675	44.8867	x		France	Cont
France	FRSA85	Pyr	1.1675	44.8867	x		France	Cont
France	FRSJ030A	NCE	5.1386	45.5031	x			
France	FRSJ030B	NCE	5.1386	45.5031	x			
France	FRSJ030C	NCE	5.1386	45.5031	x			
France	FRSJ10	NCE	5.1386	45.5031	x			
France	FRSJ11	NCE	5.1386	45.5031	x			
France	FRSJ28	NCE	5.1386	45.5031	x			
France	FRSJ31	NCE	5.1386	45.5031	x			
France	FRSJ32	NCE	5.1386	45.5031	x			
France	FRSJ9	NCE	5.1386	45.5031	x			
France	FRSN117	Pyr	3.7900	44.8911	x		France	Cont
France	FRSN118	Pyr	3.7900	44.8911	x		France	Cont
France	FRSN120	Pyr	3.7900	44.8911	x		France	Cont
France	FRSN121	Pyr	3.7900	44.8911	x		France	Cont
France	FRSN123	Pyr	3.7900	44.8911	x		France	Cont
France	FRSN124	Pyr	3.7900	44.8911	x		France	Cont
France	FRSN125	Pyr	3.7900	44.8911	x		France	Cont
France	FRSN126	Pyr	3.7900	44.8911	x		France	Cont
France	FRSN127	Pyr	3.7900	44.8911	x		France	Cont
France	FRSo091A	NCI	7.3361	47.4839	x			
France	FRSo091B	NCI	7.3361	47.4839	x			
France	FRSo90	NCI	7.3361	47.4839	x			
France	FRSo92	NCI	7.3361	47.4839	x			
France	FRSS3	NCE	4.2125	45.9486	x			
France	FRSS4	NCE	4.2125	45.9486	x			
France	FRSS5	NCE	4.2125	45.9486	x			
France	FRSS6	NCE	4.2125	45.9486	x			
France	FRVa17	NCE	5.4114	45.2569	x			
France	FRVa18	NCE	5.4114	45.2569	x			
France	FRVe129	NCE	4.6633	45.3692	x			
France	FRVe22	NCE	4.6633	45.3692	x			
France	FRVe23	NCE	4.6633	45.3692	x			
France	FRVy7	NCE	4.6572	45.7383	x			
Germany	DEEb3996	NCE	13.8109	52.8331	x	x		
Greece	GREp6406	Balk	21.1692	39.7705	x	x		
Ireland	IECL1	Ire	-7.9480	53.2678	x	x	Cloghan	Large
Ireland	IECL10	Ire	-7.9480	53.2678	x	x	Cloghan	Large
Ireland	IECL11	Ire	-7.9480	53.2678	x	x	Cloghan	Large
Ireland	IECL12	Ire	-7.9480	53.2678	x	x	Cloghan	Large
Ireland	IECL13	Ire	-7.9480	53.2678	x	x	Cloghan	Large
Ireland	IECL14	Ire	-7.9480	53.2678	x	x	Cloghan	Large
Ireland	IECL15	Ire	-7.9480	53.2678	x	x	Cloghan	Large
Ireland	IECL16	Ire	-7.9480	53.2678	x	x	Cloghan	Large
Ireland	IECL17	Ire	-7.9480	53.2678	x	x	Cloghan	Large
Ireland	IECL18	Ire	-7.9480	53.2678	x	x	Cloghan	Large
Ireland	IECL19	Ire	-7.9480	53.2678	x	x	Cloghan	Large
Ireland	IECL2	Ire	-7.9480	53.2678	x	x	Cloghan	Large
Ireland	IECL20	Ire	-7.9480	53.2678	x	x	Cloghan	Large
Ireland	IECL3	Ire	-7.9480	53.2678	x	x	Cloghan	Large
Ireland	IECL4	Ire	-7.9480	53.2678	x	x	Cloghan	Large
Ireland	IECL5	Ire	-7.9480	53.2678	x	x	Cloghan	Large
Ireland	IECL6	Ire	-7.9480	53.2678	x	x	Cloghan	Large
Ireland	IECL7	Ire	-7.9480	53.2678	x	x	Cloghan	Large

Ireland	IECL8	Ire	-7.9480	53.2678	x	x	Cloghan	Large
Ireland	IECL9	Ire	-7.9480	53.2678	x	x	Cloghan	Large
Ireland	IEDY1	Ire	-7.2500	55.0000	x	x	Derry	Large
Ireland	IEDY10	Ire	-7.2500	55.0000	x	x	Derry	Large
Ireland	IEDY11	Ire	-7.2500	55.0000	x	x	Derry	Large
Ireland	IEDY12	Ire	-7.2500	55.0000	x	x	Derry	Large
Ireland	IEDY13	Ire	-7.2500	55.0000	x	x	Derry	Large
Ireland	IEDY14	Ire	-7.2500	55.0000	x	x	Derry	Large
Ireland	IEDY15	Ire	-7.2500	55.0000	x	x	Derry	Large
Ireland	IEDY16	Ire	-7.2500	55.0000	x		Derry	Large
Ireland	IEDY17	Ire	-7.2500	55.0000	x	x	Derry	Large
Ireland	IEDY18	Ire	-7.2500	55.0000	x	x	Derry	Large
Ireland	IEDY19	Ire	-7.2500	55.0000	x	x	Derry	Large
Ireland	IEDY2	Ire	-7.2500	55.0000	x	x	Derry	Large
Ireland	IEDY20	Ire	-7.2500	55.0000	x	x	Derry	Large
Ireland	IEDY3	Ire	-7.2500	55.0000	x	x	Derry	Large
Ireland	IEDY4	Ire	-7.2500	55.0000	x	x	Derry	Large
Ireland	IEDY5	Ire	-7.2500	55.0000	x	x	Derry	Large
Ireland	IEDY6	Ire	-7.2500	55.0000	x	x	Derry	Large
Ireland	IEDY7	Ire	-7.2500	55.0000	x	x	Derry	Large
Ireland	IEDY8	Ire	-7.2500	55.0000	x	x	Derry	Large
Ireland	IEDY9	Ire	-7.2500	55.0000	x		Derry	Large
Ireland	IEE1RV	Ire	-8.3505	54.9503	x	x	Gweed	Large
Ireland	IEE2RV	Ire	-7.5152	54.9754	x	x	Derry	Large
Ireland	IEE3RV	Ire	-7.5152	54.9754	x	x	Derry	Large
Ireland	IEE4RV	Ire	-7.5152	54.9754	x	x	Derry	Large
Ireland	IEGw1	Ire	-8.2300	55.0500	x	x	Gweed	Large
Ireland	IEGw17	Ire	-8.2300	55.0500	x	x	Gweed	Large
Ireland	IEGw1RV	Ire	-8.3833	55.0500	x	x	Gweed	Large
Ireland	IEGw26	Ire	-8.2300	55.0500	x	x	Gweed	Large
Ireland	IEGw3	Ire	-8.2300	55.0500	x	x	Gweed	Large
Ireland	IEGw4	Ire	-8.2300	55.0500	x	x	Gweed	Large
Ireland	IEGw43	Ire	-8.2300	55.0500	x	x	Gweed	Large
Ireland	IEGw46	Ire	-8.2300	55.0500	x	x	Gweed	Large
Ireland	IEGw5	Ire	-8.2300	55.0500	x	x	Gweed	Large
Ireland	IEGw51	Ire	-8.2300	55.0500	x	x	Gweed	Large
Ireland	IEGw51A	Ire	-8.2300	55.0500	x	x	Gweed	Large
Ireland	IEGw51B	Ire	-8.2300	55.0500	x	x	Gweed	Large
Ireland	IEGw51C	Ire	-8.2300	55.0500	x	x	Gweed	Large
Ireland	IEGw55	Ire	-8.2300	55.0500	x	x	Gweed	Large
Ireland	IEGw55B	Ire	-8.2300	55.0500	x	x	Gweed	Large
Ireland	IEGw5b	Ire	-8.2300	55.0500	x		Gweed	Large
Ireland	IEGw5C	Ire	-8.2300	55.0500	x	x	Gweed	Large
Ireland	IEGw64	Ire	-8.2300	55.0500	x	x	Gweed	Large
Ireland	IEGwTILES	Ire	-8.2300	55.0500	x	x	Gweed	Large
Italy	ITAn23	NCI	7.6966	45.8224	x			
Italy	ITCh16	NCI	7.6229	45.6217	x			
Italy	ITCh17	NCI	7.6229	45.6217	x	x		
Italy	ITCh18	NCI	7.6229	45.6217	x			
Italy	ITGa33	NCI	7.8482	45.8519		x		
Italy	ITGa36	NCI	7.8482	45.8519	x	x		
Italy	ITGa38	NCI	7.8482	45.8519	x	x		
Italy	ITMa9815	NCI	14.1157	42.0834	x	x		
Italy	ITMa9830	NCI	14.1157	42.0834	x	x		
Italy	ITMa9832	NCI	14.1157	42.0834	x	x		
Italy	ITMa9833	NCI	14.1157	42.0834	x	x		
Italy	ITMa9834	NCI	14.1157	42.0834	x	x		
Italy	ITMa9835	NCI	14.1157	42.0834	x	x		
Italy	ITMa9849	NCI	14.1157	42.0834	x	x		
Italy	ITMa9850	NCI	14.1157	42.0834	x	x		

Italy	ITMC32500	NCI	10.8360	46.2387	x	
Italy	ITPr0001	NCI	10.2480	46.2870	x	x
Italy	ITPr0004	NCE	10.2480	46.2870	x	x
Italy	ITSC54303	NCI	8.8320	44.4773	x	x
Italy	ITSi11	Slta	16.4911	39.3522	x	x
Italy	ITSi17	Slta	16.4911	39.3522	x	x
Italy	ITSi21	Slta	16.4911	39.3522	x	x
Italy	ITTg47	NCI	7.5712	45.8072	x	x
Italy	ITTg48	NCI	7.5712	45.8072	x	x
Italy	ITTg49	NCE	7.5712	45.8072	x	x
Italy	ITTr17692	NCI	11.8333	46.2500	x	
Italy	ITVB54317	NCI	9.0648	44.5553	x	x
Macedonia	MKBi2450	Balk	20.7688	41.5169	x	
Macedonia	MKJa9212	Balk	21.4189	41.6891	x	x
Macedonia	MKJa9222	Balk	21.4189	41.6891	x	
Macedonia	MKJa9223	Balk	21.4189	41.6891	x	x
Macedonia	MKKo194	Balk	22.3942	41.1544	x	x
Macedonia	MKKo195	Balk	22.3942	41.1544	x	x
Macedonia	MKPe3834	Balk	21.1675	41.0089	x	
Macedonia	MKPe3835	Balk	21.1675	41.0089	x	x
Macedonia	MKPe3836	Balk	21.1675	41.0089		x
Macedonia	MKPe3896	Balk	21.1675	41.0089	x	x
Macedonia	MKPe9494	Balk	21.1675	41.0089	x	x
Macedonia	MKPe9505	Balk	21.1675	41.0089	x	x
Macedonia	MKPe9645	Balk	21.1675	41.0089	x	x
Montenegro	MEBj381	Balk	19.7011	42.8657	x	x
Montenegro	MEBj382	Balk	19.7011	42.8657	x	x
Montenegro	MEBj383	Balk	19.7011	42.8657	x	x
Montenegro	MEDu3403	Balk	19.0412	43.1455	x	x
Montenegro	MEDu3430	Balk	19.0412	43.1455	x	x
Poland	POBie115	NCE	22.5734	53.6439	x	x
Poland	POBie140	NCE	22.5734	53.6439	x	
Poland	POBie141	NCE	22.5734	53.6439	x	x
Poland	POBie151	NCE	22.5734	53.6439	x	x
Poland	POBie355	NCE	22.5734	53.6439	x	x
Poland	POBie373	NCE	22.5734	53.6439	x	x
Poland	POBie376	NCE	22.5734	53.6439	x	x
Poland	POBie377	NCE	22.5734	53.6439	x	x
Poland	POBie392	NCE	22.5734	53.6439	x	x
Poland	POBie912	NCE	22.5734	53.6439	x	x
Poland	POBPN315	NCE	23.9001	52.7095	x	x
Poland	POBPN316	NCE	23.9001	52.7095	x	x
Poland	POBPN318	NCE	23.9001	52.7095	x	x
Poland	POBPN319	NCE	23.9001	52.7095	x	x
Poland	POBPN320	NCE	23.9001	52.7095	x	x
Poland	POBPN345	NCE	23.9001	52.7095	x	x
Poland	POBPN346	NCE	23.9001	52.7095	x	x
Poland	POBPN347	NCE	23.9001	52.7095	x	x
Poland	POBPN402	NCE	23.9001	52.7095	x	x
Poland	POBPN411	NCE	23.9001	52.7095	x	x
Serbia	RSBe178	Balk	20.0800	45.6147	x	x
Serbia	RSKo40169	Balk	20.9981	44.7290	x	
Serbia	RSMF53266	Balk	19.6625	45.1707	x	x
Serbia	RSMF566	Balk	19.6625	45.1707	x	x
Serbia	RSMK10066	Balk	20.8106	43.2967	x	x
Serbia	RSMK1078	Balk	20.8106	43.2967	x	x
Serbia	RSMK1276	Balk	20.8106	43.2967	x	x
Serbia	RSMK17377	Balk	20.8106	43.2967	x	x
Serbia	RSMK2449	Balk	20.8106	43.2967	x	x
Serbia	RSMK578	Balk	20.8106	43.2967	x	x

Serbia	RSMK678	Balk	20.8106	43.2967	x	x		
Serbia	RSMP35866	Balk	20.3619	42.8397	x			
Serbia	RSMP35966	Balk	20.3619	42.8397	x	x		
Serbia	RSVa7841	Balk	19.7363	44.3148	x	x		
Serbia	RSVa7842	Balk	19.7363	44.3148	x	x		
Serbia	RSVa7855	Balk	19.7363	44.3148	x	x		
Slovenia	SICe142	NCI	14.9457	46.1730				x
Slovenia	SIDo2040	NCI	14.7974	45.5015	x	x		
Slovenia	SIDo2041	NCI	14.7974	45.5015				x
Slovenia	SIDr2778	NCI	14.0292	46.3588	x	x		
Slovenia	SIDr2779	NCI	14.0292	46.3588	x	x		
Slovenia	SIGo2042	Balk	15.5612	45.8578	x	x		
Slovenia	SIGr973	NCI	14.1325	46.1055	x	x		
Slovenia	SIGr974	NCI	14.1325	46.1055	x	x		
Slovenia	SIHo15910	Balk	16.3295	46.8110	x	x		
Slovenia	SIIg1563	NCI	14.5429	45.9470	x	x		
Slovenia	SIIg1564	NCI	14.5429	45.9470	x			
Slovenia	SIIg1565	NCI	14.5429	45.9470	x	x		
Slovenia	SIIg1628	NCI	14.5429	45.9470	x	x		
Slovenia	SIIg1648	NCI	14.5429	45.9470	x	x		
Slovenia	SIIg1766	NCI	14.5429	45.9470	x	x		
Slovenia	SIIg1773	NCI	14.5429	45.9470	x	x		
Slovenia	SIIg1847	NCI	14.5429	45.9470	x	x		
Slovenia	SIIg2143	NCI	14.5429	45.9470	x	x		
Slovenia	SIKn6167	NCI	13.7844	46.4695	x	x		
Slovenia	SIKn6380	NCI	13.7844	46.4695	x	x		
Slovenia	SIKo6781	NCI	14.8203	45.6570	x			
Slovenia	SIKo6782	NCI	14.8203	45.6570	x	x		
Slovenia	SIKo6827	NCI	14.8203	45.6570	x	x		
Slovenia	SIKo6845	NCI	14.8203	45.6570	x	x		
Slovenia	SIKr1042	NCI	14.2471	45.8215	x	x		
Slovenia	SIKr14709	Balk	15.4761	45.8956	x	x		
Slovenia	SILe1145	Balk	16.4575	46.5511	x	x		
Slovenia	SILe1146	Balk	16.4575	46.5511	x	x		
Slovenia	SILe1147	Balk	16.4575	46.5511	x	x		
Slovenia	SILe1163	Balk	16.4575	46.5511	x	x		
Slovenia	SING54318	NCI	13.6571	45.9447	x	x		
Slovenia	SING54320	NCI	13.6571	45.9447	x	x		
Slovenia	SIPd1045	NCI	13.9402	45.5129	x	x		
Slovenia	SIPd1372	NCI	13.9402	45.5129	x	x		
Slovenia	SIPd1374	NCI	13.9402	45.5129	x	x		
Slovenia	SIPh3126	Balk	15.2567	46.5193	x	x		
Slovenia	SIPh3131	Balk	15.2567	46.5193	x	x		
Slovenia	SIPh3489	Balk	15.2567	46.5193	x	x		
Slovenia	SIPk16394	NCI	14.0292	46.3588	x	x		
Slovenia	SIRa16104	Balk	15.3403	45.6859	x	x		
Slovenia	SISe16100	Balk	15.2350	45.5078	x			
Slovenia	SISe16101	Balk	15.2350	45.5078	x	x		
Slovenia	SISi1378	NCI	13.9402	45.5129	x	x		
Slovenia	SISi1380	NCI	13.9402	45.5129	x			
Slovenia	SISi1381	NCI	13.9402	45.5129	x	x		
Slovenia	SISi1382	NCI	13.9402	45.5129				x
Slovenia	SISi1383	NCI	13.9402	45.5129	x	x		
Slovenia	SISi1384	NCI	13.9402	45.5129				x
Slovenia	SISn1043	NCI	14.4014	45.5733	x	x		
Slovenia	SISn1044	NCI	14.4014	45.5733	x	x		
Spain	ESArE135	Iber	-4.2000	43.0333	x			
Spain	ESCoE138	Pyr	-3.6272	43.0193	x		Nav	Cont
Spain	ESEM69	Pyr	-3.4503	43.1423	x	x	Nav	Cont
Spain	ESNa1131	Pyr	-1.6455	43.1757	x	x	Nav	Cont

Spain	ESNa1286	Pyr	-1.6455	43.1757	x	x	Nav	Cont
Spain	ESNa137	Pyr	-1.6455	43.1757	x	x	Nav	Cont
Spain	ESNa1379	Pyr	-1.6455	43.1757	x	x	Nav	Cont
Spain	ESNa1576	Pyr	-1.6455	43.1757	x	x	Nav	Cont
Spain	ESNa1577	Pyr	-1.6455	43.1757	x	x	Nav	Cont
Spain	ESNa1579	Pyr	-1.6455	43.1757	x	x	Nav	Cont
Spain	ESNa172	Pyr	-1.6455	43.1757	x	x	Nav	Cont
Spain	ESNa1757	Pyr	-1.6455	43.1757	x	x	Nav	Cont
Spain	ESNa1758	Pyr	-1.6455	43.1757	x	x	Nav	Cont
Spain	ESNa239	Pyr	-1.6455	43.1757		x	Nav	Cont
Spain	ESNa240	Pyr	-1.6455	43.1757	x	x	Nav	Cont
Spain	ESNa318	Pyr	-1.6455	43.1757	x	x	Nav	Cont
Spain	ESNa399	Pyr	-1.6455	43.1757	x	x	Nav	Cont
Spain	ESNa406	Pyr	-1.6455	43.1757	x	x	Nav	Cont
Spain	ESNa460	Pyr	-1.6455	43.1757	x	x	Nav	Cont
Spain	ESNa461	Pyr	-1.6455	43.1757	x	x	Nav	Cont
Spain	ESNa463	Pyr	-1.6455	43.1757	x	x	Nav	Cont
Spain	ESNa47	Pyr	-1.6455	43.1757	x	x	Nav	Cont
Spain	ESNa509	Pyr	-1.6455	43.1757	x	x	Nav	Cont
Spain	ESNa598	Pyr	-1.6455	43.1757	x	x	Nav	Cont
Spain	ESNa633	Pyr	-1.6455	43.1757	x	x	Nav	Cont
Spain	ESNa739	Pyr	-1.6455	43.1757	x	x	Nav	Cont
Spain	ESNa752	Pyr	-1.6455	43.1757	x	x	Nav	Cont
Spain	ESNa798	Pyr	-1.6455	43.1757	x	x	Nav	Cont
Spain	ESNa803	Pyr	-1.6455	43.1757	x	x	Nav	Cont
Spain	ESNa861	Pyr	-1.6455	43.1757	x	x	Nav	Cont
Spain	ESPE47	Iber	-4.9997	43.1049	x	x		
Spain	ESPE57	Iber	-4.9997	43.1049	x	x		
Spain	ESRa0640	Iber	-3.8794	40.9036	x	x		
Spain	ESRa2653	Iber	-3.8794	40.9036	x	x		
Spain	ESRa3443	Iber	-3.8794	40.9036	x	x		
Spain	ESRa3444	Iber	-3.8794	40.9036	x	x		
Spain	ESRa3445	Iber	-3.8794	40.9036	x	x		
Spain	ESRa3446	Iber	-3.8794	40.9036	x	x		
Spain	ESRa3447	Iber	-3.8794	40.9036	x	x		
Spain	ESRa3448	Iber	-3.8794	40.9036	x	x		
Spain	ESRa3449	Iber	-3.8794	40.9036	x	x		
Spain	ESRa3451	Iber	-3.8794	40.9036	x	x		
Switzerland	CHBa0441	NCE	6.2311	46.4628	x	x		
Switzerland	CHBa1816	NCE	6.2311	46.4628	x	x		
Switzerland	CHBa1817	NCE	6.2311	46.4628	x	x		
Switzerland	CHBa1818	NCE	6.2311	46.4628	x	x		
Switzerland	CHBa1819	NCE	6.2311	46.4628	x	x		
Switzerland	CHBa1820	NCE	6.2311	46.4628	x	x		
Switzerland	CHBa1821	NCE	6.2311	46.4628	x	x		
Switzerland	CHBa3002	NCE	6.2311	46.4628	x	x		
Switzerland	CHCh7622	NCE	6.9974	46.9327	x	x		
Switzerland	CHPo7628	NCE	6.9974	46.9327	x	x		
Switzerland	CHVI4746	NCI	6.8927	46.2043	x	x		
Switzerland	CHVI4747	NCE	6.8927	46.2043	x	x		
Switzerland	CHVI4748	NCI	6.8927	46.2043	x	x		
Turkey	Svolnu290	Out	31.7238	40.8988	x	x		
Turkey	Svolnu302	Out	31.7238	40.8988	x	x		
Turkey	Svolnu303	Out	31.7238	40.8988	x	x		
Turkey	Svolnu304	Out	31.7238	40.8988	x	x		
Turkey	Svolnu312	Out	31.7238	40.8988	x	x		
Turkey	Svolnu313	Out	31.7238	40.8988	x	x		
Turkey	Svolnu392	Out	31.7238	40.8988	x	x		
Turkey	Svolnu393	Out	31.7238	40.8988	x	x		

NCE = North-Central European

NCI = North-Central Italian

SIta = South Italian

Balk = Balkan

Iber = Iberian

Pyr = Pyrenean

OM = Orkney Mainland

OW = Orkney Westray

OS = Orkney South Ronaldsay

Grimn = Grimness

Wind = Windwick

Main1 = Mainland1

Main2 = Mainland2

Swart = Swartmill

Gweed = Gweedore

Nav = Navarra

B Île = Belle Île

Cont = Continental

Large = Large island size

Med = Medium island size

Small = Small island size

X = sample available

Appendix 5. Analysis of Variance (ANOVA) post-hoc tests on Centroid Size (CS) for *Sorex minutus* mandibles.

Parametric ANOVA post-hoc test (Tukey–Kramer) on CS for *S. minutus* mandibles (pairwise *p* values).

	1	2	3	4	5	6	7	8	9	10	11
1-Balkan	-										
2-Iberian	0.9996	-									
3-Ireland	0.0000	0.0000	-								
4-North-Central European	0.0000	0.0000	0.1160	-							
5-North-Central Italian	0.0000	0.4774	0.0000	0.0000	-						
6-Orkney Mainland	0.0000	0.0002	0.8594	0.0002	0.0006	-					
7-Orkney South Ronaldsay	0.0000	0.0000	0.8693	0.9999	0.0000	0.0875	-				
8-Orkney Westray	0.0000	0.0006	0.7900	0.0004	0.0075	1.0000	0.0766	-			
9-Pyrenean	0.0000	0.0545	0.0001	0.0000	0.7729	0.1705	0.0000	0.4400	-		
10-South Italian	1.0000	1.0000	0.0378	0.0021	0.9282	0.1658	0.0066	0.2121	0.6731	-	
11-Outgroup	0.9981	0.9691	0.0000	0.0000	0.0318	0.0000	0.0000	0.0000	0.0019	1.0000	-

Non-parametric ANOVA post-hoc test (Tamhane) on CS for *S. minutus* mandibles (pairwise *p* values).

	1	2	3	4	5	6	7	8	9	10	11
1-Balkan	-										
2-Iberian	1.0000	-									
3-Ireland	0.0000	0.0000	-								
4-North-Central European	0.0000	0.0000	0.0421	-							
5-North-Central Italian	0.0021	0.5889	0.0000	0.0000	-						
6-Orkney Mainland	0.0000	0.0004	0.9031	0.0000	0.0032	-					
7-Orkney South Ronaldsay	0.0000	0.0000	0.4536	1.0000	0.0000	0.0005	-				
8-Orkney Westray	0.0000	0.0006	0.6080	0.0000	0.0081	1.0000	0.0001	-			
9-Pyrenean	0.0000	0.0467	0.0004	0.0000	0.9999	0.2793	0.0000	0.5037	-		
10-South Italian	1.0000	1.0000	0.9840	0.9429	1.0000	0.9966	0.9569	0.9976	1.0000	-	
11-Outgroup	1.0000	0.9975	0.0007	0.0003	0.0681	0.0019	0.0004	0.0025	0.0141	1.0000	-

Appendix 6. Multivariate Analysis of Variance (MANOVA) post-hoc tests on shape variables for *Sorex minutus* mandibles.

Parametric MANOVA post-hoc tests (Hotelling T^2) on shape variables among groups of *S. minutus* mandibles (pairwise p values).

	1	2	3	4	5	6	7	8	9	10	11
1-Balkan	-	0.0022	0.0000	0.0000	0.0002	0.0000	0.0000	0.0000	0.0000	0.0964	0.0010
2-Iberian	0.1217	-	0.0000	0.0002	0.0194	0.0000	0.0000	0.0000	0.0028	Fail	Fail
3-Ireland	0.0000	0.0000	-	0.0000	0.0000	0.0000	0.0000	0.0000	0.0000	0.0005	0.0001
4-North-Central European	0.0000	0.0098	0.0000	-	0.0000	0.0000	0.0000	0.0000	0.0000	0.0000	0.0000
5-North-Central Italian	0.0124	1.0000	0.0000	0.0000	-	0.0000	0.0000	0.0000	0.0000	0.0556	0.0001
6-Orkney Mainland	0.0000	0.0000	0.0000	0.0000	0.0000	-	0.0000	0.0000	0.0000	0.1151	0.0003
7-Orkney South Ronaldsay	0.0000	0.0026	0.0000	0.0000	0.0000	0.0000	-	0.0000	0.0000	0.0360	0.0082
8-Orkney Westray	0.0000	0.0000	0.0000	0.0000	0.0000	0.0000	0.0000	-	0.0000	0.0044	0.0000
9-Pyrenean	0.0000	0.1531	0.0000	0.0000	0.0000	0.0000	0.0000	0.0000	-	0.0009	0.0089
10-South Italian	1.0000	Fail	0.0293	0.0009	1.0000	1.0000	1.0000	0.2403	0.0503	-	Fail
11-Outgroup	0.0534	Fail	0.0034	0.0000	0.0060	0.0149	0.4514	0.0000	0.4882	Fail	-

Below diagonal, Bonferroni corrected p values. Above diagonal, uncorrected p values.

Non-parametric MANOVA post-hoc tests on shape variables among groups of *S. minutus* mandibles (pairwise p values).

	1	2	3	4	5	6	7	8	9	10	11
1-Balkan	-	0.0158	0.0000	0.0000	0.0000	0.0000	0.0000	0.0000	0.0000	0.0049	0.0001
2-Iberian	0.8690	-	0.0017	0.0064	0.1099	0.0007	0.0000	0.0000	0.0446	0.0191	0.0088
3-Ireland	0.0000	0.0935	-	0.0000	0.0000	0.0000	0.0000	0.0000	0.0000	0.0006	0.0002
4-North-Central European	0.0000	0.3520	0.0000	-	0.0000	0.0000	0.0000	0.0000	0.0000	0.0024	0.0000
5-North-Central Italian	0.0000	1.0000	0.0000	0.0000	-	0.0000	0.0000	0.0000	0.0000	0.0035	0.0001
6-Orkney Mainland	0.0000	0.0385	0.0000	0.0000	0.0000	-	0.0006	0.0000	0.0000	0.0350	0.0052
7-Orkney South Ronaldsay	0.0000	0.0000	0.0000	0.0000	0.0000	0.0330	-	0.0000	0.0000	0.0005	0.0008
8-Orkney Westray	0.0000	0.0000	0.0000	0.0000	0.0000	0.0000	0.0000	-	0.0000	0.0001	0.0000
9-Pyrenean	0.0000	1.0000	0.0000	0.0000	0.0000	0.0000	0.0000	0.0000	-	0.1044	0.0344
10-South Italian	0.2695	1.0000	0.0330	0.1320	0.1925	1.0000	0.0275	0.0055	1.0000	-	0.5720
11-Outgroup	0.0055	0.4840	0.0110	0.0000	0.0055	0.2860	0.0440	0.0000	1.0000	1.0000	-

Below diagonal, Bonferroni corrected p values. Above diagonal, uncorrected p values.

Appendix 7. Analysis of Variance (ANOVA) post-hoc tests on Centroid Size (CS) for *Sorex minutus* skulls.

Parametric ANOVA post-hoc test (Tukey–Kramer) on CS for *S. minutus* skulls (pairwise *p* values).

	1	2	3	4	5	6	7	8	9	10	11
1-Balkan	-										
2-Iberian	0.0009	-									
3-Ireland	1.0000	0.0001	-								
4-North-Central European	0.0002	0.0000	0.0006	-							
5-North-Central Italian	1.0000	0.0019	0.9921	0.0000	-						
6-Orkney Mainland	0.9890	0.0119	0.7933	0.0000	0.9997	-					
7-Orkney South Ronaldsay	0.9946	0.0174	0.8760	0.0000	0.9999	1.0000	-				
8-Orkney Westray	0.5078	0.1505	0.1398	0.0000	0.7354	0.9860	0.9911	-			
9-Pyrenean	1.0000	0.0060	0.9992	0.0006	1.0000	0.9999	1.0000	0.8741	-		
10-South Italian	1.0000	0.5180	1.0000	0.8526	1.0000	1.0000	1.0000	0.9994	1.0000	-	
11-Outgroup	1.0000	0.1168	1.0000	0.1733	1.0000	1.0000	1.0000	0.9940	1.0000	1.0000	-

Non-parametric ANOVA post-hoc test (Tamhane) on CS for *S. minutus* skulls (pairwise *p* values).

	1	2	3	4	5	6	7	8	9	10	11
1-Balkan	-										
2-Iberian	0.3315	-									
3-Ireland	1.0000	0.2030	-								
4-North-Central European	0.0594	0.0050	0.0556	-							
5-North-Central Italian	1.0000	0.4253	1.0000	0.0082	-						
6-Orkney Mainland	1.0000	0.6699	0.9807	0.0037	1.0000	-					
7-Orkney South Ronaldsay	1.0000	0.6218	0.3023	0.0007	1.0000	1.0000	-				
8-Orkney Westray	0.5362	0.9434	0.0003	0.0000	0.4399	1.0000	0.9116	-			
9-Pyrenean	1.0000	0.4161	1.0000	0.0133	1.0000	1.0000	1.0000	0.5983	-		
10-South Italian	1.0000	0.9453	1.0000	0.9992	1.0000	1.0000	1.0000	1.0000	1.0000	-	
11-Outgroup	1.0000	0.6249	1.0000	0.4519	1.0000	1.0000	1.0000	1.0000	1.0000	1.0000	-

Appendix 8. Multivariate Analysis of Variance (MANOVA) post-hoc tests on shape variables for *Sorex minutus* skulls.

Parametric MANOVA post-hoc tests (Hotelling T^2) on shape variables among groups of *S. minutus* skulls (pairwise p values).

	1	2	3	4	5	6	7	8	9	10	11
1-Balkan	-	0.0046	0.0000	0.0000	0.4654	0.0000	0.0000	0.0000	0.0003	0.1610	0.0233
2-Iberian	0.2534	-	0.0002	0.0035	0.0011	0.0000	0.0000	0.0000	0.2338	Fail	Fail
3-Ireland	0.0000	0.0120	-	0.0000	0.0000	0.0000	0.0000	0.0000	0.0000	0.0101	0.0000
4-North-Central European	0.0000	0.1944	0.0000	-	0.0000	0.0000	0.0000	0.0000	0.0000	0.2786	0.0015
5-North-Central Italian	1.0000	0.0607	0.0000	0.0000	-	0.0000	0.0000	0.0000	0.0000	0.0226	0.0078
6-Orkney Mainland	0.0000	0.0000	0.0000	0.0000	0.0000	-	0.0000	0.0000	0.0000	0.0035	0.0000
7-Orkney South Ronaldsay	0.0000	0.0000	0.0000	0.0000	0.0000	0.0000	-	0.0000	0.0000	0.0764	0.0004
8-Orkney Westray	0.0000	0.0000	0.0000	0.0000	0.0000	0.0000	0.0000	-	0.0000	0.0097	0.0000
9-Pyrenean	0.0157	1.0000	0.0000	0.0000	0.0010	0.0000	0.0000	0.0000	-	Fail	0.9437
10-South Italian	1.0000	Fail	0.5540	1.0000	1.0000	0.1949	1.0000	0.5339	Fail	-	Fail
11-Outgroup	1.0000	Fail	0.0000	0.0842	0.4299	0.0001	0.0193	0.0015	1.0000	Fail	-

Below diagonal, Bonferroni corrected p values. Above diagonal, uncorrected p values.

Non-parametric MANOVA post-hoc tests on shape variables among groups of *S. minutus* skulls (pairwise *p* values).

	1	2	3	4	5	6	7	8	9	10	11
1-Balkan	-	0.0002	0.0000	0.0000	0.0830	0.0000	0.0000	0.0000	0.0001	0.2640	0.0218
2-Iberian	0.0110	-	0.0000	0.0000	0.0245	0.0000	0.0000	0.0000	0.0036	0.0324	0.0000
3-Ireland	0.0000	0.0000	-	0.0000	0.0000	0.0000	0.0000	0.0000	0.0000	0.0030	0.0000
4-North-Central European	0.0000	0.0000	0.0000	-	0.0001	0.0000	0.0000	0.0000	0.0000	0.0070	0.0000
5-North-Central Italian	1.0000	1.0000	0.0000	0.0055	-	0.0000	0.0000	0.0000	0.0008	0.1390	0.0108
6-Orkney Mainland	0.0000	0.0000	0.0000	0.0000	0.0000	-	0.0000	0.0000	0.0000	0.0004	0.0000
7-Orkney South Ronaldsay	0.0000	0.0000	0.0000	0.0000	0.0000	0.0000	-	0.0000	0.0000	0.0006	0.0000
8-Orkney Westray	0.0000	0.0000	0.0000	0.0000	0.0000	0.0000	0.0000	-	0.0000	0.0000	0.0000
9-Pyrenean	0.0055	0.1980	0.0000	0.0000	0.0440	0.0000	0.0000	0.0000	-	0.0762	0.0001
10-South Italian	1.0000	1.0000	0.1650	0.3850	1.0000	0.0220	0.0330	0.0000	1.0000	-	0.9104
11-Outgroup	1.0000	0.0000	0.0000	0.0000	0.5940	0.0000	0.0000	0.0000	0.0055	1.0000	-

Below diagonal, Bonferroni corrected *p* values. Above diagonal, uncorrected *p* values.

Appendix 9. Analysis of Variance (ANOVA) of *Sorex minutus* mandibles.

Parametric ANOVA post-hoc test (Tukey–Kramer) on CS for *S. minutus* mandibles (pairwise *p* values).

	1	2	3	4	5	6	7	8	9	10	11	12
1-Ireland Cloghan	-											
2-Ireland Derry	0.3242	-										
3-Ireland Gweedore	0.0253	0.9943	-									
4-O Mainland 1	0.9939	0.0395	0.0018	-								
5-O Mainland 2	0.9725	0.9277	0.2317	0.4147	-							
6-O SR Grimness	0.0054	0.9218	1.0000	0.0004	0.0653	-						
7-O SR Windwick	0.0766	0.9999	1.0000	0.0065	0.4943	0.9997	-					
8-O W Swartmill	1.0000	0.1647	0.0088	0.9995	0.8676	0.0016	0.0305	-				
9-O W Ness	0.9984	0.9261	0.3066	0.7189	1.0000	0.1138	0.5545	0.9828	-			
10-Pyrenean Navarra	0.0000	0.0000	0.0000	0.0000	0.0000	0.0000	0.0000	0.0000	0.0000	-		
11-Pyrenean Belle Île	0.1915	0.0000	0.0000	0.9667	0.0006	0.0000	0.0000	0.3556	0.0124	0.0002	-	
12-Pyrenean France	0.0009	0.8185	1.0000	0.0001	0.0128	1.0000	0.9984	0.0002	0.0412	0.0000	0.0000	-

O = Orkney, SR = South Ronaldsay, W = Westray.

Appendix 10. Analysis of Variance (ANOVA) of *Sorex minutus* skulls.

Parametric ANOVA post-hoc test (Tukey–Kramer) on CS for *S. minutus* skulls (pairwise *p* values).

	1	2	3	4	5	6	7	8	9	10
1-Ireland Cloghan	-									
2-Ireland Derry	1.0000	-								
3-Ireland Gweedore	0.2629	0.4309	-							
4-O Mainland 1	0.7358	0.8753	1.0000	-						
5-O Mainland 2	0.1609	0.3100	1.0000	1.0000	-					
6-O SR Grimness	0.5370	0.7312	1.0000	1.0000	1.0000	-				
7-O SR Windwick	0.3144	0.4932	1.0000	1.0000	1.0000	1.0000	-			
8-O W Ness	0.0076	0.0188	0.9697	0.8653	0.8655	0.8242	0.9624	-		
9-O W Swartmill	0.1365	0.2513	1.0000	0.9993	1.0000	0.9993	1.0000	0.9959	-	
10-Pyrenean Navarra	0.7195	0.8866	0.9956	1.0000	0.9958	1.0000	0.9977	0.4177	0.9642	-

O = Orkney, SR = South Ronaldsay, W = Westray.

Non-parametric ANOVA post-hoc test (Tamhane) on CS for *S. minutus* skulls (pairwise *p* values).

	1	2	3	4	5	6	7	8	9	10
1-Ireland Cloghan	-									
2-Ireland Derry	1.0000	-								
3-Ireland Gweedore	0.1864	0.2943	-							
4-O Mainland 1	0.9929	0.9995	1.0000	-						
5-O Mainland 2	0.6075	0.7936	1.0000	1.0000	-					
6-O SR Grimness	0.4125	0.6003	1.0000	1.0000	1.0000	-				
7-O SR Windwick	0.0573	0.0799	1.0000	1.0000	1.0000	1.0000	-			
8-O W Ness	0.0001	0.0001	0.9913	0.9983	0.9989	0.5594	0.7247	-		
9-O W Swartmill	0.0698	0.1114	1.0000	1.0000	1.0000	1.0000	1.0000	1.0000	-	
10-Pyreanean Navarra	0.8372	0.9602	1.0000	1.0000	1.0000	1.0000	1.0000	0.1230	0.9997	-

O = Orkney, SR = South Ronaldsay, W = Westray.

Appendix 11. Multivariate Analysis of Variance (MANOVA) of *Sorex minutus* mandibles.

Parametric MANOVA post-hoc tests (Hotelling T^2) on shape variables among groups of *S. minutus* mandibles (pairwise p values).

	1	2	3	4	5	6	7	8	9	10	11	12
1-Ireland Cloghan	-	0.2099	0.1667	Fail	0.0000	0.0035	0.0178	0.0000	0.0000	0.0080	0.0095	0.0000
2-Ireland Derry	1.0000	-	0.1352	0.1351	0.0000	0.0001	0.0000	0.0000	0.0000	0.0006	0.0004	0.0000
3-Ireland Gweedore	1.0000	1.0000	-	Fail	0.0000	0.0244	0.0017	0.0008	0.0001	0.0016	0.0027	0.0000
4-O Mainland 1	Fail	1.0000	Fail	-	0.0032	Fail	Fail	Fail	Fail	0.0347	Fail	0.0004
5-O Mainland 2	0.0000	0.0000	0.0003	0.2085	-	0.0017	0.0015	0.0000	0.0000	0.0000	0.0000	0.0000
6-O SR Grimness	0.2305	0.0041	1.0000	Fail	0.1102	-	0.4906	0.0029	0.0002	0.0285	0.0013	0.0001
7-O SR Windwick	1.0000	0.0005	0.1125	Fail	0.0974	1.0000	-	0.0001	0.0003	0.0000	0.0014	0.0000
8-O W Swartmill	0.0016	0.0000	0.0500	Fail	0.0001	0.1926	0.0065	-	0.0146	0.0000	0.0003	0.0000
9-O W Ness	0.0019	0.0003	0.0037	Fail	0.0000	0.0164	0.0209	0.9633	-	0.0000	0.0005	0.0000
10-Pyrenean Navarra	0.5261	0.0381	0.1074	1.0000	0.0000	1.0000	0.0007	0.0000	0.0000	-	0.0012	0.0000
11-Pyrenean Belle Île	0.6297	0.0271	0.1782	Fail	0.0000	0.0884	0.0948	0.0183	0.0335	0.0769	-	0.0021
12-Pyrenean France	0.0000	0.0000	0.0000	0.0243	0.0000	0.0063	0.0000	0.0000	0.0000	0.0005	0.1395	-

Above diagonal, Bonferroni uncorrected p values. Below diagonal, Bonferroni corrected p values. O = Orkney, SR = South Ronaldsay, W = Westray.

Non-parametric MANOVA post-hoc tests on shape variables among groups of *S. minutus* mandibles (pairwise *p* values).

	1	2	3	4	5	6	7	8	9	10	11	12
1-Ireland Cloghan	-	0.0796	0.0452	0.0000	0.0000	0.0000	0.0000	0.0000	0.0000	0.0000	0.0023	0.0000
2-Ireland Derry	1.0000	-	0.0871	0.0000	0.0000	0.0000	0.0000	0.0000	0.0000	0.0000	0.0006	0.0000
3-Ireland Gweedore	1.0000	1.0000	-	0.0000	0.0000	0.0000	0.0000	0.0000	0.0000	0.0000	0.0047	0.0000
4-O Mainland 1	0.0000	0.0000	0.0000	-	0.0000	0.0001	0.0000	0.0000	0.0000	0.0000	0.0110	0.0000
5-O Mainland 2	0.0000	0.0000	0.0000	0.0000	-	0.0044	0.0264	0.0000	0.0000	0.0000	0.0000	0.0000
6-O SR Grimness	0.0000	0.0000	0.0000	0.0066	0.2904	-	0.0123	0.0000	0.0000	0.0000	0.0002	0.0000
7-O SR Windwick	0.0000	0.0000	0.0000	0.0000	1.0000	0.8118	-	0.0000	0.0000	0.0000	0.0001	0.0000
8-O W Swartmill	0.0000	0.0000	0.0000	0.0000	0.0000	0.0000	0.0000	-	0.0000	0.0000	0.0000	0.0000
9-O W Ness	0.0000	0.0000	0.0000	0.0000	0.0000	0.0000	0.0000	0.0000	-	0.0000	0.0000	0.0000
10-Pyrenean Navarra	0.0000	0.0000	0.0000	0.0000	0.0000	0.0000	0.0000	0.0000	0.0000	-	0.0001	0.0000
11-Pyrenean Belle Île	0.1518	0.0396	0.3102	0.7260	0.0000	0.0132	0.0066	0.0000	0.0000	0.0066	-	0.0210
12-Pyrenean France	0.0000	0.0000	0.0000	0.0000	0.0000	0.0000	0.0000	0.0000	0.0000	0.0000	1.0000	-

Above diagonal, Bonferroni uncorrected *p* values. Below diagonal, Bonferroni corrected *p* values. O = Orkney, SR = South Ronaldsay, W = Westray.

Appendix 12. Multivariate Analysis of Variance (MANOVA) of *Sorex minutus* skulls.

Parametric MANOVA post-hoc tests (Hotelling T^2) on shape variables among groups of *S. minutus* skulls (pairwise p values).

	1	2	3	4	5	6	7	8	9	10
1-Ireland Cloghan	-	0.1673	0.2792	Fail	0.0002	0.1180	0.1734	0.0028	0.0428	0.0003
2-Ireland Derry	1.0000	-	0.6732	Fail	0.0023	0.0659	0.2971	0.0073	0.0041	0.0000
3-Ireland Gweedore	1.0000	1.0000	-	Fail	0.0001	0.2050	0.2727	0.0012	0.0525	0.0002
4-O Mainland 1	Fail	Fail	Fail	-	0.3488	Fail	Fail	Fail	Fail	0.0379
5-O Mainland 2	0.0102	0.1026	0.0035	1.0000	-	0.0001	0.0044	0.0000	0.0000	0.0000
6-O SR Grimness	1.0000	1.0000	1.0000	Fail	0.0029	-	0.7743	0.0485	0.1161	0.0000
7-O SR Windwick	1.0000	1.0000	1.0000	Fail	0.2000	1.0000	-	0.1981	0.2553	0.0001
8-O W Ness	0.1253	0.3292	0.0549	Fail	0.0000	1.0000	1.0000	-	0.6917	0.0000
9-O W Swartmill	1.0000	0.1856	1.0000	Fail	0.0000	1.0000	1.0000	1.0000	-	0.0001
10-Pyrenean Navarra	0.0130	0.0001	0.0093	1.0000	0.0000	0.0005	0.0064	0.0002	0.0043	-

Above diagonal, Bonferroni uncorrected p values. Below diagonal, Bonferroni corrected p values. O = Orkney, SR = South Ronaldsay, W = Westray.

Non-parametric MANOVA post-hoc tests on shape variables among groups of *S. minutus* skulls (pairwise *p* values).

	1	2	3	4	5	6	7	8	9	10
1-Ireland Cloghan	-	0.0076	0.0190	0.0000	0.0000	0.0002	0.0000	0.0000	0.0000	0.0000
2-Ireland Derry	0.3420	-	0.3101	0.0020	0.0004	0.0036	0.0001	0.0000	0.0000	0.0000
3-Ireland Gweedore	0.8550	1.0000	-	0.0000	0.0000	0.0104	0.0002	0.0000	0.0000	0.0000
4-O Mainland 1	0.0000	0.0900	0.0000	-	0.0270	0.0000	0.0000	0.0000	0.0000	0.0000
5-O Mainland 2	0.0000	0.0180	0.0000	1.0000	-	0.0002	0.0000	0.0000	0.0000	0.0000
6-O SR Grimness	0.0090	0.1620	0.4680	0.0000	0.0090	-	0.1864	0.0000	0.0000	0.0000
7-O SR Windwick	0.0000	0.0045	0.0090	0.0000	0.0000	1.0000	-	0.0000	0.0000	0.0000
8-O W Ness	0.0000	0.0000	0.0000	0.0000	0.0000	0.0000	0.0000	-	0.6730	0.0000
9-O W Swartmill	0.0000	0.0000	0.0000	0.0000	0.0000	0.0000	0.0000	1.0000	-	0.0000
10-Pyrenean Navarra	0.0000	0.0000	0.0000	0.0000	0.0000	0.0000	0.0000	0.0000	0.0000	-

Above diagonal, Bonferroni uncorrected *p* values. Below diagonal, Bonferroni corrected *p* values. O = Orkney, SR = South Ronaldsay, W = Westray.